AD NUMBER

AD829332

NEW LIMITATION CHANGE

TO

Approved for public release, distribution unlimited

FROM

Distribution: Further dissemination only as directed by Air Force Aero Propulsion Lab., Wright-Patterson AFB, OH 45433, FEB 1968, or higher DoD authority.

AUTHORITY

AFAPL ltr, 30 Jun 1975

INVESTIGATION OF THE LOW SPEED FIXED GEOMETRY SCRAMJET "INLET DESIGN PRACTICE MANUAL"

Edited by

James Johnson

TECHNICAL REPORT AFAPL-TR-68-7

February 1968

GENERAL APPLIED SCIENCE Labs.,Inc.
MERRICK AND STEWART AVENUES, WESTBURY, L.I. NEW YORK 11590 • 516-333-6960

NOTICE

When Government drawings, specifications, or other data are used for any purpose other than in connection with a definitely related Government procurement operation, the United States Government thereby incurs no responsibility nor any obligation whatsoever; and the fact that the Government may have formulated, furnished, or in any way supplied the said drawings, specifications, or other data, is not to be regarded by implication or otherwise as in any manner licensing the holder or any other person or corporation, or conveying any rights or permission to manufacture, use, or sell any patented invention that may in any way be related thereto.

This report is subject to special export controls and each transmittal to foreign governments or foreign nationals may be made only with the prior approval of the Air Force Aero Propulsion Laboratory, Wright-Patterson AFB, Ohio 45433.

This document may be further distributed by any holder only with specific prior approval of the Air Force Aero Propulsion Laboratory, Wright-Patterson AFB, Ohio. 45433,

Copies of this report should not be returned unless return is required by security considerations, contractual obligations, or notice on a specific document.

INVESTIGATION OF THE LOW SPEED

FIXED GEOMETRY SCRAMJET

"INLET DESIGN PRACTICE MANUAL"

Edited by James Johnson

FOREWORD

This report was prepared by the General Applied Science Laboratories, Inc., Westbury, New York, a wholly owned subsidiary of The Marquardt Corporation, on Contract F-33(615)-67-C-1084, Task 3012, "Investigation of the Low Speed Fixed Geometry Scramjet." The work was administered under the direction of the Air Force Aero Propulsion Laboratory, Air Force Systems Command. Mr. R. Canny, (APRP) was the project engineer for the laboratory.

The studies presented began in September 1966 and were concluded in August 1967. Mr. James Johnson was responsible for the technical direction of this program at GASL. The technical efforts were performed by the following scientists; Messrs. M. Abbett and G. Bleich for the two-dimensional flow analysis and programming, and Drs. S. Angelucci and C. Ruger for the three-dimensional flow analysis and programming.

This report, GASL TR-667, was submitted November 1967.

ABSTRACT

Computer programs have been written to aid the design and analysis of two-dimensional, axisymmetric, and three-dimensional supersonic inlets. This report presents the fundamental analytic techniques, the use and operation of the computer programs, and the application to the design of supersonic inlets. The programs are written in Fortran IV for use on the 7094 high speed digital computer.

The two-dimensional and axisymmetric programs presented herein are written for generalized inviscid supersonic internal flow problems with uniform or non-uniform inlet entry conditions for entropy, total enthalpy, pressure, Mach number and flow direction. The program capabilities include the intersections and reflections of both family waves, the formation of shocks or expansions at corners, the formation of shocks by coalescence of waves from smooth walls, and the formation of contact discontinuities.

The three-dimensional programs presented herein are written for the calculation of the inviscid supersonic flow fields associated with basic elements of three-dimensional supersonic inlets. The methods utilized exact and linearized supersonic flow theory with engineering approximations to yield solutions to the following unit problems; delta wing flow, conical shock interacting with a plane surface, plane shock interacting with a conical surface, and the interaction of two different conical flow fields.

TABLE OF CONTENTS

LIST OF ILLUSTRATIONS

LIST OF ILLUSTRATIONS

LIST OF ILLUSTRATIONS

ILLUSTRATIONS TO APPENDIXES

LIST OF ILLUSTRATIONS

LIST OF TABLES

NOMENCLATURE FOR SECTION IV

a	speed of sound, $a^2 = \gamma P/\rho$
b	$\sqrt{M^2-1} \; / \; \rho \; u^2$
c_p, c_v	coefficients of specific heat
G	$\frac{(\tau-\lambda)\ \tau}{y}\ j$
h	specific static enthalpy, $h = \frac{\gamma}{\gamma-1}\ p/\rho$
H	specific total enthalpy, $H = h + q^2/2$
M	Mach number, $M = q/a$
p	pressure
q	magnitude of the velocity vector, $q^2 = u^2 + v^2$
R	gas constant
S	entropy
u	velocity component in x direction
v	velocity component in y direction
x	abscissa (horizontal axis = z in cylindrical polar frame (z, r, θ) for axisymmetric flow)
y	ordinate (vertical axis = 4 in cylindrical polar frame for axisymmetric flow)
δ	angle flow turns when going through oblique shock
ν	c_p/c_v, the ratio of specific heats
λ	characteristic slope
μ	viscosity (=0 in this report

ν Prandtl-Meyer turning angle (see equation 15)

ρ density

σ angle oblique shock makes with incident flow

τ streamline slope, $\tau = v/u$

θ angle velocity vector makes with x axis

Subscripts

$( )_x$ $\frac{\partial}{\partial x}$

1, 2 conditions in front of and behind shock, respectively

A,B,C,etc. variable is to be evaluated at the indicated point

Superscripts

j 0 for two-dimensional flow
1 for axisymmetric flow

——— averaged quantity, also indicates a line between two points

I, II down running and up running characteristic respectively

The following is standard notation on the figures

_____ _ _____ down running characteristic

---------- up running characteristic

═══════ oblique shock

_____ contact discontinuity (interface, slip stream)

I

INTRODUCTION

The use of three-dimensional flow fields in the design of supersonic and hypersonic inlets has been under experimental and analytical investigation at GASL for several years under Air Force sponsorship as reported in References 1 through 6. Three-dimensional designs can be used for either fixed or variable geometry inlet configurations over a wide flight Mach number range to obtain, for example, high inlet contraction ratios and capture mass flows, to prevent boundary layer separation, and to reduce heating loads to the inlet structure. General use of three-dimensional designs however, has been limited by the development of practical analytic techniques. In most cases where three-dimensional analytic techniques are available, they are either so highly restricted, or complicated and time consuming, that they are impractical for use in a typical inlet design effort.

Practical methods for the design and analysis of three-dimensional supersonic inlets have been under development at GASL for the Air Force Aero Propulsion Laboratory as part of the overall investigations of the low speed range supersonic combustion ramjet (SCRAMJET). These methods combine exact and linearized three-dimensional theory with engineering approximations to yield solutions to unit problems which are basic elements of three-dimensional supersonic internal flow fields, i.e., delta wing flow, conical shock interacting with a plane surface, plane shock interacting with a conical surface, and the interaction of two different conical flow fields. A combination of these unit problems can be used to design and analyze a large variety of supersonic and hypersonic three-dimensional inlets.

These methods for two and three dimensional inlet design and analysis, have been programmed in Fortran IV for use on the IBM 7094 digital computer. This report presents the complete description of the fundamental analysis, the program use and operation, and the application to the design of three and two dimensional supersonic inlets. This work was performed for the Wright-Patterson Air Force Base Aero Propulsion Laboratory under contract F33(615)-67-C-1084.

II

PROGRAM OBJECTIVES AND APPROACH

The overall objective of this effort was to generate digital computer programs for aid in the design and analysis of two and three dimensional supersonic inlets. The analytic techniques which form the basis of this work have been developed at GASL during the past several years under Air Force sponsorship. The purpose of this report is to present these fundamental analytic techniques, the use and operation of the computer programs, and the application to the design of supersonic inlets. The aim is to provide a practical tool for two and three dimensional inlet design, in addition to a detailed description of the analysis. To this end, the following sections describe;

Section III - A discussion of the methodology used for three-dimensional inlet design and the use of the computer programs in these efforts.

Section IV - A complete description of the two-dimensional and axisymmetric internal flow field analysis and computer programs.

Section V - A complete description of the three-dimensional analysis and computer program elements.

It is seen then, that this report can be used as a "Design Manual" to aid in three-dimensional inlet design, or as an initial step in developing a more sophisticated or modified analysis. In either case, it must be noted that the current work presented here has limitations which should be the object of continuing study. These limitations will be clear as they arise in the following sections in this report. A summary of the overall limitations however, is given here.

(1) Viscous effects are neglected

(2) Completely supersonic flow required

(3) Completely supersonic leading edges required

(4) Three-dimensional computations only for unit problems.

III

METHODS FOR THREE-DIMENSIONAL INLET DESIGN

The detailed three-dimensional and two-dimensional analytic techniques and computer programs will be described in the following sections. It is necessary here, however, to describe the overall methodology for using these techniques before going into the analysis.

The overall inlet design process is schematically shown in Figure 1. It is seen that several steps are required in the design process:

a) choice or definition of inlet design performance characteristics

b) choice or definition of inlet design concept, e.g., two-dimensional, three-dimensional, with or without centerbody, etc.

c) two-dimensional calculations to define essential performance properties

d) three-dimensional corrections to define exact performance properties

e) evaluation of performance with respect to initial required performance levels

f) repeat steps (b) to (e) until required performance is obtained.

A summary of each of the above design process steps is given in the following discussion.

The initial steps (a) and (b) are closely interrelated since the required inlet design performance characteristics generally dictate the choice of the inlet design concept. The requirement of fixed geometry operation over a wide Mach number range, for example, might require a more highly three-dimensional inlet design (with possibly one or more inlet central bodies) than a fixed geometry inlet design for a more restricted Mach number

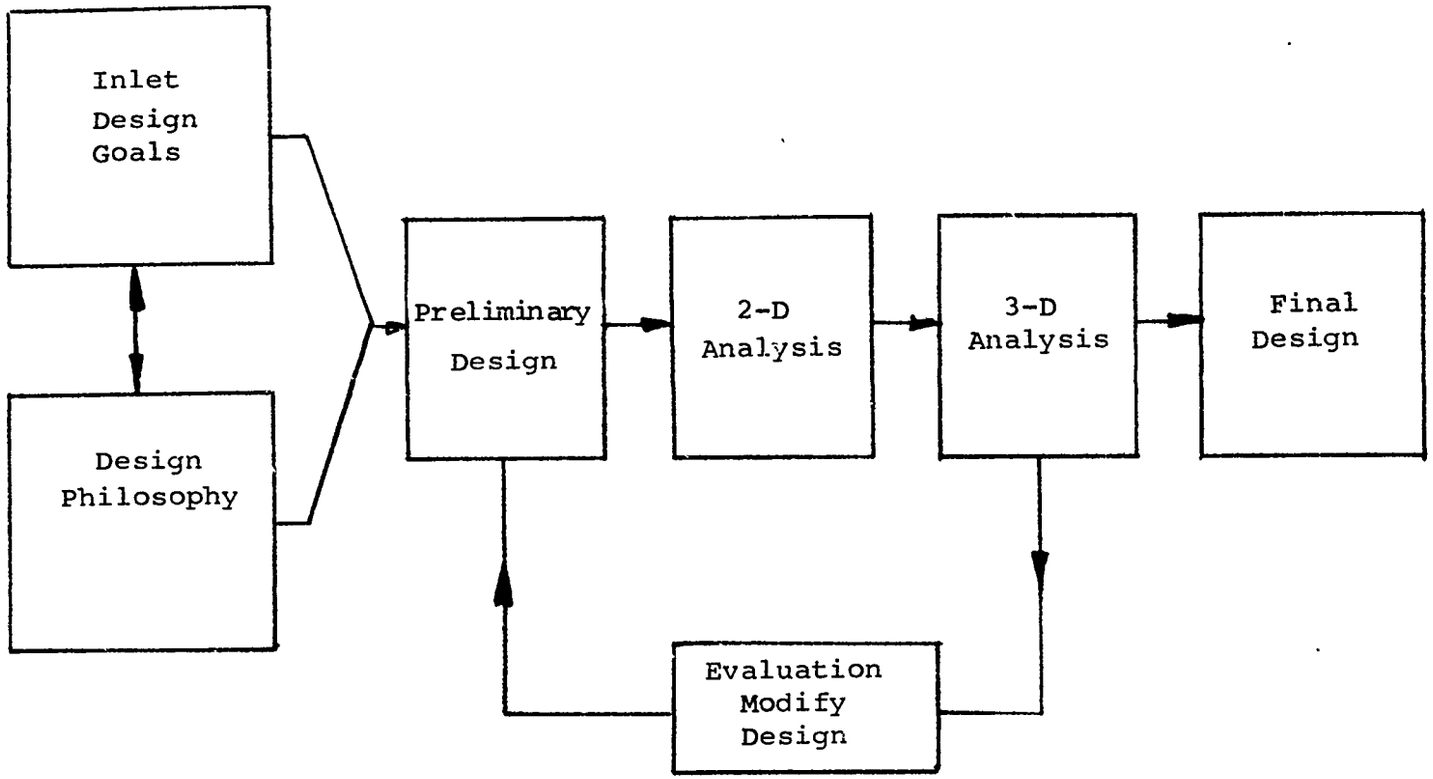

FIGURE 1 - INLET DESIGN PROCESS

range of flight operation. Other requirements might lead to a variable geometry inlet design to attain performance goals. In any case, these initial steps of the design process require decisions based upon inlet design experience.

The next step (c) utilizes the two-dimensional and/or axisymmetric computer programs described in Section IV. This step would be the final step for a completely two-dimensional or axisymmetric design. For the case of a three-dimensional design, however, it forms the first step. Several overall inlet design geometries are roughed out by the inlet designer and the computer program provides a detailed analysis of each one. The overall properties of the various inlet flow fields are then evaluated with respect to the initial design goals and the most promising designs are chosen for further consideration by including the effects of three-dimensionality.

The next step (d) utilizes the three-dimensional computer program elements described in Section V. The basic elements of a large variety of supersonic three-dimensional inlet flow fields are programmed for machine calculation in this phase of the design process. These elements as shown in Figure 2 are the delta wing flow field, the interaction of a conical shock with a plane surface, the interaction of a plane shock with a conical surface, and the interaction of two different conical shocks. The techniques used for these machine computations however, can also be used manually to compute the flow field of almost any supersonic three-dimensional configuration. The level of three dimensionality designed into the inlet geometry in this step of course depends again upon the initial design goals. The overall procedure here again is to investigate various geometries until the desired performance conditions are achieved. However, here the overall configuration is known from the two-dimensional and axisymmetric analysis of step (c). The procedures in this step are to incorporate, for example, various leading edge sweep angles, cone angles, etc.

An inlet configuration is now defined and analyzed. Step (e) calls for an evaluation of the resulting performance based upon the initial design performance goals. At this point, either these goals are satisfied or steps (c) and (d) are repeated. In this manner then the required inlet performance characteristics are achieved.

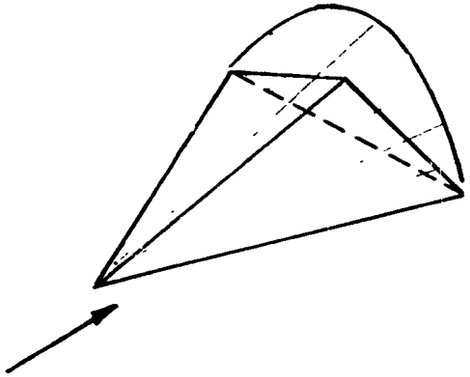

a) Swept Wedge Flow

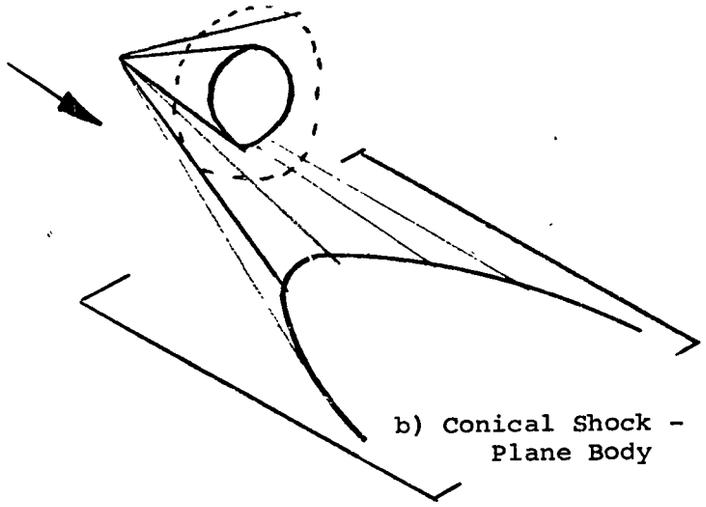

b) Conical Shock - Plane Body

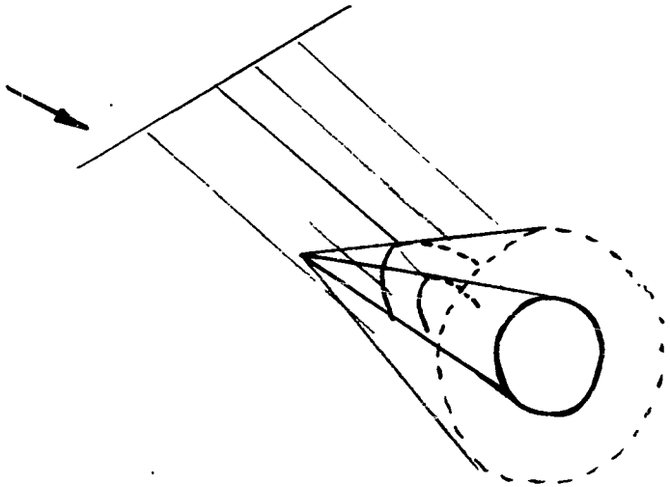

c) Plane Shock - Conical Body

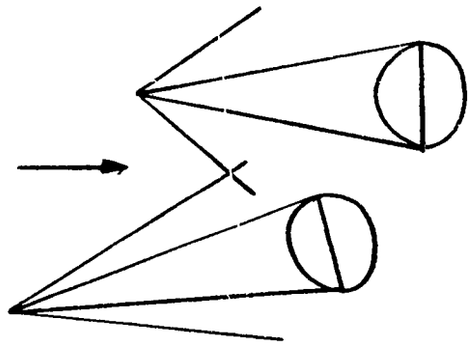

d) Double Conical Shock

FIGURE 2 - THREE DIMENSIONAL SUPERSONIC INLET FLOW ELEMENTS

IV

TWO-DIMENSIONAL AND AXISYMMETRIC SUPERSONIC INTERNAL FLOW COMPUTER PROGRAM

A. Summary and Introduction

A computer program has been written for the computation of two-dimensional and axisymmetric inviscid supersonic internal flows for configurations typical of supersonic and hypersonic inlets. The program is designed for use either for the design and analysis of completely two-dimensional or axisymmetric inlets, or as part of the design effort of a three-dimensional inlet as described in Section III. The program is written in Fortran IV for use on the IBM 7094 and the CDC 6600 high speed digital computers.

The overall computer program can be summarized as follows:

General - Calculation of complete inviscid two-dimensional and axisymmetric supersonic internal flow fields.

Input - Uniform or non-uniform entry conditions for entropy, total enthalpy, pressure, Mach number and flow direction.

Capabilities

- Intersection and reflections of waves of same and opposite families - no limit to number.
- Formation of shocks at compression corners.
- Formation of shocks by coalesence of waves from smooth walls.
- Formation of contact discontinuities.
- Reflection of waves from walls.
- Perfect gas.

Output - Fluid mechanic and thermodynamic parameters, wave locations and contact discontinuity location at each point of the characteristic mesh.

A complete detailed description of this computer program is given in this section. Part B describes the types of flows considered and summarizes the assumptions and simplifications in the analysis and computer program. In Part C the Euler equations of motion are presented and non-dimensionalized. In addition, the special forms of the governing equations are given here for characteristic, oblique shock, and Prandtl Meyer expansion computations. Part D describes the manner in which the computation is performed and gives outlines of the various types of computations. Appendix I gives most of the information required by the user of the program. In Appendix III some sample calculations are presented.

A person who wishes to use the program with a minimum amount of effort should skim Part B and Part D. He should carefully read, in order, Part C-a and Appendices I-III.

B. Outline of the Program

a) Type of Flows Considered

The program computes internal flows typical of supersonic and hypersonic inlets. Included in the flow field computation are weak shocks of both families, their formation at sharp corners and by the coalesence of characteristics (envelope shocks), the intersection of shocks of the same and opposite families, the reflection of shocks on the inlet walls, the intersection of weak shocks and slip streams, and centered corner expansions. The gas is considered to be an inviscid perfect gas of constant ratio of specific heats. Since the method of characteristics is used to perform the calculation, the flow must remain supersonic throughout. Strong shocks are not considered.

b) General Comments - Approximations and Simplifications

A schematic representation of a typical inlet is given in Figure 3. The flow impinges on the inlet at some specified angle of attack. There may be an expansion, a shock, or neither, at the leading edge of the lower wall and at the cowl. Due to smooth or abrupt compressions along the two walls, shocks may form. In addition, expansion waves may be generated by smooth or sharp expansions of the walls. The shocks and expansions will then interact in complicated ways.

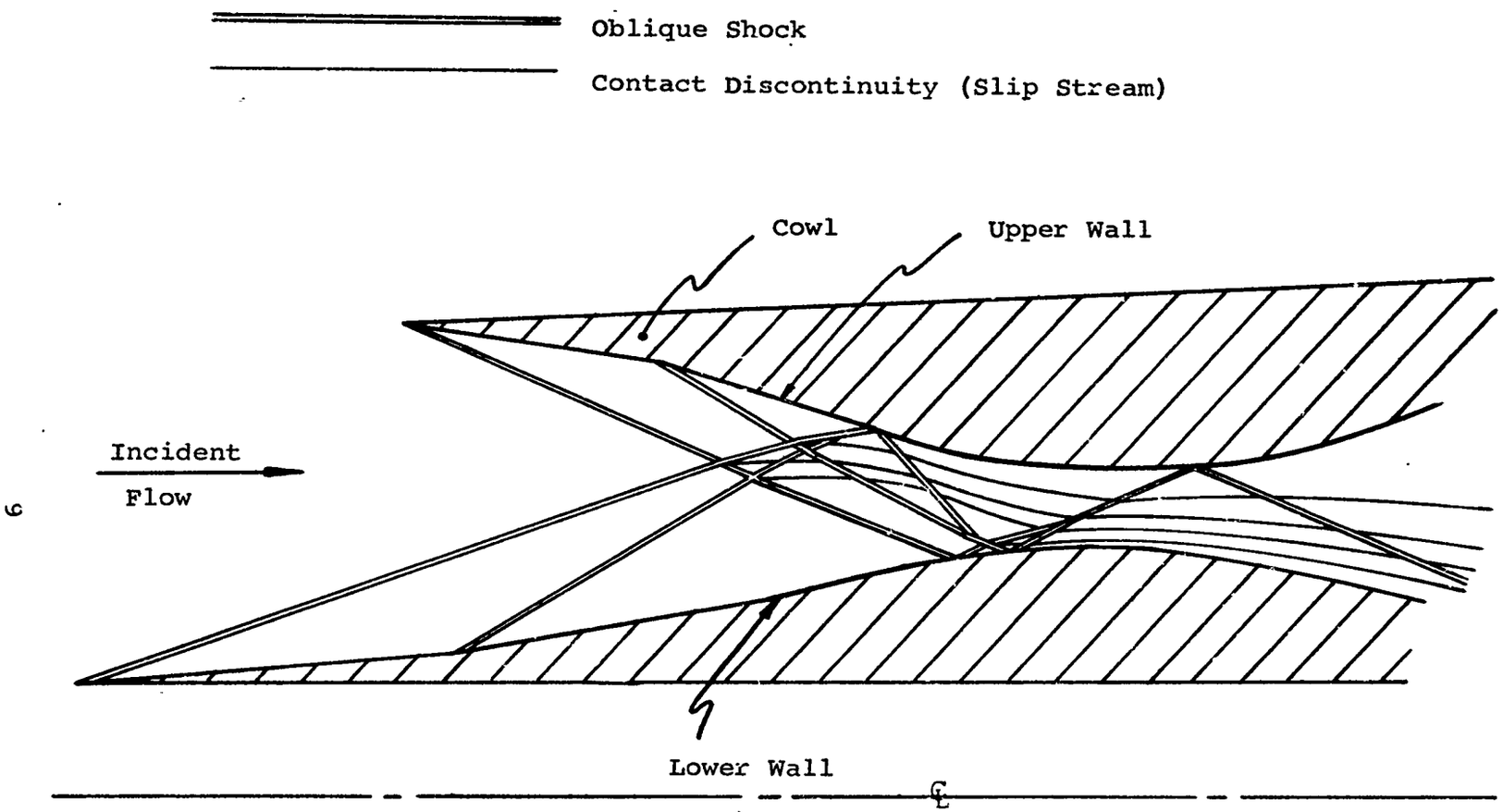

FIGURE 3 - TYPICAL INLET CONFIGURATION (AXISYMMETRIC)

Because of storage and time considerations and the desire to keep the program as simple as possible while retaining sufficient accuracy, various assumptions and simplifications have been made. These are outlined here with their justification.

1. Intersection of Two Weak Shocks of the Same Family

In general, such an intersection will result in the two shocks continuing as either two shocks and a contact discontinuity or as one shock, an expansion fan, and a contact discontinuity (Figure 4). However, in cases of interest here the second shock or expansion fan ($\overline{OE}$ of Figure 4) and the contact disconuity ($\overline{OD}$) usually have a much smaller effect on the flow field than does the primary shock ($\overline{OC}$). Hence, in the program, two shocks of the same family intersecting are continued as only one shock of that family.

2. Intersection of Two Shocks of Opposite Families

When two weak shocks of opposite families intersect they will in general continue as two shocks of opposite families and a contact discontinuity (Figure 5). In the program such an intersection is treated with no simplifications.

3. Intersection of a Weak Shock and a Contact Discontinuity

Ordinarily such an intersection will continue as a shock, a centered expansion, and a contact discontinuity (Figure 6). Presently, the contact discontinuity is dropped when it intersects an oblique shock.

4. Formation of Attached Oblique Shocks By Discontinuous Compression

This is done in a straightforward fashion (Figure 7) with no simplifying assumptions.

5. Reflection of Oblique Shocks from Walls

This is done in a staightforward fashion, the shock being reflected with strength such that the reflected shock has a turning angle which is minus that of the incident shock. (Figure 8).

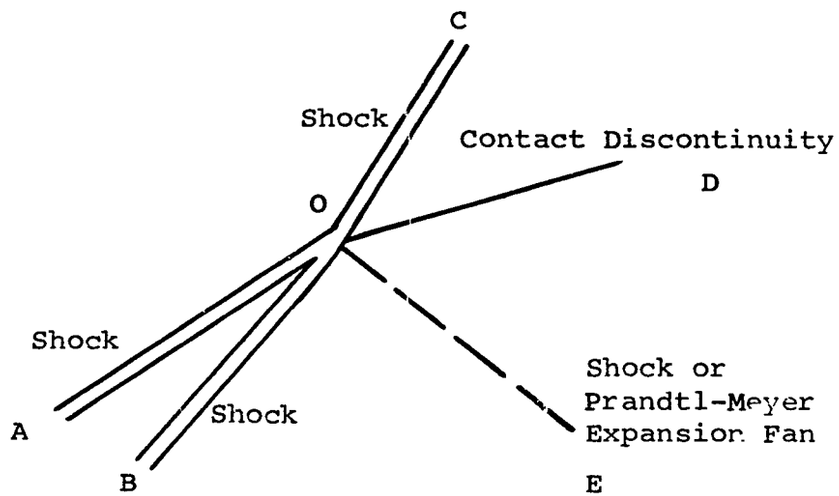

FIGURE 4 - INTERSECTION OF TWO SHOCKS OF THE SAME FAMILY

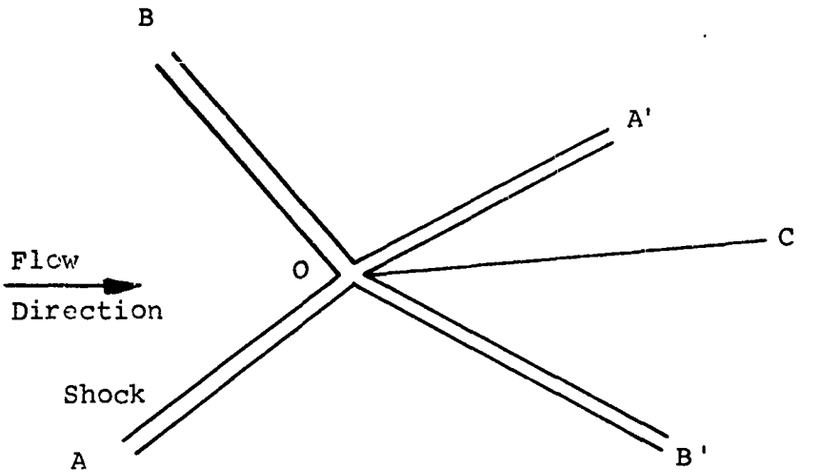

FIGURE 5 - INTERSECTION OF TWO SHOCKS OF OPPOSITE FAMILIES

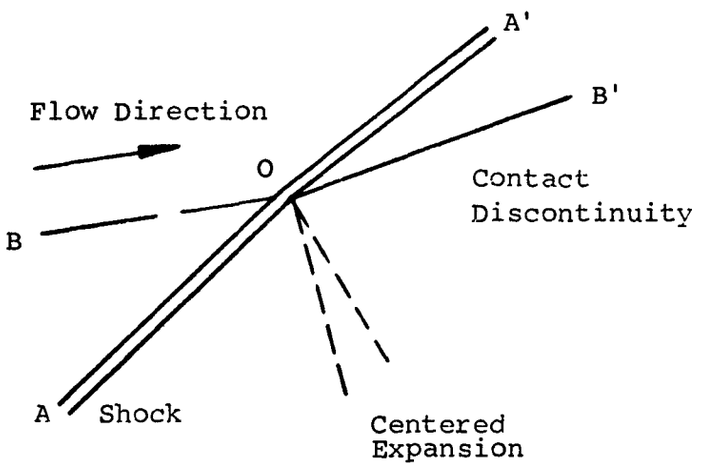

FIGURE 6 - INTERSECTION OF AN OBLIQUE SHOCK
AND A CONTACT DISCONTINUITY

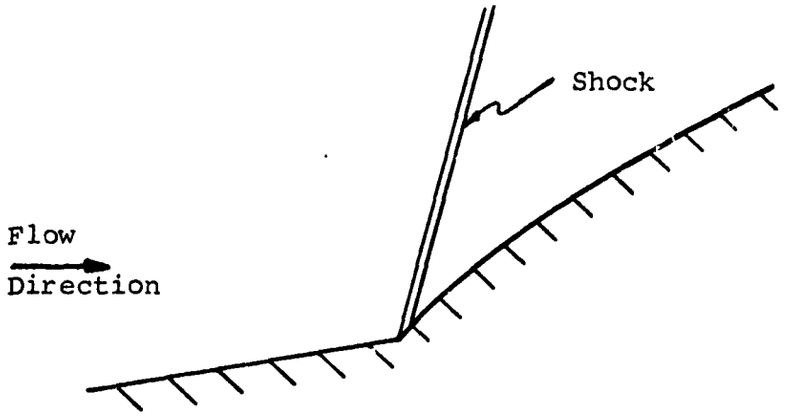

FIGURE 7 - FORMATION OF ATTACHED OBLIQUE SHOCKS BY DISCONTINUOUS COMPRESSIONS

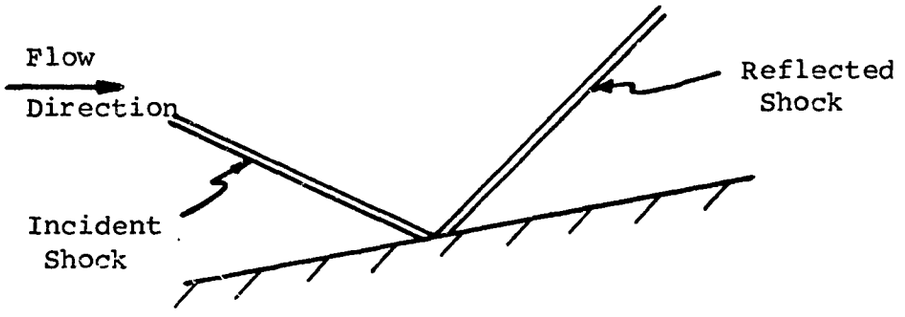

FIGURE 8 - REFLECTION OF AN OBLIQUE SHOCK FROM A WALL

6. Formation of Detached Oblique Shocks By Coalescence of Characteristics

After each point of the characteristic mesh has been computed, tests are made to detect the crossing of characteristics of the same family, indicating the formation of an oblique shock. When such a crossing occurs, a shock is entered in the flow field at that point and its subsequent development is followed. (Figure 9)

7. Centered Expansions Due to Discontinuous Expansion Corners

These are performed by dividing the turning angle of the corner into a finite number of segments and then making regular characteristic computations. (Figure 10)

8. Reflection of an Oblique Shock from the Axis of Symmetry

In the case of axisymmetric flow, the possible flow configurations arising when an oblique shock reflects on the axis of symmetry, are several and complicated. There is no provision in the program to treat this problem. One can expect the program to usually blow up as an oblique shock approaches the symmetry axis. However, it may be that the shock will reflect, as from a wall, away from the symmetry axis.

9. Compression Corner on the Symmetry Axis in Axisymmetric Flow

The only compression corner allowed on the symmetry axis in axisymmetric flow is at the leading edge of the lower wall. In addition, the initial data line must go through the leading edge of the lower wall. (See Part D-a)

10. Viscous Effects

At present there is no consideration of viscous effects in the program.

C. Analysis

a) Non-Dimensionalization and General Equations of Motion

The dimensional Euler equations of motion for the steady, inviscid, nonisentropic flow of a perfect gas of constant specific heat ratio, γ, are

continuity $$(\bar{\rho}\,\bar{y}^{j}\,\bar{u})_{\bar{x}} + (\bar{\rho}\,\bar{y}^{j}\,\bar{v})_{\bar{y}} = 0 \qquad (1)$$

momentum $$\bar{\rho}\bar{u}\bar{u}_{\bar{x}} + \bar{\rho}\bar{v}\bar{u}_{\bar{y}} + \bar{p}_{\bar{x}} = 0 \qquad (2a)$$

$$\bar{\rho}\bar{u}\bar{v}_{\bar{x}} + \bar{\rho}\bar{v}\bar{v}_{\bar{y}} + \bar{p}_{\bar{y}} = 0 \qquad (2b)$$

energy $$\bar{u}\bar{s}_{\bar{x}} + \bar{v}\bar{s}_{\bar{y}} = 0 \qquad (3)$$

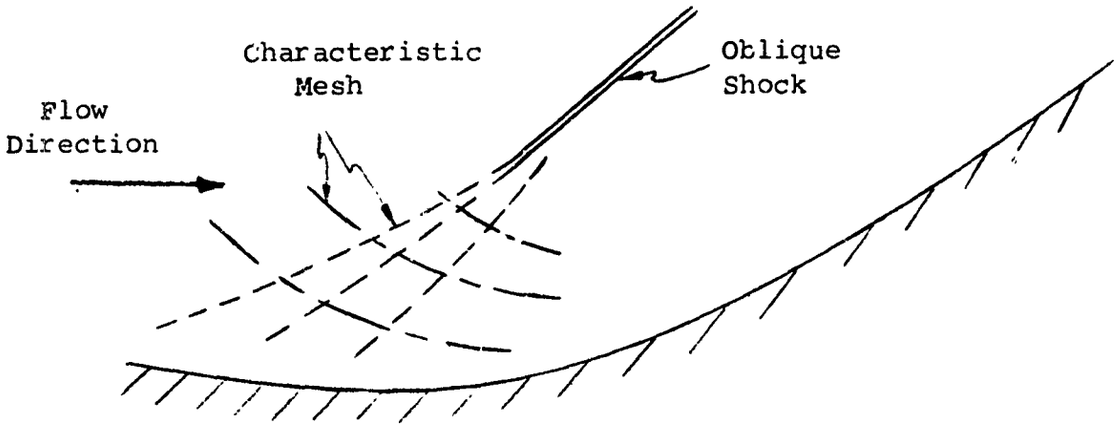

FIGURE 9 - FORMATION OF A DETACHED OBLIQUE SHOCK
BY COALESCENCE OF COMPRESSION WAVES

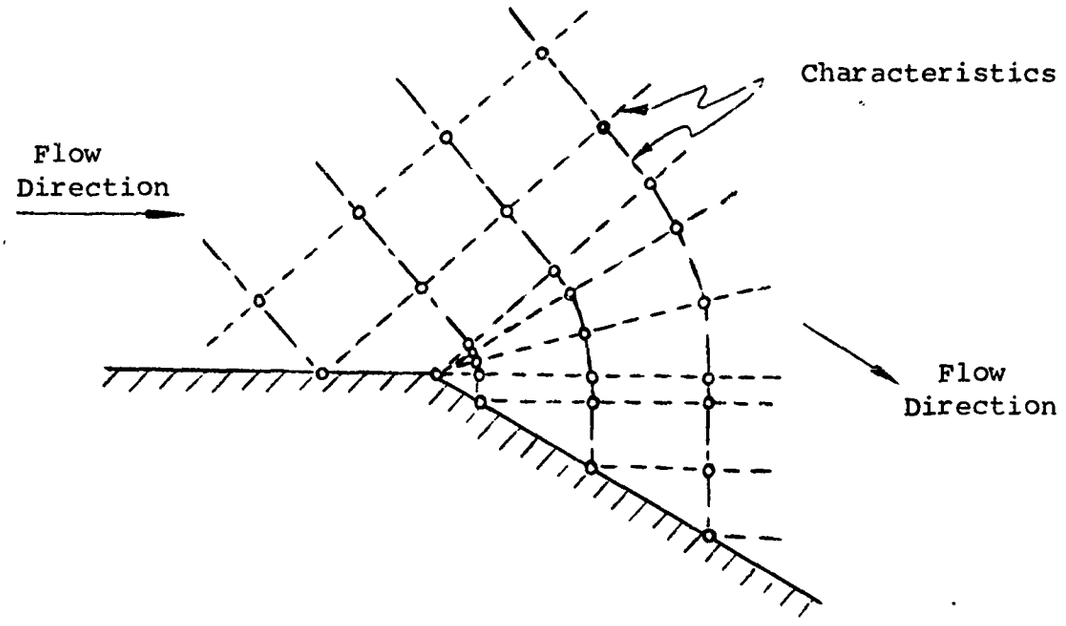

FIGURE 10 - CENTERED EXPANSIONS DUE TO
DISCONTINUOUS EXPANSION CORNERS

where x and y are axes of a right handed cartesian frame (cylindrical frame) with velocity components u and v respectively. The x axis is positive in the general direction of the incident flow. j=0 for two dimensional flow and j=1 for axisymmetrical flow, ρ is the density, p the pressure, S the entropy, and the bars indicate dimensional quantities. Now we divide all pressures by reference pressure $\bar{p}_o$, densities by $\bar{\rho}_o$, temperatures by $\bar{T}_o$, lengths by $\bar{l}_o$, velocities by $\sqrt{\bar{p}_o/\bar{\rho}_o} = \sqrt{\bar{R}\,\bar{T}_o}$ where $\bar{R}$ is the gas constant and $\bar{p}_o = \bar{\rho}_o \bar{R}\bar{T}_o$, and we subtract $\bar{S}_o$ from all entropies and divide the difference by c_v. Then, in non-dimensional quantities p, ρ, u, v, x, y, S, the equations are, (w , $\bar{\ }_o$, $\rho = \bar{\rho}/\rho_o$, $S = (\bar{S}-\bar{S}_\infty)/c_v$, etc.

$$(\rho u y^j)_x + (\rho v y^j)_y = 0 \tag{4}$$

$$\rho u u_x + \rho v u_y + p_x = 0 \tag{5a}$$

$$\rho u v_x + \rho v v_y + p_y = 0 \tag{5b}$$

$$u S_x + v S_y = 0 \tag{6}$$

where

$$S = \ln(p) - \gamma \ln(\rho) \tag{7}$$

The user of this program is free to pick any reference length, $\bar{l}_o$, he chooses. If the incident flow is uniform and the simplified input is used (see Appendix I), the reference pressure and temperature are chosen to be the free stream (i.e. incident) static pressure and temperature. The non-dimensional specific static enthalpy is given by

$$h = \frac{\gamma}{\gamma-1}\frac{p}{\rho} \tag{8}$$

and the specific total enthalpy by

$$H = h + \frac{u^2+v^2}{2} = \frac{a^2}{\gamma-1} + \frac{q^2}{2} \tag{9}$$

where q ($=\sqrt{u^2 + v^2}$) is the modulus of the velocity and a^2 ($=\gamma p/\rho$) is the square of the speed of sound.

Since the flow is inviscid and steady, H and S are constant along a streamline. When there are shocks, the entropy, S, suffers a jump increase.

For completeness, the remaining parts of this section will present well known special forms of the governing equations to be used when we make certain computations, e.g., characteristic computations. All variables in the equations are non-dimensional. Those readers wishing more detailed explanations of the mathematical character of supersonic, inviscid, perfect gas flows should look in any standard text book on gas dynamics, e.g., References 7,8,9.

b) Characteristic Equations

Along characteristic, or Mach, lines, in the absence of shock waves, the Euler equations can be combined so that we have only total derivatives of certain quantities in the direction of the characteristic line. It is well known that for our cases the characteristic directions are given by

$$\lambda^{I} = \frac{dy}{dx} = \frac{uv - a\sqrt{u^2 + v^2 - a^2}}{u^2 - a^2} \qquad (10a)$$

$$\lambda^{II} = \frac{dy}{dx} = \frac{uv + a\sqrt{u^2 + v^2 - a^2}}{u^2 - a^2} \qquad (10b)$$

$$\lambda^{III} = \frac{dy}{dx} = \frac{v}{u} = \tau \qquad (10c)$$

Henceforth, λ^{I} will be referred to as a down-running characteristic and λ^{II} as an up-running characteristic. Along $\lambda^{I,II}$ the Euler equations can be combined to give

$$\frac{d\tau}{dx} \pm b\,\frac{dp}{dx} = \left[\frac{(\tau - \lambda^{I,II})\,\tau}{y}\right] \cdot j \qquad (11)$$

where

$b = \sqrt{M^2 - 1}\ /\rho u^2$ and M (=q/A) is the Mach number.

Along λ^{III}, the streamline, we have

$$dS = dH = 0 \text{ (no snocks)} \qquad (12)$$

We can write equations (11a) in differential form as:

$$\Delta\tau - b\Delta p = \left[\frac{(\tau - \lambda^{I})\ \tau}{y}\right] .j\ \Delta x = G^{I}\ \Delta x \cdot j \qquad (13a)$$

along a down running characteristic and

$$\Delta\tau + b\Delta p = \left[\frac{(\tau - \lambda^{II})\ \tau}{y}\right] \Delta x \cdot j = G^{II}\ \Delta x \cdot j \qquad (13b)$$

along an up running characteristic.

c) Oblique Shocks - Rankine Hugoniot Equations

Let subscript 1 refer to the conditions in front of (upstream) the shock and subscript 2 refer to the conditions behind (downstream) the shock and let σ be the acute angle the incident flow makes with the shock wave.

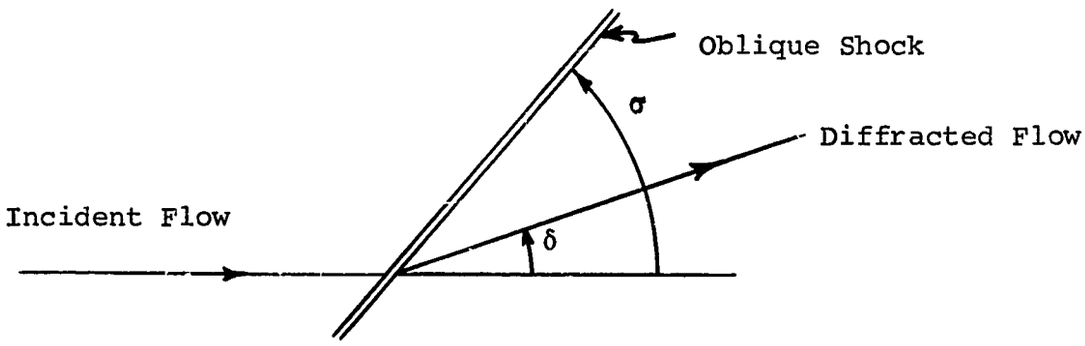

δ is the turning angle of the flow. The Rankine Hugoniot equations are

$$\frac{p_2}{p_1} = \frac{2\gamma M_1^2 \sin^2 \sigma - (\gamma-1)}{\gamma + 1} \tag{14a}$$

$$\frac{\rho_2}{\rho_1} = \frac{(\gamma+1)\ p_2 + (\gamma-1)\ p_1}{(\gamma+1)\ p_1 + (\gamma-1)\ p_2} \tag{14b}$$

$$\tan^2 \delta = \tan \frac{(\rho_2/\rho_1 - 1)}{(\tan^2 \sigma + \rho_2/\rho_1)} \tag{14c}$$

$$M_2^2 = \frac{(\gamma-1)\ M_1^2 \sin^2 \sigma + 2}{\sin^2 (\sigma-\delta)\ [2\gamma M_1^2 \sin^2 \sigma - (\gamma-1)]} \tag{14d}$$

$$S_2 = S_1 + \ln \left[\frac{2\gamma M_1^2 \sin^2 \sigma - (\gamma-1)}{\gamma + 1}\right] - \gamma \ln \left[\frac{(\gamma+1)\ M_1^2 \sin^2 \sigma}{(\gamma-1)\ M_1^2 \sin^2 \sigma + 2}\right] \tag{14e}$$

$$H_2 = H_1 \tag{14f}$$

$$\tan^{-1} (\tau_2) = \tan^{-1} (\tau_1) + \delta \tag{14g}$$

$$c_2 = \sqrt{2 \left(H_2 - \frac{\gamma}{\gamma-1} \frac{p_2}{\rho_2}\right)} \tag{14h}$$

d) Prandtl-Meyer Expansion

The Prandtl-Meyer relation is

$$\nu = \sqrt{\frac{\gamma+1}{\gamma-1}} \tan^{-1} \sqrt{\frac{\gamma-1}{\gamma+1} (M^2-1)} - \tan^{-1} \sqrt{M^2-1} \tag{15}$$

where ν is the angle turned from Mach = 1 to reach the Mach number

M. If we have a corner with other than sonic velocity just prior to the corner, then denoting the conditions just prior to the expansion by subscript 1 and just after the expansion by subscript 2, we have

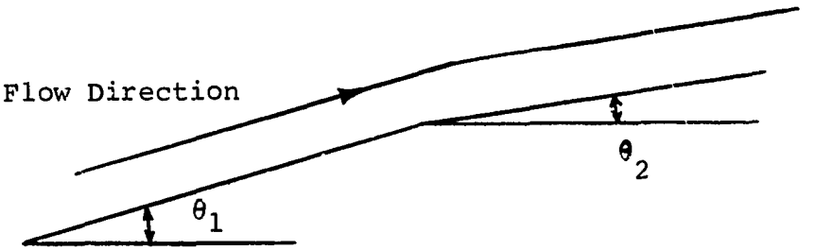

$$\theta_1 - \theta_2 = \nu_2 - \nu_1 \tag{16a}$$

$$\frac{p_2}{p_1} = \frac{\left(1 + \frac{\gamma-1}{2} M_1^2\right)^{\frac{\gamma}{\gamma-1}}}{\left(1 + \frac{\gamma-1}{2} M_2^2\right)^{\frac{\gamma}{\gamma-1}}} \tag{16b}$$

$$\frac{\rho_2}{\rho_1} = \frac{\left(1 + \frac{\gamma-1}{2} M_1^2\right)^{\frac{1}{\gamma-1}}}{\left(1 + \frac{\gamma-1}{2} M_2^2\right)^{\frac{1}{\gamma-1}}} \tag{16c}$$

$$H_2 = H_1 \tag{16d}$$

$$S_2 = S_1 \tag{16e}$$

$$\tau_2 = \tan \theta_2 \tag{16f}$$

$$q_2 = \sqrt{\gamma \frac{p_2}{\rho_2}}\, M_2 \tag{16g}$$

D. The Program - General Outline

a) Initial Conditions - Boundary Conditions - Coordinate Systems

As indicated previously, the purpose of the program is to compute supersonic and hypersonic inviscid inlet flows. The coordinate system and body geometry are represented schematically in Figure 11. The x axis is aligned in the general direction of the free stream flow (it is the axis of symmetry in the case of axisymmetric flow) but need not be exactly parallel to the incident flow. It is positive in the general direction of the incident flow. The y axis is normal to the x axis and is positive in the direction determined by rotating the positive x axis 90° counterclockwise. It corresponds to the radial axis in a cylindrical (x,r,θ) frame in the case of axisymmetric flow. It is assumed that the tips of both the cowl and the lower wall are pointed and of small enough included angle relative to the incident flow so that any tip shocks are attached and there are no regions of subsonic flow. Furthermore, for axisymmetric flow with a lower leading edge on the axis of symmetry, it is assumed that, in the coordinate system used, the x coordinate of the tip of the cowl is greater than or equal to the x coordinate of the tip of the lower wall.

The line 'parallel' to the y axis through the tip of the lower wall, $\overline{AA}'$, is considered to be the "data line" of the incident flow (see Appendix I).

The geometry of the upper and lower walls must be specified.

b) Order of Progression of The Computation

1. In The Absence of Shocks

The computation proceeds along down running characteristics issuing either from points on the initial data line, ($\overline{AA}'$, Figure 11) or from the upper wall. Referring to Figure 12, let us follow the outline of a typical computation, forgetting for the moment the possibility of shocks or centered expansions. Mesh points are indicated by circles and the flow is completely specified initially along the initial data line, $\overline{AA}'$. The flow field at point C can be computed for the known conditions at points A and B (see Part D-c-1), where C is the point of intersection of the up running characteristic from A and the down running characteristic from B. The down running characteristic

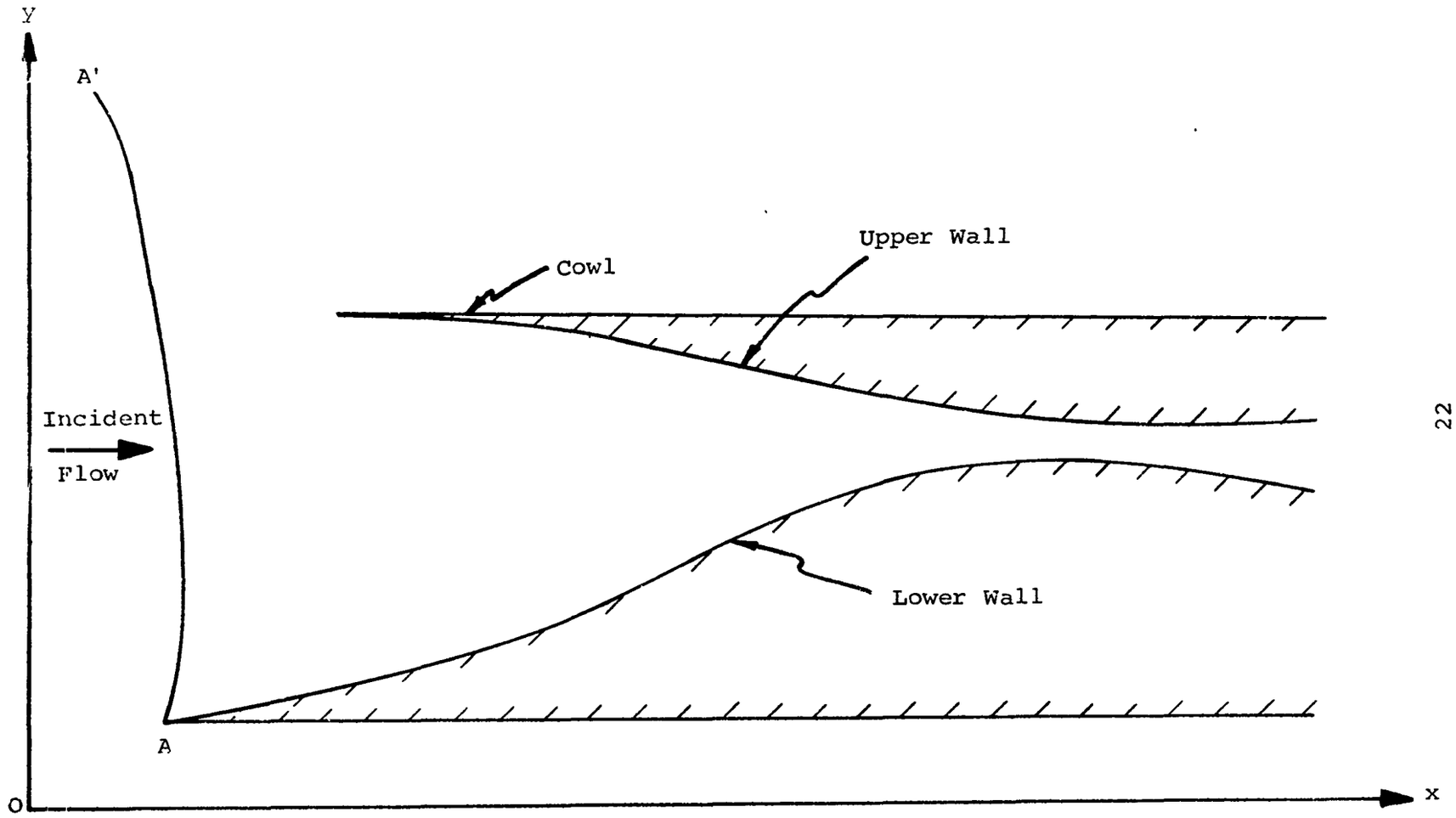

FIGURE 11 - SCHEMATIC OF COORDINATE SYSTEM AND BODY GEOMETRY

from C intersects the wall at D, and the flow conditions at D can then be obtained from the known conditions at C and the specified wall slope at D. (See D-c-2)

The computation proceeds in this manner working along down running characteristics from the initial data line to the bottom wall. Eventually, however, one of the down running characteristics will cross the cowl as illustrated in Figure 13a. C, the point formed by the intersection of the characteristics from D and B, is computed as an ordinary point. Then the conditions at E, the tip of the cowl, are obtained by interpolation between points A, B, C, and D. The computation is continued by working along the down running characteristic issuing from E (forget for the moment the possibility of a shock at E), Figure 13b. When that characteristic is completed, the intersection, with the upper wall of the up running characteristic $\overline{FG}$, from point F, can be determined. The flow conditions at G can then be computed using the known conditions at F and the specified wall slope at G. Then the computation can be continued in a normal fashion working along the down running characteristic issuing from G.

In the absence of shocks and centered corner expansions, the entire inlet flow field could be computed in this fashion. In actual fact however, there will often be not only one, but several oblique shocks (of either or both families) which complicate matters somewhat.

2. In the Presence of Attached Shocks

Although up and down running characteristics have equal stature in the mathematical theory of supersonic inviscid flow, the situation is somewhat different in the program. That is to say, since the computation proceeds along down running characteristics, we have implicitly created a favoritism between the characteristics of opposite families. This difference is important when shocks and contact discontinuities are present.

This unequal treatment of characteristics of different families does not affect the basic order of the computation when up running shocks are present. (See Figure 14)

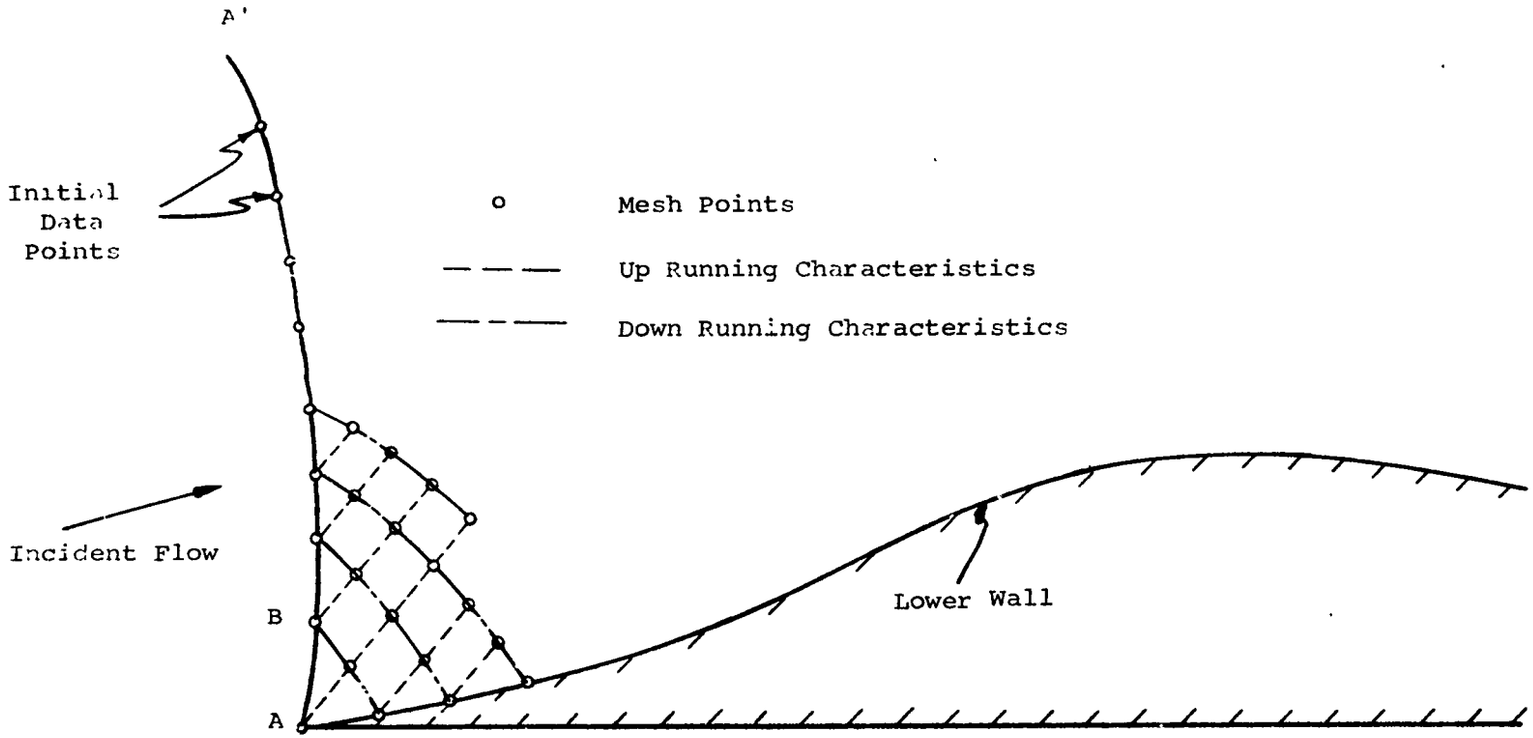

FIGURE 12 - SCHEMATIC OF COMPUTATION PROCEDURE

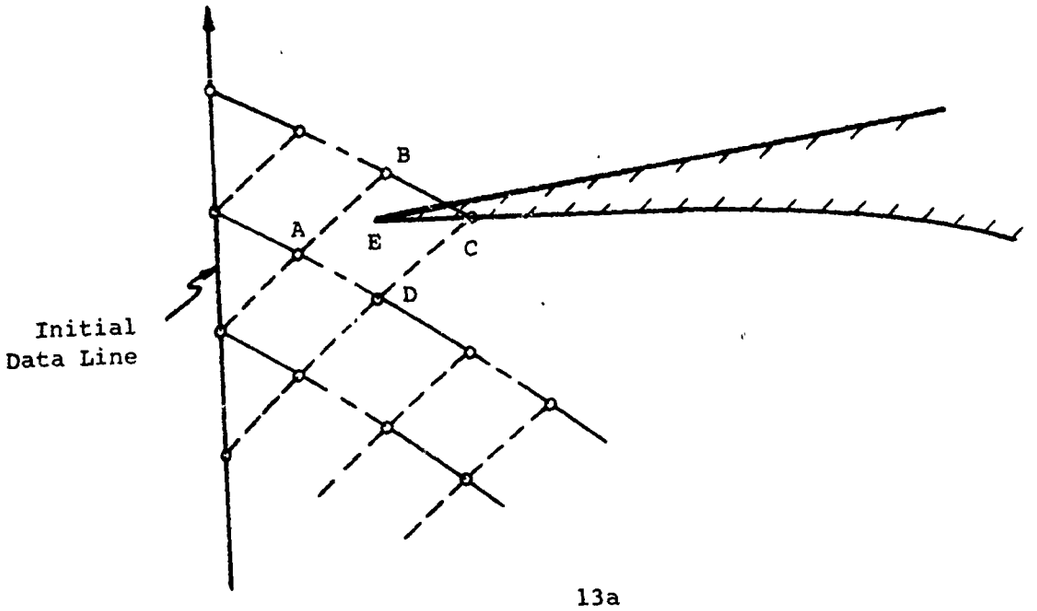

13a

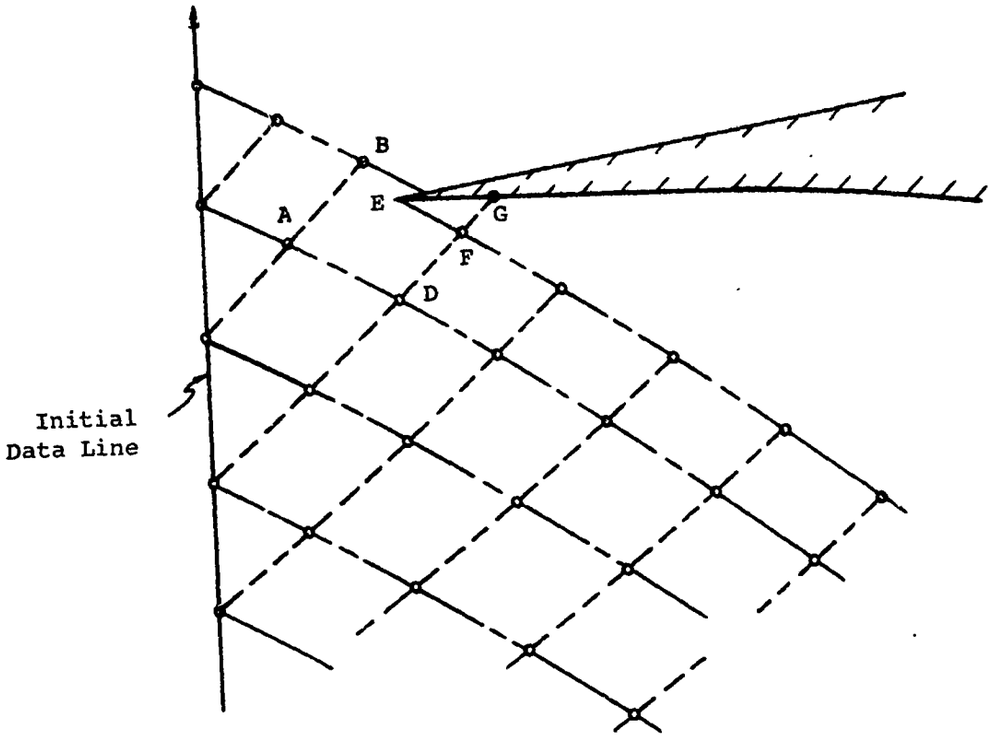

13b

FIGURE 13 - MODIFICATION OF CHARACTERISTIC MESH AT THE COWL

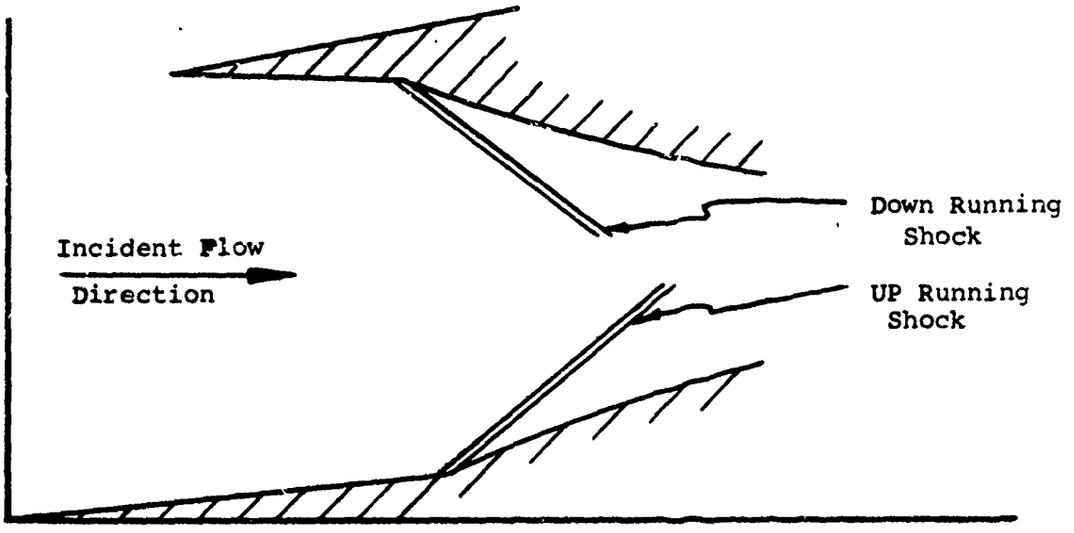

FIGURE 14 - SKETCH OF DOWN RUNNING AND UP RUNNING SHOCKS

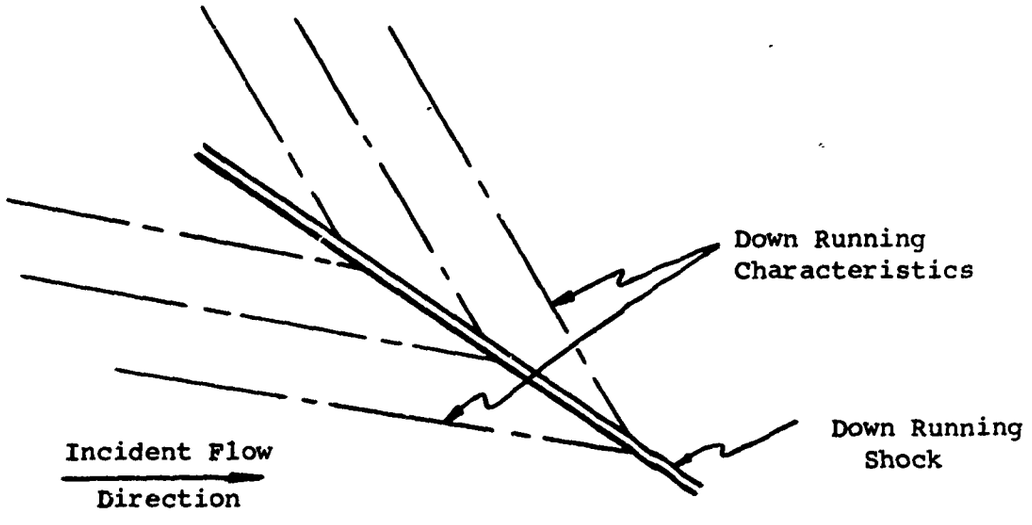

FIGURE 15 - PATTERN OF DOWN RUNNING CHARACTERISTICS
NEAR DOWN RUNNING SHOCK

If there are such shocks, the intersection of each shock with each down running characteristic defines a mesh point (actually two, one in front of and one behind the shock, see Part D-e-1). The only complication in the program is that, as it proceeds along a down running characteristic, the program must be instructed to look for the intersection of the down running characteristic with any up running shocks from the previous down running characteristics. When such an intersection occurs, a special computation must be made.

However, the situation is not quite so simple when there are down running shocks. For, the down running characteristics down stream of the shock terminate at the shock (see Figure 15), i.e. characteristics terminate at a shock of the same family. Thus, as the program proceeds along a down running characteristic, it must make a special provision upon encountering a down running shock since the down running characteristic does not continue on the other side (up stream) of the shock.

The proceedure that is followed in such cases is illustrated in Figure 16 for the case of a compression corner on the upper wall. When such a corner is detected, the conditions upstream of the shock are obtained by a regular characteristic wall computation between the corner and A, the data at A being computed by interpolation on the previous down running characteristic. The program then computes the down running characteristic, $\overline{BC}$, that would issue from B if no compressive corner were present. All the data computed on characteristics upstream of and including $\overline{BC}$ is referred to as region I and is stored for later use by the program.

With the specified turning angle and the conditions in front of the shock at B, the shock angle and the conditions behind the shock can be determined (see Part C-c). The shock will always have a slope less than the local slope of the down running characteristics in region I, hence, the shock will always be in region I. The intersection, E, of the shock and the next up running characteristic of region I is determined and the conditions upstream of the shock are determined by interpolation between points, O and P. In region I+1, the region behind the shock, $\overline{FE}$ is the down running characteristic from the upper wall to the point E. It is assumed that the conditions at F are equal to the conditions behind the shock at B. Then, the flow behind the shock and the shock slope at E can be determined by simultaneously solving the compatibility equation (Eq. 13) along $\overline{FE}$ and the Rankine-Hugoniot equations across the shock.

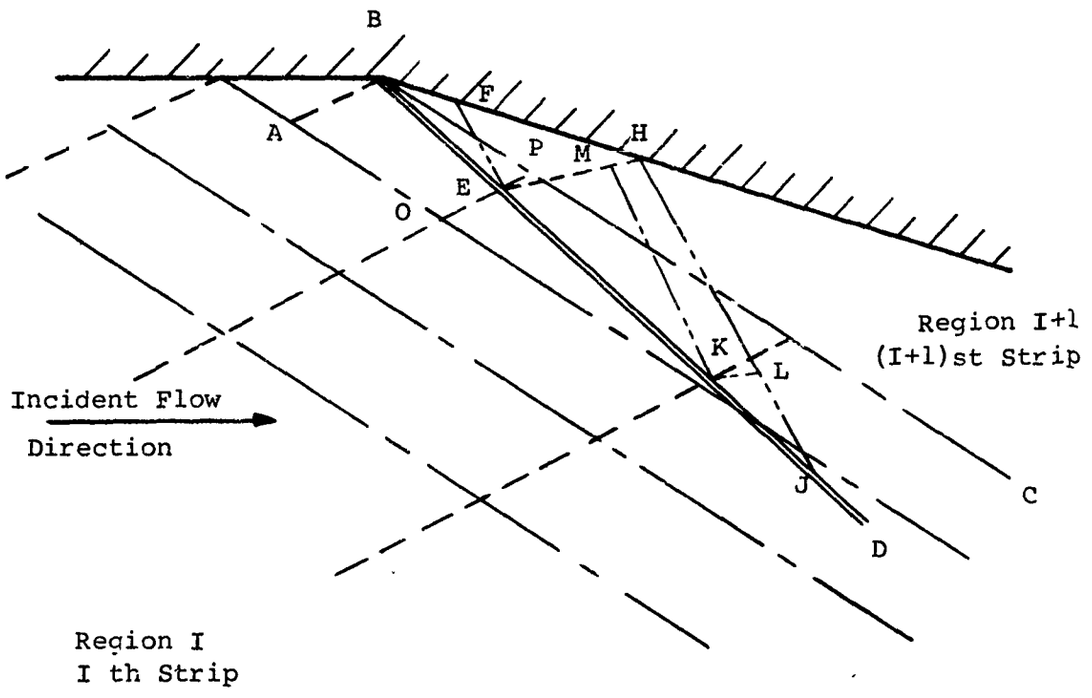

Down Running Characteristic (Region I)

Up Running Characteristic (Region I)

Down Running Characteristic (Region II)

Up Running Characteristic (Region II)

FIGURE 16 - CHARACTERISTIC MESH AT COMPRESSION CORNER ON THE UPPER WALL

With the known conditions behind the shock at E, the intersection, H, of the up running characteristic from E with the upper wall can be determined. The flow field at H can be determined by solving the compatibility equation (13b) along $\overline{EH}$ using the known wall slope at H.

Now we work along the down running characteristic, $\overline{HJ}$, in region I+1. If the shock, $\overline{BD}$, crosses the next up running characteristic of region I at a point K before it intersects $\overline{HJ}$, then the conditions in front of the shock at K are determined by interpolation in the characteristic mesh of region I. By interpolation, the point M, on $\overline{EH}$, whose down running characteristic passes through K, and the data at M are determined. The flow behind the shock at K is determined by simultaneously solving the compatibility equation along $\overline{MK}$ with the Rankine Hugoniot jump conditions across the shock at K.

Then the location and conditions at L are determined by a regular characteristic computation between H and K. This process continues until the down running characteristic, $\overline{HJ}$, intersects the shock, $\overline{BD}$, at a point J. The conditions in front of the shock at J are determined by interpolation as above; the conditions behind by using the compatibility equation along $\overline{LJ}$ and the jump conditions at J.

The result is that the flow field is divided into a number of regions, or strips, the boundaries of which are down running shocks.

3. In the Presence of Detached Shocks

It may happen that shocks are formed by the coalesence of compression waves due to a smooth turning of either of the walls (see Part D-f-2). The formation of up running shocks by such a process in no way affects the progression of the computation on the gross scale now under discussion.

However, if a down running shock is formed by the coalescence of compression waves, we again divide the flow field into two strips as illustrated in Figure 17.

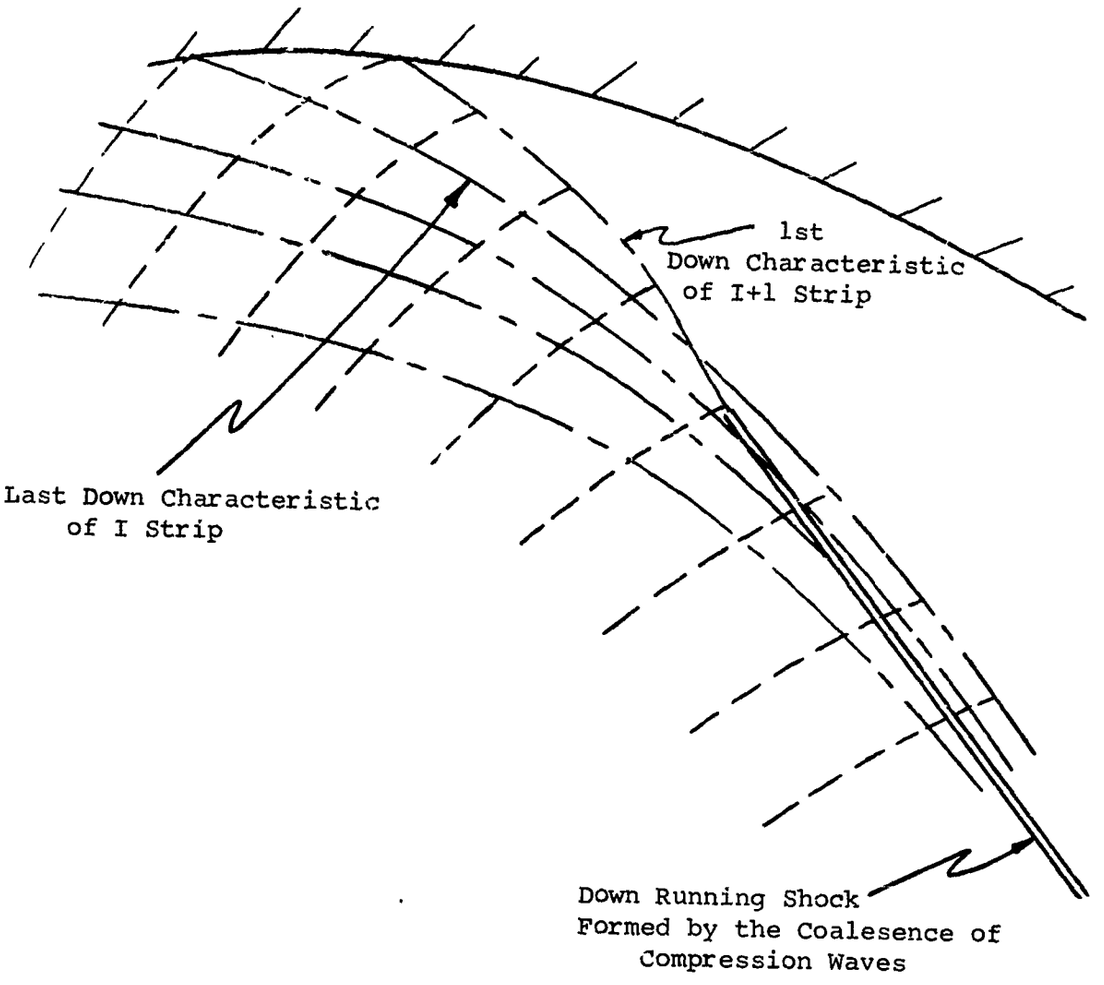

FIGURE 17 - DOWN SHOCK FORMED BY THE COALESENCE OF COMPRESSION WAVES

4. The Presence of Centered Expansions on the upper or lower walls causes no essential change in the progression of the computation (see Part D-d).

c) Computation of Regular Points

Now that we have indicated the gross order of progression of the computer program, we can look into the various specific computations in a little more detail.

1. Interior Flow Field Points

As mentioned in Part I of this section, regular interior points are determined by the intersection of a down running characteristic with the up running characteristic issuing from a mesh point on the previous down running characteristic. This is illustrated in Figure 18 where C is the point to be computed. All of the points, including B, on the (I-1) st down running characteristic have been computed, as have all the points through A on the i th characteristic. Point C is the next point to be computed.

First Equations 13a and 13b are written in finite difference form:

$$(\tau_C - \tau_A) - \bar{b}_{AC} (p_C - p_A) = \bar{G}^{I}_{AC} (x_C - x_A)\, j \qquad (17a)$$

$$(\tau_C - \tau_B) + \bar{b}_{BC} (p_C - p_B) = \bar{G}^{II}_{BC} (x_C - x_B)\, j \qquad (17b)$$

where the barred quantities are averaged quantities on the appropriate characteristic. Equations 17a and 17b are solved simultaneously to give

$$p_C = \frac{\bar{b}_{AC} p_A + b_{BC} p_B - \tau_A + \tau_B - \left[\bar{G}^{I}_{AC} (x_C - x_A) - \bar{G}^{II}_{BC} (x_C - x_B) \right] j}{\bar{b}_{AC} + \bar{b}_{BC}} \qquad (18a)$$

$$\tau_C = \tau_A + \bar{b}_{AC} (p_C - p_A) + \bar{G}^{I}_{AC} (x_C - x_A) j \qquad (18b)$$

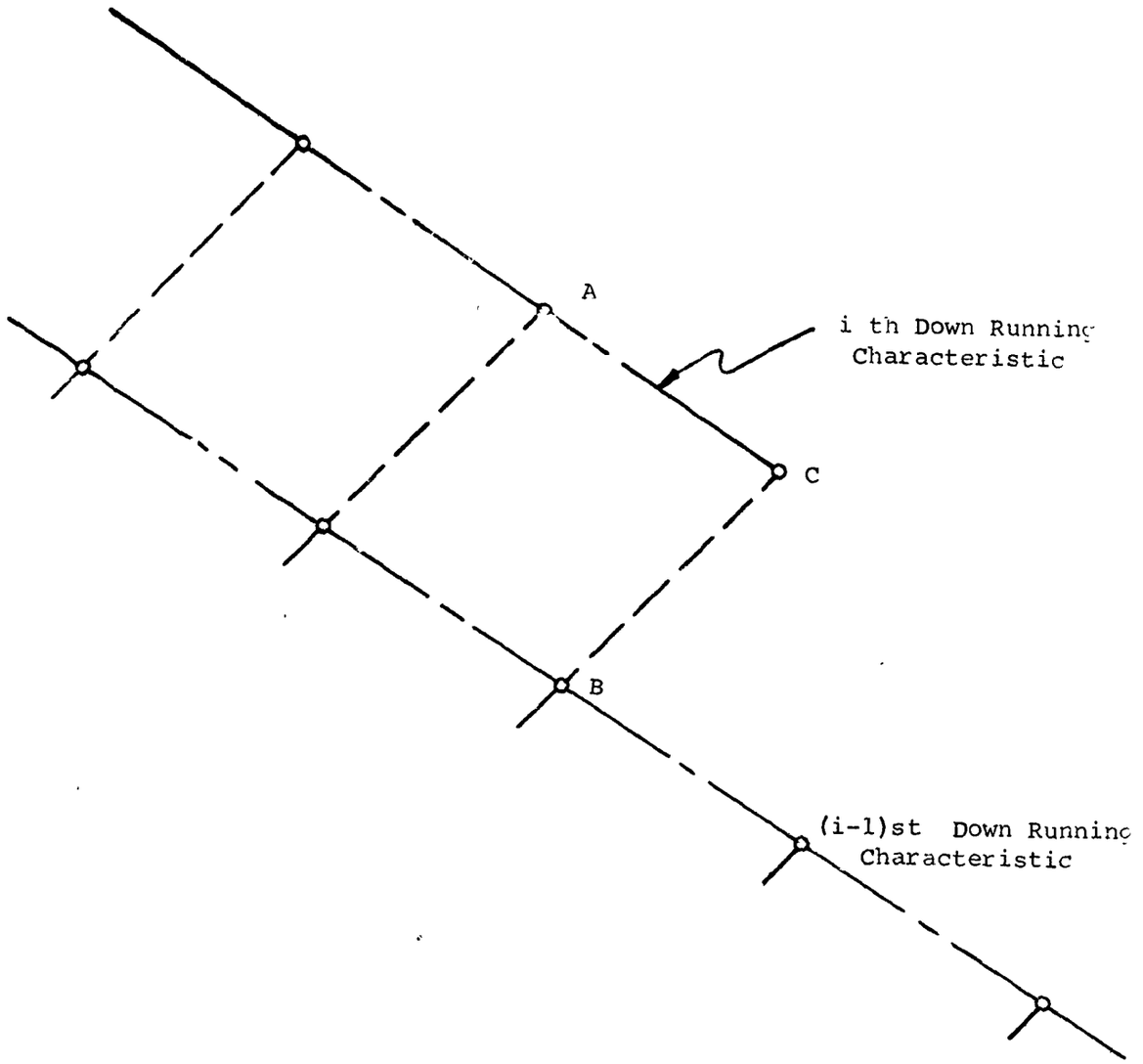

FIGURE 18 - REGULAR INTERIOR POINT COMPUTATION

In addition, we have the following definitions and equations available:

$$S_C = \ln p_c - \gamma \ln \rho_C, \text{ or } \rho_C = e^{\frac{\ln(p_C)-S_C}{\gamma}} \tag{19a}$$

$$H_C = \frac{\gamma}{\gamma-1} p_C/\rho_C + \frac{q_C^2}{2} ; \text{ or } q_c = \sqrt{2\left(H_C - \frac{\gamma}{\gamma-1}\frac{p_C}{\rho_C}\right)} \tag{19b}$$

$$q_c^2 = u_C^2 + v_C^2 ; \text{ or } u_C^2 = \frac{q_C^2}{1+\tau_C^2} \tag{19c}$$

$$\tau_C = \frac{v_C}{u_C} ; \text{ or } v_C = u_C \tau_C \tag{19d}$$

Now, it is fairly common to perform a regular computation in somewhat the following form.

1) Get the location of C by the intersection of characteristics from A and B.

2) Compute p_C and τ_C using (18a) and (18b) where, in the first pass, the averaged quantities are taken as those at A or B, whichever is appropriate.

3) Project the streamline of slope τ_C back from C to intersect the line $\overline{AB}$ connecting A and B (not shown in Figure 18).

4) Since S and H are constant along streamlines (in the absence of shocks) obtain H_C and S_C by linear interpolation along $\overline{AB}$.

5) Use equations 19 to determine u_C, v_C, ρ_C from the known p_C, τ_C, S_C, H_C.

6) Compute the coefficients b_C, G_C^I, G_C^{II}, etc., average the coefficients along each characteristic, and iterate until the characteristic slopes at C do not change within some specified tolerance.

However, if one proceeds in this manner, and if the flow is nonisentropic, he will find that the linear interpolation in step 4 introduces errors that can become quite large (Reference 4). These errors are quite evident when, after computing a number of characteristics, one checks the mass flow, where the error can exceed 40%.

A much better way of proceeding is to set up a mass flow-entropy, enthalpy table. The fact that S and H are constant along streamlines (and that we can compute the change in S through a shock) means that we can set up functions defined pointwise for S and H with mass flow as independent variable. Then we replace steps 4-5 by another process.

4-5 a) guess S_C and H_C, compute ρ_C, u_C, v_C.

b) compute the mass flow through $\overline{AC}$, subtract it from the known mass flow below A to get the mass flow at C.

c) go to the mass flow - S, H table and obtain S_C, H_C

d) compare with the guessed values of S_C and H_C and iterate until convergence.

Then continue with 6) in the indicated manner.

The result is a very accurate computation with the error in the integrated mass flow often less than 1% in the computation of two-dimensional flows. Of course, the mass flow-entropy table must be modified when there are shocks.

The dependence of S and H on mass flow are determined initially from the known conditions on the initial data line.

This technique is used in the present program.

The increment of mass flow across $\overline{AC}$ is given by

$$\overline{\rho q} \sin [\tan^{-1} \bar{\tau} - \tan^{-1} \bar{\lambda}^{I}] \Delta \text{ area} \qquad (20)$$

where the barred quantities are averaged between A and C and Δarea is the area between A and C, given by,

$$\Delta\text{area} = \sqrt{(x_C - x_A)^2 + (y_C - y_A)^2} \quad \text{for 2-dim. flow (j=0)} \quad (21a)$$

$$\Delta\text{area} = \sqrt{1 + \bar{\lambda}^{I^2}}\,(y_A^2 - y_C^2) \quad \text{for axi-sym. flow (j=1)} \quad (21b)$$

2. Boundary Points

Boundary points are computed in the same manner as interior points, except for a few simplifications. First, since in an entirely inviscid flow the boundaries are streamlines, we know a priori what S and H are along the boundary (the case of shocks is explained in Part D-g), and we need not do the mass flow - S, H iteration required at interior points. In addition, $\tau_C = v_C/u_C = dy/dx$ on the boundaries is a specified function of x. To compute a point on the lower wall we use Equation 17a along the down running characteristic to get p_C. To compute a point on the upper wall we use 17b along an up running characteristic. Naturally, averations are made in averaging coefficients when the equations are solved.

3. Centerline Points

When the flow is axisymmetric, it may happen that the lower wall ends at the axis of symmetry and then the lower wall computation must be replaced by a symmetry condition. The only effect this has, in the absence of shocks, is that G^I and G^{II}, which take the indeterminate form 0/0 at y = 0, must be evaluated by L'Hospital's rule.

$$G^{I,II}\Big|_{y=0} = (\tau - \lambda^{I,II})\,\frac{\tau}{y}\Big|_{y=0} = -\lambda^{I,II}\,\frac{d\tau}{dy}\Big|_{y=0} \quad (22)$$

The program requires a cusp at the trailing edge of the lower wall.

There is no provision to compute the reflection of shocks at the axis of symmetry.

d. Centered Expansion on the Boundaries

Everytime we compute the location of an upper or lower boundary point, a test is made to determine whether or not there is a corner between the current point and the last point on that boundary. If a corner has been detected, the next operation is to find out whether or not it is an expansion or a compression corner. The latter is treated in Part D-f.

If it is an expansion corner, the conditions just upstream of the corner are first determined (see Figure 19). Then the total turning angle , $\Delta\theta$, of the flow is determined. This turning angle is divided into a number of increments, n, of size $\delta(\Delta\theta)=\Delta\theta/n$, and the conditions corresponding to the flow which has turned from the state just prior to the corner, say θ, to $\theta'=\theta + m\ \delta\ (\Delta\theta)$, m=1,n, are determined. This is done by determining the change in Mach number to go from θ to $\theta + m\ \delta\ (\Delta\theta)$ from Equation 15). Then the rest of the conditions can be determined by using Equation 16.

If the expansion is on the upper boundary, a new down running characteristic is put in the mesh for each value of m, and the regular upper boundary point computation is bypassed until all of the down running characteristics issuing from the corner have been computed (see Figure 19a).

If the expansion is on the lower wall, a number, n+1, of mesh points is put at the corner and the current down running characteristic is finished by making a series of regular interior point computations as indicated in Figure 19b.

e. Computation of Interior Shock Points

1. Up Running Shock Points

In Figure 20, $\overline{AB}$ is a down running characteristic along which we know everything, including the location and slope of any up running shocks crossing $\overline{AB}$. Such a characteristic shock intersection is designated by two points (H,I of Figure 20) which have the same physical coordinates, one having the properties of the flow just in front of the shock and the other properties just behind the shock. We want to compute $\overline{CD}$, the next down running characteristic.

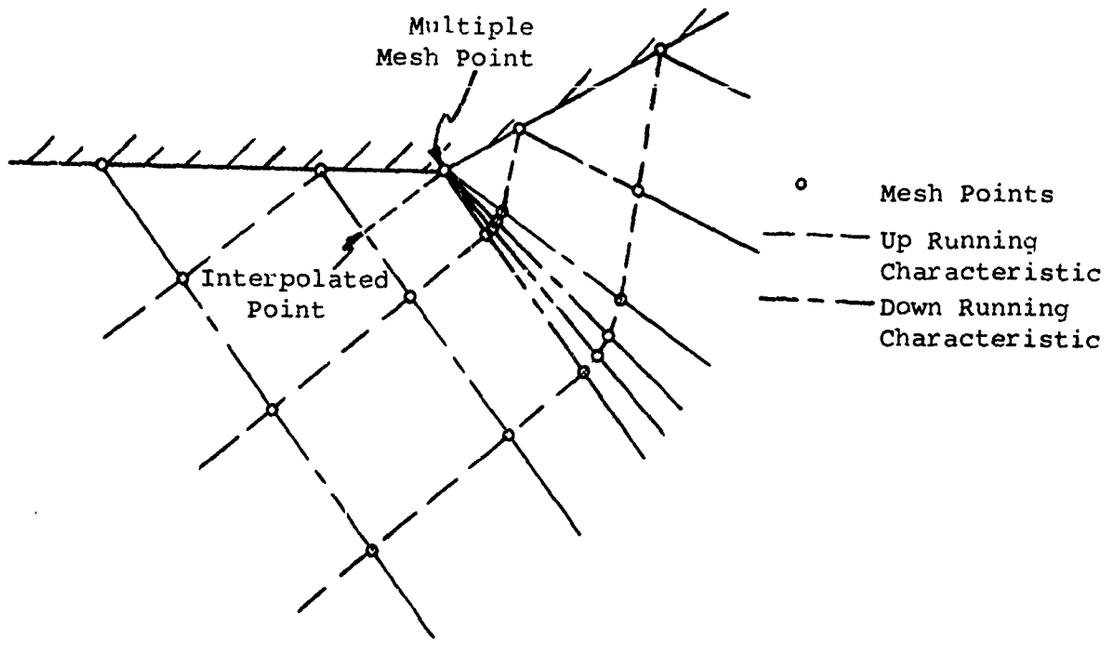

FIGURE 19a - EXPANSION ON UPPER BOUNDARY

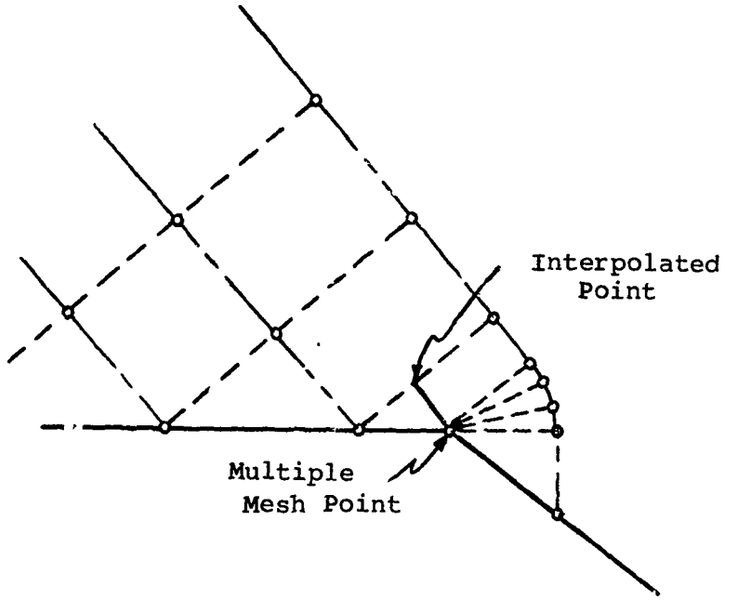

FIGURE 19b - EXPANSION ON LOWER BOUNDARY

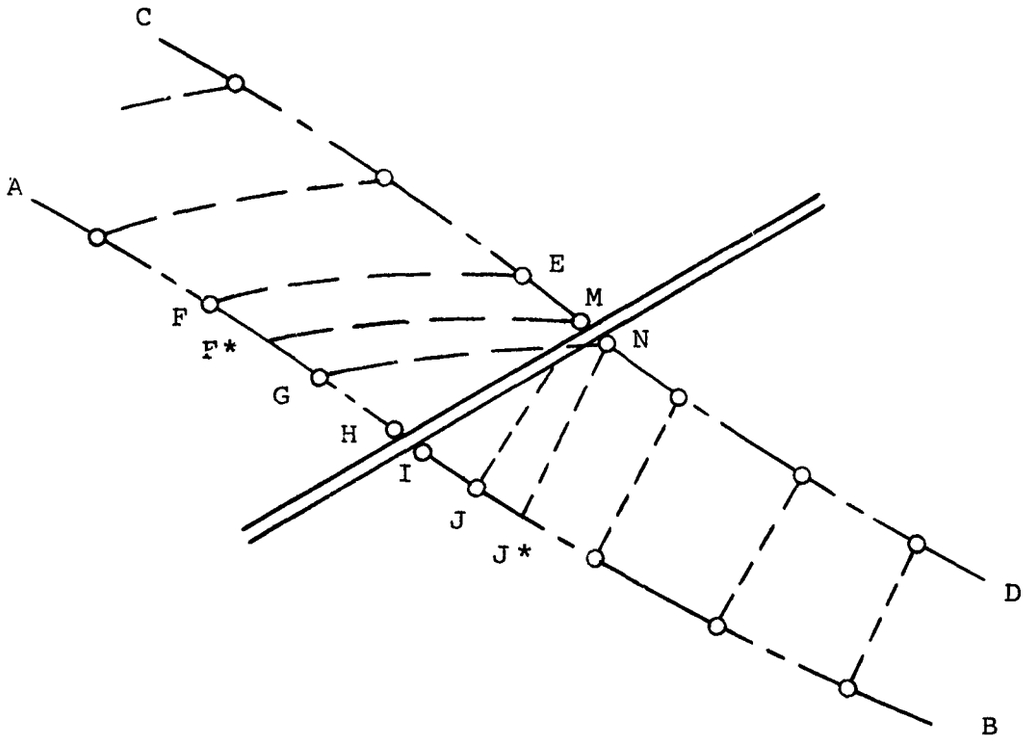

FIGURE 20 - PROGRESS OF THE COMPUTATION IN THE PRESENCE OF AN UP RUNNING SHOCK

Supposing the shock to be the first up running shock to cross $\overline{CD}$, all points through E on $\overline{CD}$ can be computed as ordinary points. As each such point is computed, we test to see if the down characteristic and the shock intersect before we can compute any other regular points. When such an intersection occurs, we locate it (M in Figure 20) by intersecting the down characteristic $\overline{EM}$ from E, the last good regular point, with the up characteristic, $\overline{F^*M}$, from F*, an interpolated point on $\overline{AB}$. The conditions at M are determined by a regular characteristic computation between F* and E.

Now we must determine the new shock slope at M and the conditions behind the shock at N. To do this, a point J* on $\overline{AB}$ is found by interpolation such that the up running characteristic, $\overline{J^*N}$, from J*, intersects the shock at N. Then the compatibility equation (13b) along $\overline{J^*N}$ is solved simultaneously with the Rankine Hugniot conditions across the shock to determine everything including the shock slope, at N. In outline, the process of solution is:

1) guess σ, the shock slope at M;

2) compute, p, ρ, τ, M^2 at N from Rankine Hugniot equations (14) and the known conditions at M,

3) compute p', at N from the known conditions at J* using the compatibility equation (17b) along $\overline{J^*N}$ and the τ from 2, above,

4) compare p' and p; if they do not agree, guess another value of σ and repeat the process until convergence.

When the iteration has converged, an additional test is made on p_N/p_M. If an expansion has caused the shock to become so weak that, within the numerical accuracy of the computation, the shock no longer has finite strength, it is desirable to eliminate it from the flow field. Thus if $p_N/p_M \leq 1$, we drop the shock.

2. Down Running Shock Points

The intersection of a down running characteristic and a down running shock were outlined in Part D-b-2, although the manner in which the iteration is carried out was not given. The iteration is performed exactly as in the case of a down characteristic up shock intersection detailed in Part D-e-1, except that the

compatibility equation is 17a written along a down running characteristic (see Figure 16 and Part D-b-2). There is presently no provision to drop a down shock which has become very weak. This should not cause any trouble in the use of the program.

f. How Are Shocks Started?

Shocks may arise in two fashions, differing only in their smoothness. There may be sharp compressive corners in the flow field which will give rise to attached oblique shocks (Figure 7)(the case of strong shocks is not considered here). Or, a continuous smooth compression may coalesce into a shock as illustrated in Figure 9.

1. Formation of Attached Oblique Shocks by Sharp Corners

a) Lower Boundary - When a corner is encountered on the lower boundary, the conditions just in front of the shock are found by an ordinary lower boundary computation (Part D-c-2) along MA of Figure 21 where M is an interpolated point. The turning angle of the flow is specified and the conditions behind the shock at B and the shock slope at (A,B) are completely determined from Equations 14 where $\delta = \tan^{-1}\tau_B - \tan^{-1}\tau_A$. The intersection of the shock with the down running characteristic (E of Figure 21) is found and the conditions in front of the shock are determined by a regular characteristic compuation between G and H where G is an interpolated point on the previous down characteristic and H is the last computed point in front of the shock on the current characteristic. C is the point on the wall behind the shock whose up running characteristic intersects the shock at (E,F). The conditions at C are assumed to equal those at B. A regular shock computation between E, F, and C is then performed (see Part D-e) determining the conditions at F and the slope of the shock at (E,F). Then D is computed as a regular boundary point.

b) Upper Boundary - The computation of the formation of shocks on the upper boundary has been outlined in Part D-b-2 except that no indication was given of the equations used to determine the conditions behind the shock. However, the equations are those indicated in the preceeding paragraph and there is no need to duplicate here a description of the computational procedure outlined in Parts D-b-2 and D-f-1.

2. Shocks Formed by Coalescence of Smooth Compressions

The formation of oblique shocks by the coalescence of a smooth compression is manifested numerically by the crossing of characteristics of the same family as illustrated in Figure 9 for a

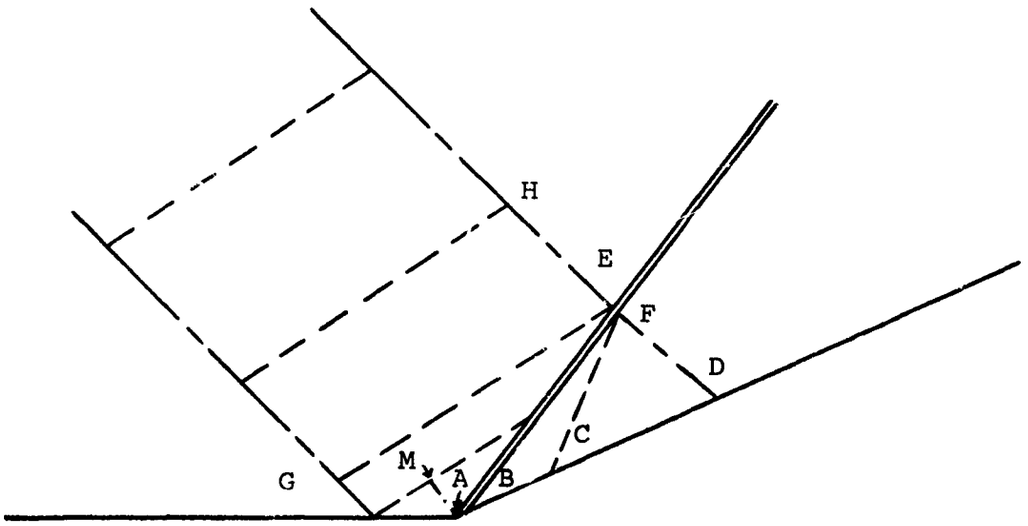

FIGURE 21 - FORMATION OF ATTACHED OBLIQUE SHOCK ON LOWER WALL

compression from the lower wall. In the program such shocks are detected by testing each regularly computed mesh point to see if there has been a crossing of either characteristic family. In such an instance a shock of that family is initiated.

g. Reflection of Oblique Shocks at the Walls

1. Up Running Shock Reflected at the Upper Wall

The reflection of an up running shock at the upper wall is illustrated in Figure 22. It is easy to detect such a reflection since the counter indicating the mesh point of the shock on the down running characteristic approaches one (1) as the shock approaches the boundary. When such a reflection occurs, we proceed in a manner similar to that used when we have a sharp compressive corner on the upper wall. Referring to Figure 22, $\overline{AB}$ is assumed to have been completely computed. The location, (C,D,F) of the intersection is determined and the conditions at C in front of the incident shock are determined by a regular upper wall computation (H is an interplated point on $\overline{AB}$). Then the slope of the incident shock at the point of intersection and the conditions at D (behind the incident shock but in front of the reflected shock) are determined by a regular up shock-down characteristic computation (Part D-e-1). The characteristic $\overline{DE}$ is then completed in the usual manner.

Now since the up shock reflects as a down shock, the latter will separate the flow field into two strips, say the I'th strip in front of the reflected shock and the (I+1) st strip behind it. The incident shock turns the flow toward the wall, and we can think of there being an effective compressive corner at the point of reflection which turns the flow from its direction at D, between the two shocks, to the direction parallel to the wall at F, behind the reflected shock. Thus, after $\overline{DE}$ is computed the reflection is treated exactly as a sharp compressive corner (see Part D-f-1-b).

2. Down Running Shock Reflected at the Lower Wall

The configuration arising when a down running shock reflects at the lower wall is illustrated in Figure 23. While working along the down running characteristic, $\overline{DEF}$, in the I'th strip, tests are made to see if the characteristic intersects the lower wall before it intersects the down shock, $\overline{GA}$, separating the I'th and (I-1)st strips. When this happens, the point of intersection (A,B,C) of the shock with the wall is determined. The conditions at A are determined by interpolating on the (I-1)st strip. The conditions at B are determined by making a regular down shock computation as previously

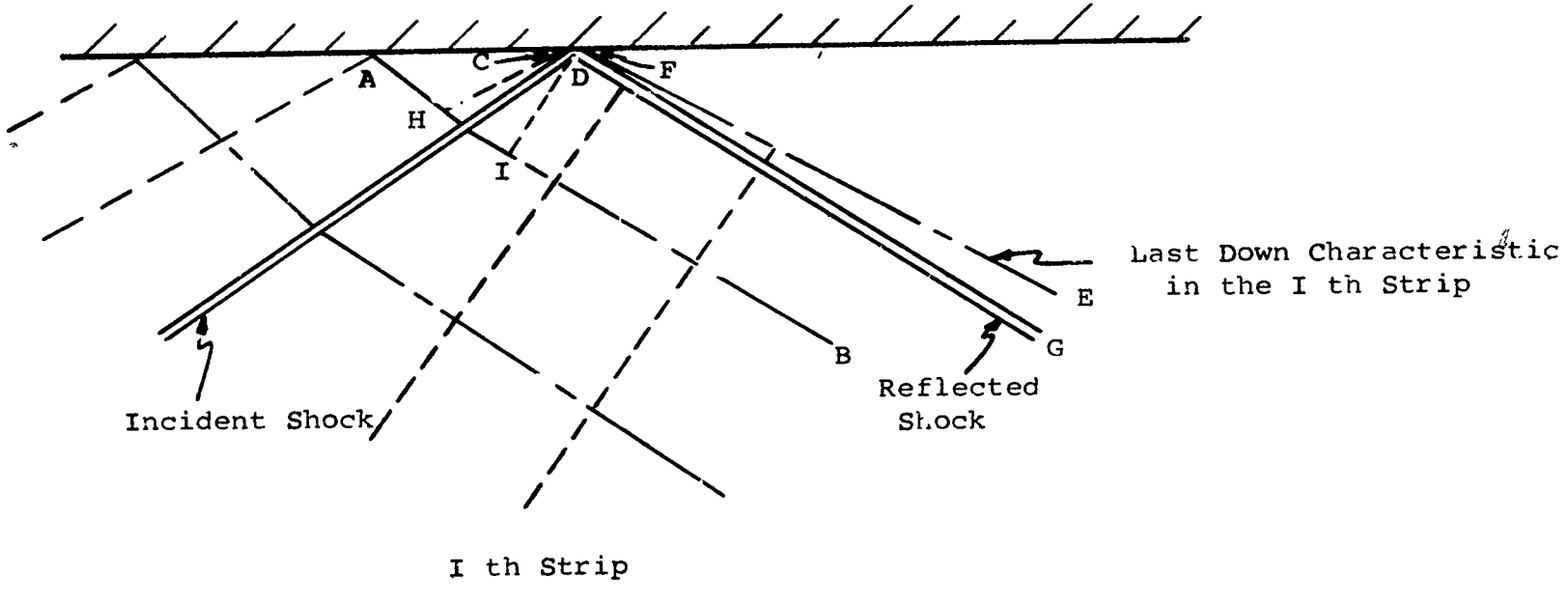

FIGURE 22 - REFLECTION OF AN UP RUNNING SHOCK AT THE UPPER WALL

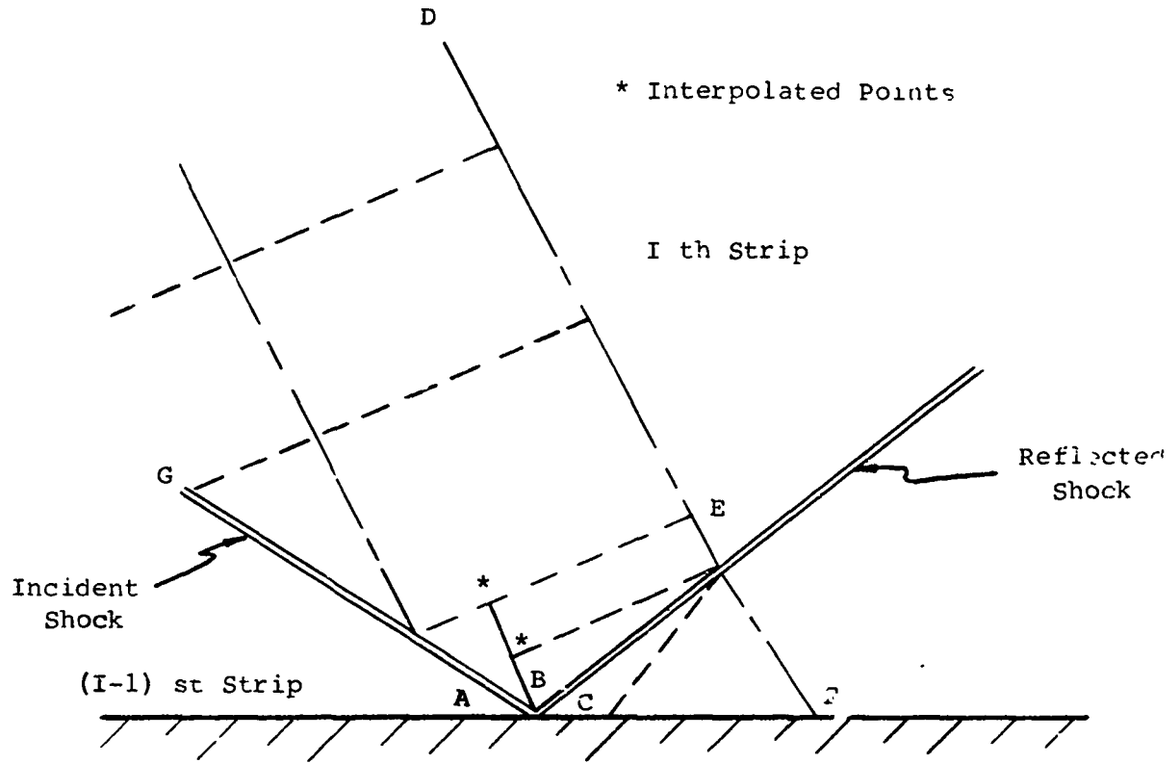

FIGURE 23 - REFLECTION OF A DOWN RUNNING SHOCK AT THE LOWER WALL

outlined. The incident shock turns the flow toward the wall at B, between the two shocks. The slope of the reflected shock and the flow at C is then determined by requiring the known flow at D to turn back parallel to the wall at C. By extrapolating the reflected shock we find E, the last good computed point on $\overline{DEF}$. By a procedure identical with the case of a sharp compressive corner on the lower wall (Part D-f-1) the rest of $\overline{DEF}$ is recomputed as indicated in the figure.

h. Intersection of Shocks of the Same Family

In general, such an intersection will be continued as a shock, a contact discontinuity, and a reflected expansion or shock as is illustrated in Figure 4. We neglect the contact discontinuity and reflected expansion or shock because they should be weak compared to the shock $\overline{OC}$.

i. Intersection of Shocks of Opposite Family

This situation is illustrated in Figure 24. Such an intersection will result in the diffraction of the two incident shocks and the creation of a contact discontinuity along which the pressure and velocity direction are continuous. While working along the down characteristic $\overline{AB}$ in the Ith strip, tests are made to determine whether or not the down shock $\overline{COB}$ separating the two strips intersects an up shock of the (I-1)st strip. When this happens, the point of intersection, O, is determined. The conditions at O (in front of both intersecting shocks) are obtained by interpolation on the (I-1)st strip. The slopes at O of the two incident shocks and the conditions at E and F are then determined, the slopes being assumed equal to the slope at the nearest previous shock point and the conditions at E and F being then computed directly using the Rankine Hugoniot relations.

The slope of the diffracted up shock, $\overline{OK}$, is then guessed and the conditions at G are determined, including τ_G. Then the slope of the diffracted down shock, $\overline{OB}$, is determined which gives $\tau_H=\tau_G$. Then p_G and p'_H are compared and, if they disagree, the slope of $\overline{OK}$ is changed an an iteration is performed. Then the intersection, K, of the down characteristic, $\overline{AB}$, with the diffracted up shock, $\overline{OK}$, is determined as are the other intersections indicated in the figure.

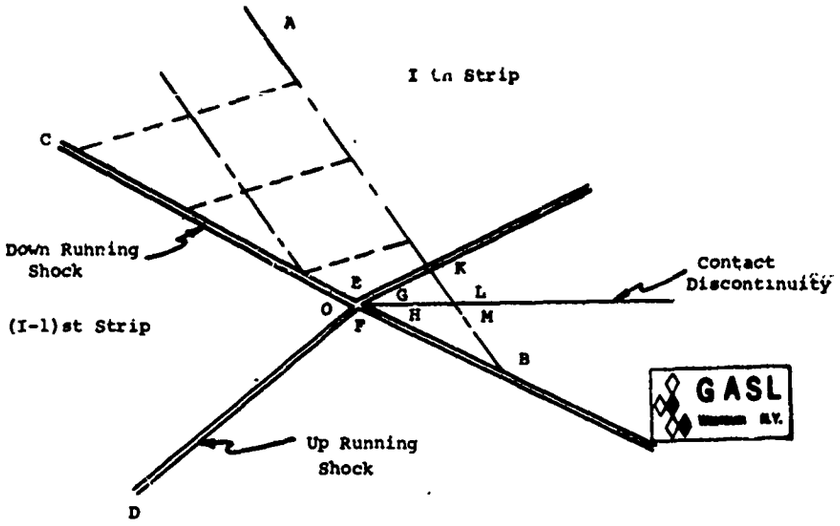

FIGURE 24 - INTERSECTION OF SHOCKS OF OPPOSITE FAMILY

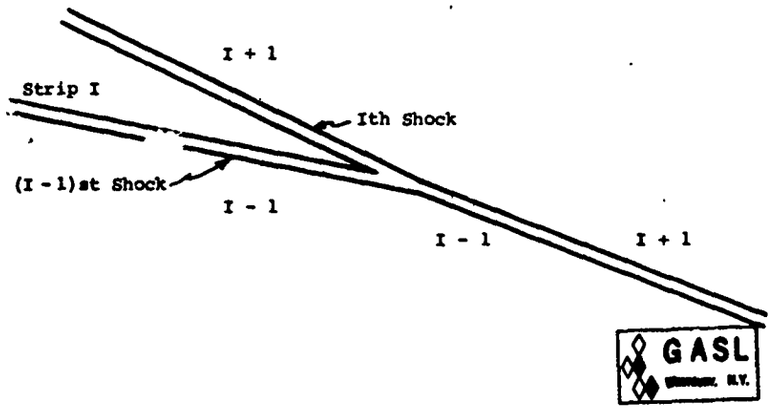

FIGURE 25 - COALESENCE OF DOWN RUNNING SHOCKS

The next down running characteristic in the Ith strip is then made in the normal fashion.

j. Intersection of Shocks with Contact Discontinuities

The situation which arises in this case is depicted in Figure 6 where it is seen that the intersecting shock and contact discontinuity are diffracted at the point of intersection with a weak centered expansion often arising at the point of intersection, O.

Currently, contact discontinuities are dropped from the computation upon intersecting a shock.

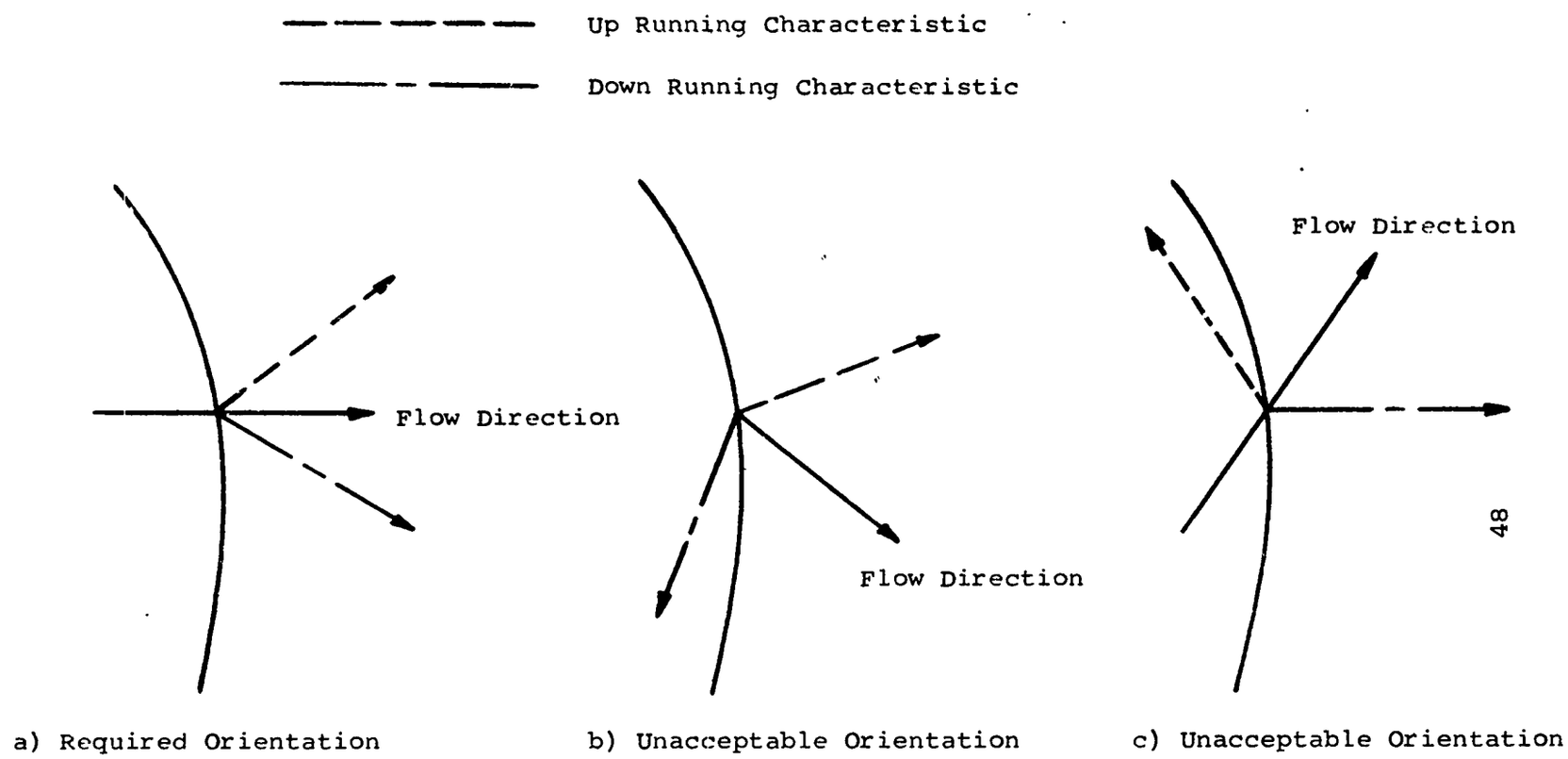

a) Required Orientation b) Unacceptable Orientation c) Unacceptable Orientation

FIGURE 26 - REQUIRED ORIENTATION OF CHARACTERISTICS WITH RESPECT TO THE INITIAL DATA LINE

V

THREE-DIMENSIONAL SUPERSONIC FLOW COMPUTER PROGRAM ELEMENTS

A. Summary and Introduction

Computer programs have been written for machine computation of the basic flow elements which compose a large variety of three-dimensional supersonic inlet flow fields. A combination of these unit problems can be used to design and analyze three-dimensional inlets as described in Section III. The programs are written in Fortran IV for use on the IBM 7094 high speed digital computer.

The overall program can be summarized as follows:

General - Computer calculation of the basic elements of three-dimensional supersonic inlet flow fields

- Plane shock - conical body
- Conical shock - plane body
- Conical shock-conical shock
- Delta wing

Input
- Uniform free stream conditions
- Supersonic leading edges
- Any combination of Mach number, body surface angle and leading edge sweep angle
- Perfect gas

Output
- Aerodynamic flow properties along the axis of symmetry of the locus of the three-dimensional wave intersections
- Aerodynamic properties, incident and reflected wave angles and locations, immediately behind the three-dimensional wave intersections
- Complete flow field behind intersections calculated for plane shock - conical body and conical shock - plane body

Complete descriptions of these program elements are given in this section. The problems are divided into two parts. Firstly, the swept wedge (Part B) which is considered to be infinite, i.e., no end expansions. This problem requires the analytic description of a shock envelope and flow field composed of a central conical region between two two-dimensional regions which extend from the central region boundaries to the leading edges. Secondly, for the remaining problems (Parts C, D and E) the initial shock envelopes and flow fields are either purely conical or two-dimensional and therefore are known a priori.

For each of the above problems, once the initial shock envelope and the associated flow field is determined, the various three-dimensional reflection and intersection curves are computed by using linearized and two-dimensional supersonic flow theory and working in planes normal to the tangent of the intersection curve. The flow fields behind the intersection curves are then constructed from two-dimensional characteristics with entropy variations.

It is suggested that the reader study the analysis given in Parts B through E before using these programs, in order to fully understand the approximations involved. The operating instructions, including the input formats, definition of symbols, and example problems, are given in the Appendices to this section.

B-1 Swept Wedge Flow (Delta Wing)

According to linear theory[11] the effect of the vertex of a supersonic swept wedge is limited to a region inside the free-stream Mach cone from the vertex. In the analysis presented herein the two dimensional leading edge shock and flow field (the region outside this central Mach cone) are obtained from exact oblique shock theory applied in a plane normal to the wedge leading edge. Since an exact solution for the region influenced by the vertex Mach cone is nonexistent, linear theory is used on the base plane of the wedge to obtain the flow properties inside the Mach cone corresponding to the two dimensional Mach number. This cone is assumed to divide the two- and three-dimensional regions. Similar to the solution of Babaev[12] and Fowell[13] for a swept flat plate at an angle of attack, a second order curve is used as an approximation for the shock envelope in the 3-D central region. The flow conditions behind the reflection of the wedge shock from a plane surface are then determined from oblique shock theory in planes normal to the tangent of the intersection curve.

The supersonic flow over a swept wedge as shown schematically in Figure 28 is considered here. The sweep angle is designated by and the wedge angle in the plane of symmetry is denoted . The leading edges are assumed to be supersonic and the wedge is taken to be of infinite span.

As is well known[11], the influence of the wedge apex (0') is only felt inside of a Mach cone whose vertex is at 0'. Outside of this cone the flow field behind the leading edge shock is two-dimensional. This region may be analyzed in the usual way by breaking the free stream Mach number into two components, tangent and normal to the leading edge. Oblique shock theory can then be used in the plane normal to the leading edge to determine the flow behind the two-dimensional portion of the shock. The wedge angle in this normal plane is determined geometrically to be

$$\lambda_n = \tan^{-1}\left(\frac{\tan \lambda}{\cos \chi}\right) \qquad (23)$$

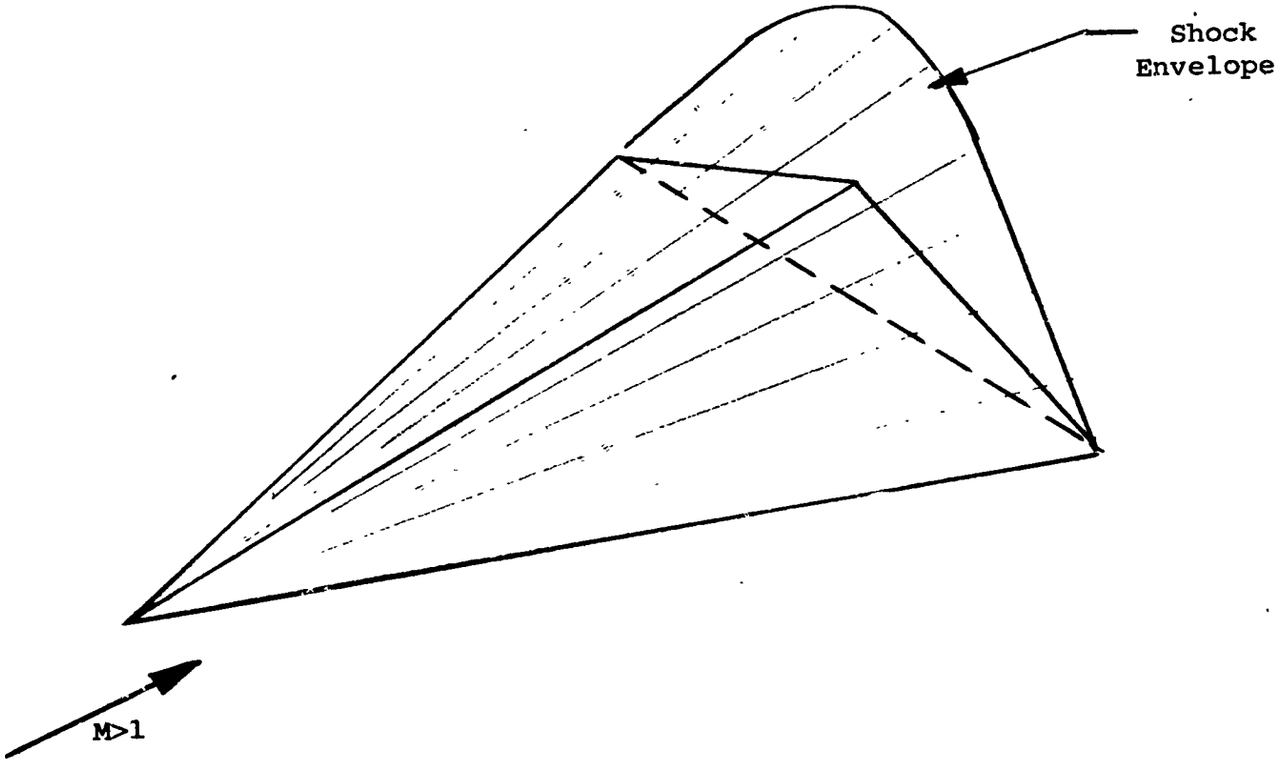

FIGURE 27 - SCHEMATIC OF SWEPT WEDGE FLOW

and the flow deviation on the wedge surface with respect to line O'C (Fig.28), is

$$\sigma_1 = \cos^{-1}(\cos\lambda \sin\chi) - \tan^{-1}\left(\frac{M_{n_1}}{M_{t_1}}\right) \qquad (30)$$

The general shape of the swept wedge shock consists of the two plane shocks attached to the leading edges, as described above, connected through the central region by a curved section which is determined by the three-dimensional nature of the flow. In order to analyze this central region it is necessary to make some approximations concerning the shock shape and the distribution of the flow properties. The local Mach cone defined by μ_1, with the vertex at O' and an axis along O'C is assumed to separate the two-dimensional flow field from the central portion, which is conical under the assumption of linear theory[14]. Due to the conical nature of the central flow, the element of the wedge shock in the vertical plane of symmetry ($x = 0$) is a straight line and, therefore, a linear function of z. In a plane normal to the z' axis the shock is assumed to be a parabola, which is tangent to the two-dimensional shocks at their points of intersection with the local Mach cone (Fig. 29). A parabola is chosen since this family of curves have asymptotes, which is desired since the curve must match with the straight two dimensional shock. The angles that the two-dimensional shocks make with the base plane of the wedge in the y-z and x-y planes are respectively:

$$\beta^* = \tan^{-1}(\tan\theta_{1n}\cos\lambda) \qquad (31)$$

$$\theta_s = \tan^{-1}(\tan\theta_{1n}\sin\chi) \qquad (32)$$

Using these relations the two-dimensional shock angle in the plane normal to the z' axis can be found as

$$\theta_c' = \tan^{-1}\left\{\left[\cos\lambda\tan(\beta^*-\lambda) + \sin\lambda\right]\tan\chi\right\} \qquad (33)$$

The points of intersection of the two-dimensional shocks with the local Mach cone in the plane $z' = \cos\lambda$ are given by $x_j' = \pm\cos\theta_c'\cos\lambda\left\{\tan(\beta^*-\lambda)\sin\theta_c' + \left[\tan^2\mu_1 - \tan^2(\beta^*-\lambda)\cos^2\theta_c'\right]^{\frac{1}{2}}\right\}$

$$y_j' = \left|x_j'\right|\tan\theta_c' - \cos\lambda\tan(\beta^*-\lambda) \qquad (34)$$

$$z_j' = \cos\lambda$$

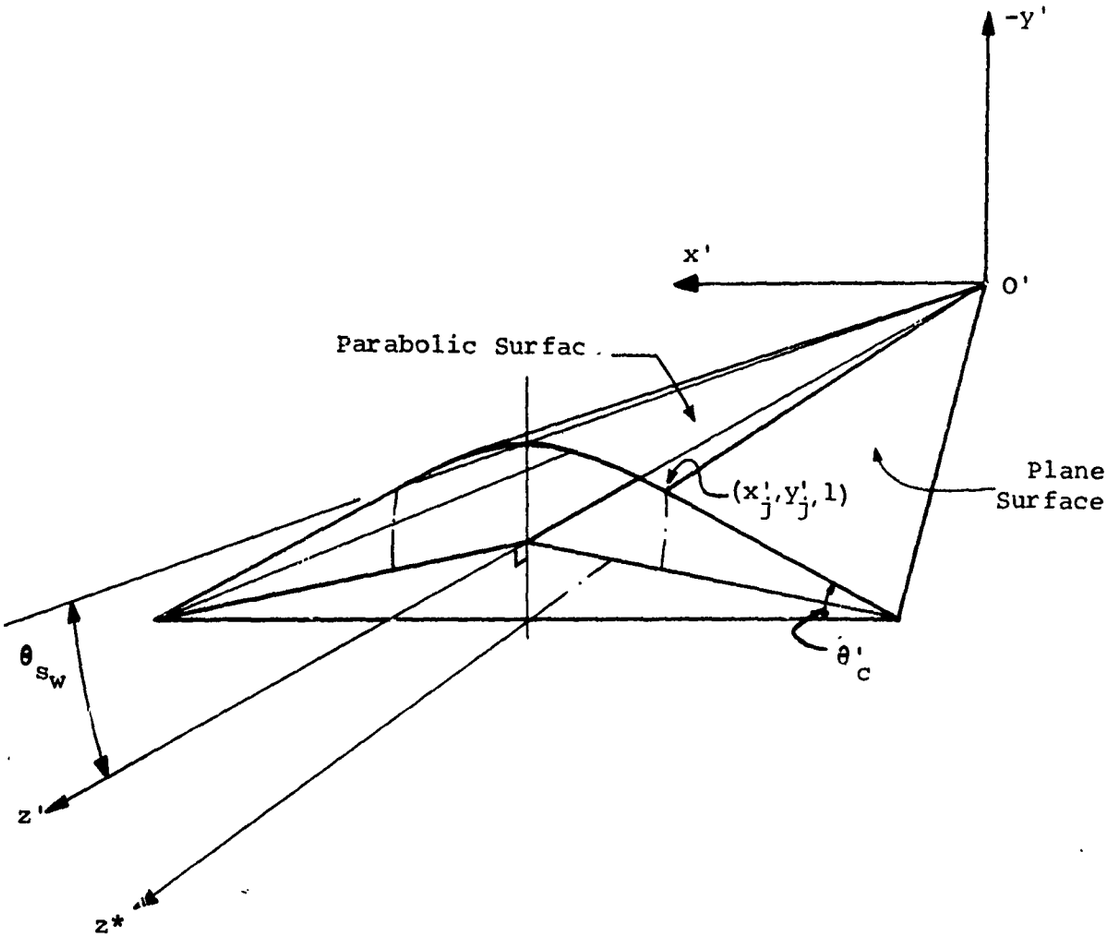

FIGURE 29 - SHOCK CONFIGURATION

Since the central portion of the wedge shock is represented by a parabola tangent to the two-dimensional shocks in a plane z' = const. and is linear in z', the three-dimensional shock envelope is represented by a parabolic sheet whose equation is

$$x'^2 = Az' \ (y' + hz') \tag{35}$$

The constants A and h are determined by requiring, as stated previously, that the shocks pass through the point (x'_j, y'_j, z'_j) and have slope $\tan \theta'_c$ in the plane z' = const. at that point. The resulting values of these constants are

$$A = \frac{2\left|x'_j\right|}{\tan\theta'_c} \ \frac{1}{\cos \lambda}$$

$$h = \left(\frac{x'^2_j}{A \cos \lambda} - y'_j\right) \frac{1}{\cos\lambda} \tag{36}$$

The constant h, as can be seen from (36), is the tangent of the angle θ_{sw} that the three-dimensional shock makes with the z' axis in the plane of symmetry (y-z).

Linear theory has been used in the conical region to obtain the variation of the flow properties from their uniform values in the two-dimensional region to the plane of symmetry. For this present work the variations of the properties in the y direction has been neglected. Therefore the variations used are truly valid only on the baseplane (x-z*) of the wedge. However, for small wedge angles (<10 degrees approximately) which are generally used in supersonic and hypersonic inlet designs the approximation is good for the whole region. Since the local Mach cone has been used previously to construct the shock and linear theory uses the free stream Mach cone, the conical rays of linear theory must be adjusted to fit into the local Mach cone. Thus, given the ratio $(x/z)_i$, which represents the slope of a conical ray i, the adjusted parameter used in linear theory is

$$\zeta_i = \left|\frac{x}{z}\right|_i \left(\frac{\cos^2 \lambda - \left|y'_j\right| \sin \lambda}{\left|x'_j\right|}\right) n \tag{37}$$

where $n = \tan \chi \sqrt{M_\infty^2 - 1}$. The resulting variations of pressure and Mach number in the conical region are

$$\frac{P_{1_i}}{P_\infty} = \frac{P_1}{P_\infty} \frac{1 + \tfrac{1}{2} \gamma M_\infty^2 C_{pi}}{1 + \tfrac{1}{2} \gamma M_\infty^2 C_{po}} \tag{38}$$

and

$$M_{1_i} = M_1 \left\{ \frac{\left(1 - \frac{C_{pi}}{2}\right)^2 + u_i^2}{\left(1 - \frac{C_{po}}{2}\right)^2 + \left(\frac{n}{\sqrt{1-n^2}} \tan \lambda\right)^2} \right\}^{1/2} \tag{39}$$

where the pressure coefficients from linear theory[11] for the two-dimensional and conical regions are respectively,

$$C_{po} = \frac{2 \tan \lambda}{\sqrt{(M_\infty^2 - 1)\ (1 - n^2)}} \tag{40}$$

and

$$C_{pi} = C_{po} \left[1 - \frac{2}{\pi} \sin^{-1} \left(\frac{n^2 - \zeta_i^2}{1 - \zeta_i^2} \right)^{1/2} \right] \tag{41}$$

and the lateral velocity u_i (x-direction) is

$$u_i = \frac{n \tan \lambda}{\pi \sqrt{1-n^2}} \left\{ \cos^{-1} \left[\frac{n^2 - \zeta_i}{n(1-\zeta_i)} \right] - \cos^{-1} \left[\frac{n^2 + \zeta_i}{n(1+\zeta_i)} \right] \right\} \tag{42}$$

The flow deviation with respect to the z' axis in the conical region is

$$\sigma_{1i} = \sigma_1 \left[\frac{1 - \frac{C_{po}}{2}}{\left(\frac{n}{\sqrt{1-n^2}}\right) \tan \lambda} \right] \tan^{-1} \left[\frac{u_i}{1 - \frac{C_{pi}}{2}} \right] \tag{43}$$

where σ_1 (Eq. 30) represents the flow deviation in the two-dimensional region.

B-2 Swept Wedge Shock Reflection

A swept wedge shock reflecting from a plane surface is considered next. The three-dimensional wedge shock intersects a plane body along a curve which ends in two straight lines (Fig.30), corresponding to the intersection of the two-dimensional portions of the shock with the plane. For the case under consideration, where the plane body is parallel to the base plane of the wedge, the two straight line sections are parallel to the leading edges of the wedge. The central curved portion of the intersection curve is represented by the second order equation

$$x_i = \pm \left[A\,(Bz_i^2 + 2Cz_i + D)\right]^{1/2} \tag{44}$$

where

$$\begin{aligned} B &= \cos\lambda\,(\sin\lambda + h\cos\lambda) \\ C &= r\,(h\sin\lambda\cos\lambda + \sin^2\lambda - 1/2) \\ D &= r^2\sin\lambda\,(h\sin\lambda - \cos\lambda) \end{aligned} \tag{45}$$

and where r is the distance between the plane and the base of the wedge. Values of z_i are obtained by incrementing from the value of $z_{i=0}$ obtained from Eq (44) with $x_{i=0}=0$, i.e., $z_i=z_o+i\,\Delta z$.

For each point on the curve the angle between the tangent to the curve and the z axis is given by

$$\chi_i' = \tan^{-1}\left[\frac{A(Bz_i + C)}{|x_i|}\right] \tag{46}$$

When the value of χ_i' reaches $(\pi/2)-\chi$, the intersection curve becomes a straight line and the incrementation of z_i can be stopped.

The intersection curve represents the line along which the shock reflects from the plane body. The flow field between the incident and reflected shocks has been assumed to be the same as the flow on the wedge surface, i.e., no variation in the y-direction (Fig.30). In order to obtain the flow conditions behind the reflected shock, it is necessary to use the oblique shock relations in planes normal to the tangents of the intersection

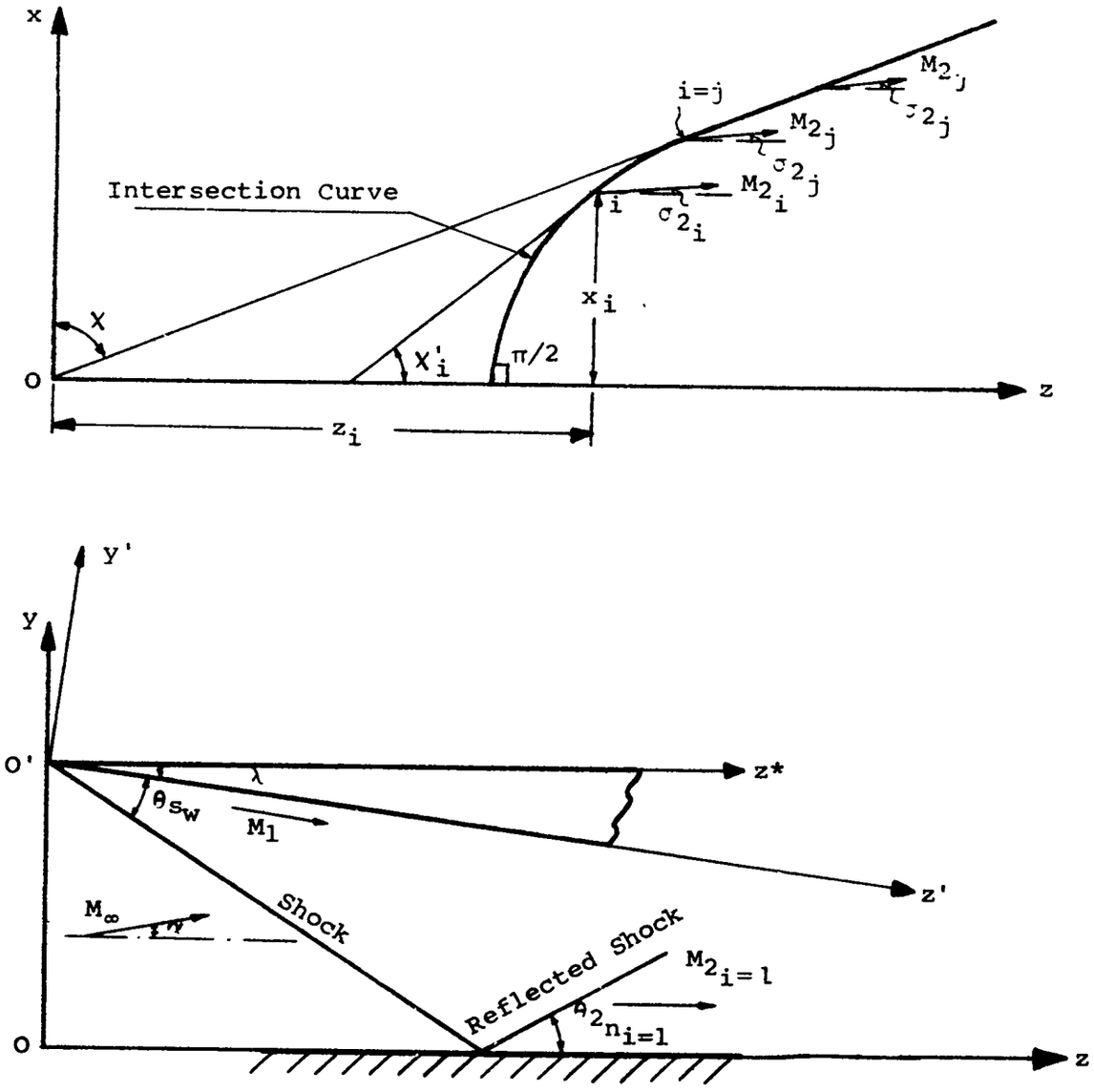

FIGURE 30 - WEDGE SHOCK REFLECTION

curve for each point i. To simplify the procedure the components of the Mach number between the incident and reflected shocks in the x-y-z directions are found first.

$$M_{l_{xi}} = M_{li}\left[\cos\chi\cos(\chi^* - \sigma_{li}) - \cos\lambda_n \sin\chi \sin(\chi^* - \sigma_{li})\right]$$

$$M_{l_{yi}} = -M_{li} \sin\lambda_n \sin(\chi^* - \sigma_{li}) \tag{47}$$

$$M_{l_{zi}} = M_{l_i}\left[\sin\chi\cos(\chi^* - \sigma_{li}) + \cos\lambda_r \cos\chi \sin(\chi^* - \sigma_{li})\right]$$

where the angle between the leading edge and the z' axis on the wedge surface is

$$\chi^* = \cos^{-1}(\cos\lambda \sin\chi) \tag{48}$$

Then the Mach number components normal and tangent to the intersection curve on the plane surface are easily found from

$$M_{l_{n_i}} = M_{l_{z_i}} \sin\chi_i' - M_{l_{x_i}} \cos\chi_i'$$

$$M_{l_{t_i}} = M_{l_{z_i}} \cos\chi_i' + M_{l_{x_i'}} \sin\chi_i' \tag{49}$$

The total Mach number in the plane normal to the intersection curve is

$$M_{N_i} = (M_{n_i}^2 + M_{l_{y_i}}^2)^{1/2} \tag{50}$$

and the corresponding flow deflection is

$$\delta_{l_i} = \tan^{-1}\left|\frac{M_{l_{y_i}}}{M_{l_{n_i}}}\right| \tag{51}$$

since the flow behind the reflected shock must be parallel to the plane body. The oblique shock relations are also used to find the change in flow properties across the reflected shock:

$$M_{2_{N_i}} \; ; \; \left(\frac{P_2}{P_1}\right)_i \; ; \; \left(\frac{a_2}{a_1}\right)_i \; ; \; \theta_{2_i} \text{ and } \Delta S_i$$

These conditions together with the relation

$$M_{2_{t_i}} = M_{1_{t_i}} \left(\frac{a_1}{a_2}\right)_i \tag{52}$$

give the flow properties behind the reflected shock

$$M_{2_i} = (M^2_{2_{N_i}} + M^2_{2_{t_i}})^{1/2} \tag{53}$$

$$\frac{p_{2_i}}{p_\infty} = \left(\frac{P_2}{P_1}\right)_i \frac{p_{1_i}}{p_\infty} \tag{54}$$

$$\theta_{2_{n_i}} = \theta_{2_i} - \delta_{1_i} \tag{55}$$

$$\sigma_{2_i} = \chi_i' - \tan^{-1}\left(\frac{M_{2_{N_i}}}{M_{2_{t_i}}}\right) \tag{56}$$

$$\Delta S_{2_i} = \Delta S_1 + \Delta S_i \tag{57}$$

These relations give the flow conditions immediately behind the curved portion of the intersection curve for each point i. The point i for which the value of χ_i' reaches $(\pi/2 - \chi)$ gives the conditions behind the two-dimensional shock reflection.

The flow conditions in the whole region of the plane surface behind the shock intersection can be found by using two-dimensional characteristics which take the variations of entropy, due to the curvature of the shock, into account. This method has been applied to the conical flow problems of Sections C and E and has been presented in such a manner (separate subroutine in the computer program), that it can easily be used in this wedge program.

Other methods of solution for supersonic flow over the wedge, which are more complicated than the approximation of linear theory used here, include an exact solution similar to the indirect method for a swept flat plate at an angle of attack of Ref. 12. Also, the present solutions can be improved by using three-dimensional linear theory to give an approximation which allows variation of the flow properties in the y-direction. A method for determining the y-variation of the flow, which should yield a better approximation than three-dimensional linearized theory, is to use the conical flow variation between the body and shock of an equivalent cone, whose surface pressure is matched to the surface pressure of the wedge at the same free stream Mach number. In any case, the methods of the present work and the analytic techniques presented above can either be used directly in an inlet design and analysis effort or as a starting point for additional investigations.

The program operation and example problems are described completely in Appendices V and VI.

C-1 Impingement of a Conical Shock on a Plane Surface

The configuration examined here is the supersonic flow over a cone of half angle γ_b at zero angle of attack, in the presence of a plane surface inclined by an angle θ_1 with respect to the cone axis (Fig.31).

The intersection curve of the conical shock, (γ_c) produced by the cone, with the plane surface, (x', z' plane), is represented by the second order equation

$$x'_i = \left\{ -(Az'^2_i - 2Bz'_i + C) \right\}^{\frac{1}{2}} \tag{58}$$

where

$$\begin{aligned} A &= \sin^2\theta_1 - \tan^2\gamma_c \cos^2\theta_1 \\ B &= r \sin\theta_1 + q \tan^2\gamma_c \cos\theta_1 \\ C &= r^2 - q^2 \tan^2\gamma_c \end{aligned} \tag{59}$$

where θ_1 is the inclination of the plane surface to the free stream direction and where r and q are the coordinates of the origin 0', which is assumed to be in the y', z' plane (Fig. 31). Values of z'_i are obtained by incrementing from the value of $z'_{i=o}$, obtained from Equation (58) with $x'_i = 0$, i.e., $z'_i = z'_o + i\,\Delta z'$.

For each point of the intersection curve, the angle between the tangent to the curve and the z' axis is given by

$$\Omega_i = \tan^{-1} \left| \frac{B - Az'_i}{x'_i} \right| \tag{60}$$

The intersection curve is cut off when Ω_i becomes 5^o or less in order to work on only one side of the cone. The conical flow field of a cone at zero angle of attack is completely defined by the values of the critical Mach number M_1^* and the flow direction angle ψ_1 for each conical ray angle γ [15]. The Mach number components along and normal to a conical ray of angle γ are, from Ref. 15.

$$\begin{aligned} M_r &= u/a \\ M_t &= M_r \tan(\psi_1 - \gamma) \end{aligned} \tag{61}$$

where

$$u = \sqrt{\frac{\gamma-1}{\gamma+1}}\; M_1^* \; \frac{1}{[1+\tan^2(\psi_1 - \gamma)]^{\frac{1}{2}}}$$

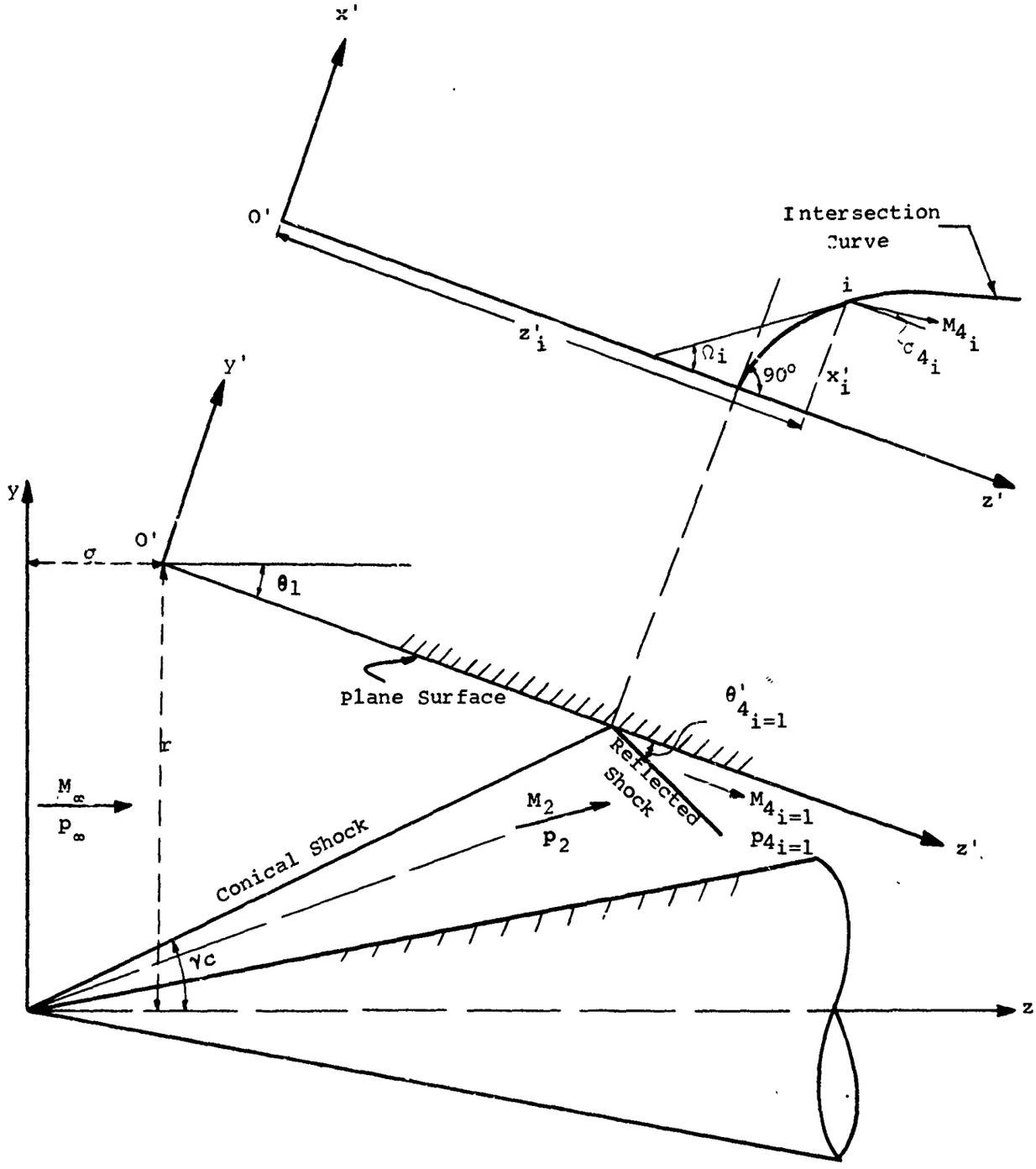

FIGURE 31 - CONICAL SHOCK-PLANE BODY GEOMETRY

and

$$a = \sqrt{\frac{\bar{\gamma}-1}{2}}\left(1 + \frac{\bar{\gamma}-1}{\bar{\gamma}+1} M_1^{*2}\right)^{\frac{1}{2}} \tag{62}$$

represent the velocity along the conical ray and the speed of sound non-dimensionalized with respect to the limiting velocity, respectively. The Mach number components immediately behind the conical shock, which is represented by the conical ray $\gamma = \gamma_c$, are found from Eqs. (61) and (62) by setting $\gamma = \gamma_c$. In order to calculate the flow field beind the reflected shock, the oblique shock relations are used in a plane normal to the tangent of the intersection curve for each point i. The components of the Mach number immediately behind the conical shock in the x', y', z' directions are found first;

$$\begin{aligned}
M_{2_{x_i'}} &= M_r \sin\gamma_c \cos\varphi_i + M_t \cos\gamma_c \sin\varphi_i \\
M_{2_{y_i'}} &= M_r (\sin\gamma_c \cos\varphi_i \cos\theta_1 + \cos\gamma_c \sin\theta_1) \\
&\quad + M_t (\cos\gamma_c \cos\varphi_i \cos\theta_1 - \sin\gamma_c \sin\theta_1) \\
M_{2_{z_i'}} &= M_r (\cos\gamma_c \cos\theta_1 - \sin\gamma_c \cos\varphi_i \sin\theta_1) \\
&\quad - M_t (\cos\gamma_c \cos\varphi_i \sin\theta_1 + \sin\gamma_c \cos\theta_1)
\end{aligned} \tag{63}$$

where

$$\varphi_i = \tan^{-1}(x_i'/y_i') \text{ with } y_i' = r - z_i' \sin\theta_1$$

Then the upstream Mach number components normal and tangent to the intersection curve on the plane surface are found from

$$\begin{aligned}
M_{2_{n_i}} &= M_{2_{z_i'}} \sin\Omega_i - M_{2_{x_i'}} \cos\Omega_i \\
M_{2_{t_i}} &= -M_{2_{z_i'}} \cos\Omega_i - M_{2_{x_i'}} \sin\Omega_i
\end{aligned} \tag{64}$$

The total Mach number and the flow deflection in the plane normal to the intersection curve are

$$M_{2_{N_i}} = (M_{2_{n_i}}^2 + M_{2_{y_i'}}^2)^{\frac{1}{2}} \tag{65}$$

$$\delta_{2_i} = \tan^{-1}(M_{2_{y_i'}}/M_{2_{n_i}}) \tag{66}$$

With the oblique shock relations giving the change in flow properties across the shock as

$$M_{4_{N_i}} \; ; \quad (p_4/p_2)_i \; ; \; a_4/a_2)_i \; ; \; \theta_{4_i}$$

and the relation

$$M_{4_{t_i}} = M_{2_{t_i}} \, (a_2/a_4)_i \tag{67}$$

the flow properties behind the reflected shock can be found from

$$M_{4_i} = (M^2_{4_{N_i}} + M^2_{4_{t_i}})^{\frac{1}{2}} \tag{68}$$

$$p_{4_i}/p_\infty = (p_4/p_2)_i \; p_c/p_\infty \tag{69}$$

$$\sigma_{4_i} = \pi/2 - \Omega_i + \tan^{-1} (M_{4_{t_i}}/M_{4_{N_i}}) \tag{70}$$

$$\theta'_{4_i} = \theta_{4_i} - \delta_{2_i} \tag{71}$$

$$S_{4_i} = \frac{\bar{\gamma}-1}{2\bar{\gamma}} \, S_2/R + \frac{1}{2\bar{\gamma}} \left[\ln \left(\frac{2\bar{\gamma} M^2_{2_{N_i}} \sin^2\theta_{4_i} - (\bar{\gamma}-1)}{\bar{\gamma}+1} \right) \right.$$
$$\left. - \bar{\gamma} \ln \left(\frac{(\bar{\gamma}+1) M^2_{2_{N_i}} \sin^2\theta_{4_i}}{(\bar{\gamma}-1) M^2_{2_{N_i}} \sin^2\theta_{4_i} + 2} \right) \right] \tag{72}$$

where p_c/p_∞ and S_2/R represent the pressure ratio and the entropy increase across the conical shock. The shock angle, θ'_{4_i} is referred to the plane surface.

C-2 Characteristic Subroutine

The flow properties on the plane surface behind the reflection curve are determined by using two-dimensional characteristics. The flow conditions immediately behind the reflected shock on the plane surface are calculated by the methods of the preceding section. Due to the conical flow in front of the reflected shock, the properties behind the shock vary in the y-direction. Therefore, the flow is truly three-dimensional. However, the y-variations are small for most cases of interest in inlet design ($\gamma_b < 10^o$ approximately) and thus a two-dimensional characteristic calculation on the plane surface has been assumed appropriate.

On the plane surface, whose coordinates are redefined as ρ, ψ the intersection curve is considered a data line, since the flow conditions immediately behind it are known (Fig.32). Due to the flow symmetry about the plane x=x'=0, the ρ axis must be a streamline and therefore can be considered as a wall with zero flow deviation (θ=0). The data line terminates when either a five degree slope or a Mach reflection is reached. The program computes the characteristic mesh between the data line, the wall and the second family characteristic line from the last data point. The characteristic equations include the effect of entropy due to the varying strength of the reflected shock. This subroutine can also be applied to find the flow field behind the intersection curves of any of the problems considered in this report.

The data required for the characteristic equations at each point (ρ_i, ψ_i) on the data line are: the flow deviation, θ, with respect to the ρ axis, the local entropy $\bar{S}_i=(S_i-S_\infty)/2c_p$, the local velocity, w_i, non-dimensionalized with respect to the local limiting velocity and the local Mach angle μ_i. The values of w_i and μ_i can be found from the known Mach number behind the intersection curve from the relations:

$$w_i = M_i \frac{\sqrt{\frac{\gamma-1}{2}}}{\sqrt{1+\frac{\gamma-1}{2} M_i^2}} \qquad (73)$$

$$\mu_i = \sin^{-1} (1/M_i)$$

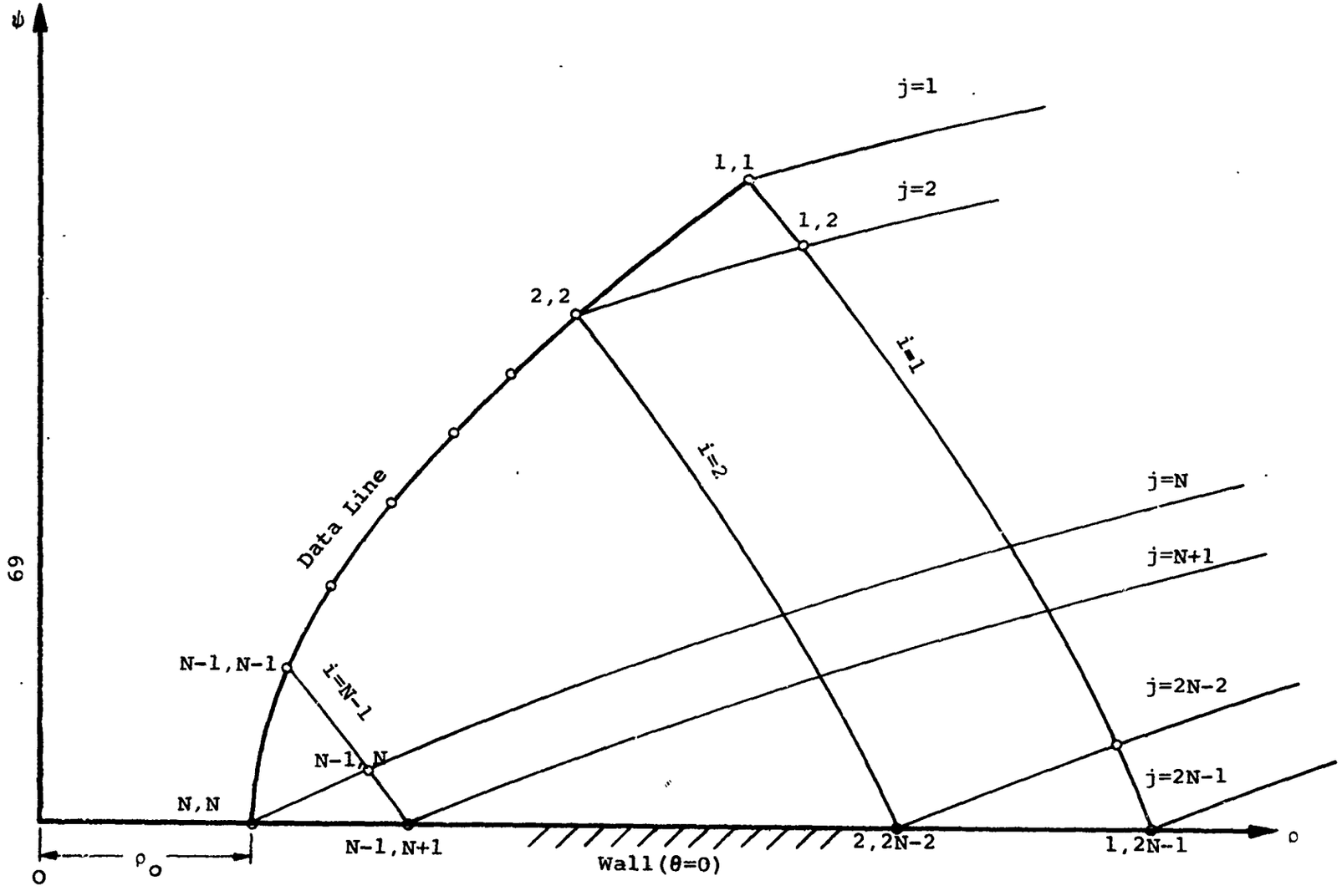

FIGURE 32 - CHARACTERISTIC MESH

The equations which determine the location of a typical point Q_3 in Fig. 33 are

$$\psi_3-\psi_1 = (\rho_3-\rho_1)\ [\tan\ (\theta + \mu)\ ]_{1,3} \qquad (74)$$
$$\psi_3-\psi_2 + (\rho_3-\rho_2)\ [\tan\ (\theta - \mu)\ ]_{2,3}$$

where the double subscript indicates the average value between the two points. The relations which hold along the first and second family characteristic lines are, respectively

$$\left(\frac{\cot\tan\ \mu}{w}\right)_{1,3}\ (w_3-w_1)-(\theta_3-\theta_1)= -\frac{2}{\overline{\gamma-1}}\ (\sin^2\mu\ \cos\mu)_{1,3} \cdot$$
$$\cdot\ \frac{ds}{dn}\ \overline{Q_1Q_3} \qquad (75)$$
$$\left(\frac{\cot\tan\ \mu}{w}\right)_{2,3}(w_3-w_2)-(\theta_3-\theta_2)= \frac{2}{\overline{\gamma-1}}\ (\sin^2\mu\ \cos\mu)_{2,3}\ \frac{ds}{dn}\ \overline{Q_2Q_3}$$

where ds/dn represents the entropy variation between the points Q_1 and Q_2 normal to the streamlines.

The characteristic grid consists of first and second family characteristics designated by j=1,2....2N-1 and i=1,2....N-1 respectively, where N is the number of data points (Fig.32.) If the Eqs.(74) are rearranged into a form suitable for computation there results

$$\rho_{i,j}= \frac{\psi_{i+i,j} - \psi_{i,j-1}-\rho_{i+i,j}\tan(\overline{\theta+\mu})+ \rho_{i,j-1}\ \tan(\overline{\theta-\mu})}{\tan\ (\overline{\theta-\mu}) - \tan\ (\overline{\theta+\mu})} \qquad (76)$$

$$\psi_{i,j}= \psi_{i,j-1} + (\rho_{i,j} - \rho_{i,j-1})\ \tan\ (\overline{\theta-\mu})$$

where

$$\tan(\overline{\theta+\mu})=\tfrac{1}{2}[\tan(\theta_{i+1,j}+\mu_{i+1,j})+\tan(\theta_{i,j}+\mu_{i,j})] \qquad (77)$$

and

$$\tan(\overline{\theta-\mu})=\tfrac{1}{2}[\tan(\theta_{i,j-1}-\mu_{i,j-1}) + \tan(\theta_{i,j}-\mu_{i,j})]$$

For the first approximation of these averages only the values at the known point are used. The order of computation is to start at the point i=N, j=N and to move

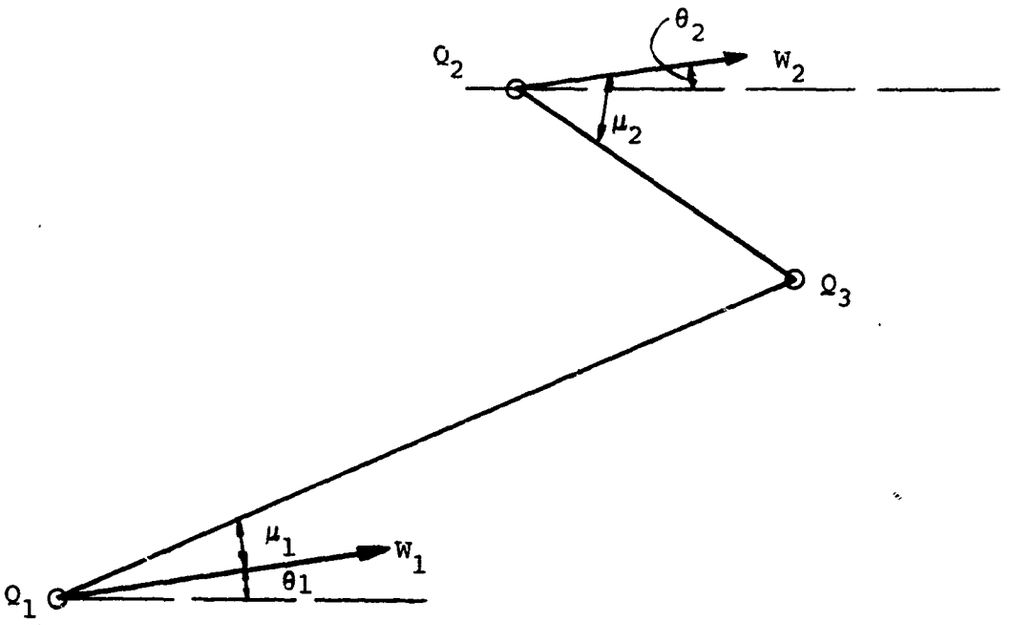

FIGURE 33 - CHARACTERISTIC UNIT PROBLEM

along second family characteristic lines, (i=const.), from the data line, toward the wall. This can be represented, in subscript form, by

$$i = N,\ N-1,\ N-2,\ldots 1$$

$$j = i,\ i+1,\ i+2,\ldots 2N-1$$

A wall point is obtained whenever i=2N-j. At these points $\psi_{i,j} = \theta_{i,j}=0$ and

$$\rho_{i,j}=\rho_{i,j-1} + \psi_{i,j-1} \left|\text{ctan}(\overline{\theta-\mu})\right| \tag{78}$$

where

$$\text{ctan}(\overline{\theta-\mu})=\tfrac{1}{2}[\text{ctan}(\theta_{i,j-1}-\mu_{i,j-1})-\text{ctan}\ \mu_{i,j}] \tag{79}$$

Eqs. (75) , solved for w and θ, give

$$w_{i,j} = \frac{1}{\Delta}\,(\Omega_{i+1,j} + \Omega_{i,j-1}) \tag{80}$$

$$\theta_{i,j}= \frac{1}{\Delta}\,[\Omega_{i,j-1}\left(\frac{\overline{\text{ctan}\mu_{i+1,j}}}{w_{i+1,j}}\right) - \Omega_{i+1,j}\left(\frac{\overline{\text{ctan}\mu_{i,j-1}}}{w_{i,j-1}}\right)] \tag{81}$$

where

$$\Omega_{i+1,j}= -\frac{2}{\overline{\gamma}-1}\,(\overline{\sin^2\mu_{i+1,j}\cos\mu_{i+1,j}})\,(\overline{\frac{ds}{dn}})_{i+1,j}$$
$$-\theta_{i+1,j}+w_{i+1,j}\left(\frac{\overline{\text{ctan}\mu_{i+1,j}}}{w_{i+1,j}}\right)$$

$$\Omega_{i,j-1}= \frac{2}{\overline{\gamma}-1}\,(\overline{\sin^2\mu_{i,j-1}\cos\mu_{i,j-1}})\,(\overline{\frac{ds}{dn}})_{i,j-1} \tag{82}$$
$$+\theta_{i,j-1}+w_{i,j-1}\left(\frac{\overline{\text{ctan}\mu_{i,j-1}}}{w_{i,j-1}}\right)$$

$$\Delta =\left(\frac{\overline{\text{ctan}\mu_{i+1,j}}}{w_{i+1,j}}\right) + \left(\frac{\overline{\text{ctan}\mu_{i,j-1}}}{w_{i,j-1}}\right)$$

and where

$$\bar{L}_{i+1,j}=[(\psi_{i,j}-\psi_{i+1,j})^2+(\rho_{i,j}-\rho_{i+1,j})^2]^{\frac{1}{2}}$$

$$\bar{L}_{i,j-1}=[(\psi_{i,j}-\psi_{i,j-1})^2+(\rho_{i,j}-\rho_{i,j-1})^2]^{\frac{1}{2}}$$

$$\left(\frac{ds}{dn}\right)=\frac{\bar{S}_{i,j-1}-\bar{S}_{i+1,j}}{\bar{L}_{i+1,j}(\overline{\sin\mu_{i+1,j}})+\bar{L}_{i,j-1}(\overline{\sin\mu_{i,j-1}})}$$

$$\overline{\sin\mu_{i+1,j}}=\tfrac{1}{2}(\sin\mu_{i+1,j}+\sin\mu_{i,j})$$

$$\overline{\sin\mu_{i,j-1}}=\tfrac{1}{2}(\sin\mu_{i,j-1}+\sin\mu_{i,j})$$

$$\overline{\sin^2\mu_{i+1,j}\cos\mu_{i+1,j}}=\tfrac{1}{2}(\sin^2\mu_{i+1,j}\cos\mu_{i+1,j}+\sin^2\mu_{i,j}\cos\mu_{i,j}) \qquad (83)$$

$$\overline{\sin^2\mu_{i,j-1}\cos\mu_{i,j-1}}=\tfrac{1}{2}(\sin^2\mu_{i,j-1}\cos\mu_{i,j-1}+\sin^2\mu_{i,j}\cos\mu_{i,j})$$

$$\left(\frac{\overline{\operatorname{ctan}\mu_{i+1,j}}}{w_{i+1,j}}\right)=\tfrac{1}{2}\left(\frac{\operatorname{ctan}\mu_{i+1,j}}{w_{i+1,j}}+\frac{\operatorname{ctan}\mu_{i,j}}{w_{i,j}}\right)$$

$$\left(\frac{\overline{\operatorname{ctan}\mu_{i,j-1}}}{w_{i,j-1}}\right)=\tfrac{1}{2}\left(\frac{\operatorname{ctan}\mu_{i,j-1}}{w_{i,j-1}}+\frac{\operatorname{ctan}\mu_{i,j}}{w_{i,j}}\right)$$

The Mach angle and the non-dimensionalized entropy are

$$\mu_{i,j}=\sin^{-1}\left[\left(\frac{\bar{\gamma}-1}{2}\,\frac{1-w_{i,1}^2}{w_{i,j}^2}\right)^{\frac{1}{2}}\right] \tag{84}$$

$$\bar{S}_{i,j}=\bar{S}_{i,j-1}-\frac{d\tilde{s}}{dn}\,\bar{L}_{i,j-1}\left(\overline{\sin\mu_{i,j-1}}\right) \tag{85}$$

At the wall, (i=2N-j), the flow properties are

$$w_{i,j}=w_{i,j-1}+\frac{1}{\left(\frac{\overline{\cot\mu_{i,j-1}}}{w_{i,j-1}}\right)}\left[\theta_{i,j-1}+\frac{2}{\bar{\gamma}-1}\right. \tag{86}$$

$$\left.\text{x}\ \left(\sin^2\mu_{i,j-1}\cos\mu_{i,j}\right)\left(\frac{d\tilde{s}}{dn}\right)\bar{L}_{i,j-1}\right] \tag{87}$$

where $\theta_{i,j}=0$

$$\left(\frac{d\tilde{s}}{dn}\right)=\frac{\bar{S}_{i,j-1}-\bar{S}_{N,N}}{\bar{L}_{i,j-1}\left(\overline{\sin\mu_{i,j-1}}\right)}$$

Since the wall is a streamline, the entropy has the constant value $S_{N,N}$ and the pressure distribution can be found from

$$\frac{p_{i,j}}{p_\infty}=\frac{p_{N,N}}{p_\infty}\left(\frac{1-w_{i,j}^2}{1-w_{N,N}^2}\right)^{\frac{\bar{\gamma}}{\bar{\gamma}-1}} \tag{88}$$

For this particular problem, $p_{N,N}/p_\infty$ is p_{4_1}/p_∞.

The program operation and example problems are given in Appendices V and VI.

D Intersection of Two Conical Shocks of Different Strengths

D-1 Conical Flow Fields

The problem examined here is the flow field immediately behind the intersection of two conical shocks of different strength. The conical shocks are generated by two unequal cones, one of which is at a small angle of attack with respect to the free-stream velocity. The cone axes are assumed to be in a plane. These assumptions, which simplify the analytical solution of the problem, are consistent with common geometrical configurations of inlets.

The analysis includes the definition of the intersection curve between the two conical shocks, the definition of an orthogonal reference frame attached to the intersection curve, and the use of the two-dimensional oblique shock relations in the plane defined by the normal and binormal to the intersection curve.

In the analysis that follows, the cone with the axis parallel to the free-stream direction will be denoted as the "base cone" while the designation "second cone" will be used for the cone at a small angle of attack.

The flow fields of the two conical bodies are found first. For the base cone, the velocity along a conical ray line (γ = const.) in a spherical coordinate system, and the speed of sound nondimensionalized with respect to the limiting velocity are respectively[15]

$$u = \sqrt{\frac{\bar{\gamma}-1}{\bar{\gamma}+2}} \quad \frac{M_1^*}{\sqrt{1+\tan^2(\psi_1^*-\gamma)}}$$

$$a = \frac{\bar{\gamma}-1}{2}\left(1-\frac{\bar{\gamma}-1}{\bar{\gamma}+1} M_1^{*2}\right)^{\frac{1}{2}} \qquad (89)$$

where M_1^* and ψ_1^*, which represent the critical Mach number and the flow direction, are tabulated in Ref.15. The Mach number components along and normal to the conical ray line γ =const. become (Fig.34)

$$M_r = u/a$$
$$M_t = M_r \tan(\psi_1^* - \gamma) \tag{90}$$

The effect of a small angle of attack on the conical flow field can be considered as a perturbation of the flow conditions for no angle of attack. It has been shown in Ref. 11 that a circular cone at a small angle of attack produces a circular conical shock having the same half angle as the shock which would be produced by the same concial body at no angle of attack, but inclined slightly with respect to the free stream direction in the plane containing the body axes (z^*) and the free-stream velocity vector, Fig.35. Therefore, the total nondimensional velocity components in a cylindrical coordinate system u, v, and w, along the z axis, along the r axes and normal to the meridian plane respectively, may be defined by (16)

$$u_i = u_1 \cos\gamma - v_1 \sin\gamma + \alpha u_2 \cos\varphi_i$$
$$\bar{v}_i = v_1 \cos\gamma + u_1 \sin\gamma + \alpha v_2 \cos\varphi_i \tag{91}$$
$$w_i = \alpha w_2 \sin\varphi_i$$

where φ_i is the meridian angle defined in Fig.35, which is incorrectly defined in Ref. 16. The velocity components u_1 and v_1 are the zero-angle of attack values along and normal to the conical ray $\gamma = \gamma_2$, where γ_2 is the shock angle, and are given by

$$u_1 = \sqrt{\frac{\bar{\gamma}-1}{\bar{\gamma}+1}}\, M^*_{1,2} \quad \frac{1}{\sqrt{1+\tan^2(\psi^*_{1,2}-\gamma_2)}} \tag{92}$$
$$v_1 = u_1 \tan(\psi^*_{1,2}-\gamma_2)$$

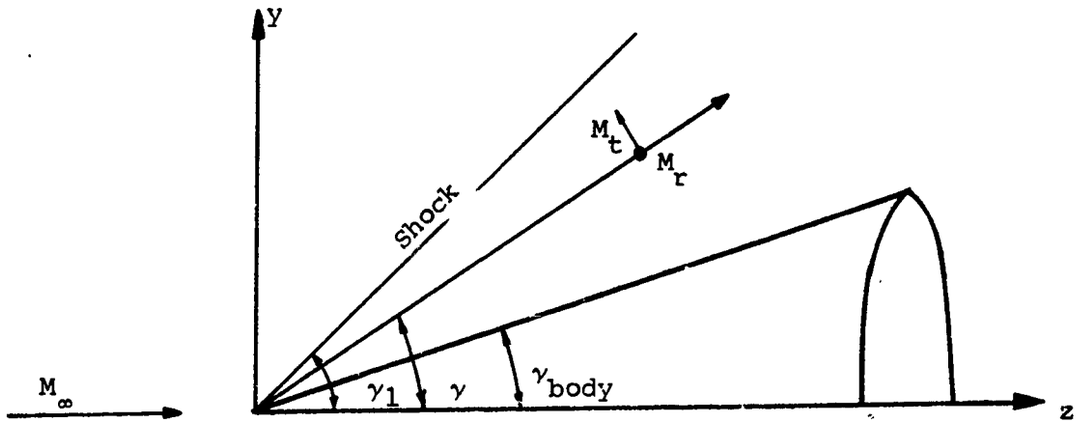

FIGURE 34 - BASE CONE FLOW

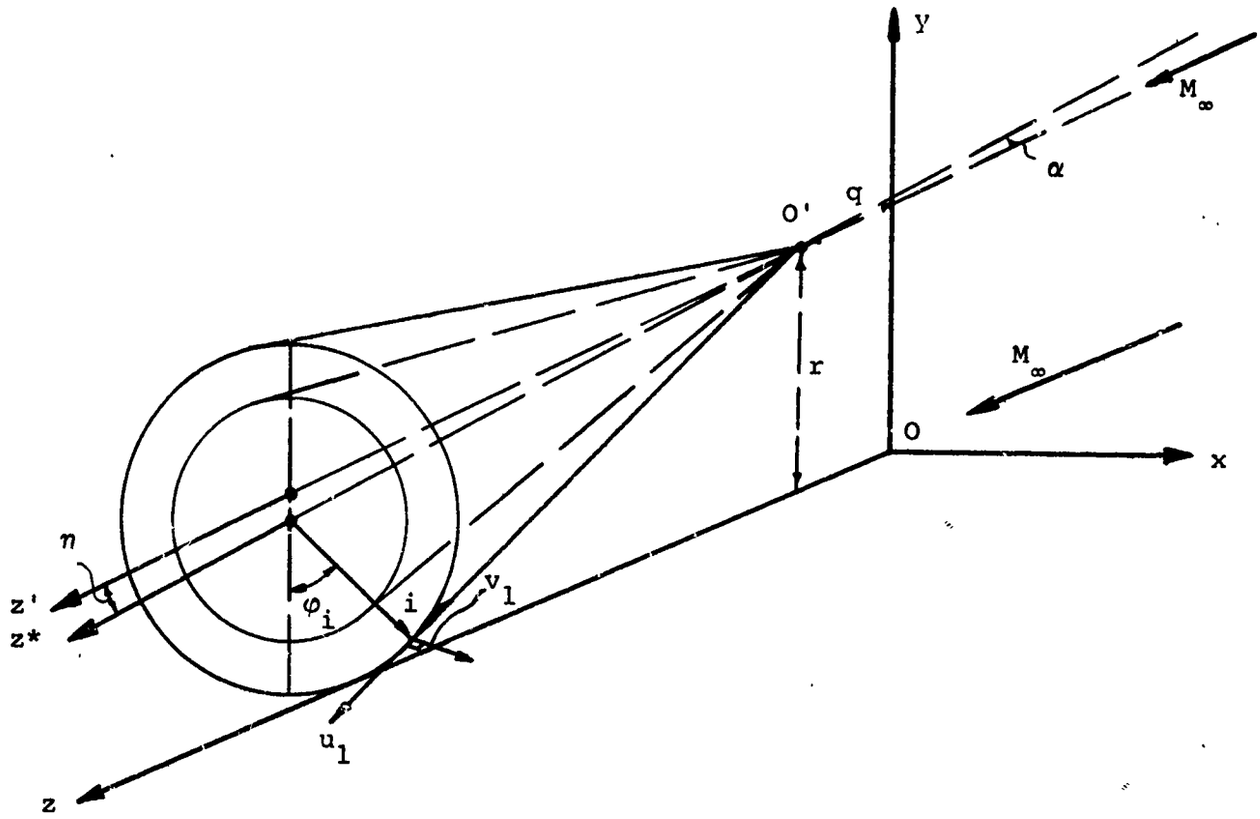

FIGURE 35 - SECOND CONE FLOW

where $M^*_{1,2}$ and $\psi^*_{1,2}$ are the critical Mach number and the flow direction of the second cone flow with no angle of attack. The perturbation velocities derived from Ref.16 are

$$u_2 = \sqrt{\frac{\bar{\gamma}-1}{\bar{\gamma}+1}}\left[- M^*_{1,2}\ \psi_2^*\ \sin\ \psi^*_{1,2} + M^*_2\ \cos\ \psi^*_{1,2} \right]$$

$$v_2 = \sqrt{\frac{\bar{\gamma}-1}{\bar{\gamma}+1}}\left[M^*_{1,2}\ \psi_2^*\ \cos\ \psi^*_{1,2} + M^*_2\ \sin\ \psi^*_{1,2} \right] \qquad (93)$$

$$w_2 = \sqrt{\frac{\bar{\gamma}-1}{\bar{\gamma}+2}}\quad M^*_{w,2}$$

where the flow direction ψ^*_2 and the critical Mach numbers M^*_2 and $M^*_{w,2}$ are tabulated in Ref. 16.

To complete the definition of the flow field of the second cone, the local speed of sound and the second cone shock axis inclination must be defined. The speed of sound non-dimensionalized with respect to the limiting velocity, is

$$a_{2i} = \sqrt{\frac{\bar{\gamma}-1}{2}}\left[1- \frac{\bar{\gamma}-1}{\bar{\gamma}+1}\ M^{*2}_i \right]^{\frac{1}{2}} \qquad (94)$$

where the total critical Mach number M^*_i, is

$$M^*_i = M^*_{1,2} + \alpha\ M^*_2\ \cos\ \varphi_i \qquad (95)$$

The inclination of the shock axis with respect to the free-stream direction is given by

$$\theta_1 = \alpha\ (1-\eta/\alpha) \qquad (96)$$

where η/α, tabulated in Ref.16, represents the ratio between the deviation of the shock axes from the cone axis and the angle of attack (Fig.36).

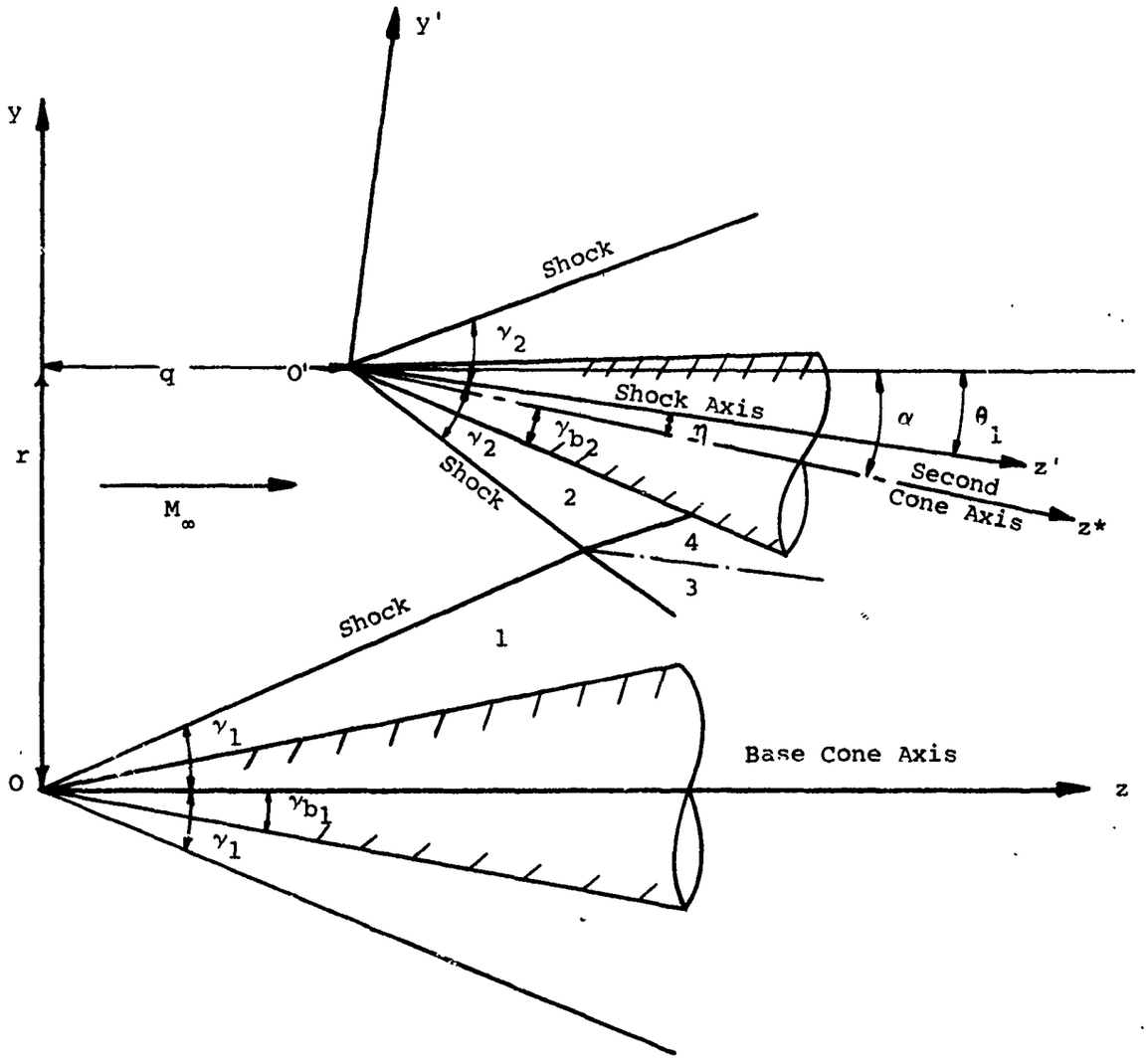

FIGURE 36 - CONICAL-CONICAL SHOCK INTERSECTION

D-2 Shock Intersection

In the preceding section, the conical flow fields have been defined. In order to calculate the flow field behind the intersection of the two conical shocks, it is first necessary to determine the intersection curve. On the base cone a conical coordinative system, ρ, ψ is defined as shown in Fig. 37. The intersection curve of the base cone shock, of angle ν_1, and the second cone shock, of angle ν_2, whose axis is inclined by an angle θ_1 to the free stream direction, is represented in this coordinate system by

$$\frac{1}{\rho_i} = -(D_1 + C_1 \cos\psi_i) + \left[(D_1 + C_1 \cos\psi_i)^2 - (A_1 \cos^2\psi_i + 2E_1 \cos\psi_i + B_1)\right]^{\frac{1}{2}} \tag{97}$$

where

$$\begin{aligned} A_1 &= \left[(a_2-1)\sin^2\gamma_1\right]/F_1 \\ B_1 &= \left[(c_2+b_1^2)\cos^2\gamma_1\right]/F_1 \\ C_1 &= \left[(e_2 b_2^2 \sin\theta_1 - d_2\cos\theta_1)\sin\nu_1\right]/F_1 \\ D_1 &= -\left[(e_2 b_2^2 \cos\theta_1 + d_2 \sin\theta_1)\cos\nu_1\right]/F_1 \\ E_1 &= (f_2 \sin\gamma_1 \cos\gamma_1)/F_1 \end{aligned} \tag{98}$$

and where

$$\begin{aligned} b_1^2 &= \tan^2\nu_1 \\ b_2^2 &= \tan^2\nu_2 \\ a_2 &= \cos^2\theta_1 - b_2^2 \sin^2\theta_1 \\ c_2 &= \sin^2\theta_1 - b_2^2 \cos^2\theta_1 \\ d_2 &= r\cos\theta_1 + q\sin\theta_1 \\ e_2 &= r\sin\theta_1 - q\cos\theta_1 \\ f_2 &= \cos\theta_1 \sin\theta_1 (1+b_2^2) \\ F_1 &= d_2^2 - b_2^2 e_2^2 \end{aligned} \tag{99}$$

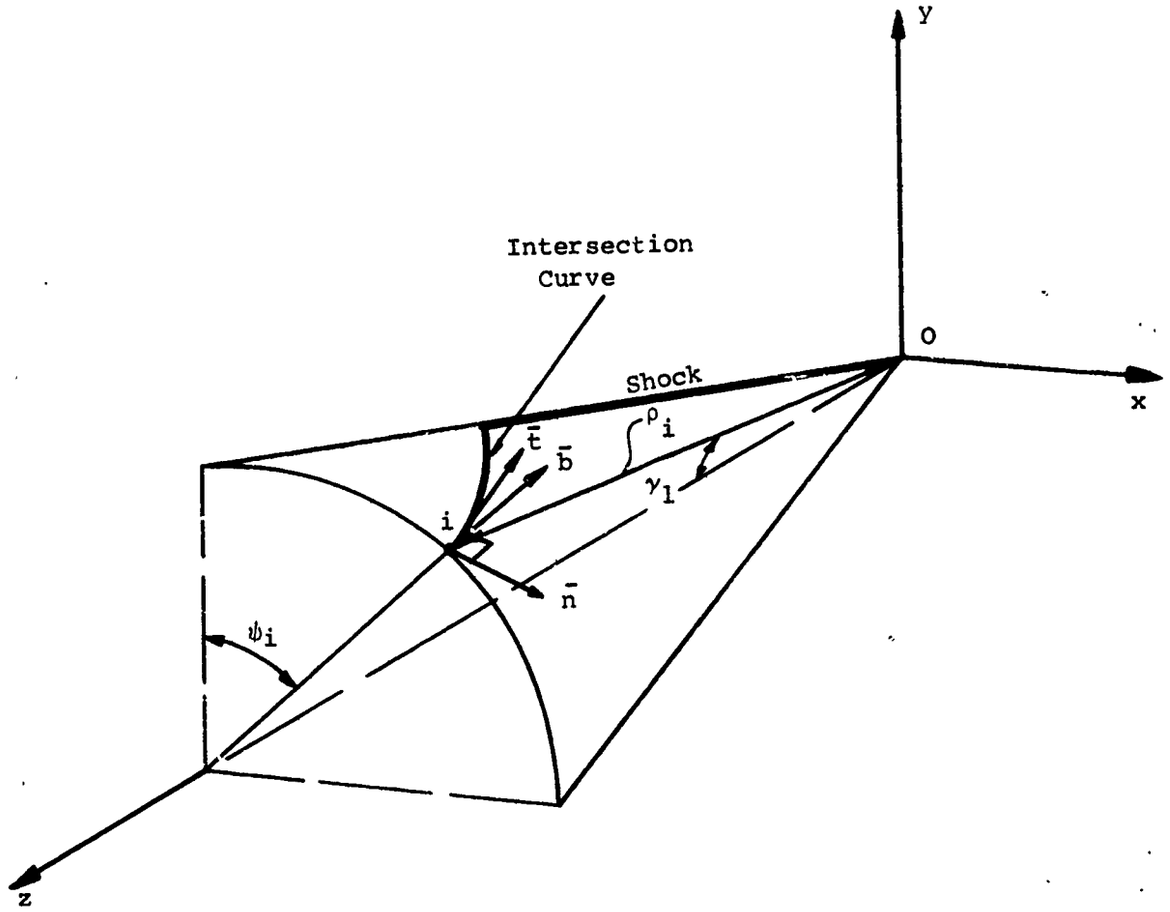

FIGURE 37 - BASE CONE COORDINATES

The curve is computed by inserting values of ψ_i given by, $\psi_i = i\Delta\psi, i=0,1,2\cdots\psi_{max}/\Delta\psi$ into Eq.(97) where ψ max. represents the furthest point out on the intersection curve, before the curve bends in again

$$\psi_{max} = \cos^{-1}\left[\frac{D_1C_1-E_1}{C_1^2-A_1} + \sqrt{\left(\frac{D_1C_1-E_1}{C_1^2-A_1}\right)^2 - \frac{D_1^2-B_1}{C_1^2-A_1}}\right]$$

In order to determine the planes normal to the tangent to the intersection curve, the direction cosines of the tangent, bi-normal and normal with respect to the x-y-z directions must be found. Following the procedure of Ref.17, the direction cosines of the tangents to the intersection curve are found as

$$\begin{aligned}
\cos(\hat{tx})_i &= \sin\gamma_1\ (\rho_i' \sin^2\psi_i - \rho_i \cos\psi_i)/\Delta_i^* \\
\cos(\hat{ty})_i &= \sin\gamma_1 \sin\psi_i(\rho_i' \cos\psi_i+\rho_i')/\Delta_i^* \\
\cos(\hat{tz})_i &= \rho_i' \cos\gamma_1 \sin\psi_i/\Delta_i^*
\end{aligned} \tag{100}$$

where

$$\rho_i' = -\frac{1}{\sin\psi_i}\left(\frac{\partial\rho}{\partial\psi}\right)_i = \rho_i^2\left[C_1 - \frac{(C_1^2-A_1)\cos\psi_i+D_1C_1-E_1}{\sqrt{(C_1^2-A_1)\cos^2\psi_i+2(D_1C_1-E_1)\cos\psi_i+D_1^2-B_1}}\right] \tag{101}$$

and

$$\Delta_i^* = \left[(\rho_i')^2 \sin^2\psi_i+\rho_i^2 \sin^2\gamma_1\right]^{\frac{1}{2}} \tag{102}$$

The bi-normal to the curve is the normal to the plane tangent to the cone at the generic point i, and the direction cosines are given by

$$\begin{aligned}
\cos(\hat{bx})_i &= \cos\gamma_1 \sin\psi_i \\
\cos(\hat{by})_i &= \cos\gamma_1 \cos\psi_i \\
\cos(\hat{bz})_{any\,i} &= -\sin\gamma_1
\end{aligned} \tag{103}$$

Finally, the vector normal to the curve can be found from the vector product $\bar{n} = \bar{t} \times \bar{b}$ and lies on the plane

tangent to the cone at the generic point i. Its direction cosines are

$$\begin{aligned}
\cos(\hat{nx})_i &= \cos(\hat{ty})_i \cos(\hat{bz})_i - \cos(\hat{tz})_i \cos(\hat{by})_i \\
\cos(\hat{ny})_i &= \cos(\hat{tz})_i \cos(\hat{bx})_i - \cos(\hat{tx})_i \cos(\hat{bz})_i \\
\cos(\hat{nz})_i &= \cos(\hat{tx})_i \cos(\hat{by})_i - \cos(\hat{ty})_i \cos(\hat{bx})_i
\end{aligned} \tag{104}$$

The Mach number components, immediately behind the base cone shock ($\gamma=\gamma_1$), in the $\bar{t}$, $\bar{b}$ and $\bar{n}$ directions are from Eq. (89) and (90).

$$\begin{aligned}
M_{\bar{t}_{1_i}} &= M_{x_{1_i}} \cos(\hat{tx})_i + M_{y_{1_i}} \cos(\hat{ty})_i + M_{z_{1_i}} \cos(\hat{tz})_i \\
M_{\bar{n}_{1_i}} &= M_{x_{1_i}} \cos(\hat{nx})_i + M_{y_{1_i}} \cos(\hat{ny})_i + M_{z_{1_i}} \cos(\hat{nz})_i \\
M_{\bar{b}_{1_i}} &= M_{x_{1_i}} \cos(\hat{bx})_i + M_{y_{1_i}} \cos(\hat{by})_i + M_{z_{1_i}} \cos(\hat{bz})_i
\end{aligned} \tag{105}$$

where

$$\begin{aligned}
M_{x_{1_i}} &= (M_r \sin\gamma_1 + M_t \cos\gamma_1) \sin\psi_i \\
M_{y_{1_i}} &= (M_r \sin\gamma_1 + M_t \cos\gamma_1) \cos\psi_i \\
M_{z_{1_i}} &= M_r \cos\gamma_1 - M_t \sin\gamma_1
\end{aligned} \tag{106}$$

The Mach number component and the flow deviation in the plane normal to the tangent to the intersection curve are

$$M_{N_{1_i}} = (M_{\bar{n}_{1_i}}^2 + M_{\bar{b}_{1_i}}^2)^{\frac{1}{2}} \tag{107}$$

$$\delta_{1_i} = \left| \Gamma_i - \tan^{-1} \left(\frac{M_{\bar{b}_{1_i}}}{M_{\bar{n}_{1_i}}} \right) \right| \tag{108}$$

where Γ_i, which represents the angle between the direction of the free-stream Mach number and the normal ($\bar{n}$) to the intersection curve at each point i in this plane, is given by

$$\Gamma_i = \tan^{-1} \left[\frac{\cos(\hat{bz})_i}{\cos(\hat{nz})_i} \right] \tag{109}$$

For the second cone, a similar procedure is carried out to find the Mach number components along the $\bar{t}$, $\bar{b}$, and $\bar{n}$ directions, when the value of φ_i, corresponding to the generic point i of the intersection curve, is known. The coordinates of the generic point ρ_i, ψ_i in the x',y', directions (Fig. 36) are

$$x'_i = \rho_i \sin\psi_i \sin\gamma_1$$

$$y'_i = (\rho_i \cos\psi_i \sin\gamma_1 - r) \cos\alpha + (\rho_i \cos\gamma_1 - q) \sin\alpha \tag{110}$$

from which

$$\varphi_i = \tan^{-1}\left|\frac{x'_i}{y'_i}\right| \tag{111}$$

For the second cone, the relations corresponding to equations (105) become from equations (91), (94), and (111) with $\gamma = \gamma_2$

$$\begin{aligned} M_{\bar{t}_{2_i}} &= M_{x_{2_i}} \cos(\hat{tx})_i + M_{y_{2_i}} \cos(\hat{ty})_i + M_{z_{2_i}} \cos(\hat{tz})_i \\ M_{\bar{n}_{2_i}} &= M_{x_{2_i}} \cos(\hat{nx})_i + M_{y_{2_i}} \cos(\hat{ny})_i + M_{z_{2_i}} \cos(\hat{nz})_i \\ M_{\bar{b}_{2_i}} &= M_{x_{2_i}} \cos(\hat{bx})_i + M_{y_{2_i}} \cos(\hat{by})_i + M_{z_{2_i}} \cos(\hat{bz})_i \end{aligned} \tag{112}$$

where

$$\begin{aligned} M_{x_{2_i}} &= \frac{\bar{v}_i}{a_{2_i}} \sin\varphi_i + \frac{\bar{w}_i}{a_{2_i}} \cos\varphi_i \\ M_{y_{2_i}} &= \left(-\frac{\bar{v}_i}{a_{2_i}} \cos\varphi_i + \frac{\bar{w}_i}{a_{2_i}} \sin\varphi_i\right) \cos\alpha - \frac{\bar{u}_i}{a_{2_i}} \sin\alpha \\ M_{z_{2_i}} &= \left(-\frac{\bar{v}_i}{a_{2_i}} \cos\varphi_i + \frac{\bar{w}_i}{a_{2_i}} \sin\varphi_i\right) \sin\alpha + \frac{\bar{u}_i}{a_{2_i}} \cos\alpha \end{aligned} \tag{113}$$

The Mach number component and the flow deviation in the plane normal to the tangent to the intersection curve are represented, similar to Eqs. (107) and (108) by

$$M_{N_{2_i}} = \left[(M_{\bar{n}_{2_i}})^2 + (M_{\bar{b}_{2_i}})^2 \right]^{\frac{1}{2}} \tag{114}$$

$$\delta_{2_i} = \left| \tau_i - \tan^{-1} \left(\frac{\bar{M}_{t_{2_i}}}{\bar{M}_{n_{2_i}}} \right) \right| \tag{115}$$

The oblique shock relations in the plane normal to the tangent to the intersection curve are used to find the flow conditions at each point i, immediately behind the intersection of the two shocks, which due to the conical nature of the flow field, remain valid only in the immediate vicinity of the point. In this present work, the flows of the base cone and the second cone are considered to be deflected by the angles δ_{2_i} and δ_{1_i} respectively. Using the oblique shock relations with $M_{N_{1_i}}$ and δ_{2_i}, the Mach number behind the shock M_B, the shock angle θ and the pressure and speed of sound ratios P_2/P_1, A_2/A_1 are found for the lower portion of the intersection. The total Mach number behind the shock intersection is

$$M_{3_i} = (M_{3_{t_i}}^2 + M_{B_{1_i}}^2)^{\frac{1}{2}} \tag{116}$$

where $M_{3_{t_i}} = \bar{M}_{t_{1_i}} / (A_2/A_1)_i$ (117)

The total pressure ratio and the total entropy change are

$$(p_3/p_\infty)_i = \left(\frac{P_2}{P_1}\right)_i \frac{P_1}{P_\infty} \tag{118}$$

$$S_{3_i} = \frac{\bar{\gamma}-1}{2\bar{\gamma}} \frac{S_1}{R} + \frac{1}{2\bar{\gamma}} \left\{ \ell n \left[\frac{2\bar{\gamma} M_{N_{1_i}}^2 \sin^2\theta_{3_i} - (\bar{\gamma}-1)}{\bar{\gamma}+1} \right] - \bar{\gamma}\, \ell n \left[\frac{(\bar{\gamma}+1) M_{N_{1_i}}^2 \sin^2\theta_{3_i}}{(\bar{\gamma}-1) M_{N_{1_i}}^2 \sin^2\theta_{3_i} + 2} \right] \right\} \tag{119}$$

where p_1/p_∞ and S_1/R are the values immediately behind the base cone shock.

Using $M_{N_{2_i}}$ and δ_{1_i}, the upper portion of the flow behind the shock intersection is calculated in a similar manner from the oblique shock relations. The flow properties immediately behind the shock are

$$M_{4_{t_i}} = M_{t_{2_i}} / (A_2/A_1)_i \tag{120}$$

$$M_{4_i} = (M_{4_{t_i}}^2 + M_{B_{2_i}}^2)^{-} \tag{121}$$

$$\frac{p_{4_i}}{p_\infty} = \left(\frac{p_2}{p_1}\right)_i \frac{p_2}{p_\infty} \left[\frac{(\bar{\gamma}+1) - (\bar{\gamma}-1)(M^*_{1,2} + \alpha M^*_2 \cos\phi_i)^2}{(\bar{\gamma}+1) - (\bar{\gamma}-1)(M^*_{1,2})^2} \right]^{\frac{\bar{\gamma}}{\bar{\gamma}-1}} \cdot e^{-\frac{S_2}{R} \alpha \cos\phi_i} \tag{122}$$

$$S_{4_i} = \frac{\bar{\gamma}-1}{2\bar{\gamma}} \left(\frac{S_{1,2}}{R} + \alpha \frac{S_2}{R} \cos\phi_i\right) + \frac{1}{2\bar{\gamma}} \left\{ \ell n \left[\frac{2\bar{\gamma} M_{N_{2_i}}^2 \sin^2\theta_{4_i} - (\bar{\gamma}-1)}{\bar{\gamma}+1} \right] - \bar{\gamma}\, \ell n \left[\frac{(\bar{\gamma}+1) M_{N_{2_i}}^2 \sin^2\theta_{4_i}}{(\bar{\gamma}-1) M_{N_{2_i}}^2 \sin^2\theta_{4_i} + 2} \right] \right\} \tag{123}$$

The last two expressions contain factors which represent the contribution of the angle of attack of the second cone. In the present analysis, the shock strengths have been assumed to be constant through the intersections. An iterative procedure can be used to improve the results. The iteration consists of varying the flow deviations δ_{1_i} and δ_{2_i} until the pressures in the lower and upper region behind the shock intersection are matched.

In order to define the flow field behind the shock intersection, the characteristic subroutine can be used in a plane which contains the projection of the intersection curve. This curve becomes the data line and the flow properties immediately behind it are obtained by averaging the values in the upper and lower regions and finding the flow deviation in this plane from the projections of the normal and tangent Mach number components.

The program operation and example problems are given in Appendix V and VI.

E. Impingement of a Plane Shock On a Conical Surface

The impingement of a plane shock from a two-dimensional wedge of angle δ_1 on a conical body is treated here. In order to treat the most general case, the shock of the conical body is included (Fig. 38). The intersection of the conical and plane shocks is found first. After the plane shock passes through the conical shock it is no longer planar, due to the effects of the conical flow field. The local inclination of this shock can be found by using variations in the conical field between the conical shock and the cone surface as shown by dashed lines in Figure . In this analysis the computation is carried out only at the cone shock and at the cone surface. The properties obtained by crossing the "plane" shock at the cone surface are used in the manner discussed in the preceding sections to obtain the shock reflected from the cone surface. The flow field behind the reflected shock is found by using the Characteristic Subroutine after transforming the reflection curve, which lies on the cone body, into a curve on a plane.

The computation starts by using oblique shock theory for the given wedge angle, δ_1, and free stream Mach number to obtain

$$M_1,\ \theta_1,\ p_1/p_\infty \text{ and } a_1/a_\infty$$

which represent the uniform flow properties behind the plane shock. As in the previous sections, the conical field of the cone at zero-angle of attack is defined by imputing the parameters, γ_c, $M^*_{1_c}$, ψ_{1_c}, p_c/p_∞, T_c/T_∞ and S_2/R behind the conical shock and γ_b, $M^*_{1_b}$, ψ_{1_b}, p_b/p_∞ on the body (see Ref. 15). This data allows the conical flow properties to be computed. The Mach number components along and normal to the conical ray γ = const.are

$$M_r = u/a$$
$$M_t = M_r \tan(\psi_1 - \gamma) \qquad (124)$$

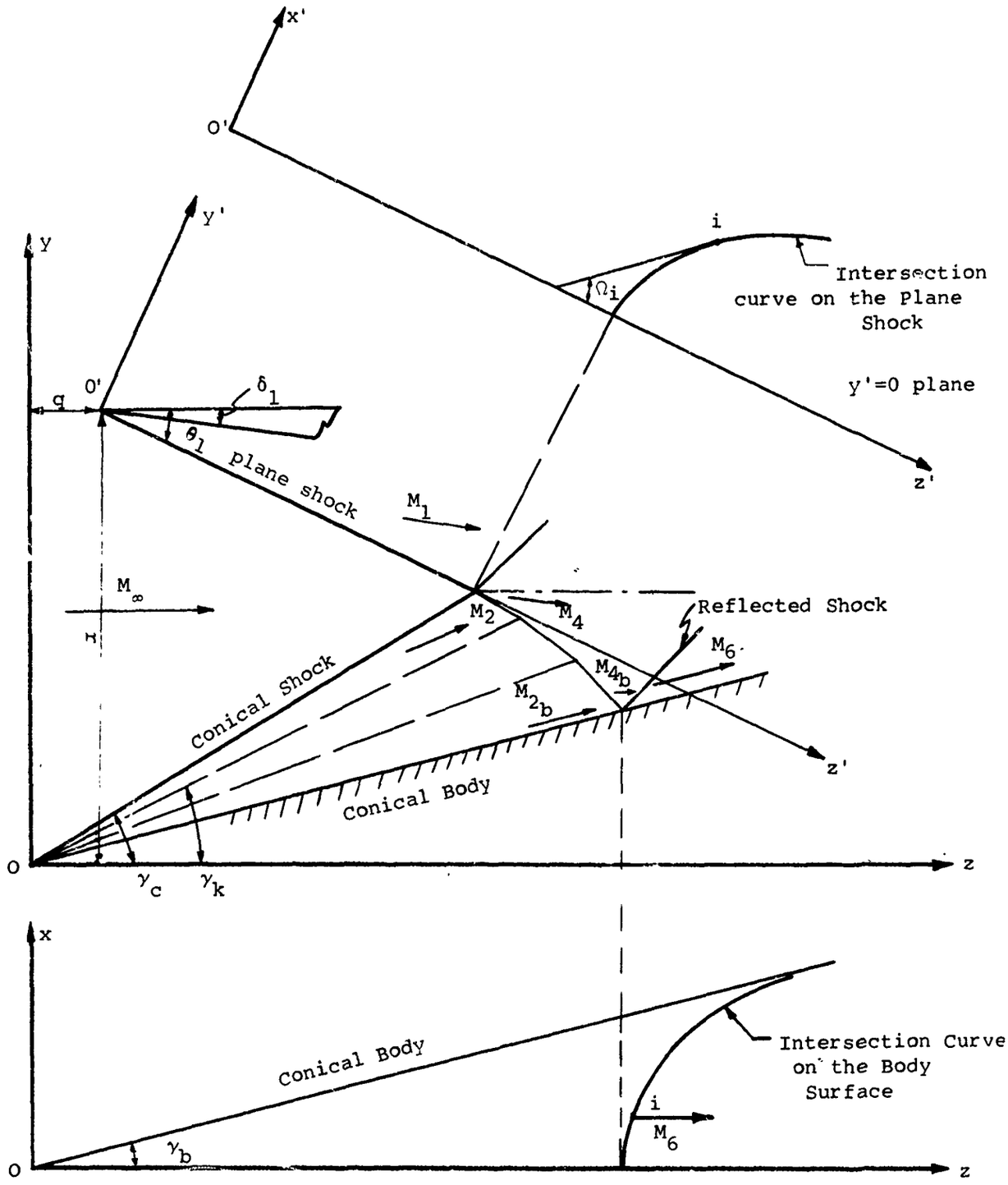

FIGURE 38 - CONICAL BODY-PLANE SHOCK CONFIGURATION

where

$$u = \sqrt{\frac{\bar{\gamma}-1}{\bar{\gamma}+1}}\, M_1^* \cos(\psi_1 - \nu) \tag{125}$$

$$a = \sqrt{\frac{\bar{\gamma}-1}{2}}\ \sqrt{1 - \frac{\bar{\gamma}-1}{\bar{\gamma}+1} M_1^{*2}}$$

The intersection of the conical shock and the plane shock on the z'-x' plane, (Fig. 38), is given by

$$x'_i = \left\{ - (Az'^2_i - 2Bz'_i + C) \right\}^{\frac{1}{2}} \tag{126}$$

where

$$A = \sin^2\theta_1 - b^2 \cos^2\theta_1$$

$$B = r \sin\theta_1 + b^2 q \cos\theta_1 \tag{127}$$

$$C = r^2 - b^2 q^2$$

$$b^2 = \tan^2\gamma c$$

and where z'_i is obtained by incrementing from the value of z' corresponding to x' = 0 (z'_o) and is given by

$$z'_i = z'_o + i\ \Delta z' \tag{128}$$

The angle between the tangent to the intersection curve and the z'-axis is

$$\Omega_i = \tan^{-1} \left| \frac{B - Az'_i}{x'_i} \right| \tag{129}$$

The computationof the intersection is terminated when $\Omega_i < 5^\circ$ in order to work on one side of the cone. The conical flow Mach number components immediately behind the shock, $(\gamma = \gamma_c)$, in the x'-y'-z' directions are

$$\begin{aligned}
M_{2_{x'_i}} &= M_r \sin\gamma_c \sin\varphi_i + M_t \cos\gamma_c \sin\varphi_i \\
M_{2_{y'_i}} &= M_r (\sin\gamma_c \cos\varphi_i \cos\theta_1 + \cos\gamma_c \sin\theta_1) \\
&\quad + M_t (\cos\gamma_c \cos\varphi_i \cos\theta_1 - \sin\gamma_c \sin\theta_1) \\
M_{2_{z'_i}} &= M_r (\cos\gamma_c \cos\theta_1 - \sin\gamma_c \cos\varphi_i \sin\theta_1) \\
&\quad - M_t (\cos\gamma_c \cos\varphi_i \sin\theta_1 + \sin\gamma_c \cos\theta_1)
\end{aligned} \tag{130}$$

where the meridian angle φ_i is

$$\varphi_i = \tan^{-1} \left(\frac{x_i}{y_i} \right) \tag{131}$$

with

$$\begin{aligned}
x_i &= x'_i \\
y_i &= q + z'_i \sin\theta_1
\end{aligned} \tag{132}$$

Equations (130) projected along the normal and the tangent to the intersection curve with z', x' plane become

$$\begin{aligned}
M_{2_{n_i}} &= M_{2_{z'_i}} \sin\Omega_i - M_{2_{x'_i}} \cos\Omega_i \\
M_{2_{t_i}} &= -M_{2_{z'_i}} \cos\Omega_i - M_{2_{x'_i}} \sin\Omega_i
\end{aligned} \tag{133}$$

With the total Mach number component in the generic plane normal to the intersection curve at point i given by

$$M_{2_{N_i}} = (M_{2_{y'_i}}^2 + M_{2_{n_i}}^2)^{\frac{1}{2}} \tag{134}$$

and the strength of the plane shock given by,

$$\delta_{1_i}^* = \tan^{-1}\left(\frac{\tan\theta_1}{\sin\Omega_1}\right) - \tan^{-1}\left[\frac{\tan(\theta_1-\delta_1)}{\sin\Omega_i}\right] \tag{135}$$

the oblique shock relations can be used to find the flow properties behind the lower region of the shock intersection. The properties thus found are the Mach number component $M_{4_{N_i}}$, the shock angle, θ_{4_i}, in the plane normal to the intersection curve and the pressure and speed of sound ratios $(P_4/P_2)_i$ and $(a_4/a_2)_i$, respectively. The tangent Mach number component $M_{4_{t_i}}$, the total Mach number M_{4_i}, the pressure ratio $(p_4/p_\infty)_i$, the speed of sound ratio $(a_4/a_\infty)_i$ and the change of entropy S_{4_i} are respectively

$$M_{4_{t_i}} = M_{2_{t_i}} \left(\frac{a_2}{a_4}\right)_i \tag{136}$$

$$M_{4_i} = \left\{ (M_{4_{N_i}})^2 + (M_{4_{t_i}})^2 \right\}^{\frac{1}{2}}$$

$$(p_4/p_\infty)_i = (P_4/P_2)_i \ (p_c/p_\infty)$$

$$(a_4/a_\infty)_i = (a_4/a_2)_i \ \sqrt{T_c/T_\infty}$$

$$S_{4_i} = \frac{1}{2\bar{\gamma}} \left\{ (\bar{\gamma}-1)\frac{S_2}{R} + \left[\ln\left(\frac{2\bar{\gamma} M_{2_{N_i}}^2 \sin^2\theta_{4_i} - (\bar{\gamma}-1)}{\bar{\gamma}+1} \right) - \bar{\gamma} \ln\left(\frac{(\bar{\gamma}+1) M_{2_{N_i}}^2 \sin^2\theta_{4_i}}{(\bar{\gamma}-1) M_{2_{N_i}}^2 \sin^2\theta_{4_i} + 2} \right) \right] \right\}$$

The flow deviation with respect to the z' axis is

$$\sigma_{4_i} = \Omega_i - \tan^{-1}\left| \frac{M_{4_{N_i}}}{M_{4_{t_i}}} \right| \tag{137}$$

For the eventual computation of the upper intersection region it will be useful to know the strength of the conical shock, which is

$$\delta_{2_i}^{*} = \tan^{-1}\left(\frac{M_{2_{y'_i}}}{M_{2_{n_i}}}\right) - \tan^{-1}\left(\frac{\tan\theta_1}{\sin\Omega_i}\right) \tag{138}$$

In each plane normal to the intersection curve a new orthogonal coordinate system, (ζ,η), is defined, in which ζ is in the x'-z' plane and is coincident with the normal direction previously defined, (Fig. 39). The angle of the lower shock, referred to the ζ axis, is

$$\theta'_{4_i} = \theta_{4_i} - \tan^{-1}\left(\frac{M_{2_{y'_i}}}{M_{2_{n_i}}}\right) \tag{139}$$

For each normal plane the point η_{i_1}, ζ_{i_1} of intersection between the shock and the conical body is found from the following;

$$\eta_{i_1} = -\frac{Q}{P} + \sqrt{\left(\frac{Q}{P}\right)^2 - \frac{N}{P}} \tag{140}$$

$$\zeta_{i_1} = -\eta_{i_1}\,\text{cotan}\left|\theta'_{4_i}\right|$$

where

$$\begin{aligned} P &= L + e_1\,(E\,e_1 + 2\,G) \\ Q &= e_1\,F + H \end{aligned} \tag{141}$$

and where

$$\begin{aligned} E &= \cos^2\Omega_i + \sin^2\Omega_i(\sin^2\theta_1 - b^2\cos^2\theta_1) \\ F &= -x_i'\cos\Omega_i - (F_1\sin\theta_1 + b^2 F_2\cos\theta_1)\sin\Omega_i \\ G &= -\sin\theta_1\cos\theta_1\sin\Omega_i\,(1+b^2) \\ H &= F_1\cos\theta_1 - b^2 F_2\sin\theta_1 \\ L &= \cos^2\theta_1 - b^2\sin^2\theta_1 \end{aligned} \tag{142}$$

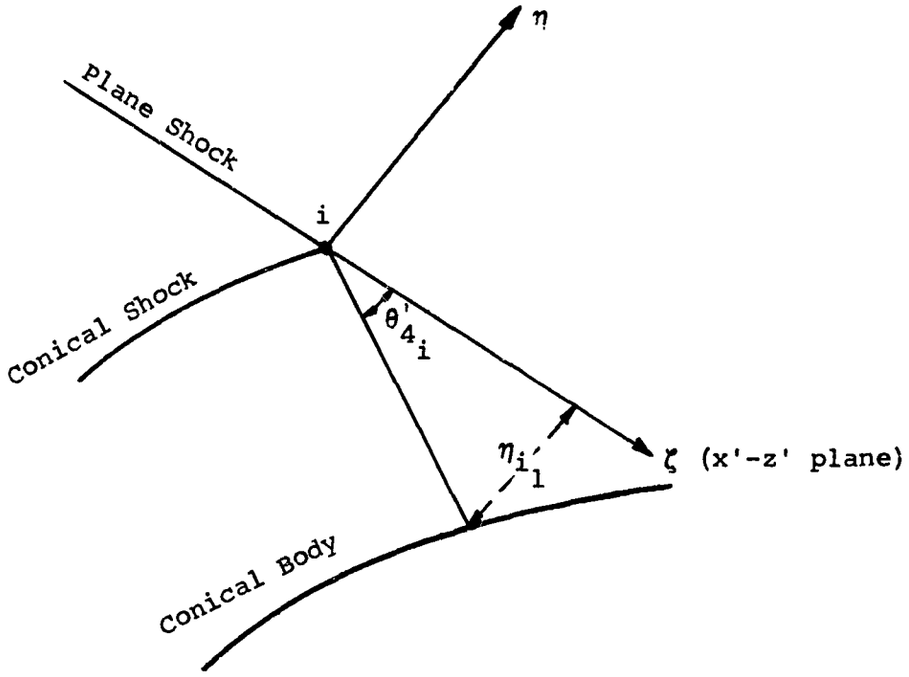

FIGURE 39 - GENERIC PLANE NORMAL TO THE INTERSECTION CURVE

$$N = (x_i')^2 + F_1^2 - b^2 F_2^2$$

$$F_1 = r - z_i' \sin\theta_1 \tag{143}$$

$$F_2 = q + z_i' \cos\theta_1$$

$$e_1 = -\text{cotan} \left| \theta_{4_i}' \right|$$

The coordinates of these intersection points on the body are transformed into a conical coordinate system, ρ, φ, which represents the polar distance from the conical body apex and the meridian angle in the z = constant plane, respectively, (see Fig. 40). This transformation is given by

$$\rho_i = + \left\{ x_{i_1}^2 + y_{i_1}^2 + z_{i_1}^2 \right\}^{\frac{1}{2}}$$

$$\varphi_i = \tan^{-1} \left| x_{i_1} / y_{i_1} \right| \tag{144}$$

where

$$x_{i_1} = x_i' - \zeta_{i_1} \cos \Omega_i$$

$$y_{i_1} = r + \eta_{i_1} \cos \theta_1 - \sin \theta_1 (z_i' + \zeta_{i_1} \sin \Omega_i)$$

$$z_{i_1} = q + \eta_{i_1} \sin \theta_1 + \cos \theta_1 (z_i' + \zeta_{i_1} \sin \Omega_i) \tag{145}$$

In order to analytically represent the intersection of the shock on the conical body, a second order curve of the form

$$a_k \varphi^2 + b_k \rho^2 + d_k \rho + 1 = 0 \tag{146}$$

is fitted to three selected points

$$\rho_o, \varphi_o;\ \rho_1, \varphi_1;\ \rho_2, \varphi_2$$

which are the center line point, a point in the region near the center line and one of the last points, respectively. The

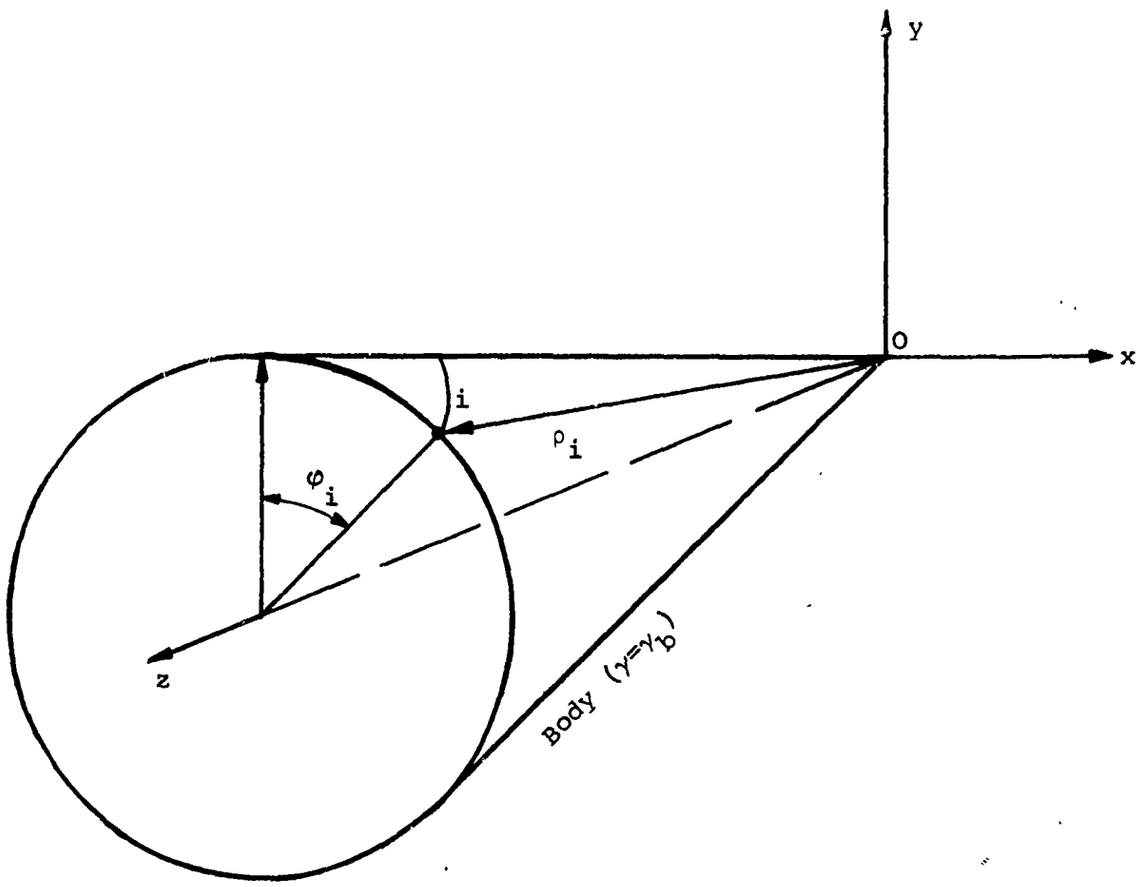

FIGURE 40 - CONICAL COORDINATE SYSTEM ON CONE SURFACE

coefficients of Eq. (146) are

$$a_k = (\rho_2-\rho_1)\ (\rho_1-\rho_o)\ (\rho_2-\rho_o)/\Delta_k$$
$$b_k = [\varphi_1^2\ (\rho_2-\rho_o)-\varphi_2^2\ (\rho_1-\rho_o)]/\Delta_k \qquad (147)$$
$$d_k = [\varphi_2^2\ (\rho_1^2-\rho_o^2)-\varphi_1^2\ (\rho_2^2-\rho_o^2)]/\Delta_k$$

where $\Delta_k = \rho_o[\varphi_1^2\ \rho_2\ (\rho_2-\rho_o)-\varphi_2^2\ \rho_1(\rho_1-\rho_o)]$

Similar to Section D a set of coordinates tangent, binormal and normal to the curve represented by Eq. (146) are defined. Their direction cosines with respect to the x-y-z axes are

$$\cos(\hat{tx})_i = (\varphi_i \sin \varphi_i \sin \gamma_b - AA_i \cos \varphi_i)/BB_i$$
$$\cos(\hat{ty})_i = (\varphi_i \cos \varphi_i \sin \gamma_b + AA_i \sin \varphi_i)/BB_i \qquad (148)$$
$$\cos(\hat{tz})_i = (\varphi_i \cos \gamma_b)/BB_i$$

$$\cos(\hat{bx})_i = \sin \varphi_i \cos \gamma_b$$
$$\cos(\hat{by})_i = \cos \varphi_i \cos \gamma_b \qquad (149)$$
$$\cos(\hat{bz})_i = -\sin \gamma_b$$

and

$$\cos(\hat{nx})_i = NA_i$$
$$\cos(\hat{ny})_i = NB_i \qquad (150)$$
$$\cos(\hat{nz})_i = \Delta\Delta_i$$

where

$$AA_i = \left(b_k \rho_i + \frac{d_k}{2}\right) \frac{\rho_i \sin \gamma_b}{a_k}$$

$$BB_i = \left\{\varphi_i^2 + AA_i^2\right\}^{\frac{1}{2}}$$

$$\begin{aligned} \Delta\Delta_i &= \cos(\hat{tx})_i \cos(\hat{by})_i - \cos(\hat{ty})_i \cos(\hat{bx})_i \\ NA_i &= \cos(\hat{ty})_i \cos(\hat{bz})_i - \cos(\hat{tz})_i \cos(\hat{by})_i \\ NB_i &= \cos(\hat{tz})_i \cos(\hat{bx})_i - \cos(\hat{tx})_i \cos(\hat{bz})_i \end{aligned} \qquad (151)$$

Next it is desired to find the flow field behind the "plane" shock near the conical surface. The Mach number components of the conical flow field in front of the "plane" shock on the conical body are

$$\begin{aligned} M_{2_{x'_{bi}}} &= M_r \sin \gamma_b \sin \omega_i + M_t \cos \gamma_b \sin \omega_i \\ M_{2_{y'_{bi}}} &= M_r (\sin \gamma_b \cos \omega_i \cos \theta_1 + \cos \gamma_b \sin \theta_1 \\ &\quad + M_t (\cos \gamma_b \cos \omega_i \cos \theta_1 - \sin \gamma_b \sin \theta_1) \\ M_{2_{z'_{bi}}} &= M_r (\cos \gamma_b \cos \theta_1 - \sin \gamma_b \cos \omega_i \sin \theta_1) \\ &\quad - M_t (\cos \gamma_b \cos \omega_i \sin \theta_1 + \sin \gamma_b \cos \theta_1) \end{aligned} \qquad (152)$$

where M_r is found from Eqs. (124) and (125) with $\gamma = \gamma_b$, $M_1^* = M_{1_b}^*$ and $\psi_1 = \psi_{1_b}$. The components normal and tangent to the original intersection curve are

$$\begin{aligned} M_{2_{n_{bi}}} &= M_{2_{z'_{bi}}} \sin \Omega_i - M_{2_{x'_{bi}}} \cos \Omega_i \\ M_{2_{t_{bi}}} &= -M_{2_{z'_{bi}}} \cos \Omega_i - M_{2_{x'_{bi}}} \sin \Omega_i \end{aligned} \qquad (153)$$

The flow field behind the shock near the conical body can be found by using

$$M_{2_{N_{bi}}} = \left\{ M_{2_{n_{bi}}}^{2} + M_{2_{y'_{bi}}}^{2} \right\}^{\frac{1}{2}} \tag{154}$$

and $\delta_{1_i}^{*}$ (Eq. 135), in the oblique shock relations. The shock strength has been assumed to be constant; however, the flow behind the shock near the body differs from that of the lower region of the shock intersection since the flow field in front of the shock is conical. In the usual manner the properties obtained are: the normal Mach number $M_{4_{N_{bi}}}$, the shock angle $\theta_{4_{bi}}$, the pressure and speed of sound ratios $(P_4/P_2)_{bi}$ and $(a_4/a_2)_{bi}$. The tangent Mach number and the total change in entropy are

$$M_{4_{t_{bi}}} = M_{2_{t_{bi}}} (a_2/a_4)_{bi}$$

$$S_{4_{bi}} = \frac{1}{2\bar{\gamma}} \left\{ (\bar{\gamma}-1) \frac{S_2}{R} + \left[\ell n \left(\frac{2\bar{\gamma} M_{2_{N_{bi}}}^{2} \sin^2 \theta_{4_{bi}} - (\bar{\gamma}-1)}{\bar{\gamma}+1} \right) \right. \right. \tag{155}$$

$$\left. \left. - \bar{\gamma}\, \ell n \left(\frac{\frac{\bar{\gamma}+1}{\bar{\gamma}-1} M_{2_{N_{bi}}}^{2} \sin^2 \theta_{4_{bi}}}{(\bar{\gamma}-1) M_{2_{N_{bi}}}^{2} \sin^2 \theta_{4_{bi}} + 2} \right) \right] \right\}$$

The Mach number components normal and binormal to the original intersection curve are

$$M_{4_{n_{bi}}} = M_{4_{N_{bi}}} \cos (\gamma_{b_i}^{*} + \theta_{1_i}^{*} - \delta_{1_i}^{*})$$

$$M_{4_{b_{bi}}} = M_{4_{N_{bi}}} \sin (\gamma_{b_i}^{*} + \theta_{1_i}^{*} - \delta_{1_i}^{*}) \tag{156}$$

where after much geometry

$$\theta_{1_i}^{*} = \cos^{-1}\left[\frac{\cos\theta_1}{(1-\cos^2\Omega_i \sin^2\theta_1)^{\frac{1}{2}}}\right]$$

and

$$\gamma_{b_i}^{*} = \cos^{-1}\left\{\left[1-\cot^2\Omega_i \cos\theta_1 \left(\sin\theta_1 \left(\frac{\partial y}{\partial t}\right)_{i_1} - \cos\theta_1\right)\right] / (1+\cos^2\theta_1 \cot^2\Omega_i)^{\frac{1}{2}} \left[1 + \left(\frac{\partial y}{\partial t}\right)^2_{i_1} + \left(\sin\theta_1 \left(\frac{\partial y}{\partial t}\right)_{i_1} - \cos\theta_1\right)^2 \cot^2\Omega_i\right]^{\frac{1}{2}}\right\}$$

where

$$\left(\frac{\partial y}{\partial t}\right)_{i_1} = [\sin\theta_1 \cos\theta_1 \cot^2\Omega_i\, y_{i_1} + K_i \cos\theta_1 \cot\Omega_i - (\cos^2\theta_1 \cot^2\Omega_i - \tan^2\gamma_b)\, z_{i_1}] / [(\sin^2\theta_1 \cot^2\Omega_i + 1)\, y_{i_1} + K_i \sin\theta_1 \cot\Omega_i - z_{i_1} \sin\theta_1 \cos\theta_1 \cot^2\Omega_i]$$

with

$$K_i = -\alpha_i + \sqrt{\alpha_i^2 - \beta_i}$$

$$\alpha_i = \cot\Omega_i (\sin\theta_1\, y_{i_1} - \cos\theta_1\, z_{i_1})$$

$$\beta_i = (\sin^2\theta_1 \cot^2\Omega_i + 1)\, y_{i_1}^2 - 2 \sin\theta_1 \cos\theta_1 \cot^2\Omega_i\, y_{i_1} z_{i_1} + (\cos^2\theta_1 \cot^2\Omega_i - \tan^2\gamma_b)\, z_{i_1}^2$$

To obtain the flow field behind the reflected shock it is necessary to find the upstream Mach number components in the directions tangent, normal, and binormal to the reflection curve which are

$$M_{4_{t_i}} = M_{4_{x_{bi}}} \cos(\hat{tx})_i + M_{4_{y_{bi}}} \cos(\hat{ty})_i + M_{4_{z_{bi}}} \cos(\hat{tz})_i$$

$$M_{4_{n_i}} = M_{4_{x_{bi}}} \cos(\hat{nx})_i + M_{4_{y_{bi}}} \cos(\hat{ny})_i + M_{4_{z_{bi}}} \cos(\hat{nz})_i$$

$$M_{4_{b_i}} = M_{4_{x_{bi}}} \cos(\hat{bx})_i + M_{4_{y_{bi}}} \cos(\hat{by})_i + M_{4_{z_{bi}}} \cos(\hat{bz})_i \tag{157}$$

where

$$M_{4_{x_{bi}}} = M_{4_{n_{bi}}} \cos \Omega_i - M_{4_{t_{bi}}} \sin \Omega_i$$

$$M_{4_{y_{bi}}} = M_{4_{b_{bi}}} \cos \theta_1 - M_{4_{n_{bi}}} \sin \Omega_i \sin \theta_1 + M_{4_{t_{bi}}} \cos \Omega_i \sin \theta_1$$

$$M_{4_{z_{bi}}} = M_{4_{n_{bi}}} \sin \Omega_i \cos \theta_1 - M_{4_{t_{bi}}} \cos \Omega_i \cos \theta_1 + M_{4_{b_{bi}}} \sin \theta_1 \tag{158}$$

Then the total Mach number component in a plane normal to the reflection curve

$$M_{4_{N_i}} = \left\{ M_{4_{n_i}}^2 + M_{4_{b_i}}^2 \right\}^{\frac{1}{2}} \tag{159}$$

and the flow deflection across the reflected shock in this plane

$$\delta_{4_i} = \tan^{-1} \left| M_{4_{\bar{b}i}} / M_{4_{\bar{n}i}} \right| \tag{160}$$

can be used in the oblique shock relations to give the flow properties behind the reflected shock on the cone surface. The results are finally given by the following relations:

$$M_{6_i} = \left\{ M_{6_{\bar{t}_i}}^2 + M_{6_{N_i}}^2 \right\}^{\frac{1}{2}} \tag{161}$$

where $M_{6_{N_i}}$ is obtained from the oblique shock relations and

$$M_{6_{\bar{t}_i}} = M_{4_{\bar{t}_i}} \left(\frac{a_4}{a_6} \right)_i \tag{162}$$

The shock angle with respect to the body is

$$\theta_{6_i}' = \theta_{6_i} - \delta_{4_i} \tag{163}$$

The pressure ratio is

$$(p_6/p_\infty)_i = \left(\frac{p_6}{p_4} \right)_i \left(\frac{p_4}{p_2} \right)_{bi} \left(\frac{p_b}{p_\infty} \right) \tag{164}$$

The flow deviation in the ρ, φ plane with respect to the ρ axes is

$$\sigma_{6_i} = \cos^{-1} \left[\frac{2a_k \varphi_i}{\sqrt{(2a_k \varphi_i)^2 + (2b_k \rho_i + d_k)^2}} \right] - \tan^{-1} \left(M_{6_{N_i}} / M_{6_{\bar{t}_i}} \right) \tag{165}$$

and the total change in entropy is

$$S_{6_i} = S_{4_{bi}} + \frac{1}{2\bar{\gamma}}\left[\ell n\left(\frac{2\bar{\gamma}\, M_{4_{N_{bi}}}^2 \sin^2\theta_{6_i} - (\bar{\gamma}-1)}{\bar{\gamma}+1}\right)\right.$$

$$\left. -\bar{\gamma}\,\ell n\left(\frac{(\bar{\gamma}+1)\, M_{4_{N_{bi}}}^2 \sin^2\theta_{6_i}}{(\bar{\gamma}-1)\, M_{4_{N_{bi}}}^2 \sin^2\theta_{6_i} + 2}\right)\right] \qquad (166)$$

To find the flow field on the body, the characteristic subroutine can be used in the ρ, ω plane, with the above conditions which are valid immediately behind the reflected shock.

The program operation and example problems are given in Appendices V and VI.

APPENDIX I

HOW TO USE THE PROGRAM
(Two-Dimensional and Axisymmetric Flow Computer Program)

1. General Comments

Very often instructions for operating a computer program are more complicated than even the program itself. Many quite useful programs have been rendered almost useless because the answers to prospective users questions are either not provided by the instruction manual or are hidden in a plethora of jargon. The important questions which are answered here are:

a. What does the program do?

b. What are its restrictions and limitations?

c. What input data are required by physics?

d. What additional input data are required to make the program work?

e. What is the required form of the input data?

f. What is given in return (i.e. what are the outputs)?

g. How is the output to be interpreted?

h. What might go wrong? What can be done about it?

Answers and parts of answers to some of these questions have already been given. In such instances, the appropriate sections will be designated and that information will not be repeated in this section. The questions and answers are:

a. What does the program do?

The program computes the inviscid supersonic internal flow of a perfect gas of constant specific heat ratio for configurations typical of supersonic and hypersonic inlets. (Also see Section IV-A,B).

b. What are its restrictions and limitations?

In standard notation:

γ = constant (constant ratio of specific heats)

$p = \rho RT$ (perfect gas equation of state)

$\mu = 0$ (inviscid)

$M > 1$ (supersonic)

c. What input data are required by physics?

Referring to Figure 11, the physics of these flows requires one to specify the flow conditions completely on some initial data line (which is not characteristic) ($\overline{AA}'$ of Figure 11) and the geometry ($y(x)$, $y'(x)$) of both the walls. When this data has been specified (maximum ordinate of the initial data must be great enough so that a down characteristic from that point intersects the leading edge of the upper wall) the entire inviscid flow in the inlet can be determined, so long as it remains everywhere supersonic.

Needless to say, one must also specify γ, the ratio of specific heats.

d. What additional input data is required to make the program work?

In addition to the physically required data, the program needs the following information: abscissa of upper and lower leading edges, maximum abscissa of the upper wall to be computed, angle of attack of the free stream flow with respect to the horizontal axis, spacing of mesh points on the initial data line (uniform incident flow), a code indicating whether data along the initial line is supplied or the simplified input is used, a code indicating whether the flow is two-dimensional or axi-symmetrical, and other codes related to the wall geometry. In addition, for the convenience of the user, provision is made for inputing and outputing the date and a run indentification number.

e. What is the required input data?
Physical Data

As mentioned before all input data must be nondimensionalized in the manner specified in Part C-a, Non Dimensionalization and General Equations of Motion. Read Part C-a before continuing with this section.

If the incident flow is uniform, the user may specify the incident Mach number, M, the specific heat ratio, γ, and, in the case of two-dimensional flow, the angle of attack. In this case the reference pressure and temperature will be assumed to be the incident pressure and temperature.

In the case of uniform incident flow, the leading edge of the lower wall must be upstream of the leading edge of the upper wall. However, if it is not, this requirement can be overcome by extending the lower wall upstream of its leading edge parallel to the incident flow. This can not be done in the case of axisymmetric flow when the leading edge of the lower wall has a sharp corner on the axis of symmetry. If it is desired to have the output referred to another pressure and temperature, it is necessary to input data on the initial data line point by point, the data being referred to the desired reference pressure and temperature.

If the incident flow is non-uniform, it is necessary to specify the data point by point, starting at the leading edge of the lower wall. A reference pressure and temperature (and length, if desired) must be chosen. Then the coordinates of each data point must be specified along with the Mach number, the angle the streamline makes with the x axis, and either the static pressure and temperature or the total enthalpy and total pressure (all non-dimensionalized).

It is important to realize that the initial data line may not be arbitrarily specified. The first point must be at the leading edge of the lower wall and the subsequent points must be in order of increasing ordinate. Also, the initial data line must be oriented so that the characteristics emanating therefrom point downstream from the data line (see Figure 26). In addition, the inital data line must be upstream of the leading edge of the upper wall (cowl).

The required data are:

1) Free stream Mach number, M (simplified input, uniform incident flow) or x,y,M, θ, either p and T or p_t and H on the initial data.

2) Specific heat ratio, γ.

3) Abscissae of the two leading edges and the maximum abscissa to be computed on the upper wall. All lengths must be dimensionally the same or non-dimensionalized consistently. If non-dimensionalized, the program does not need to know how this was done, nor is there any way of telling it.

4) Angle-of-attack in degrees measured positive counter-clockwise from the horizontal axis. (Two-dimensional, uniform incident flow, only.)

5) The code for two-dimensional/axisymmetrical flow is an integer which is zero (0) if the flow is two-dimensional and one (1) if it is axisymmetrical.

6) The run identification number and the date are read in as integers, the identification number having a maximum of 5 digits.

7) Miscellaneous control integers.

8) y(x) on the lower and upper walls in the form of second order polynomials. There are a maximum of 9 second order polynomials on each wall. The polynomials are of the form

$$y(x) = a_i + b_i\ (x-x_i) + c_i\ (x-x_i)^2,\ i=1,\ 9$$

for top and bottom. a_i, b_i, c_i, and x_i must be specified for each polynomial.

Note: - A more complicated, but extremely versatile way of specifying body geometries is given in Appendix A. It can be used to specify body geometries in virtually any manner.

9) The x coordinate of every sharp corner on the upper and lower wall, but not including the leading edges. In addition, the user must supply dy/dx before and after the corner. There are a maximum of six such corners on each wall.

f. What is given in return? (What are the output?)

Data at each mesh point, including the location of the point, are written on scratch tape in the following form:

1) abscissa and ordinate of the point (in the same units or non-dimensionalized in the same manner as the input lengths).

2) pressure divided by the reference pressure

3) temperature divided by the reference temperature

4) the streamline angle, θ

5) Mach number

6) $(S-S_o)/C_v$ where S is dimensional entropy (S_o is the entropy corresponding to the place where p_o and T_o are).

7) total enthalpy divided by the ratio of reference pressure to reference density.

8) the mass flow between the mesh point and the lower wall divided by [square root of (reference pressure x reference density) times the square of the length used to non-dimensionalize lengths (if they are non-dimensionalized)].

$$\text{i.e.} \quad \frac{\text{mass flow}}{\sqrt{\rho_o \, p_o} \quad \ell_o^2} \qquad p_o = \rho_o \, R \, T_o$$

In addition, in axisymmetric flow the mass flow is also divided by π.

9) Pitot pressure divided by the reference pressure.

g. How is the output to be interpreted?

The output is given as a function of mesh points on each down running characteristic. In each strip the down running characteristics are identified integrally beginning with 1 for the first point to be computed (see Part D-b on the order of progression of the computation) in that strip. Similarly, the strips are identified integrally beginning with 1 for the strip containing the initial data line.

These should be no problem so far as reference quantities are concerned.

There is a little problem arising from the way in which the computation proceeds. It will be recalled that (see Part D-b-2,3) when a down shock is initiated, the region between (see Figure 16) the last down characteristic $\overline{BC}$, in the previous strip (Ith strip) and the down shock, $\overline{BD}$, separating the two strips (i.e., the region between $\overline{BC}$ and $\overline{BD}$) is computed first as a part of the Ith strip without considering the influence of the compression at B, and then is recomputed as a part of the (I+1)st strip taking into account the compression. This is necessary since we have no way of knowing a priori just where the shock, $\overline{BD}$, will go. We only know that it will always be upstream of $\overline{BC}$.

For this reason, in computing the Ith strip, we write out all of the data in that strip up to and including all of the data on $\overline{BC}$. Then, in recomputing the region common to both strips, we output the new "good" data between $\overline{ED}$ and $\overline{BC}$. Thus, one must be careful to pick the "good" data for the common region.

But this is made simple by the following device.

Recall that the various strips are separated by down running shocks. In general, the Ith down shock will separate the Ith and the (I+1)st strip. Neglecting, for the moment, the effect of any other down shocks, the data ambiguity is a result of the fact that some of the data computed in the Ith strip is not valid because it is downstream of the Ith shock. So the proper procedure is to plot first the down running shocks and to use their locations as a guide in determining which data has become invalid.

Note that, if two down running shocks coalesce, being continued as one shock, downstream of the coalescence the difference between the strip number on either side of the shock will be greater than one (Figure 25).

h. How long will a computation take?

The program is written in Fortran IV for use with IBSYS 13 on the IBM 7094. A typical case will take about 1-4 minutes execution time.

On the CDC 6600, the same computation would be completed in less than 2 minutes including compilation time.

i. What might go wrong and what can be done about it?

Any computer program developed to compute phenomena as complicated as those under consideration here is bound to have trouble from time to time. Prospective users should be neither surprised nor frightened by this fact. A good program will have difficulties, but they should not occur too frequently under normal use nor should they occur when relatively "simple" cases are being computed. But, when troubles arise, the user should be given every opportunity to get around the difficulties in order to obtain the information (or at least some of it) desired.

The difficulties of this flow field program will ordinarily fit into two categories, those resulting from computational inaccuracies and those resulting from logical complications caused by extremely complicated flow field patterns.

1) Problems resulting from computational inaccuracies - The usual reason for problems to arise because of computation inaccuracies is that dependent variables have large variations on the scale of a mesh size or less. For instance, if one has an expansion corner, the pressure, density and streamline orientation are discontinuous at the corner. Hence, we make provisions to compute the flow near the corner in special ways in order to retain the desired accuracy. If we did not make such provision, we not only would lose accuracy, but we would usually find that the errors made would be so large that the computation would soon fail to converge in one of the many subsequent iterations.

Suppose that in some region one of the boundaries changes so rapidly, relative to the local mesh scale, that there are large changes in the pressure, density, and streamline orientation during one mesh interval on the body. Then, even though things are smooth, because of the rapid changes it is not unlikely that, in addition to inaccuracies, there will be difficulties and/or failures in attempting to converge in some iteration.

One obvious solution is to decrease the mesh size by decreasing the initial mesh size. This can be done within limits (the computer has limited storage capacity), though a price is paid in increased computer time. If it is impossible to refine the mesh enough, an alternative is to replace the rapid smooth turning with a sharp corner strategically placed and oriented. Then, locally, near the corner, the solution will not describe well the flow over the original body, but the engineer can usually correct the computed flow to give him the required information.

In certain cases the user is justified in relaxing certain tolerances in order to allow an iteration to converge. Such action must be done with an appreciation for the effect that this will have on the computation. Some tolerances can be relaxed by an order of magnitude under certain conditions without having a marked effect on the accuracy of the computation. Others should not be relaxed by even a factor of two. Such decisions require a quite intimate knowledge of the program and should not usually be attempted by infrequent users.

2) Logical problems resulting from extremely complicated flow field patterns - For such problems all of the prescriptions applicable to inaccuracy problems also apply, in addition to a few others. The problems we are now discussing result from very complicated flow field patterns. For example, if three down running shocks converge near the lower wall (perhaps they converge just before, or the reflected shocks converge just after, or some combination happens) near a sharp corner, it would not be too surprising to find that the program gets a little confused trying to keep track of what happened, what is happening, and what might happen. Sometimes the program will fail to work perfectly for such reasons. This does not mean that it is useless or that the user is lost. There are many alternatives available, including those already discussed under a), above.

Another "corrective" measure is best explained by an illustrative example. Suppose that for a given geometry and Mach number, such a complicated pattern develops in a particular region and the program gets confused and stops. Very often a change in Mach number (in both directions) will spread things out so that they are not quite so concentrated. One can use this to infer his desired results.

j. Special control cards; Tape Assignments

The program is written in FORTRAN IV for use on the IBM 7094 or CDC 6600 computer.

Approximately 72,000 octal locations are needed on the CDC 6600. No special control cards are needed other than specifications of the use of logical tape 5 for input, 6 for output, and 3 and 4 as scratch tapes.

On the IBM 7094, the same tape assignments are used. Because of storage requirements, it is necessary to use the alternate input- output option, the ALTIO routines. This is dome by specifying ALTIO as one of the options on the $IBJOB control card.

2. Input

Input are read on logical tape 5 and the results written on logical tape 6. In addition, the results are stored on logical tape 4 for use during the computation. But that tape can be used later also. Logical tape 3 is also used as a scratch tape.

The data for several cases can be stacked.

INPUT DATA

All Integers Must Be Right Adjusted

Card No.	Columns	Datum-Fortran Symbols	Format	Must be Right Adjusted	Recommended Value	Description
1	1-5	NRUN	I5	Yes		Run number
	6-10	MONTH				Number of the month
	11-15	MDAY				Number of the day
	16-20	MYEAR				Last two digits of the year
	21-25	IUNFLO			Must be ≥0	0-If initial data is uniform and to be computed from given Mach number and γ. In this case the initial data line is the line x=XBEG (see card #2). If the initial data is to be read for each mesh point, then IUNFLO equals the number of such points.
	26-30	JA			Must be 0 or 1	0 for two-dimensional flow, 1 for axisymmetric flow.
	31-35	ILWFTS			≤9	Number of quadratic fits on the lower wall $[y(x)=a_i+b_i(x-x_i)+c_i(x-x_i)^2]$
	36-40	IUPFTS			≤9	Number of quadratic fits on the upper wall $[y(x)=a_i+b_i(x-x_i)+c_i(x-x_i)^2]$

Card No.	Columns	Datum-Fortran Symbols	Format	Must be Right Adjusted	Recommended Value	Description
1	41-45	INPT	I5	Yes	+1	INPT=+1 if IUNFLO ≠ 0 and p and T are to be specified. INPT=-1 if IUNFLO ≠0 and p_T and H are to be specified.
	46-50	ICŌRNL			≤6	Number of corners on lower wall (not counting lower leading edge)
	51-55	ICŌRNU			6	Number of corners on upper wall (not counting upper leading edge
2	1-10	MACH	E10.8	Optional		$\gamma=c_p/c_v$, the ratio of specific heats. Angle of attack of free stream with respect to x axis, positive counter-clockwise
	11-20	GAMMA				
	21-30	ALPHA				
	31-40	DY				Δy interval for initial line x coordinate of the leading edge of the upper wall
	41-50	XAU				
	51-60	XEND				Maximum abscissa of the upper wall. The computation will be stopped when this value is reached and the next case will be begun.
	61-70	XBEG				Abscissa of the leading edge of the lower wall.

Card No.	Columns	Datum-Fortran Symbols	Format	Must be Right Adjusted	Recommended Value	Description
3	1-10	XFLAGL(1)	E10.8	Optional		x coordinate of the sharp corners on the lower wall.
	11-20	(2)				
	21-30	(3)				
	51-60	(6)				There are a maximum of 6 such corners. They must be in order beginning at the first sharp corner <u>after</u> the leading edge. There are ICORNL corners (See card #1) *
4	1-10	TFLAGL(1,1)				τ=dy/dx on the <u>upstream edge</u> of the sharp corners on the lower wall, in order. *
	11-20	(1,2)				
	51-60	(1,6)				
5	1-10	TFLAGL(2,1)				τ=dy/dx on the <u>downstream side</u> of the sharp corners on the lower wall, in order. *
	11-20	(2,2)				
	51-60	(2,6)				
6	1-10	XFLAGU(1)				x coordinate of the sharp corners on the upper wall (maximum of 6). They must be in order beginning with the 1st corner <u>after</u> the leading upper edge. There are ICORNU corners (See card # 1) *
	11-20	(2)				
	51-60	(6)				

* If there are no corners, insert blank data cards.

Card No.	Columns	Datum-Fortran Symbols	Format	Must be Right Adjusted	Recommended Value	Description
7	1-10	TFLAGU(1,1)	E10.8	Optional		τ=dy/dx on the upstream side of the sharp corners on the upper wall, in order. *
	11-20	(1,2)				
	.					
	.					
	.					
	51-60	(1,6)				
8	1-10	TFLAGU(2,1)				τ=dy/dx on the downstream side of the sharp corners on the upper wall, in order. *
	11-20	(2,2)				
	.					
	.					
	.					
	51-60	(2,6,				
9	1-10	YLBC(1,1)				Coefficients in the first of the second order polynomial fits for y(x) on the lower wall. $y(x)=a_1+b_1(x-x_1)+c_1(x-x_1)^2$ $x_1 \leq x \leq x_2$ where a_1 is in columns 1-10, b_1 is in columns 11-20, c_1 is in columns 21-30, x_1 is in columns 31-40. There are a maximum of 9 such fits. The actual number of such fits is ILWFTS which is a datum on the first card.
	11-20	(1,2)				
	21-30	(1,3)				
	31-40	(1,4)				

Card No.	Columns	Datum-Fortran Symbols	Format	Must be Right Adjusted	Recommended Value	Description
10	1-10	YLBC(2,1)	E10.8	Optional		Coefficients of the second of the second order polynomial fits for y(x) on the lower wall. $y(x)=a_2+b_2(x-x_2)+c_2(x-x_2)^2$, $x_2 \le x \le x_3$ where a_2 is in columns 1-10, b_2 is in columns 11-20, c_2 is in columns 21-30, x_2 is in columns 31-40.
	11-20	(2,2)				
	21-30	(2,3)				
	31-40	(2,4)				
9+ILWFTS-1 (ILWFTS≤9)	1-10	YLBC((ILWFTS,1)				Coefficients of the last of the second order fits for y(x) on the lower wall.
		.				
		.				
		.				
		YLBC (ILWFTS,4)				
9+ILWFTS	1-10	YUBC(1,1)				Coefficients of the 1st of the 2nd order polynomial fits for y(x) on the upper wall. $y(x)=a_1+b_1(x-x_1)+c_1(x-x_1)^2$ $x_1 \le x \le x_2$ where a_1 is in columns 1-10, b_1 is in columns 11-20, c_1 is in columns 11-30, x_1 is in columns 31-40,
	11-20	(1,2)				
	21-30	(1,3)				
	31-40	(1,4)				
9+ILWFTS+ IUPFTS-1	1-10	YUBC(IUPFTS,1)				Coefficients of the last of the 2nd order polynomial fits for y(x) on the upper wall.
	11-2-					
	21-30	.				
	31-40	. (IUPFTS,4)				
		.				

If the specified initial data is uniform with given Mach number, there are no more data cards. If the initial data is non-uniform, it is read on the following cards. The first point is the point corresponding to the minimum value of y and will usually correspond to the leading edge of the lower wall (the axis point, for axially symmetric flow). Recall that the coordinate system is right handed, with x, the abscissa, positive in the general direction of the flow. The characteristics issuing from the data line must point downstream of the initial line.

Card No.	Columns	Datum Fortran Symbols	Format	Must be Right Adjusted	Recommended value	Description
9+ILWFTS+ IUPFTS	1-10	X(1,1)	E10.8	Optional		x, abscissa of the 1st data point (must equal XBEG, card number 2).
	11-20	Y(1,1)				y, ordinate of the first data point.
	21-30	TAU(1,1)				Angle (in degrees) made by the streamline through the first data point.
	31-40	SM(1,1)				Mach number of the first data point.
	41-50	P(1,1)				Static pressure (INPT=+1) or total pressure (INPT=-1 of the first data point (non-dimensionalized).
	51-60	H(1,1)				Static temperature (INPT=+1) or total enthalpy (INPT=-1) of the first data point (non-dimensionalized).
9+ILWFTS+ IUPFTS+1						Second data card for initial data line.
. . .						
9+ILWFTS+ IUPFTS+IUNFLO -1						Last data card for initial data line.

3. Output

The output is done by writing on logical tape 6 as the computation proceeds. After each down running characteristic has been computed, the data along that characteristic is output. The data is nondimensionalized as indicated in Part C-a.

Sample output sheets are given in Appendix II (pp. 126-129).

At the beginning of the computation, the pertinent input data are output and identified.

At the top of the data of each down characteristic, the strip number and the number of the characteristic in that strip are printed out. These are followed by a block with important data concerning the location of contact discontinuities and up running shocks. (See page 127, Appendix II.) The contact discontinuities and the shocks are numbered from one (1) to ten (10) beginning with those nearest the upper wall as one proceeds along the characteristic. Thus, on Page 128, Appendix II, one sees that there is a contact discontinuity at the 20th mesh point on the 18th characteristic of the 3rd strip. The data on the 'upper' side of the discontinuity is at mesh point 20, while the data at the 'lower' side of the discontinuity is at mesh point 21. Similarly, there are up-running shocks at mesh points 16 and 25, the data behind the shocks being stored in points 17 and 26 respectively. The column under SIGMA gives the local slope of the shock (dy/dx of the shock) while 1/SIGMA is the inverse of the slope.

Following is the data along the characteristic, beginning at the upper wall and continuing to either the lower wall or a down running shock, as the case may be. The column of integers on the extreme left and right identify the mesh point number on that characteristic. The various quantities output are the mesh point coordinates, the non-dimensional pressure and temperature, the angle (in degrees) the streamline makes with the x axis, the Mach number, and the non-dimensional entropy, enthalpy, mass flow (between the lower wall and that mesh point), and total pressure.

The only thing to be cleared up is how to be able to distinguish whether the down characteristic ends at a down running shock or bottom wall. But this is really very easy because the initiation of a down running shock is always indicated by one of the following three

messages:

1) SHOCK ON UPPER WALL AT X = , Y=

2) REFLECTION ON UPPER WALL AT X= , Y=

3) DOWN SHOCK FORMED BY COALESENCE OF SMOOTH COMPRESSION WAVES

The first message is written when a down shock is formed by a sharp compression corner on the upper wall.

The second message is written when a down shock is formed by the reflection of an up running shock on the upper wall.

The third message is written when smooth compression waves coalesce to form an 'envelope shock'.

So, after any one of the three messages, the last point on the down running characteristics will be on the downstream side of the down running shock, until that shock reflects at the lower wall. This is indicated by the message

4) REFLECTION ON LOWER WALL AT X = , Y=

indicating that a down running shock has reflected off the lower wall, the reflected shock being an up running shock. All the down characteristics printed after message 4), will terminate on the lower wall until one of the messages 1) - 3) is again printed.

Sample output are shown in Appendix II.

APPENDIX II

SAMPLE INPUT AND OUTPUT

1. Sample Input

Sample input cards for a case with the simplified input (uniform incident flow) are given on the following pages. The data for this case are:

Two-dimensional
$\gamma = 1.4$
$M_\infty = 12.3$
Uniform incident flow
Zero degrees angle of attack
$\Delta y = 0.1$ on the initial data line
lower wall leading edge at $x = 0.0$, $y = 0.0$
upper wall leading edge at $x = 2.75$, $y = 2.75$
maximum upper wall abscissa at $x = 9.5$

The geometry of the lower wall is:

$y = 0.17633x$; $0 \le x \le 5.5$
$y = 0.96982 + 0.23087\ (x-5.5)$ $5.5 < x \le 8.1122$
$y = 1.5729 + 0.23087\ (x-8.1122) - 0.097186\ (x-8.1122)^2$ $8.1122 < x \le 9.3$
$y = 1.71$ $x > 9.3$

The geometry of the upper wall is:

$y = 2.75 - 0.08749\ (x-2.75)$ $2.75 \le x \le 5.0$
$y = 2.5527 - 0.17633\ (x-5.0)$ $5.0 < x \le 8.782$
$y = 1.8907 - 0.17633\ (x-8.782) + 0.17021\ (x-8.782)^2$ $8.782 < x \le 9.3$
$y = 1.845$ $9.3 < x$

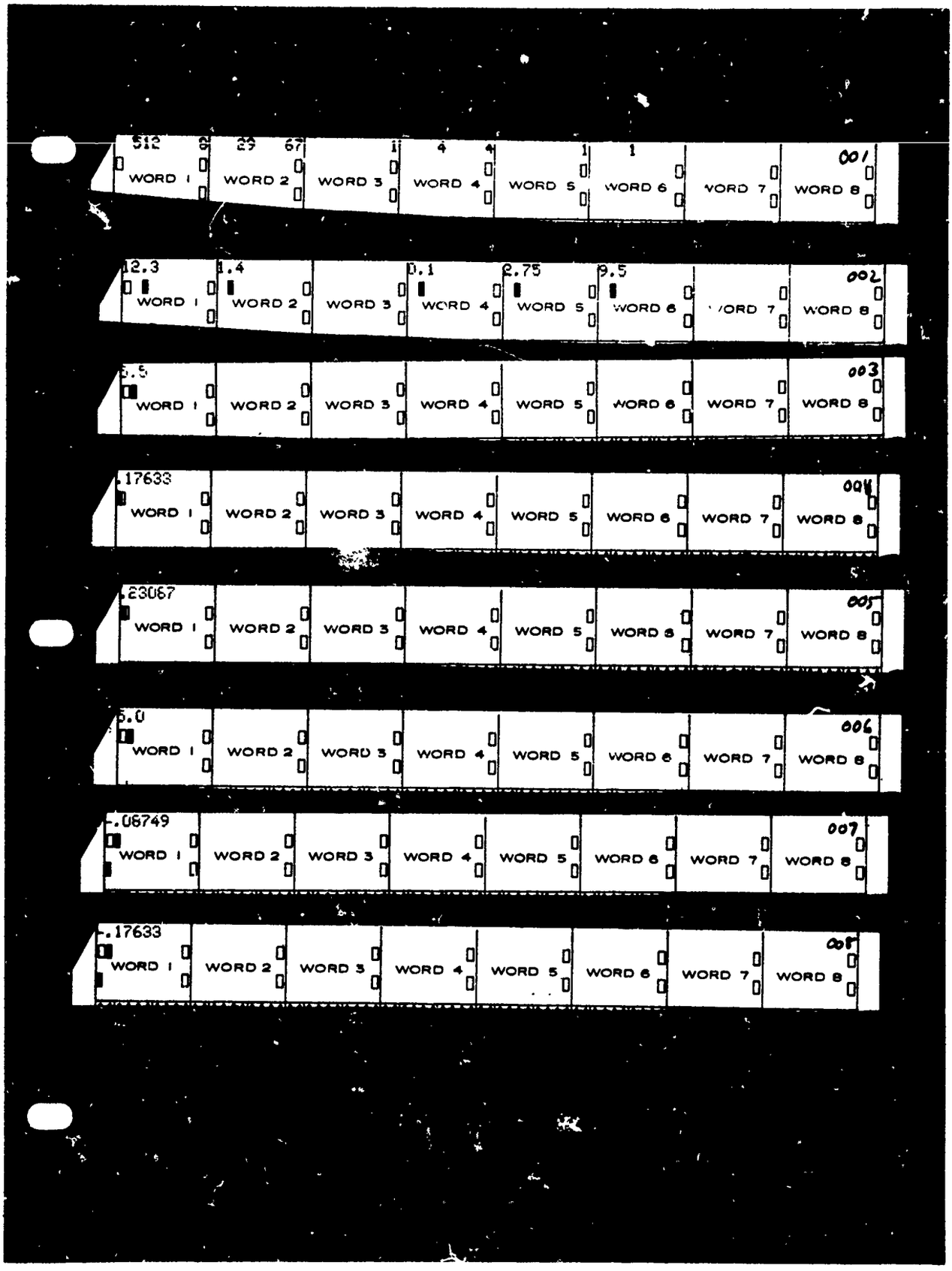

SAMPLE INPUT CARD

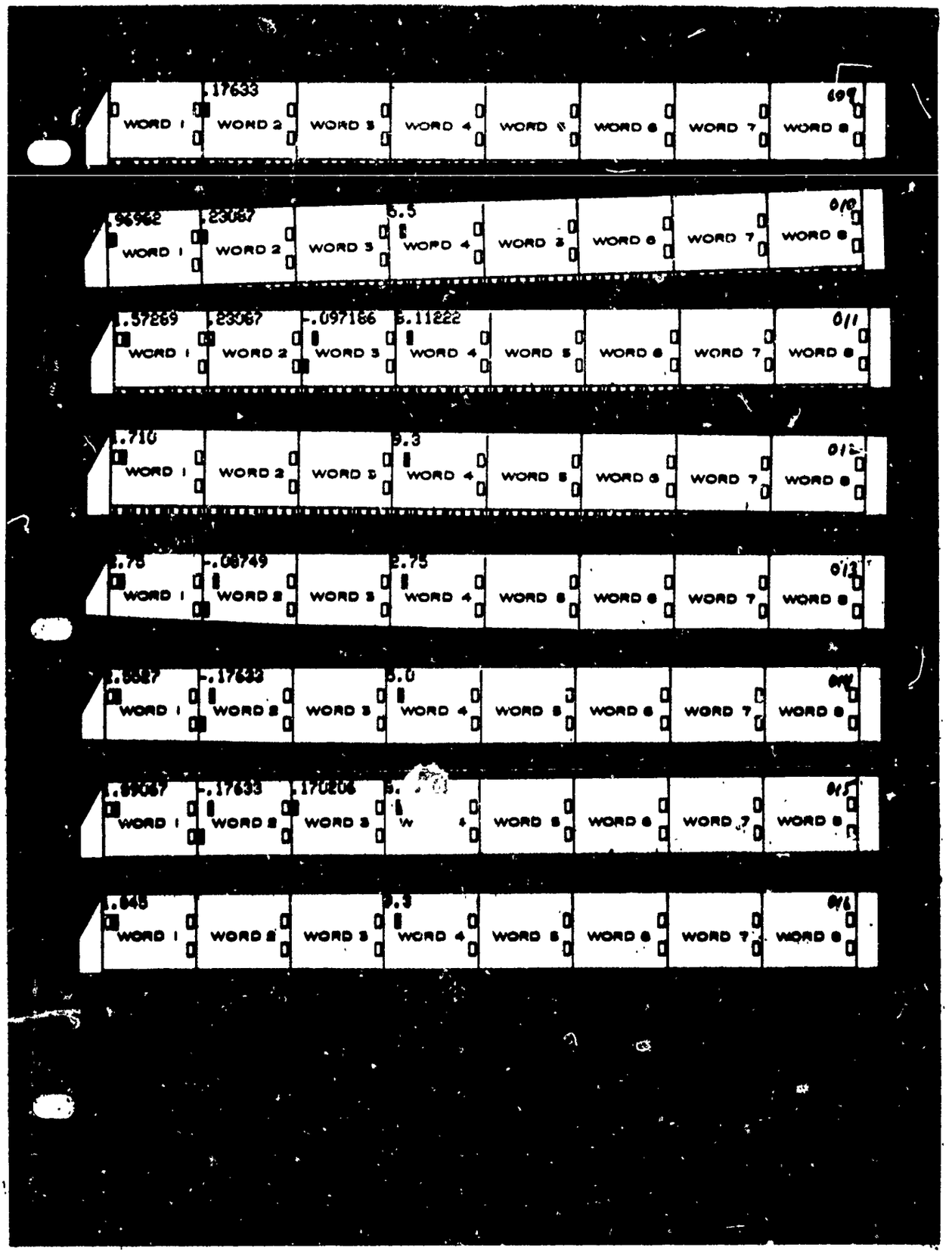

SAMPLE INPUT CARDS (cont'd)

2. Sample Output

Sample output sheets for the case of the preceding pages is given on the following pages (pp. 126-129).

The first page, Table I, gives the input data. If the simplified input is not used, just disregard those parameters which are used only for the simplified input. They are:

MACH	M_∞
ANGLE OF ATTACK	
DY	Δy on initial lines

For completeness, a review of the meaning of Table I follows:

The first two lines of output are self-explanatory.

IUNFLO = 0 means the incident flow is uniform and the simplified input is being used

MACH = 12.3 $M_\infty = 12.3$

GAMMA = 1.4 $\gamma = 1.4$

ANGLE OF ATTACK = 0 is self-explanatory

DY = 0.1 $\Delta y = 0.1$ on the initial data line which is computed internally

JA = 1 means the flow is axisymmetric

ILWFTS = 4 means there are four geometry fits on the lower wall

IUPFTS = 4 means there are four geometry fits on the upper wall

INPT = 0 means the flow is uniform and the simplified input is being used

ICORNL = 1 means there is one sharp corner on the lower wall after the leading edge

ICORNU = 1	means there is one sharp corner on the upper wall after the leading edge
X UPPER = 2.75	is the abscissa of the leading edge of the upper wall (cowl)
X FINAL = 9.5	is the maximum abscissa to be computed on the upper wall
X LOWER = 0.0	is the abscissa of the leading edge of the lower wall

Following are the abscissae and slopes (dy/dx) of each of the corners on the upper and lower walls. TAU LEFT is dy/dx on the upstream side of the corner. TAU RIGHT is dy/dx on the downstream side. Remember, the leading edges are not counted as corners in this part of the input.

Following are the coefficients of the polynomial fits for the walls. This data is self-explanatory.

Table II shows the data on the eleventh down running characteristic of the first strip. Note that the leading edge of the upper cowl has not yet been intersected. Also note that since the data at x = 0, y = 0, is on the first characteristic, one would expect to have the eleventh characteristic having an ordinate of y = 1.0 since $\Delta y = 0.1$ was input. The fact that y = 0.9 here indicates that twice a failure has occurred in an iteration and the initial Δy was temporarily halved. In this example this happened at the very beginning near the symmetry axis of the conical centerbody. The lower wall has a leading edge of 10° yielding a conical shock of 11.9°. For a more extensive discussion of how to read this table, see Appendix I, Part c.

Table III gives the data along a down running characteristic further downstream.

The shock wave pattern for this example is given in Appendix III along with some comments about the computation.

TABLE I - SAMPLE OUTPUT (2-D)

SUPERSONIC INLET-PROGRAM 1A

RUN NUMBER 512 ON 8/29/67

IUNFLO=-0 MACH= 1.2300E 01 GAMMA= 1.40E 00 ANGLE OF ATTACK= -0. DY= 1.0000E-01 JA= 1
ILWFTS= 4 IUPFTS= 4 INPT= -0 ICORNL= 1 ICORNU= 1

X UPPER= 2.7500000E 00 X FINAL= 9.5000000E 00 X LOWER= -0.

LOWER CORNERS			UPPER CORNERS		
X	TAU LEFT	TAU RIGHT	X	TAU LEFT	TAU RIGHT
5.5000000E 00	1.7633000E-01	2.3087000E-01	5.0000000E 00	-8.7490000E-02	-1.7633000E-01
-0.	-0.	-0.	-0.	-0.	-0.
-0.	-0.	-0.	-0.	-0.	-0.
-0.	-0.	-0.	-0.	-0.	-0.
-0.	-0.	-0.	-0.	-0.	-0.
-0.	-0.	-0.	-0.	-0.	-0.
-0.	-0.	-0.	-0.	-0.	-0.

COEFFICIENTS FOR GEOMETRY FITS, $Y(X)=A+B*(X-XI)+C*(X-XI)**2$, FOR X BETWEEN XI AND XI+1

LOWER WALL				UPPER WALL			
A	B	C	XI	A	B	C	XI
-0.	1.7633E-01	-0.	-0.	2.7500E 00	-8.7490E-02	-0.	2.7500E 00
9.6982E-01	2.3087E-01	-0.	5.5000E 00	2.5527E 00	-1.7633E-01	-0.	5.0000E 00
1.5729E 00	2.3087E-01	-9.7186E-02	8.1122E 00	1.8907E 00	-1.7633E-01	1.7021E-01	8.7620E 00
1.7100E 00	-0.	-0.	9.3000E 00	1.8450E 00	-0.	-0.	9.3000E 00
0.	0.	0.	0.	0.	0.	0.	0.
0.	0.	0.	0.	0.	0.	0.	0.
0.	0.	0.	0.	0.	0.	0.	0.
0.	0.	0.	0.	0.	0.	0.	0.
0.	0.	0.	0.	0.	0.	0.	0.
0.	0.	0.	0.	0.	0.	0.	0.

TABLE II - SAMPLE OUTPUT (2-D)

STEP NUMBER 11 STRIP NUMBER 1

K	INTERFACE	SHOCK	SIGMA	1/SIGMA
1	0	7	2.1007028E-01	4.7603117E 00
2	0	0	0.	0.
3	0	0	0.	0.
4	0	0	0.	0.
5	0	0	0.	0.
6	0	0	0.	0.
7	0	0	0.	0.
8	0	0	0.	0.
9	0	0	0.	0.
10	0	0	0.	0.

	X	Y	P	T	THETA(DEG)	MACH	S	H	FLOW	P TOTAL	
1	-0.	9.0000E-01	1.000E 00	1.000E 00	-0.	1.230E 01	0.	1.094E 02	1.179E 01	1.708E 05	1
2	6.1296E-01	8.5000E-01	1.000E 00	1.000E 00	0.	1.230E 01	0.	1.094E 02	1.051E 01	1.708E 05	2
3	1.2259E 00	8.0000E-01	1.000E 00	1.000E 00	0.	1.230E 01	0.	1.094E 02	9.314E 00	1.708E 05	3
4	1.8389E 00	7.5000E-01	1.000E 00	1.000E 00	0.	1.230E 01	0.	1.094E 02	8.186E 00	1.708E 05	4
5	2.4519E 00	7.0000E-01	1.000E 00	1.000E 00	0.	1.230E 01	0.	1.094E 02	7.131E 00	1.708E 05	5
6	3.0648E 00	6.5000E-01	1.000E 00	1.000E 00	0.	1.230E 01	0.	1.094E 02	6.149E 00	1.708E 05	6
7	3.0866E 00	6.4822E-01	1.000E 00	1.000E 00	0.	1.230E 01	0.	1.094E 02	6.115E 00	1.708E 05	7
8	3.0866E 00	6.4822E-01	7.293E 00	2.166E 00	8.294E 00	8.195E 00	2.873E-01	1.094E 02	6.115E 00	8.326E 04	8
9	3.2421E 00	6.5225E-01	7.580E 00	2.189E 00	8.734E 00	8.148E 00	2.868E-01	1.094E 02	4.909E 00	8.337E 04	9
10	3.4249E 00	6.5829E-01	7.788E 00	2.207E 00	9.175E 00	8.113E 00	2.870E-01	1.094E 02	3.439E 00	8.332E 04	10
11	3.6232E 00	6.6623E-01	7.906E 00	2.218E 00	9.596E 00	8.090E 00	2.884E-01	1.094E 02	1.798E 00	8.302E 04	11
12	3.8349E 00	6.7620E-01	7.943E 00	2.220E 00	1.000E 01	8.084E 00	2.875E-01	1.094E 02	8.462E-03	8.302E 04	12

TABLE III - SAMPLE OUTPUT (2-D)

STEP NUMBER 18 STRIP NUMBER 3

K	INTERFACE	SHOCK	SIGMA	1/SIGMA
1	20	16	1.1599865E-01	8.6207896E 00
2	0	25	2.4282260E 01	4.1182328E 00
3	0	0	0.	0.
4	0	0	0.	0.
5	0	0	0.	0.
6	0	0	0.	0.
7	0	0	0.	0.
8	0	0	0.	0.
9	0	0	0.	0.
10	0	0	0.	0.

	X	Y	P	T	THETA(DEG)	MACH	S	H	FLOW	P TOTAL	
1	7.1075E 00	2.1811E 00	1.222E 01	2.260E 00	-1.000E 01	8.010E 00	1.402E-01	1.094E 02	1.101E 02	1.203E 05	1
2	7.1661E 00	2.1630E 00	1.225E 01	2.263E 00	-1.002E 01	8.005E 00	1.410E-01	1.094E 02	1.075E 02	1.200E 05	2
3	7.1664E 00	2.1629E 00	1.225E 01	2.263E 00	-1.002E 01	8.005E 00	1.410E-01	1.094E 02	1.075E 02	1.200E 05	3
4	7.2039E 00	2.1512E 00	1.137E 01	2.216E 00	-1.042E 01	8.095E 00	1.415E-01	1.094E 02	1.059E 02	1.199E 05	4
5	7.2942E 00	2.1226E 00	1.142E 01	2.221E 00	-1.046E 01	8.086E 00	1.427E-01	1.094E 02	1.022E 02	1.195E 05	5
6	7.3898E 00	2.0923E 00	1.148E 01	2.226E 00	-1.049E 01	8.076E 00	1.439E-01	1.094E 02	9.841E 01	1.191E 05	6
7	7.5148E 00	2.0526E 00	1.155E 01	2.233E 00	-1.054E 01	8.063E 00	1.457E-01	1.094E 02	9.345E 01	1.186E 05	7
8	7.5237E 00	2.0497E 00	1.156E 01	2.233E 00	-1.055E 01	8.062E 00	1.458E-01	1.094E 02	9.309E 01	1.186E 05	8
9	7.7352E 00	1.9821E 00	1.168E 01	2.245E 00	-1.064E 01	8.039E 00	1.489E-01	1.094E 02	8.487E 01	1.177E 05	9
10	7.7825E 00	1.9676E 00	1.171E 01	2.248E 00	-1.066E 01	8.033E 00	1.496E-01	1.094E 02	8.306E 01	1.175E 05	10
11	7.9528E 00	1.9118E 00	1.182E 01	2.363E 00	-1.073E 01	7.820E 00	2.158E-01	1.094E 02	7.669E 01	9.956E 04	11
12	8.0614E 00	1.8761E 00	1.189E 01	2.487E 00	-1.079E 01	7.605E 00	2.854E-01	1.094E 02	7.279E 01	8.365E 04	12
13	8.1953E 00	1.8311E 00	1.198E 01	2.713E 00	-1.086E 01	7.253E 00	4.040E-01	1.094E 02	6.820E 01	6.219E 04	13
14	8.2116E 00	1.8256E 00	1.199E 01	2.742E 00	-1.087E 01	7.211E 00	4.185E-01	1.094E 02	6.766E 01	5.998E 04	14
15	8.2264E 00	1.8205E 00	1.200E 01	2.768E 00	-1.087E 01	7.174E 00	4.316E-01	1.094E 02	6.717E 01	5.805E 04	15
16	8.2699E 00	1.8056E 00	1.203E 01	2.834E 00	-1.090E 01	7.081E 00	4.635E-01	1.094E 02	6.577E 01	5.359E 04	16
17	8.2699E 00	1.8056E 00	6.173E 01	5.093E 00	3.110E-01	5.068E 00	6.299E-01	1.094E 02	6.577E 01	3.536E 04	17
18	8.2795E 00	1.8037E 00	6.173E 01	5.124E 00	3.111E-01	5.050E 00	6.385E-01	1.094E 02	6.462E 01	3.460E 04	18
19	8.4042E 00	1.7790E 00	6.171E 01	5.262E 00	3.128E-01	4.970E 00	6.758E-01	1.094E 02	5.002E 01	3.153E 04	19
20	8.4374E 00	1.7724E 00	6.170E 01	5.286E 00	3.132E-01	4.957E 00	6.820E-01	1.094E 02	4.620E 01	3.103E 04	20
21	8.4374E 00	1.7724E 00	6.170E 01	5.353E 00	3.132E-01	4.919E 00	6.998E-01	1.094E 02	4.620E 01	2.969E 04	21
22	8.4754E 00	1.7648E 00	6.169E 01	5.353E 00	3.139E-01	4.919E 00	6.998E-01	1.094E 02	4.188E 01	2.969E 04	22
23	8.7092E 00	1.7148E 00	4.793E 01	4.787E 00	-1.710E 00	5.258E 00	6.444E-01	1.094E 02	1.802E 01	3.410E 04	23
24	8.7926E 00	1.6945E 00	3.263E 01	4.194E 00	-4.625E 00	5.681E 00	6.129E-01	1.094E 02	1.150E 01	3.689E 04	24
25	8.7998E 00	1.6926E 00	3.132E 01	4.136E 00	-4.912E 00	5.726E 00	6.098E-01	1.094E 02	1.104E 01	3.718E 04	25
26	8.7998E 00	1.6926E 00	1.162E 02	6.405E 00	5.669E 00	4.405E 00	6.977E-01	1.094E 02	1.104E 01	2.984E 04	26
27	8.8340E 00	1.6921E 00	1.167E 02	6.407E 00	5.708E 00	4.404E 00	6.967E-01	1.094E 02	1.026E 01	2.992E 04	27
28	8.8299E 00	1.6885E 00	1.104E 02	6.542E 00	5.221E 00	4.448E 00	7.480E-01	1.094E 02	5.492E 00	2.992E 04	28

APPENDIX III

RESULTS

The shock wave pattern for the example case given in Appendix II is shown in Figure 41. The strip numbers are shown in the Figure in order to illustrate once again that feature of the program.

Another sample case is shown in Figure 42. This is an internal flow problem with many sharp compressions and expansions and illustrates very well the interaction of the various wave patterns. The flow is two-dimensional and at an incident Mach number of 3, $\bar{P}$ is the ratio of the local pressure to free stream pressure and M is the local Mach number. The values of $\bar{P}$ and M are indicated for various points in the flow field. Thus, at point D we have $\bar{P} = 0.109$ and $M = 4.63$. Point D is just in front of the intersection of the two shocks. Do not interpret the letters as indicating that an entire area has the specified properties. For instance, the properties of F are at a point at the wall slightly in front of the expansion corner. The properties vary along the wall between E and F.

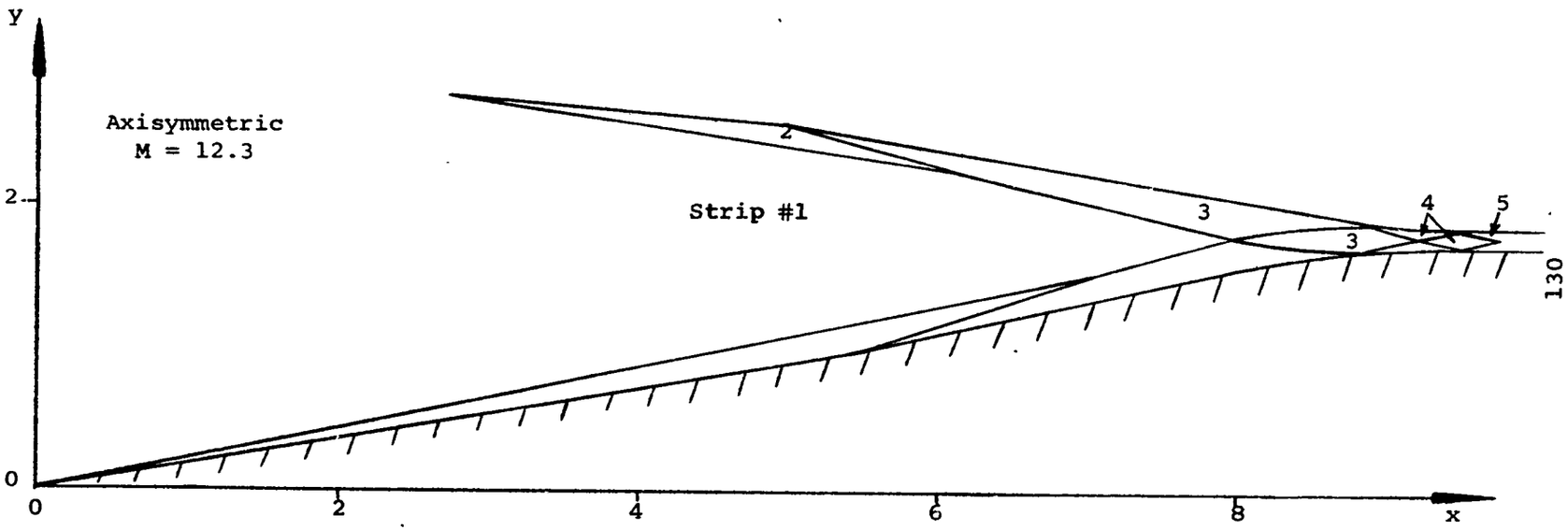

FIGURE 41 - SAMPLE COMPUTATION - SHOCK WAVE PATTERN

	$\bar{P}$	M
A	0.431	3.58
B	0.160	4.32
C	0.980	2.72
D	0.109	4.65
E	1.840	2.26
F	0.412	3.24
G	0.169	3.87
H	0.543	3.02
I	0.406	3.22
J	1.650	2.36
K	1.650	2.26
L	0.242	3.63
M	0.965	2.53
N	2.760	1.78
O	1.960	2.12
P	0.301	3.22
Q	0.768	2.55
R	1.670	2.02

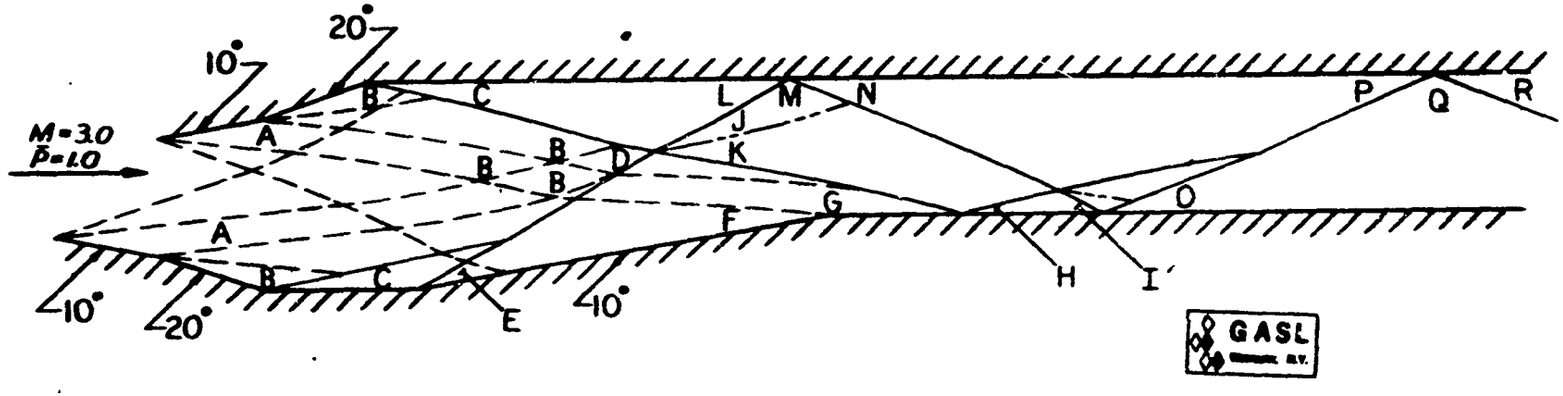

FIGURE 42 - SAMPLE INTERNAL FLOW COMPUTATION

APPENDIX IV

DISCUSSION ON THE GEOMETRY SPECIFICATION AND SUGGESTIONS ON HOW TO ACHIEVE GREATER FLEXIBILITY

It has already been stated that the geometry of the upper and lower walls is specified through a number of second order polynomial fits for y as a function of x. Presently, this number is nine, but it can be increased by simply increasing the dimension of the appropriate variables. In addition, there is provision for six corners on each wall. That number can also be increased. The dimension of the appropriate variables must be one more than the number of fits or corners, respectively.

It would not be difficult to increase the order of the polynomials. The limitations are primarily machine storage space and convenience in input. However, the polynomials could be increased to sixth order while still retaining the pattern of one data card per polynomial. It is only necessary to modify the dimension statements for YLBC and YUBC from (10, 4) to (10, 7), to change the corresponding input and output statements, and to modify the coding in functions YUB, YLB, TUB, TLB, which compute y(x) and dy/dx on the upper and lower boundaries.

These functions can be made as versatile as desired, the only penalty being that a certain amount of programming needs to be performed. Each of these functions has an argument, XIN, which is the value of the abscissa at which one would like either y or dy/dx. That is,

FUNCTION YLB (XIN) computes y(XIN) on the lower boundary,

FUNCTION TLB (XIN) computes τ=dy/dx at x=XIN on the lower boundary.

FUNCTION YUB (XIN) computes y (XIN) on the upper boundary,

FUNCTION TUB (XIN) computes τ=dy/dx at X=XIN on the upper boundary.

An example can best illustrate the method for changing the geometry routines. Suppose that the second order fits are satisfactory on the upper wall but not on the lower wall where it is desired to specify y(x) as:

$y(x) = 0$ $\quad 0 \leq x \leq 1$

$y(x) = \tanh(x-1)$ $\quad 1 < x \leq 2$

$y(x) = 0.76159$ $\quad x > 2$

then

$y'(x)=0 \qquad 0 \le x < 1$

$y'(x)=\text{sech}^2(x-1) \qquad 1 < x < 2$

$y'(x)=0 \qquad x > 2$

The procedure is to recompile FUNCTION YLB(XIN) and FUNCTION TLB(XIN) as follows:

```
$IBFTC YL
      FUNCTION YLB(XIN)
      IF(XIN.LE.1.))YLB=0.0
      IF(XIN.GT.1.).AND.XIN.LE.2.0)YLB=TANH(XIN-1.0)
      IF(XIN.GT.2.0)YLB=0.76159
      RETURN
      END
$IBFTC TL
      FUNCTION TLB(XIN)
      IF(XIN.LE.1.0)TLB=0.0
      IF(XIN.GT.1.0.AND.XIN.LE.2.0)TLB=1./COSH(XIN-1.0))**2
      ID(XIN.GT.2.0)TLB=0.0
      RETURN
      END
```

Do not forget that it is necessary to input the proper data indicating that there is a compressive corner at x=1.0 and an expansion corner at x=2.0.

APPENDIX V

PROGRAM OPERATION (THREE-DIMENSIONAL)

These programs are coded in the IBM Fortran IV language. It is designed for use with the IBSYS Monitor system for the IBM 7090/94 digital computer. The only tapes utilized are the system input tape mounted on unit B1 (logical tape 5), and the system BCD output tape mounted on unit B2 (logical tape 6).

No sense switch settings are interrogated, nor any program stops anticipated. This program may be "backed" with other runs and may be pre-processed via the IBM1401, say, in the usual manner.

Execution time for the longer programs is approximately 1 minute per case.

1. Wedge Program

The wedge program computes the shock and inviscid flow field about a swept wedge with supersonic leading edges including the effects of an angle of attack. The conditions behind the reflection of this shock from a plane surface parallel to the base of the wedge as well as the reflected shock geometry are also computed. In its present form the program uses a ratio of specific heats, γ, equal to 1.4.

Input

The card input to the program is on a single card and is read as follows:

χ, M_∞, λ, α, Δz, r

FORMAT (6E10.4)

The symbols in the input statement have the following meanings:

CHI (χ): Wedge sweep angle (deg.)
M-INF(M_∞): Free stream Mach number
LAMBDA (λ): Wedge angle in y-z plane (deg.)
ALPHA (α): Angle of attack with respect to wedge base plane (deg.)
DELTA Z (Δz) Step size in z for determining intersection curve. A typical value is 0.05r.
R(r): Distance between reflection plane and the base plane of the wedge (normalized in any convenient manner).

Output

The output consists of the conditions in the two-dimensional region and the constants that define the shock shape, followed by tables of conditions in the conical region for each computed point on the shock reflection curve. It should be noted that the conditions corresponding to the last point in these tables represent the two-dimensional shock reflection.

The meanings of the symbols in the first part of the output are:

LAMBDA-N(λn): Wedge angle in a plane normal to the leading edge (radians).
ALPHA-N (α_n): Sum of wedge angle and angle of attack in plane normal to leading edge, i.e., flow deflection across two-dimensional shock (radians).

MN-INF (M_{n_∞}): Component of free stream Mach number in a plane normal to leading edge.

MT-INF (M_{t_∞}): Component of free stream Mach number tangent to leading edge.

THETA (θ_1): Two-dimensional shock angle with respect to M_{n_∞} in a plane normal to leading edge (radians).

P1/P-INF (P_1/P_∞): Pressure jump across two-dimensional shock.

MT1 (M_{t_1}): Component of Mach number behind two-dimensional shock, tangent to leading edge.

THETA-N (θ_{1n}): Shock angle with respect to base plane of wedge in a plane normal to leading edge (radians).

M-1 (M_1): Total Mach number on wedge surface.

CHI-STAR (χ^*): Angle between z'-axis and leading edge (radians).

SIGMA-1 (σ_1): Flow deviation on wedge surface with respect to z' axes (radians).

THETA-S (θ_s): Two-dimensional shock angle with respect to the base plane of wedge in a plane parallel to the x-y plane (radians).

BETA-STAR (β^*): Two-dimensional shock angle with respect to base plane of wedge in a plane parallel to the y-z plane (radians).

THETA-CP (θ'_c): Two-dimensional shock angle with respect to base plane of wedge in a plane normal to the z' axis (radians).

A : Constant in equation of parabolic sheet (35)

XJP (x_j'): The x coordinate of the point of intersection of the two-dimensional shock and the local Mach cone in the plane $z' = \cos \lambda$

H(h): Constant in equation of parabolic sheet (36)

THETA-SW (θ_{sw}): Angle between the three dimensional shock and the z' axes in the y-z plane (radians).

The meanings of the symbols in the tables of conditions on each conical ray i are:

I(i): Designates conical ray in central region.

Z(z_i): Normalized z coordinate of the intersection point of conical ray i and the shock reflection curve on plane surface.

X(x_i): Normalized x coordinate of the intersection point of conical ray i and the shock reflection curve on plane surface.

CHI (χ'_i): Angle between the tangent to the intersection curve and the z-axes (radians).

SIGMA-1 (σ_{1_i}): Flow deviation on conical ray i (radians).

M-1(M_{1_i}): Total Mach number on conical ray i.

MT($M_{1_{t_i}}$): Upstream Mach number component tangent to intersection curve.

MN($M_{1_{n_i}}$): Upstream Mach number component normal to intersection curve, on plane surface.

MKN (M_{N_i}): Total Mach number component in a plane normal to intersection curve.

DELTA-1(δ_{1_i}): Flow deflection across reflected shock (radians).

M2T($M_{2_{t_i}}$): Component of Mach number behind reflected shock, tangent to intersection curve.

P2/P-INF (P_{2i}/P_∞): Pressure ratio behind reflected shock.

M2(M_{2_i}): Total Mach number behind reflected shock.

SIGMA-2(σ_{2i}): Flow deviation with respect to z axes behind reflected shock (radians).

THETA-P (θ_{2ni}): Reflected shock angle with respect to the reflection plane in a plane normal to the intersection curve (radians).

The subroutine which contains the oblique shock relations is equipped with four stops printed out as follows:

1) $M_\infty = 1$: If the total Mach number becomes sonic.

2) Upstream normal Mach number < 1: If the Mach number component in a plane normal to the leading edge or to the intersection curve becomes sonic.

3) Mach Reflection: If the flow deflection used in the shock relations exceeds the maximum value given by

$$\delta_m = \frac{4}{3\sqrt{3}(\gamma+1)} \frac{(M_N^2 - 1)^{3/2}}{M_N^2}$$

where M_N is the Mach number component in a plane normal to the leading edge or to the intersection curve. The computation of the intersection curve is terminated but the rest of the computation is continued for the points already obtained.

4) Imaginary roots: If a pair of roots of the cubic equation for the shock angle are imaginary.

2 Conical Shock-Plane Surface Program and Characteristic Subroutine

This program starts with the shock and flow field about a cone at zero angle of attack and computes the reflection of this shock from a plane inclined at an angle θ_1 to the cone axes. The characteristic subroutine computes the flow field behind the reflection curve on the plane surface by using two-dimensional characteristics and may be applied to any of the programs of the report. The ratio of specific heats, $\bar{\gamma}$, is an input quantity in the program, while the characteristic subroutine automatically uses the value which the main program has used.

Main Program

Input

The card input to the program is on two cards and is read as follows:

CARD 1: M_∞, θ_1, γ_c, $\bar{\gamma}$, r, q, $\Delta z'$
FORMAT (7E 10.4)

CARD 2: P_c/P_∞, M^*_{1c}, ψ_{1c}, S_2/R
FORMAT (4E 10.4)

The symbols in the input statement have the following meanings:

M-INF(M_∞): Free stream Mach number.

THETA-1(θ_1): Angle between plane surface and free stream direction (deg.)

GAMMA-C (γ_c): Conical shock angle from Reference 15 (rad.)

R (r): y distance between origins 0 and 0' (Fig.31), normalized in any convenient manner.

Q (q): Nondimensionalized z distance between 0 and 0', usually zero.

DELTA-Z($\Delta z'$): Step size in z' for determining intersection curve. A typical value is 0.05 r.

PC/P-INF (p_c/p_∞): Pressure ratio across conical shock, from Reference 15.

M1-STAR (M^*_{1c}): Critical Mach number behind conical shock, from Reference 15.

PSI (ψ_{1c}): Angle of flow behind conical shock with respect to the cone axes (rad.).

S2/R(S_2/R): Entropy change across conical shock normalized with respect to the gas constant.

Output

The output of the program consists of tables of conditions in front of and behind the reflected shock, near the plane surface, for each point i on the reflection curve.

The meanings of the symbols in the output are:

I(i): Designates point on reflection curve.

ZP(z'_i): Normalized z' coordinate of point i on reflection curve.

XP (x'_i): Normalized x' coordinate of point i on reflection curve.

OMEGA (Ω_i): Angle between the tangent of the reflection curve at point i and the z' axes. The computation terminates when $\Omega_i < 5^o$ (rad.).

M2XP ($M_{2x'_i}$): Mach number component behind conical shock in x' direction.

M2YP ($M_{2y'_i}$): Mach number component behind conical shock in y' direction.

M2ZP ($M_{2z'_i}$): Mach number component behind conical shock in z' direction.

M2N (M_{2ni}): Mach number component in front of the reflected shock, normal to the reflection curve, on the plane surface.

M?T ($M_{2_{t_i}}$): Mach number component in front of reflected shock, tangent to the reflection curve.

M2KN (M_{2N_i}): Total Mach number component in front of the reflected shock, in a plane normal to the reflection curve.

DELTA-2 (δ_{2i}): Flow deflection across the reflected shock in a plane normal to the reflection curve (radians).

P4/P2 $(p_4/p_2)_i$: Pressure jump across reflected shock.

A4/A2 $(a_4/a_2)_i$: Speed of sound ratio across reflected shock.

M4N (M_{4N_i}): Mach number component behind reflected shock in a plane normal to the reflection curve.

THETA 4 (θ_{4_i}): Reflected shock angle, in a plane normal to the reflection curve, with respect to the direction of M_{2N_i}, (radians).

M4T (M_{4t_i}): Mach number component behind reflected shock, tangent to reflection curve.

P4/P-INF (p_{4_i}/p_∞): Pressure ratio behind reflected shock.

SIGMA-4(σ_{4i}): Flow deviation behind reflected shock, with respect to z' axes (radians).

THETA-P-4(θ'_{4_i}): Reflected shock angle with respect to plane body (radians).

S(S_{4_i}): Change in entropy from the free stream value, nondimensionalized by twice the specific heat at constant pressure (2 c_p).

Characteristic Subroutine

The Characteristic Subroutine is an integral part of the program of this section, Conical-Shock-Plane Body, and the program of Section V, Plane Shock-Conical Body. In these cases no additional input is needed. The subroutine also exists as a separate program for which the input is given below. The output of the subroutine is the same for all cases and is also given below.

Input

When used as a separate program, the input is on N+1 cards and is read as follows:

CARD 1: γ, p_{NN}/p_{∞}, N
FORMAT(2E10.4, I10)

CARD 2: M_N, ρ_N, ψ_N, θ_N, S_N (Data at last point of main program)

. (One card for each data point)
.
.

CARD N+1: M_1, ρ_1, ψ_1, θ_1, S_1 (Data at first point of main program)

The symbols in the input statement have the following meanings:

GAMMA (γ): Ratio of specific heats

P/P ($p_{N,N}/p_{\infty}$): Pressure ratio at point N,N (Fig.32).

N: Number of data points.

M ($M_{i,j}$): Total Mach number at data point, i=j.

RHO ($\rho_{i,j}$): Nondimensionalized coordinate of data point (Fig.32).

PSI ($\psi_{i,j}$): Nondimensionalized coordinate of data point (Fig.32.)

THETA ($\theta_{i,j}$): Flow deviation with respect to ρ axes, at data point (radians).

S ($\bar{S}_{i,j}$): Entropy change from free stream at data point, normalized with respect to twice the specific heat at constant pressure.

Output

The output consists of the Mach angle and velocity at the data points, which is printed next to the data, and a page of output for each second family characteristic line, i=constant, which gives the flow conditions at each point along the line.

The output symbols, not defined under input, have the following meanings:

MU ($\mu_{i,j}$): Mach angle (radians).

W ($W_{i,j}$): Flow velocity, normalized with respect to the limiting velocity.

I (i): Second family characteristic line. The computation starts at I=N, Fig. 32.

P/P-INF ($p_{i,j}/p_{\infty}$): Pressure ratio at the wall points, i.e., last point on each i line.

J (j): First family characteristic line, Fig.32.

3. Double Conical Shock Program

The double conical shock program computes the flow field behind the intersection of two conical shocks of different strength when given the flow conditions behind the shocks. An option is included which allows one of the cones to be oriented by an angle attack, α, with respect to the free stream direction. The properties immediately behind the upper and lower shocks behind the intersection are found, along with the new shock angles. This data can be used in the characteristic subroutine, (Section C), to find the flow field on a plane passing through the shock intersection.

Input

The card input consists of three cards if both cones are at zero angle of attack and four cards if one cone is at an angle of attack, and is read as follows:

CARD 1: M_1^*, ψ_1^*, γ_1, p_1/p_∞, S_1/R
FORMAT (5E10.4)

CARD 2: $M^*_{1,2}$, $\psi^*_{1,2}$, γ_2, p_2/p_∞, $S_{1,2}/R$
FORMAT (5E10.4)

CARD 3: $r, q, \Delta\psi, \bar{\gamma}$, S_2/R, KALF

FORMAT (5E10.4, I10)

CARD 4: α, η/α, M_2^*, $M^*_{w,2}$, ψ_2^*

FORMAT (5E10.4)
(Only required if the angle of attack $\alpha \neq 0$)

The symbols in the input have the following meanings:

Ml* (M_1^*): Critical Mach number behind the shock of the first cone, ("base cone"), which has zero angle of attack.

PSI 1* (ψ_1^*) Flow direction angle behind the shock of the base cone, (radians).

GAMMA 1 (γ_1): Base cone shock angle, (radians).

P1/P-INF (p_1/p_∞): Pressure jump across base cone shock.

S1/R (S_1/R): Entropy increase across base cone shock, normalized with respect to the universal gas constant, Reference 15.

M12* ($M^*_{1,2}$): Critical Mach number behind the shock of the second cone, for zero angle of attack.

PS12 ($\psi^*_{1,2}$): Flow direction angle behind the shock of the second cone, for zero angle of attack, (radians).

GAMMA 2 (γ_2): Shock angle of second cone at zero angle of attack, (radians).

P2/P-INF (p_2/p_∞): Pressure ratio across the second cone shock, for zero angle of attack.

S12/R ($S_{1,2}/R$): Entropy increase across second cone shock, for zero angle of attack.

R(r): Vertical, (y), distance between cone verticies, normalized in any convenient manner.

Q (q): Normalized z distance between cone verticies.

DELTA-PSI ($\Delta\psi$): Step size in ψ for determining the intersection curve. A typical value is 5 deg. (deg.).

GAMMA-BAR ($\bar{\gamma}$): Ratio of specific heats.

S2/R (S_2/R): Entropy perturbation, due to angle of attack of second cone[16].

KALF: Index for including angle of attack of second cone; =0, zero angle of attack; $\neq 0$, nonzero angle of attack.

ALPHA (α): Angle of attack of second cone, (deg.).

ETA/ALPHA (η/α): Ratio of tilt angle of second cone shock to angle of attack [16].

M2* (M_2*): Critical Mach number perturbation, due to angle of attack, behind second cone shock.

MW2*($M^*_{w,2}$): Critical Mach number normal to meridian plane, behind second cone shock.

PSI2*(ψ_2^*): Flow direction angle perturbation, due to angle of attack, behind second cone shock, (radians).

Output

The output consists of the maximum value of ψ, three quantities which are invariant along the intersection curve and tables which describe the intersection curve, the base and second cone flows and the flows in the upper and lower intersection regions, for each point i on the intersection curve.

The meanings of the symbols in the output are:

PSI-MAX(ψmax.): Maximum value of intersection curve coordinate, ψ, before reaching double values of ρ, (degrees).

THETA-1 (θ_1): Angle between second cone shock axis and free stream direction, (radians).

COS(BZ) (cos(bz)): Direction cosine of binormal to intersection curve and z axes.

MZ1(M_{z_1}): Mach number component in z direction, behind lower cone shock.

PSI (ψ_i): Meridian coordinate of point on intersection curve, (radians).

COS(TX) ($\cos(tx)_i$): Direction cosine of tangent to intersection curve and x axes.

COS(TY) ($\cos(ty)_i$): Direction cosine of tangent to intersection curve and y axes.

COS(TZ) ($\cos(tz)_i$): Direction cosine of tangent to intersection curve and z axes.

COS(BX) ($\cos(bx)_i$): Direction cosine of binormal to intersection curve and x axes.

COS(BY) $(\cos(by)_i)$: Direction cosine of binormal to intersection curve and y axes.

COS(NX) $(\cos(nx)_i)$: Direction cosine of normal to intersection curve and x axes.

COS(NY) $(\cos(ny)_i)$: Direction cosine of normal to intersection curve and y axes.

COS(NZ) $(\cos(nz)_i)$: Direction cosine of normal to intersection curve and z axes.

RHO (ρ_i): Nondimensionalized radial coordinate of point on intersection curve.

GAMMA (Γ_i): Angle between the normal to the intersection curve and the free stream direction, (radians).

MY1 $(M_{y_{1_i}})$: Mach number component in y direction behind base cone shock.

MX1 $(M_{x_{1_i}})$: Mach number component in x direction behind base cone shock.

MT-BAR 1 $(M_{\bar{t}_{1_i}})$: Mach number component tangent to the intersection curve, behind the base cone shock.

MN-BAR 1 $(M_{\bar{n}_{1_i}})$: Mach number component along the normal to the intersection curve, behind the base cone shock.

MB-BAR 1 $(M_{\bar{b}_{1_i}})$: Mach number component along the binormal to the intersection curve, behind the base cone shock.

MN1 $(M_{n_{1_i}})$: Total Mach number component in a plane normal to intersection curve, behind the base cone shock upstream of the intersection.

DELTA 1 (δ_{1_i}): Strength of the base cone shock in a plane normal to the intersection curve, and which is assumed to be constant through the intersection, (radians).

X (x'): Nondimensionalized x' coordinate of intersection curve point i.

Y (y'): nondimensionalized y' coordinate of intersection curve point i.

Z (z'): nondimensionalized z' coordinate of intersection curve point i.

PHI (φ_i): Meridian angle of intersection curve point, (second cone coordinates), (radians).

U-BAR ($\bar{u}_i$): Velocity component behind the second cone shock along the z axes, normalized with respect to limiting velocity.

V-BAR ($\bar{v}_i$): Normalized velocity component behind the second cone shock along the r axes.

W-BAR ($\bar{w}_i$): Normalized velocity component behind the second cone shock, normal to the meridian plane.

M*(M_i^*): Total critical Mach number behind the second cone shock.

A2 (a_{2_i}): Speed of sound behind the second cone shock, normalized by the limiting velocity.

MX2 ($M_{x_{2_i}}$): Mach number component in x direction, behind second cone shock

MY2 ($M_{y_{2_i}}$): Mach number component in y direction, behind second cone shock.

MZ2 ($M_{z_{2_i}}$) Mach number component in z direction behind second cone shock.

MT-BAR 2 ($M_{\bar{t}_{2_i}}$): Mach number component tangent to the intersection curve, behind the second cone shock.

MN-BAR 2 ($M_{\bar{n}_{2_i}}$): Mach number component normal to the intersection curve, behind the second cone shock.

MB-BAR 2 ($M_{\bar{b}_{2_i}}$): Mach number component along the binormal to the intersection curve, behind the second cone shock.

MN2 ($M_{N_{2_i}}$): Total Mach number component in a plane normal to the intersection curve, behind the second cone shock.

DELTA 2 (δ_{2_i}): Strength of the second cone shock in a plane normal to the intersection curve, and which is assumed constant through the intersection, (radians).

MB1 ($M_{B_{1_i}}$): Mach number component behind lower portion of intersection, in a plane normal to the intersection curve.

THETA (θ_{3_i}): Second cone shock angle with respect to δ_{1_i}, in a plane normal to intersection curve, behind the intersection, (radians).

M3T ($M_{3_{t_i}}$): Mach number component behind lower portion of intersection, tangent to the intersection curve.

M3 (M_{3_i}): Total Mach number behind lower portion of intersection.

P3/P-INF (p_{3_i}/p_∞): Pressure ratio immediately behind lower portion of intersection.

S3 (S_{3_i}): Entropy change from free stream, behind lower portion of intersection, normalized by twice the specific heat at constant pressure.

MB2 ($M_{B_{2_i}}$): Mach number component behind upper portion of intersection, in a plane normal to the intersection curve.

THETA (θ_{4_i}): Base cone shock angle, with respect to δ_{2_i}, in a plane normal to the intersection curve, behind the intersection, (radians).

M4T ($M_{t_{4_i}}$): Mach number component behind upper portion of intersection, tangent to the intersection curve.

M4 (M_{4_i}): Total Mach number behind upper portion of intersection.

P4/P-INF (p_{4_i}/p_∞): Pressure ratio behind upper portion of intersection.

S4 (S_{4_i}): Entropy change from free stream behind upper portion of intersection, normalized by twice the specific heat at constant pressure.

4. Plane Shock - Conical Body

When given a conical flow field and a free stream Mach number, this program computes the flow behind the shock from a two-dimensional wedge, both before and after its intersection with the conical shock. The reflection curve of the modified plane shock on the conical body is then determined, together with the flow field behind the reflected shock on the cone surface. The characteristic subroutine, described in Section C, is incorporated in the program to compute the rest of the flow field on the conical body.

Input

The card input to the program consists of four cards and it is read as follows:

CARD 1: M_∞, δ_1, r, q, Δz, $\bar{\gamma}$
FORMAT (6E10.4)

CARD 2: pc/p_∞, p_b/p_∞, T_c/T_∞, S_2/R
FORMAT (4E10.4)

CARD 3: γ_c, M^*_{1c}, ψ_{1c}
FORMAT (3E10.4)

CARD 4: γ_b, M^*_{1b}, ψ_{1b}
FORMAT (3E10.4)

The meanings of the symbols in the input statement are:

M-INF (M_∞): Free stream Mach number.

DELTA-1 (δ_1): Two-dimensional wedge angle, (deg.)

R (r): y distance of the wedge vertex from the cone vertex, normalized in any convenient manner, (Figure 38).

Q (q): Normalized z distance of the wedge vertex from the cone vertex.

DELTA-Z ($\Delta z'$): Step size in z' for determining intersection curve.

GAMMA ($\bar{\gamma}$): Ratio of specific heats.

PC/P-INF (p_c/p_∞): Pressure ratio behind conical shock.

PB/P-INF (p_b/p_∞): Pressure ratio at cone surface.

TC/T-INF (T_c/T_∞): Temperature ratio behind conical shock.

S2/R (S_2/R): Entropy increase across conical shock, normalized with respect to the universal gas constant.

GAMMA (γ_c, γ_b): Conical shock and cone angles, respectively, (radians).

M1-STAR (M^*_{1c}, M^*_{1b}): Critical Mach numbers behind conical shock and on cone, respectively.

PSI-1 (ψ_{1c}, ψ_{1b}): Flow deviation behind conical shock and on cone, respectively, (radians).

Output

The output consists of many parts. The first includes some quantities in the two-dimensional and conical fields, which are independent of the shock intersection. Second, are tables describing the intersection curve of the plane and conical shocks, and the flow conditions ahead and behind the modified plane shock near the intersection. Next, the reflection curve of the modified plane shock on the cone surface is described, along with the flow conditions in front and behind this shock near the body. Finally, the conditions behind the reflected shock on the cone surface are given. The characteristic subroutine is included in the program and its output is described in Appendix V-2.

The meanings of the symbols in the output are:

GAMMA-C (γ_c): Cone shock angle, (radians).

MR (M_r): Mach number component behind the conical shock, parallel to the shock.

MT (M_t): Mach number component behind the conical shock, normal to the shock.

M-1 (M_1): Mach number behind the two-dimensional shock.

THETA-1 (θ_1): Two-dimensional shock angle, with respect to the free stream direction, (radians).

P1/P-INF(p_1/p_∞): Pressure jump across two-dimensional shock.

A1/A-INF(a_1/a_∞): Speed of sound increase across two-dimensional shock.

ZP (z'_i): Normalized z' coordinate of point on two-dimensional and conical shock intersection, on plane of two-dimensional shock.

XP (x'_i): Normalized x' coordinate of point on shock intersection curve.

OMEGA (Ω_i): Angle between the tangent to the intersection curve and the z' axes. The computation of the curve terminates when $\Omega_i<5^\circ$, (radians).

M2XP ($M_{2_{x'_i}}$): Mach number component in x' direction, behind conical shock.

M2YP ($M_{2_{y'_i}}$): Mach number component in y' direction, behind conical shock.

M2ZP($M_{2_{z'_i}}$): Mach number component in z' direction, behind conical shock.

M2NP ($M_{2_{n_i}}$): Mach number component normal to the intersection curve in the plane of the two-dimensional shock, behind the conical shock.

M2TP ($M_{2_{t_i}}$): Mach number component tangent to the intersection curve, behind the conical shock.

M2KN ($M_{2_{N_i}}$): Total Mach number component in a plane normal to the intersection curve, behind the conical shock.

DELTA (2): Flow deviation behind conical shock with respect to plane of two-dimensional shock, in a plane normal to the intersection. (First term of Eq. 138), (radians).

OMEGA-STAR: $\pi/2-\Omega_i$, (radians).

GAMMA: Free stream flow deviation with respect to the plane of the two-dimensional shock, in a plane normal to the intersection curve. (Second term of equation 138), (radians).

DELTA(2)STAR(δ^*_{2i}): Strength of the conical shock in a plane normal to the intersection curve, (radians).

DELTA (1): Flow deviation behind two-dimensional shock with respect to two-dimensional shock plane, in a plane normal to the intersection curve. (Second term of equation 135), (radians).

DELTA(1)STAR($\delta^*_{1_i}$): Strength of the plane shock in a plane normal to the intersection curve, (radians).

P4/P2 ($p_4/p_2)_i$: Pressure jump across modified plane shock.

A4/A2 ($a_4/a_2)_i$: Speed of sound increases across modified plane shock.

M4N ($M_{4_{N_i}}$): Mach number component in a plane normal to the intersection curve, in the lower intersection region.

THETA(4) (θ_{4i}): Modified plane shock angle behind intersection, with respect to upstream conical flow direction, in a plane normal to the intersection curve, (radians).

M4T ($M_{4_{t_i}}$): Mach number component tanget to the intersection curve, in the lower intersection region.

M4 (M_{4_i}): Total Mach number in the lower intersection region.

P4/P-INF($p_4/p_\infty)_i$: Pressure ratio in the lower intersection region.

A4/A-INF(a_{4_i}/a_∞): Speed of sound ratio in the lower intersection region.

SIGMA(4)(σ_{4_i}): Flow deviation in the lower intersection region with respect to the z'-axes, (radians).

THETAP(4) (θ'_{4_i}): Lower shock angle with respect to the ζ axes, Figure 39, (radians).

S4 (S_{4_i}): Entropy increase from free stream, in the lower intersection region, normalized by twice the specific heat at constant pressure.

GAMMA(K) (γ_b): Conical body half angle, (radians).

I (i): Shock - conical body intersection points.

ETA (η_{i_1}): Normalized coordinate, normal to plane of the two-dimensional shock, of intersection point of modified plane shock and conical body, (Figure 39).

ZETA (ζ_{i_1}): Normalized coordinate of intersection point, in plane of two-dimensional shock normal to intersection curve.

X (x_{i_1}): Normalized x coordinate of intersection point.

Y (y_{i_1}): Normalized y coordinate of intersection point.

Z (z_{i_1}): Normalized z coordinate of intersection point.

RHO (ρ_i): Normalized radial, conical coordinate of intersection point, (Figure 40).

PHI (φ_i): Meridian, conical coordinate of intersection point, (radians).

CHECK: Checks if x_{i_1}, y_{i_1}, z_{i_1}, lie on the conical body $(x^2_{i_1} + y^2_{i_1} - (\tan \nu_b)^2 z^2_{i_1} = 0)$

THREE POINT SELECTION: I=a, I=b, I=c : Intersection points chosen for determining reflection curve. (The program presently uses I=1, I=4 I=10).

RHO-0,RHO-1,RHO-2, (ρ_o, ρ_1, ρ_2): Normalized coordinates of the three selected points.

PHI-1,PHI-2, (φ_1, φ_2): Cooordinates of last two selected points. The coordinate $\varphi_o = 0$, (radians).

COS(TX) ($\cos(\hat{tx})_i$): Direction cosine of tangent to reflection curve and x axes.

COS(TY) ($\cos(\hat{ty})_i$): Direction cosine of tangent to reflection curve and y axes.

COS(TZ) ($\cos(\hat{tz})_i$): Direction cosine of tangent to reflection curve and z axes.

COS(BX) ($\cos(\hat{bx})_i$): Direction cosine of binormal to reflection curve and x axes.

COS(BY) ($\cos(\hat{by})_i$): Direction cosine of binormal to reflection curve and y axes.

COS(BZ) ($\cos(\hat{bz})_i$): Direction cosine of binormal to reflection curve and z axes.

COS(NX) ($\cos(\hat{nx})_i$): Direction cosine of normal to reflection curve and x axes.

COS(NY) ($\cos(\hat{ny})_i$): Direction cosine of normal to reflection curve and y axes.

COS(NZ) ($\cos(\hat{nz})_i$): Direction cosine of normal to reflection curve and z axes.

M2XP($M_{2_{x'_{bi}}}$): Mach number component, in x' direction, on conical surface.

M2YP($M_{2_{y'_{bi}}}$): Mach number component, in y' direction, on conical surface.

M2ZP($M_{2_{z'_{bi}}}$): Mach number component, in z' direction, on conical surface.

M2T($M_{2_{t_{bi}}}$): Mach number component tangent to intersection curve, on conical surface.

M2N($M_{2_{n_{bi}}}$): Mach number component normal to intersection curve, on conical surface.

M2KN($M_{2_{N_{bi}}}$): Total Mach number component in a plane normal to the intersection curve, on the conical body.

P4/P2($p_4/p_2)_{bi}$: Pressure jump across the modified plane shock near the cone.

A4/A2($a_4/a_2)_{bi}$: Speed of sound increase across the modified plane shock near the cone.

M4CN($M_{4_{N_{bi}}}$): Total Mach number component in a plane normal to the intersection curve, in front of the reflected shock, near the cone.

THETA(4)($\theta_{4_{b_i}}$): Modified plane shock angle near the cone, with respect to the direction of $M_{2_{N_{bi}}}$, (radians).

S4($S_{4_{b_i}}$): Total entropy change behind the modified plane shock near the cone, normalized by twice the specific heat at constant pressure.

M4T($M_{4_{t_{bi}}}$): Mach number component tangent to the intersection curve, in front of the reflected shock, near the cone.

M4N($M_{4_{n_{bi}}}$): Mach number component along normal to intersection curve, in front of reflected shock, near the cone.

M4B($M_{4_{b_{bi}}}$): Mach number component along binormal to intersection curve, in front of reflected shock, near the cone.

M4TB($M_{4_{t_i}}$): Mach number component tangent to the reflection curve, in front of the reflected shock, near the cone.

M4NB($M_{4_{n_i}}$): Mach number component along the normal to the reflection curve, in front of the reflected shock, near the cone.

($M_{4_{b_i}}$): Mach number component along the binormal to the reflection curve, in front of the reflected shock near the cone.

DELTA-4(δ_{4_i}): Flow deflection across the reflected shock in a plane normal to the reflection curve, (radians).

M4KN($M_{4_{N_i}}$): Total Mach number component in a plane normal to the reflection curve, in front of the reflected shock.

THETAP-6(θ'_{6_i}): Reflected shock angle with respect to the cone surface, in a plane normal to the reflection curve (radians).

P6/P4(p_6/p_4)$_i$: Pressure jump across reflected shock on cone surface.

A6/A4(a_6/a_4)$_i$: Speed of sound increase across the reflected shock on cone surface.

M6N($M_{6_{N_i}}$): Total surface Mach number component in a plane normal to the reflection curve behind the reflected shock.

M6T($M_{6_{t_i}}$): Surface Mach number component tangent to the reflection curve, behind the reflected shock.

P6/P-INF($p_6/p_\infty)_i$: Pressure ratio on cone surface behind reflected shock.

SIGMA-6(σ_{6_i}): Surface flow deviation behind the reflected shock, with respect to the β axes.

S6(S_{6_i}): Total surface entropy change behind the reflected shock, normalized by twice the specific heat at constant pressure.

APPENDIX VI

(SAMPLE PROBLEMS - THREE-DIMENSIONAL)

1. Wedge Program Example

To illustrate the use of the wedge program a particular example was carried out for the following input data:

χ = 55 deg.

M_∞ = 4.23

λ = 8 deg.

α = 0

Δz = 0.05

All lengths have been normalized with respect to r by inputting r=1. The program output is included in this appendix and the symbols are defined in Appendix V-1.

Each set of non-dimensionalized coordinates x and z represent a point on the intersection curve of the shock on the plane surface. However, if the ratio x/z is considered the variation of flow conditions on the wedge surface is determined. Each set of conditions, i, corresponds to the flow on a ray on the base plane of the wedge passing through the wedge vertex and making a angle $\tan^{-1}(x/z)_i$ with the z axes. Due to the assumption of linear theory the flow on the wedge surface is the same as that on the base plane of the wedge. The last set of conditions (i = 22) corresponds to those on the edge of the local Mach cone and therefore also to the constant conditions in the two-dimensional region. Note that the step size has been reduced by a factor of 5 for the last set of points in order to approach the two-dimensional values more closely. Figure 43 presents the variation of Mach number, pressure ratio and flow deviation across the wedge surface. Only half the wedge is shown due to its symmetry.

These conditions are also valid in front of the reflected shock. The strength of the reflected shock at any point i on the intersection curve depends on the upstream Mach number in a plane normal to the intersection curve at that point and on the

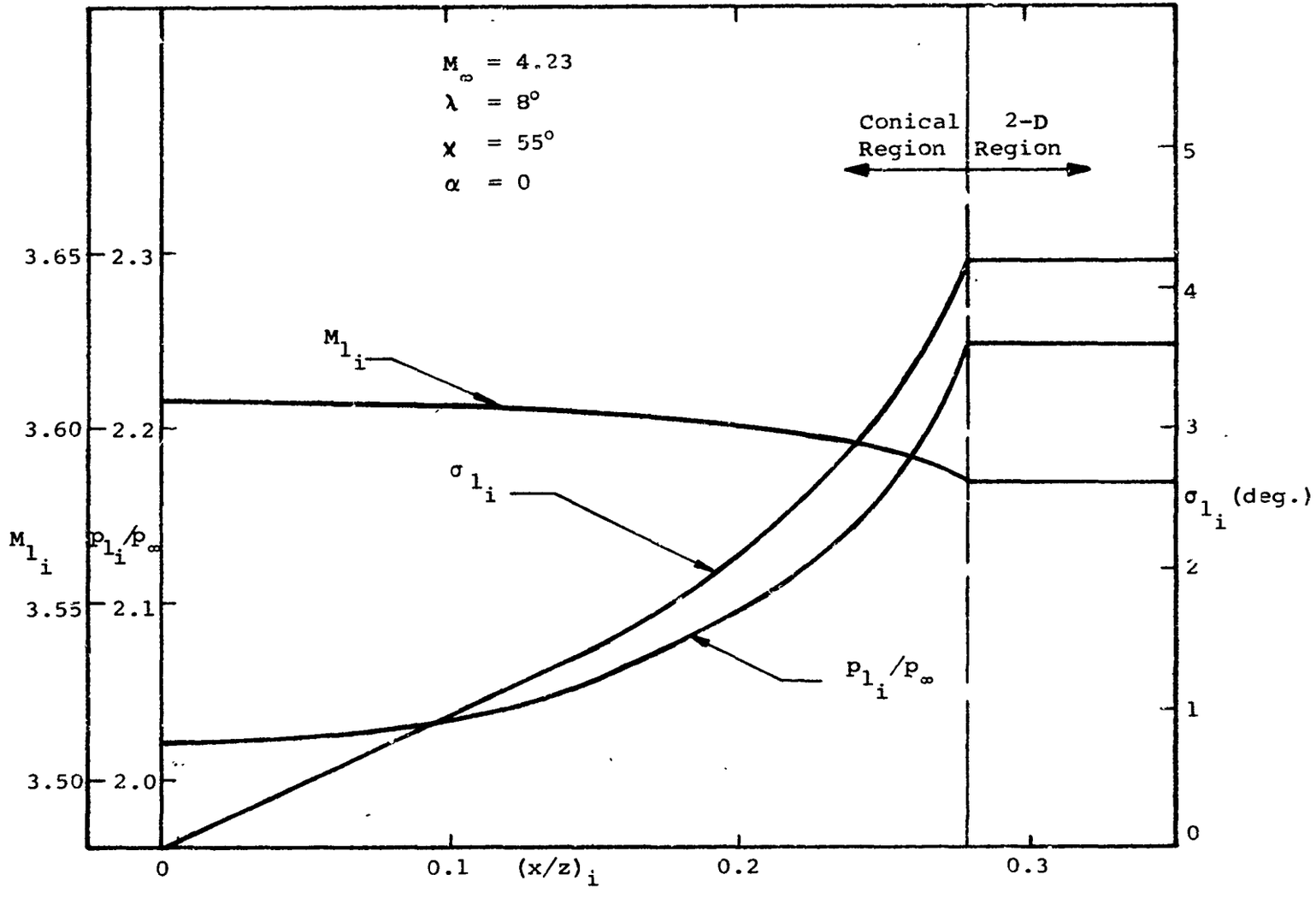

FIGURE 43 - WEDGE SURFACE CONDITIONS

deflection of the flow necessary to turn the flow parallel to the plane surface. These quantities are plotted for each point on the intersection curve in Figure 43. At first, one would expect that the shock strength would decrease as points further and further from the z axes are considered since the normal Mach number decreases. However, it is also necessary to consider the fact that the flow deflection increases as the two-dimensional region is approached. Therefore, the shock strength may increase or decrease depending on the relative effects of these two quantities. It is also possible that as the two-dimensional region is approached the required deflection will become too large for the corresponding normal Mach number, resulting in a Mach reflection. This did not occur in this example but would result in a program stop as described in Appendix V.

The conditions immediately behind the intersection curve on the plane surface are plotted in Figure 45. Figures 44 and 45 do not represent a cross section, but points on the intersection curve (Figure 30 of the main text). It can be seen that the shock strength decreases a little and then increases as the intersection curve is traversed from the z axes to the two-dimensional region. It should be noted that the values of θ_{2n_i} can be used to construct the reflected shock. In particular $\theta_{2n_{i=1}}$ is the angle between the reflected shock and the z axes in the y-z plane.

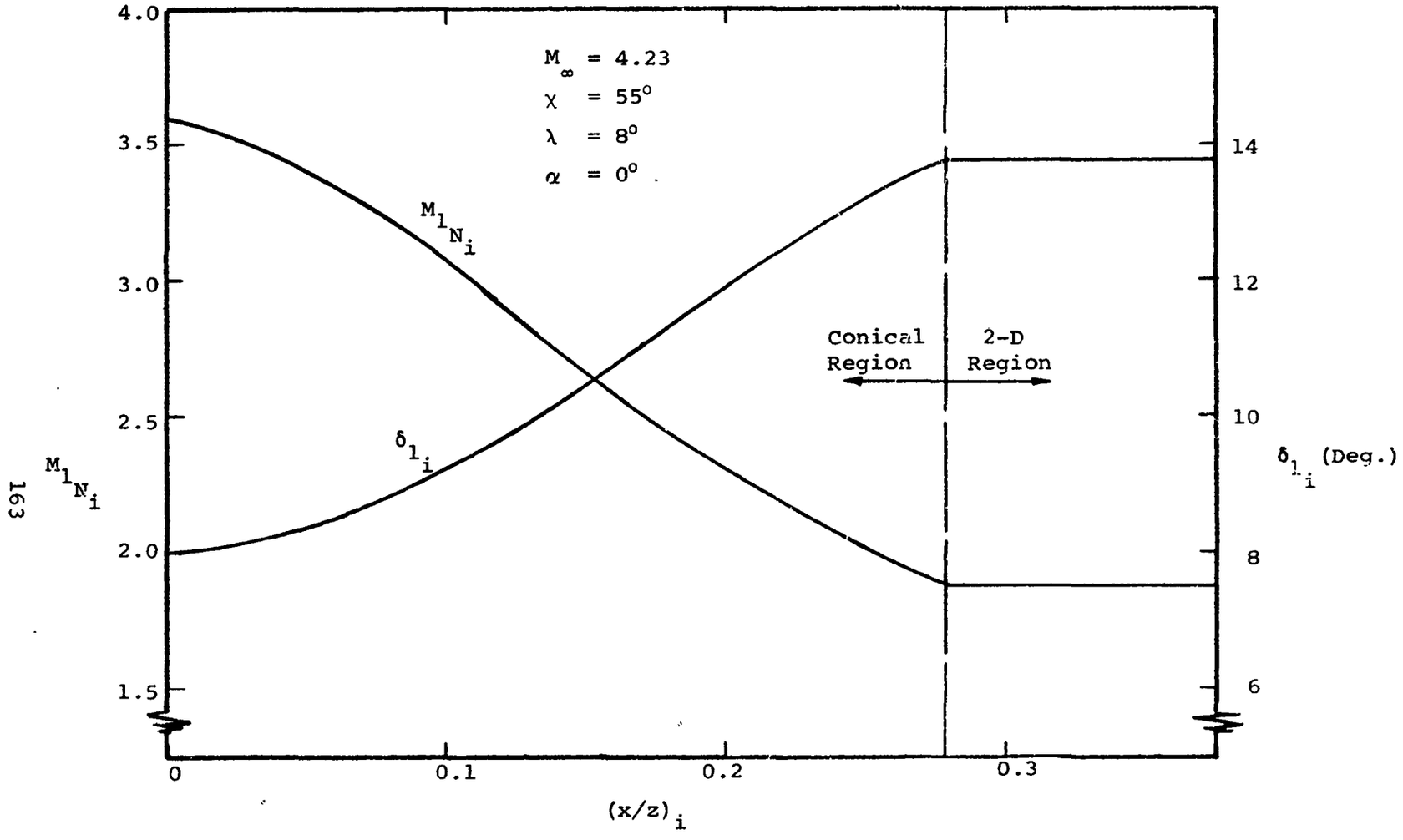

FIGURE 44 - CONDITIONS AFFECTING REFLECTED SHOCK STRENGTH

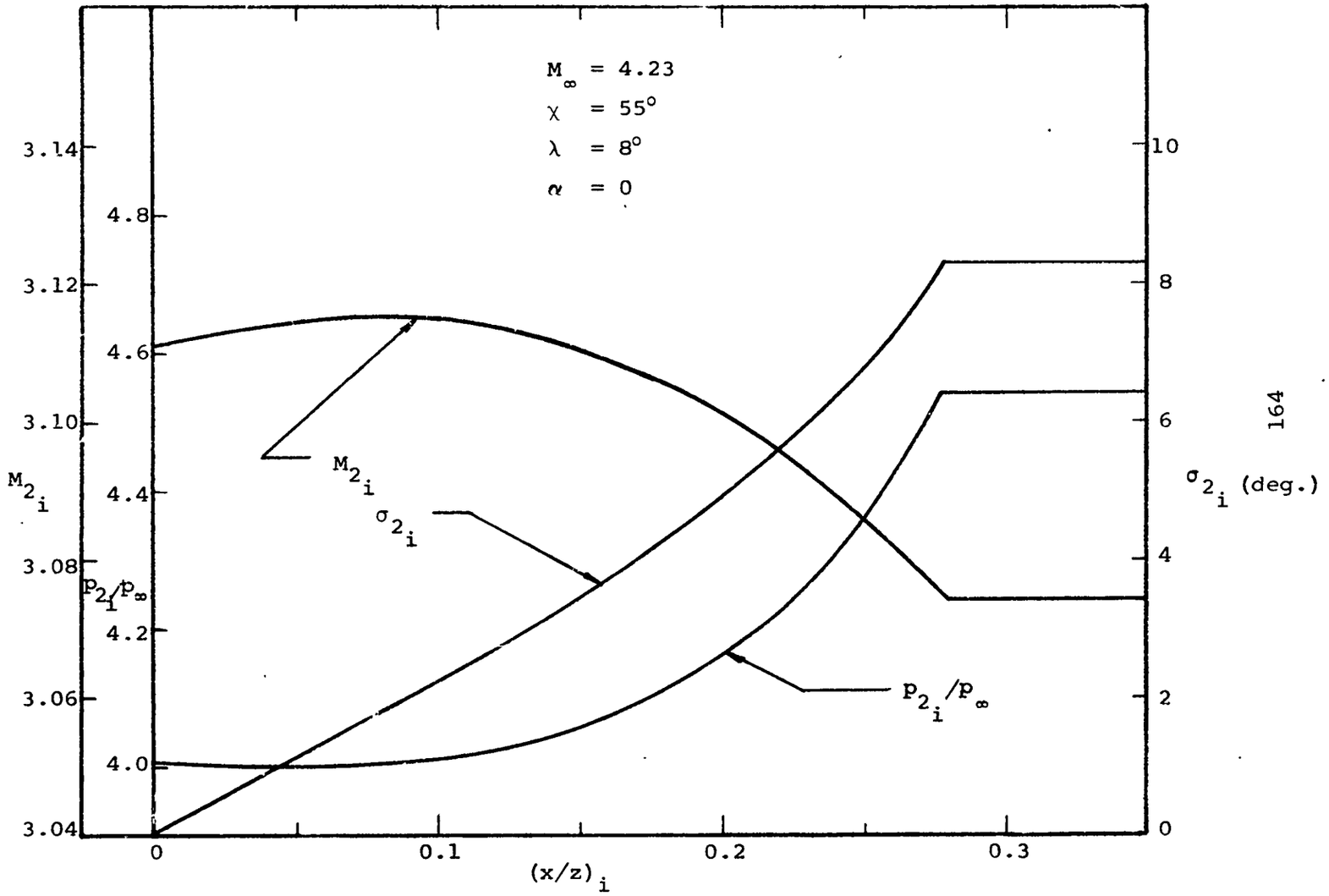

FIGURE 45 - CONDITIONS BEHIND INTERSECTION CURVE

TABLE IV - SAMPLE OUTPUT - SWEPT WEDGE

WEDGE COMPUTATION

CHI= 5.500000E 01 LAMBDA= 8.000000E 00 ALPHA= 0. R= 1.000000E 00
M-INF= 4.230000E 00 DELTA Z= 5.000000E-02 GAMMA= 1.400000E 00

LAMBDA-N= 2.402913E-01 ALPHA-N= 2.402913E-01 MN-INF= 2.426228E 00 MI-INF= 3.465013E 00 THETA= 6.374286E-01
P1/P-INF= 2.265736E 00 MT1= 3.058813E 00 THETA-N= 6.374286E-01 M-1= 3.583306E 00 CHI-STAR= 6.246290E-01
SIGMA-1= 7.674523E-02 THETA-S= 5.452279E-01 BETA-STAR= 4.016713E-01 THETA-CP= 5.241462E-01 A=-2.649042E-01
XJP= 9.255052E-01 B= 1.908921E-01 THETA-SW= 1.886229E-01

I	Z	X	CHI	SIGMA-1	M-1	P1/P-INF	MT
1	2.93626E 00	0.	1.57080E 00	-0.	3.80868E 00	2.021537E 00	0.
2	2.98626E 00	2.16858E-01	1.14473E 00	1.21989E-02	3.80780E 00	2.022940E 00	1.51627E 00
3	3.03626E 00	3.09125E-01	1.01059E 00	1.73664E-02	3.80693E 00	2.023751E 00	1.95060E 00
4	3.08626E 00	3.81567E-01	9.26460E-01	2.14191E-02	3.80604E 00	2.024572E 00	2.20628E 00
5	3.13626E 00	4.43997E-01	8.66835E-01	2.49177E-02	3.80514E 00	2.025404E 00	2.37871E 00
6	3.18626E 00	5.00176E-01	8.21771E-01	2.80809E-02	3.80423E 00	2.026252E 00	2.50393E 00
7	3.23626E 00	5.52018E-01	7.86281E-01	3.10231E-02	3.80330E 00	2.027115E 00	2.59941E 00
8	3.28626E 00	6.00645E-01	7.57500E-01	3.38151E-02	3.80236E 00	2.027999E 00	2.67484E 00
9	3.33626E 00	6.46784E-01	7.33641E-01	3.65059E-02	3.80139E 00	2.028905E 00	2.73608E 00
10	3.38626E 00	6.90934E-01	7.13515E-01	3.91335E-02	3.80040E 00	2.029840E 00	2.78890E 00
11	3.43626E 00	7.33453E-01	6.96299E-01	4.17300E-02	3.79937E 00	2.030809E 00	2.82985E 00
12	3.48626E 00	7.74610E-01	6.81401E-01	4.43258E-02	3.79831E 00	2.031818E 00	2.86672E 00
13	3.53626E 00	8.14611E-01	6.68380E-01	4.69526E-02	3.79720E 00	2.032878E 00	2.89884E 00
14	3.58626E 00	8.53620E-01	6.56904E-01	4.96473E-02	3.79602E 00	2.034003E 00	2.92718E 00
15	3.63626E 00	8.91766E-01	6.46715E-01	5.24577E-02	3.79476E 00	2.035212E 00	2.95251E 00
16	3.68626E 00	9.29155E-01	6.37614E-01	5.54533E-02	3.79339E 00	2.036537E 00	2.97549E 00
17	3.73626E 00	9.65876E-01	6.29431E-01	5.87502E-02	3.79185E 00	2.038032E 00	2.99670E 00
18	3.78626E 00	1.00200E 00	6.22043E-01	6.25833E-02	3.79003E 00	2.039812E 00	3.01681E 00
19	3.83626E 00	1.03700E 00	6.15341E-01	6.70644E-02	3.78761E 00	2.042214E 00	3.03708E 00
20	3.88626E 00	1.04465E 00	6.14074E-01	6.90085E-02	3.78694E 00	2.042868E 00	3.04147E 00
21	3.85626E 00	1.05170E 00	6.12831E-01	7.06587E-02	3.78617E 00	2.043603E 00	3.04622E 00
22	3.88626E 00	1.05872E 00	6.11610E-01	7.29599E-02	3.78507E 00	2.044775E 00	3.05186E 00

I	MN	MKN	DELTA-1	M2T	P2/P-INF	M2	SIGMA-2	THETA-P
1	3.57350E 00	3.60868E 00	1.39626E-01	0.	4.01123E 00	3.41139E 00	0.	2.40148E-01
2	3.23629E 00	3.27371E 00	1.51347E-01	1.36988E 00	4.00228E 00	3.41353E 00	2.92169E-02	2.73051E-01
3	2.99413E 00	3.03399E 00	1.62156E-01	1.76229E 00	4.01794E 00	3.41457E 00	4.12219E-02	3.00423E-01
4	2.81049E 00	2.85234E 00	1.71520E-01	1.99303E 00	4.03738E 00	3.41511E 00	5.04310E-02	3.23274E-01
5	2.66533E 00	2.70902E 00	1.79718E-01	2.14837E 00	4.05874E 00	3.41553E 00	5.82178E-02	3.44173E-01
6	2.54728E 00	2.59245E 00	1.86965E-01	2.26093E 00	4.08135E 00	3.41596E 00	6.51182E-02	3.63511E-01
7	2.44688E 00	2.49537E 00	1.93426E-01	2.34655E 00	4.10491E 00	3.41727E 00	7.14109E-02	3.81586E-01
8	2.36652E 00	2.41293E 00	1.99230E-01	2.41399E 00	4.12928E 00	3.41810E 00	7.72658E-02	3.98603E-01
9	2.29297E 00	2.34177E 00	2.04477E-01	2.46856E 00	4.15442E 00	3.41926E 00	8.27979E-02	4.14761E-01
10	2.22977E 00	2.27949E 00	2.09240E-01	2.51369E 00	4.18034E 00	3.42008E 00	8.80924E-02	4.30206E-01
11	2.17374E 00	2.22429E 00	2.13504E-01	2.55169E 00	4.20709E 00	3.42082E 00	9.32172E-02	4.45066E-01
12	2.12351E 00	2.17479E 00	2.17603E-01	2.58414E 00	4.23479E 00	3.42152E 00	9.82319E-02	4.59469E-01
13	2.07798E 00	2.12992E 00	2.21288E-01	2.61237E 00	4.26361E 00	3.42234E 00	1.03143E-01	4.73525E-01
14	2.03627E 00	2.08878E 00	2.24698E-01	2.63714E 00	4.29378E 00	3.42305E 00	1.08160E-01	4.87357E-01
15	1.99780E 00	2.05060E 00	2.27860E-01	2.65919E 00	4.32569E 00	3.42404E 00	1.13205E-01	5.01103E-01
16	1.96123E 00	2.01467E 00	2.30808E-01	2.67913E 00	4.35989E 00	3.42576E 00	1.18422E-01	5.14939E-01
17	1.92643E 00	1.98020E 00	2.33565E-01	2.69748E 00	4.39740E 00	3.42830E 00	1.23960E-01	5.29112E-01
18	1.89267E 00	1.94508E 00	2.36153E-01	2.71489E 00	4.44020E 00	3.43010E 00	1.30125E-01	5.44141E-01
19	1.85864E 00	1.90974E 00	2.38595E-01	2.73259E 00	4.49409E 00	3.43069E 00	1.37747E-01	5.61289E-01
20	1.82742E 00	1.87750E 00	2.39066E-01	2.73649E 00	4.50787E 00	3.43618E 00	1.39692E-01	5.65337E-01
21	1.83335E 00	1.88234E 00	2.38953E-01	2.74076E 00	4.52401E 00	3.43742E 00	1.41979E-01	5.69893E-01
22	1.82726E 00	1.88116E 00	2.40006E-01	2.74594E 00	4.54581E 00	3.43757E 00	1.45039E-01	5.75581E-01

2. Conical Shock-Plane surface Program Example

This program was run together with the characteristic subroutine program for the following input data.

$M_\infty = 4.0$

$\theta_1 = 10$ deg.

$\gamma_c = 0.30918$ rad. (10 deg. cone)

$\bar{\gamma} = 1.4$

$r = 2.5$

$q = 2.0$

$\Delta z = 0.01$

$p_c/p_\infty = 1.562$

$M^*_{1c} = 2.09123$

$\psi_{1c} = 0.0803353$ rad.

$S_2/R = 0.089929$

This program output is included in the appendix and the symbols are defined in Appendix V.2.

Corresponding to each value of i, the set of coordinates x' and z' represent a point on the reflection curve of the conical shock from the plane surface. This curve also represents the data line for the characteristic subroutine and is shown in Figure 46. The curve is terminated after computing a maximum number of 25 points. If it is necessary to find the flow further out on the curve the step size, Δz, would have to be increased. If a large enough step size were used the reflection curve computation would terminate either at a Mach reflection or when the slope of the curve with respect to the z' axes becomes 5° or less.

The variation of the reflected shock strength can be determined from Figure 47 where the total upstream Mach number component in a plane normal to the reflection curve ($M_{2_{N_i}}$) and and the flow deflection necessary to turn the flow parallel to the plane surface (δ_{2_i}) are plotted vs. the slope

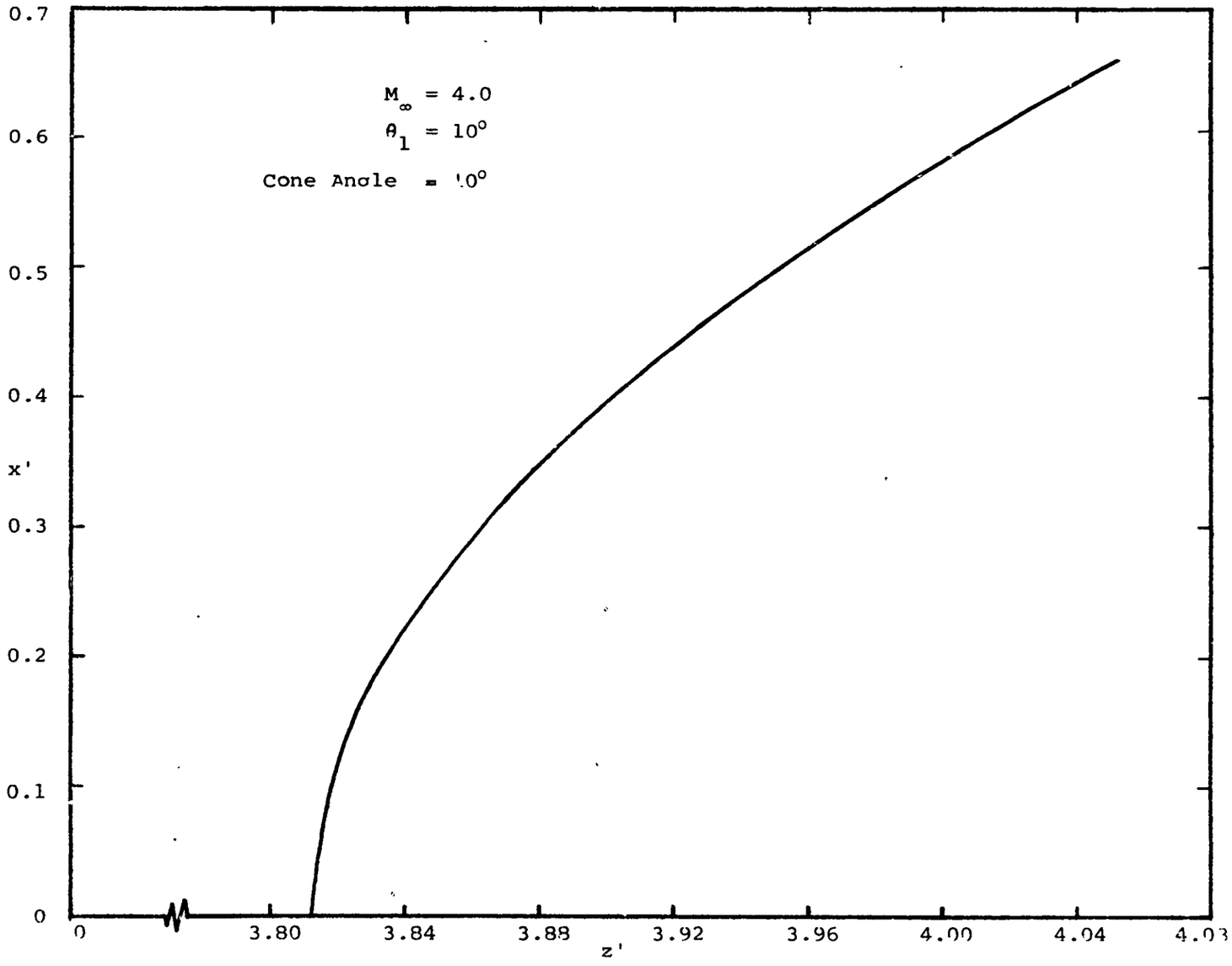

FIGURE 46 - INTERSECTION CURVE OF CONICAL SHOCK ON PLANE SURFACE

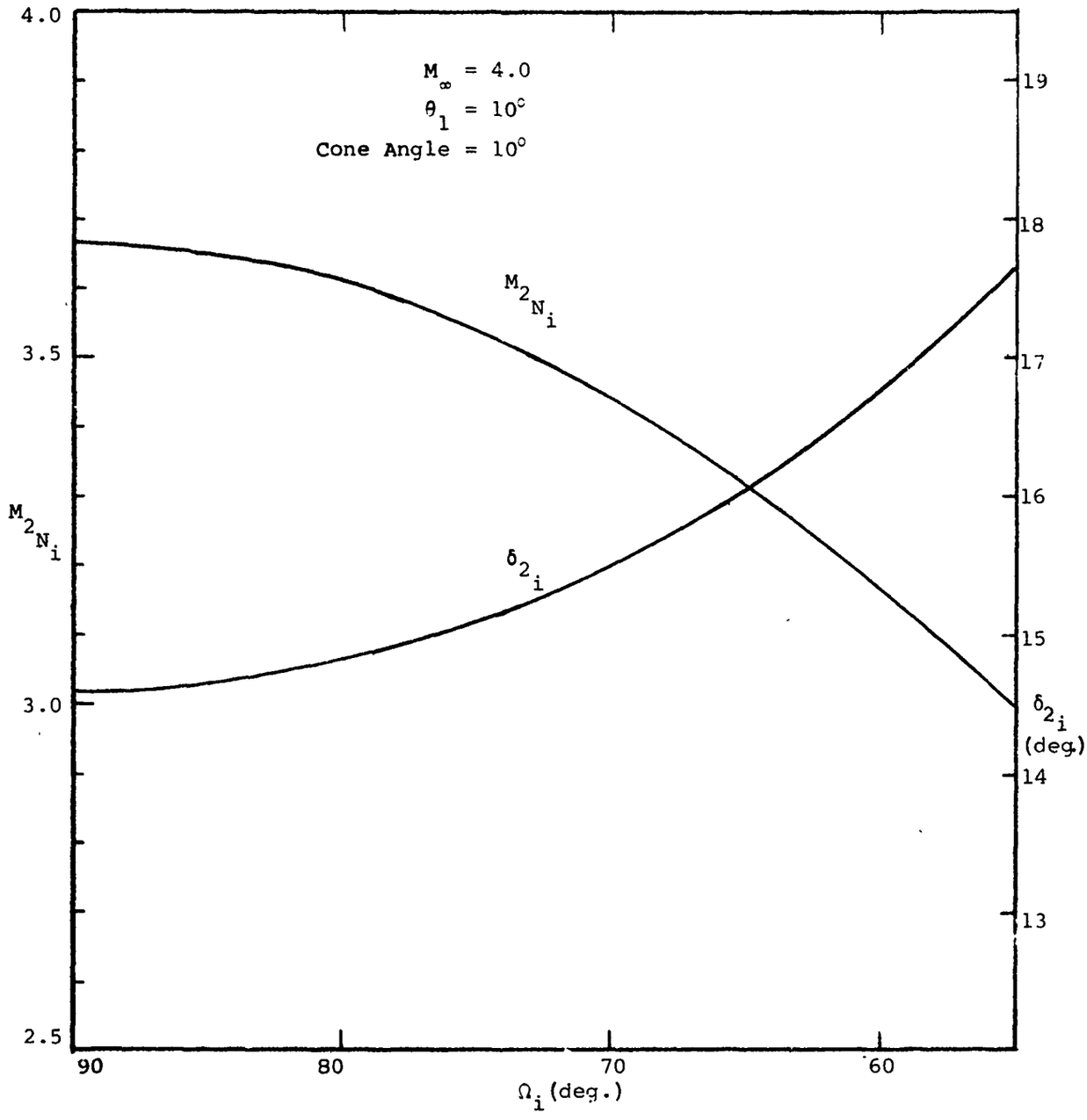

FIGURE 47 - CONDITIONS AFFECTING STRENGTH OF REFLECTED CONICAL SHOCK

of the reflection curve Ω_i . The effect of these parameters is described in Appendix VI.1 where it is also pointed out that this figure does not represent a cross-section but points along the reflection curve.

The conditions on the plane surface behind the reflection are given in Figure 48. The first part of the figure shows the pressure and Mach number variations immediately behind the reflection curve. It can be seen that a Mach relection must occur quite soon since the pressure is increasing so rapidly. The second part of the figure shows the variation of the pressure along the line of symmetry (ρ or z' axes) on the plane surface as obtained from the characteristic subroutine program.

Something should be said here about the output of the characteristic subroutine. The first page gives the value of the pressure behind the reflection curve on the centerline and the flow conditions along the reflection curve, which is now called the data line. The data is given in reverse order, i.e., the point furthest out on the curve is listed first and the centerline point is given last. The next page gives the conditions along the second family characteristic line closest to the centerline data point. This line is designated by the value of i, and the value of p/p_∞ given at the top is the pressure ratio at the intersection of this second family characteristic line and the centerline (wall). The procedure continues until the second family line from the data point furtherst out on the reflection curve has been considered.

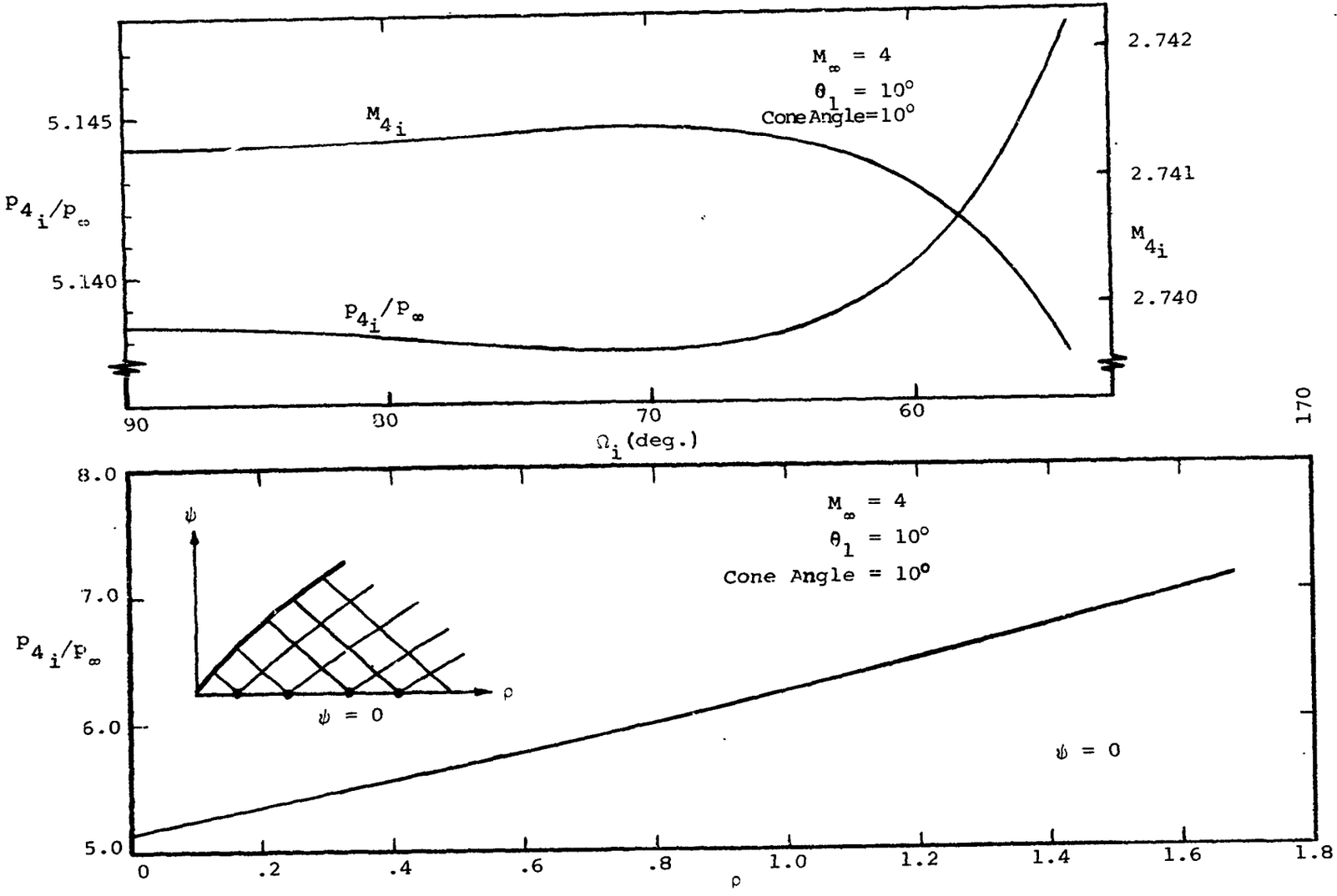

FIGURE 48 - CONDITIONS BEHIND REFLECTED SHOCK ON PLANE SURFACE

TABLE V - SAMPLE OUTPUT FOR CONICAL SHOCK - PLANE BODY PROGRAM

CONICAL SHOCK - PLANE BODY

M-INF= 4.000000E 00 THETA-B= 1.000000E 01 K= 2.500000E 00 M1-STAR= 2.091230E 00 PC/P-INF= 1.562000E 00
GAMMA= 1.400000E 00 GAMMA-C= 3.091800E-01 W= 2.000000E 00 DELTA-Z= 1.000000E-02 PSI= 8.033530E-02
SZ/R= 3.932500E-02

I	ZP	XP	OMEGA	M2XP	M2YR	M2ZP	M2N
1	3.[illegible]E 00	0.	1.570796E 00	0.	9.243344E-01	3.547845E 00	3.547845E 00
2	3.822127E 00	1.339923E-01	1.422685E 00	2.141159E-02	9.235661E-01	3.547980E 00	3.505976E 00
3	3.832127E 00	1.895305E-01	1.362956E 00	3.023476E-02	9.228004E-01	3.548115E 00	3.465517E 00
4	3.842127E 00	2.321711E-01	1.318178E 00	3.697394E-02	9.220373E-01	3.548250E 00	3.426392E 00
5	3.852127E 00	2.681395E-01	1.281272E 00	4.262944E-02	9.212768E-01	3.548384E 00	3.388529E 00
6	3.862127E 00	2.998405E-01	1.249406E 00	4.758940E-02	9.205189E-01	3.548518E 00	3.351861E 00
7	3.872127E 00	3.285284E-01	1.221326E 00	5.205324E-02	9.197636E-01	3.548651E 00	3.316327E 00
8	3.882127E 00	3.549419E-01	1.195990E 00	5.613959E-02	9.190108E-01	3.548783E 00	3.281870E 00
9	3.892127E 00	3.794976E-01	1.172892E 00	5.992566E-02	9.182606E-01	3.548916E 00	3.248437E 00
10	3.902127E 00	4.025943E-01	1.151835E 00	6.346596E-02	9.175129E-01	3.549048E 00	3.215978E 00
11	3.912127E 00	4.244528E-01	1.131925E 00	6.679920E-02	9.167677E-01	3.549179E 00	3.184446E 00
12	3.922127E 00	4.452949E-01	1.113543E 00	6.995527E-02	9.160250E-01	3.549310E 00	3.153800E 00
13	3.932127E 00	4.653423E-01	1.096313E 00	7.295728E-02	9.152848E-01	3.549440E 00	3.123998E 00
14	3.942127E 00	4.846279E-01	1.080096E 00	7.582368E-02	9.145471E-01	3.549571E 00	3.095001E 00
15	3.952127E 00	5.032026E-01	1.064779E 00	7.856941E-02	9.138118E-01	3.549700E 00	3.066776E 00
16	3.962127E 00	5.211425E-01	1.050267E 00	8.120685E-02	9.130790E-01	3.549829E 00	3.039288E 00
17	3.972127E 00	5.385099E-01	1.036486E 00	8.374632E-02	9.123487E-01	3.549958E 00	3.012506E 00
18	3.982127E 00	5.553586E-01	1.023351E 00	8.619658E-02	9.116207E-01	3.550087E 00	2.986400E 00
19	3.992127E 00	5.717325E-01	1.010822E 00	8.856515E-02	9.108952E-01	3.550214E 00	2.960943E 00
20	4.002127E 00	5.876725E-01	9.988423E-01	9.085852E-02	9.101721E-01	3.550342E 00	2.936108E 00
21	4.012127E 00	6.031421E-01	9.873685E-01	9.308232E-02	9.094514E-01	3.550469E 00	2.911870E 00
22	4.022127E 00	6.181812E-01	9.763617E-01	9.524153E-02	9.087330E-01	3.550596E 00	2.888206E 00
23	4.032127E 00	6.327863E-01	9.657875E-01	9.734053E-02	9.080171E-01	3.550722E 00	2.865094E 00
24	4.042127E 00	6.469106E-01	9.556156E-01	9.938323E-02	9.073035E-01	3.550848E 00	2.842513E 00
25	4.052127E 00	6.606150E-01	9.458185E-01	1.013731E-01	9.065922E-01	3.550973E 00	2.820443E 00

I	M2T	M2KN	DELTA-2	P4/P2	A4/A2	M4N	THETA-4
1	1.[illegible]E-01	3.600276E 00	2.548082E-01	3.289677E 00	1.213928E 00	2.741255E 00	4.886926E-01
2	-5.[illegible]E-01	3.625581E 00	2.575747E-01	3.289506E 00	1.213915E 00	2.704322E 00	4.946572E-01
3	-7.[illegible]E-01	3.586275E 00	2.602426E-01	3.289369E 00	1.213905E 00	2.668557E 00	5.005676E-01
4	-9.[illegible]E-01	3.548285E 00	2.628715E-01	3.289264E 00	1.213897E 00	2.633895E 00	5.064259E-01
5	-1.[illegible]E 00	3.511535E 00	2.654643E-01	3.289194E 00	1.213892E 00	2.600277E 00	5.122343E-01
6	-1.1058[illegible] 00	3.475904E 00	2.680215E-01	3.289158E 00	1.213889E 00	2.567648E 00	5.179949E-01
7	-1.[illegible] 00	3.441516E 00	2.705442E-01	3.289156E 00	1.213889E 00	2.535955E 00	5.237096E-01
8	-1.[illegible] 00	3.408115E 00	2.730334E-01	3.289189E 00	1.213892E 00	2.505153E 00	5.293803E-01
9	-1.[illegible] 00	3.375729E 00	2.754900E-01	3.289258E 00	1.213897E 00	2.475196E 00	5.350088E-01
10	-1.[illegible] 00	3.344300E 00	2.779150E-01	3.289363E 00	1.213904E 00	2.446043E 00	5.405968E-01
11	-1.[illegible] 00	3.313784E 00	2.803093E-01	3.289504E 00	1.213915E 00	2.417655E 00	5.461460E-01
12	-1.[illegible] 00	3.284137E 00	2.826736E-01	3.289681E 00	1.213928E 00	2.389996E 00	5.516579E-01
13	-1.[illegible] 00	3.255320E 00	2.850088E-01	3.289896E 00	1.213944E 00	2.363033E 00	5.571341E-01
14	-1.[illegible] 00	3.227295E 00	2.873156E-01	3.290149E 00	1.213963E 00	2.336732E 00	5.625760E-01
15	-1.[illegible] 00	3.200026E 00	2.895947E-01	3.290440E 00	1.213984E 00	2.311065E 00	5.679851E-01
16	-1.[illegible] 00	3.173481E 00	2.918469E-01	3.290770E 00	1.214009E 00	2.286004E 00	5.733627E-01
17	-1.[illegible] 00	3.147629E 00	2.940726E-01	3.291140E 00	1.214036E 00	2.261521E 00	5.787102E-01
18	-1.[illegible] 00	3.122441E 00	2.962731E-01	3.291549E 00	1.214067E 00	2.237593E 00	5.840287E-01
19	-1.[illegible] 00	3.097888E 00	2.984483E-01	3.291999E 00	1.214100E 00	2.214196E 00	5.893197E-01

TABLE V (Cont'd)

I							
20	-1.998113E 00	3.073945E 00	3.005991E-01	3.292490E 00	1.214137E 00	2.191307E 00	5.945844E-01
21	-2.033595E 00	3.050588E 00	3.027259E-01	3.293023E 00	1.214176E 00	2.168905E 00	5.998237E-01
22	-2.067382E 00	3.027793E 00	3.048296E-01	3.293599E 00	1.214219E 00	2.146972E 00	6.050390E-01
23	-2.099604E 00	3.005538E 00	3.069102E-01	3.294218E 00	1.214265E 00	2.125487E 00	6.102314E-01
24	-2.130379E 00	2.983803E 00	3.089686E-01	3.294881E 00	1.214314E 00	2.104433E 00	6.154019E-01
25	-2.159812E 00	2.962566E 00	3.110051E-01	3.295588E 00	1.214366E 00	2.083794E 00	6.205517E-01

I	M4T	M4	P4/P-INF	SIGMA-4	THETA-P-4	S
1	1.277591E-07	2.741255E 00	5.138476E 00	4.660606E-08	2.336244E-01	3.659544E-02
2	-4.487570E-01	2.741303E 00	5.138209E 00	-1.633115E-02	2.370826E-01	3.659241E-02
3	-8.275007E-01	2.741341E 00	5.137994E 00	-2.311048E-02	2.403256E-01	3.658997E-02
4	-7.600719E-01	2.741370E 00	5.137631E 00	-2.832288E-02	2.435544E-01	3.658812E-02
5	-8.682050E-01	2.741390E 00	5.137721E 00	-3.272630E-02	2.467700E-01	3.658687E-02
6	-9.604484E-01	2.741400E 00	5.137664E 00	-3.661413E-02	2.499734E-01	3.658623E-02
7	-1.041253E 00	2.741401E 00	5.137662E 00	-4.013690E-02	2.531654E-01	3.658620E-02
8	-1.113299E 00	2.741391E 00	5.137714E 00	-4.338397E-02	2.563470E-01	3.658679E-02
9	-1.178357E 00	2.741372E 00	5.137821E 00	-4.641349E-02	2.595188E-01	3.658801E-02
10	-1.237573E 00	2.741343E 00	5.137984E 00	-4.926598E-02	2.626816E-01	3.658987E-02
11	-1.292164E 00	2.741304E 00	5.138205E 00	-5.197095E-02	2.658367E-01	3.659236E-02
12	-1.342331E 00	2.741254E 00	5.138482E 00	-5.455061E-02	2.689843E-01	3.659551E-02
13	-1.389324E 00	2.741194E 00	5.138818E 00	-5.702225E-02	2.721253E-01	3.659932E-02
14	-1.432983E 00	2.741123E 00	5.139213E 00	-5.939969E-02	2.752604E-01	3.660380E-02
15	-1.473869E 00	2.741042E 00	5.139668E 00	-6.169409E-02	2.783904E-01	3.660897E-02
16	-1.512281E 00	2.740950E 00	5.140183E 00	-6.391466E-02	2.815158E-01	3.661481E-02
17	-1.548471E 00	2.740847E 00	5.140760E 00	-6.606919E-02	2.846373E-01	3.662137E-02
18	-1.582654E 00	2.740733E 00	5.141399E 00	-6.816415E-02	2.877557E-01	3.662862E-02
19	-1.615012E 00	2.740607E 00	5.142102E 00	-7.020520E-02	2.908714E-01	3.663660E-02
20	-1.645767E 00	2.740470E 00	5.142867E 00	-7.219722E-02	2.939853E-01	3.664532E-02
21	-1.674876E 00	2.740321E 00	5.143702E 00	-7.414439E-02	2.970978E-01	3.665477E-02
22	-1.702643E 00	2.740161E 00	5.144601E 00	-7.605048E-02	3.002096E-01	3.666498E-02
23	-1.729115E 00	2.739988E 00	5.145568E 00	-7.791880E-02	3.033212E-01	3.667595E-02
24	-1.754389E 00	2.739803E 00	5.146604E 00	-7.975226E-02	3.064334E-01	3.668771E-02
25	-1.778550E 00	2.739606E 00	5.147709E 00	-8.155356E-02	3.095466E-01	3.670027E-02

TABLE V (Cont'd)

CHARACTERISTICS PROGRAM

GAMMA= 1.400 P/P= 5.138

I	J	RHO	PSI	THETA	S	M	MU	W
1	1	2.4[illegible]E-01	6.59315E-01	-8.15536E-02	3.67003E-02	2.73961E 00	3.73650E-01	7.74709E-01
2	2	2.3[illegible]E-01	6.45311E-01	-7.97523E-02	3.66877E-02	2.73980E 00	3.73622E-01	7.74731E-01
3	3	2.2[illegible]E-01	6.31006E-01	-7.79188E-02	3.66760E-02	2.73999E 00	3.73595E-01	7.74752E-01
4	4	2.1[illegible]E-01	6.16381E-01	-7.60505E-02	3.66650E-02	2.74016E 00	3.73571E-01	7.74772E-01
5	5	2.0[illegible]E-01	6.01412E-01	-7.41444E-02	3.66548E-02	2.74032E 00	3.73548E-01	7.74790E-01
6	6	1.9[illegible]E-01	5.86073E-01	-7.21972E-02	3.66453E-02	2.74047E 00	3.73526E-01	7.74807E-01
7	7	1.8[illegible]E-01	5.70333E-01	-7.02052E-02	3.66366E-02	2.74061E 00	3.73507E-01	7.74822E-01
8	8	1.7[illegible]E-01	5.54158E-01	-6.81641E-02	3.66286E-02	2.74073E 00	3.73489E-01	7.74836E-01
9	9	1.6[illegible]E-01	5.37510E-01	-6.60692E-02	3.66214E-02	2.74085E 00	3.73472E-01	7.74849E-01
10	10	1.5[illegible]E-01	5.20343E-01	-6.39147E-02	3.66148 02	2.74095E 00	3.73458E-01	7.74861E-01
11	11	1.4[illegible]E-01	5.02603E-01	-6.16941E-02	3.66090E-02	2.74104E 00	3.73445E-01	7.74871E-01
12	12	1.3[illegible]E-01	4.84228E-01	-5.93997E-02	3.66038E-02	2.74112E 00	3.73433E-01	7.74880E-01
13	13	1.2[illegible]E-01	4.65142E-01	-5.70223E-02	3.65993E-02	2.74119E 00	3.73423E-01	7.74888E-01
14	14	1.1[illegible]E-01	4.45255E-01	-5.45506E-02	3.65955E-02	2.74125E 00	3.73414E-01	7.74895E-01
15	15	1.0[illegible]E-01	4.24453E-01	-5.19709E-02	3.65924E-02	2.74130E 00	3.73407E-01	7.74901E-01
16	16	9.[illegible]E-02	4.02594E-01	-4.92660E-02	3.65899E-02	2.74134E 00	3.73402E-01	7.74905E-01
17	17	8.[illegible]E-02	3.79497E-01	-4.64135E-02	3.65880E-02	2.74137E 00	3.73397E-01	7.74909E-01
18	18	7.[illegible]E-02	3.54919E-01	-4.33840E-02	3.65868E-02	2.74139E 00	3.73395E-01	7.74911E-01
19	19	6.[illegible]E-02	3.28528E-01	-4.01369E-02	3.65862E-02	2.74140E 00	3.73393E-01	7.74912E-01
20	20	5.[illegible]E-02	2.99847E-01	-3.66141E-02	3.65862E-02	2.74140E 00	3.73393E-01	7.74912E-01
21	21	4.[illegible]E-02	2.68140E-01	-3.27263E-02	3.65869E-02	2.74139E 00	3.73395E-01	7.74911E-01
22	22	3.[illegible]E-02	2.32171E-01	-2.83229E-02	3.65881E-02	2.74137E 00	3.73398E-01	7.74908E-01
23	23	2.[illegible]E-02	1.89531E-01	-2.31105E-02	3.65900E-02	2.74134E 00	3.73402E-01	7.74905E-01
24	24	1.[illegible]E-02	1.33992E-01	-1.63512E-02	3.65924E-02	2.74130E 00	3.73407E-01	7.74901E-01
25	25	..	0.	0.	3.65954E-02	2.74126E 00	3.73414E-01	7.74895E-01

TABLE V (cont'd)

I= 24 P/P-INF= 5.49350E 00

J	RHO	P-I	THETA	S	MU	W
24	1.000000E-02	1.33992E-01	-1.63312E-02	3.65924E-02	3.73407E-01	7.74901E-01
25	1.73295E-01	6.73966E-02	-8.15930E-03	3.65939E-02	3.76562E-01	7.72412E-01
26	3.40956E-01	0.	0	3.65954E-02	3.79740E-01	7.69911E-01

TABLE V (Cont'd)

I= 23 P/P-INF= 5.64639E 00

J	RHO	PSI	THETA	S	MU	M
23	2.00000E-02	1.89531E-01	-2.31105E-02	3.65900E-02	3.73402E-01	7.74905E-01
24	8.50485E-02	1.62125E-01	-1.97158E-02	3.65911E-02	3.74709E-01	7.73873E-01
25	2.46594E-01	9.56047E-02	-1.15439E-02	3.65930E-02	3.77870E-01	7.71377E-01
26	4.11920E-01	2.82380E-02	-3.38465E-03	3.65947E-02	3.81066E-01	7.68870E-01
27	4.81922E-01	0.	0.	3.65954E-02	3.82398E-01	7.67826E-01

TABLE V (Cont'd)

I= 22 ρ/ρ-INF= 5.76624E 00

J	RHO	PSI	THETA	S	MU	W
22	3.00000E-02	2.32171E-01	-2.83229E-02	3.65881E-02	3.73398E-01	7.74908E-01
23	7.94668E-02	2.11203E-01	-2.57128E-02	3.65890E-02	3.74402E-01	7.74115E-01
24	1.44368E-01	1.83837E-01	-2.23181E-02	3.65901E-02	3.75714E-01	7.73080E-01
25	3.03507E-01	1.17387E-01	-1.41463E-02	3.65923E-02	3.78819E-01	7.70590E-01
26	4.67045E-01	5.00573E-02	-5.98705E-03	3.65941E-02	3.82089E-01	7.68068E-01
27	5.36309E-01	2.18245E-02	-2.60242E-03	3.65949E-02	3.83425E-01	7.67022E-01
28	5.90136E-01	0.	0.	3.65954E-02	3.84455E-01	7.66215E-01

TABLE V (Cont'd)

I= 21 P/P-INF= 5.86909E 00

J	RHO	PSI	THETA	S	MU	W
21	4.00000E-02	2.68340E-01	-3.27263E-02	3.65869E-02	3.73395E-01	7.74911E-01
22	8.10976E-02	2.50490E-01	-3.05220E-02	3.65874E-02	3.74243E-01	7.74241E-01
23	1.30075E-01	2.29563E-01	-2.79120E-02	3.65882E-02	3.75260E-01	7.73446E-01
24	1.94336E-01	2.02233E-01	-2.45173E-02	3.65893E-02	3.76564E-01	7.72410E-01
25	3.51962E-01	1.35852E-01	-1.63454E-02	3.65916E-02	3.79748E-01	7.69905E-01
26	5.13993E-01	8.85010E-02	-8.18620E-03	3.65935E-02	3.82955E-01	7.67389E-01
27	5.82639E-01	4.03360E-02	-4.80158E-03	3.65943E-02	3.84295E-01	7.66341E-01
28	6.35978E-01	1.85142E-02	-2.19920E-03	3.65946E-02	3.85328E-01	7.65533E-01
29	6.81423E-01	0.	0.	3.65947E-02	3.86203E-01	7.64850E-01

TABLE V (Cont'd)

I= 20 P/P-INF= 5.96115E 00

J	RHO	PSI	THETA	S	MU	W
20	5.00000E-02	2.99847E-01	-3.66141E-02	3.65862E-02	3.73393E-01	7.74912E-01
21	8.57588E-02	2.84330E-01	-3.46688E-02	3.65865E-02	3.74142E-01	7.74321E-01
22	1.26491E-01	2.66717E-01	-3.24645E-02	3.65870E-02	3.74992E-01	7.73650E-01
23	1.75037E-01	2.45810E-01	-2.98545E-02	3.65876E-02	3.76001E-01	7.72854E-01
24	2.38740E-01	2.18514E-01	-2.64598E-02	3.65886E-02	3.77318E-01	7.71816E-01
25	3.95026E-01	1.52200E-01	-1.82880E-02	3.65909E-02	3.80508E-01	7.69308E-01
26	5.55730E-01	8.49501E-02	-1.01287E-02	3.65930E-02	3.83723E-01	7.66788E-01
27	6.23822E-01	5.67347E-02	-6.74410E-03	3.65938E-02	3.85065E-01	7.65739E-01
28	6.70745E-01	3.49172E-02	-4.14172E-03	3.65944E-02	3.86100E-01	7.64930E-01
29	7.21835E-01	1.64047E-02	-1.94253E-03	3.65950E-02	3.86978E-01	7.64245E-01
30	7.61933E-01	0.	0.	3.65954E-02	3.87755E-01	7.63640E-01

TABLE V (Cont'd)

I= 19 P/P-INF= 6.04563E 00

J	RHO	PSI	THETA	S	MU	M
19	6.00000E-02	3.28528E 01	-4.01369E-02	3.65862E-02	3.73393E-01	7.74912E-01
20	9.19752E-02	3.14517E-01	-3.83754E-02	3.65862E-02	3.74071E-01	7.74377E-01
21	1.27442E-01	2.99024E-01	-3.64302E-02	3.65864E-02	3.74820E-01	7.73785E-01
22	1.67843E-01	2.81437E-01	-3.42259E-02	3.65867E-02	3.75672E-01	7.73113E-01
23	2.15999E-01	2.60558E-01	-3.16159E-02	3.65872E-02	3.76683E-01	7.72316E-01
24	2.79196E-01	2.33297E-01	-2.82211E-02	3.65881E-02	3.78002E-01	7.71277E-01
25	4.34272E-01	1.67047E-01	-2.00493E-02	3.65904E-02	3.81199E-01	7.68766E-01
26	5.93773E-01	9.98401E-02	-1.18901E-02	3.65925E-02	3.84420E-01	7.66243E-01
27	6.61369E-01	7.16353E-02	-8.50545E-03	3.65933E-02	3.85765E-01	7.65192E-01
28	7.13911E-01	4.98235E-02	-5.90305E-03	3.65940E-02	3.86802E-01	7.64382E-01
29	7.58680E-01	3.13139E-02	-3.70391E-03	3.65945E-02	3.87681E-01	7.63697E-01
30	7.98495E-01	1.49103E-02	-1.76139E-03	3.65950E-02	3.88460E-01	7.63090E-01
31	8.34799E-01	0.	0.	3.65954E-02	3.89167E-01	7.62539E-01

TABLE V (Cont'd)

I= 18 P/P-INF= 6.12437E 00

J	RHO	PSI	THETA	S	MU	W
18	7.00000E-02	3.54919E-01	-4.33840E-02	3.65868E-02	3.73395E-01	7.74911E-01
19	9.91151E-02	3.42047E-01	-4.17817E-02	3.65866E-02	3.74018E-01	7.74418E-01
20	1.30846E-01	3.28058E-01	-4.00002E-02	3.65864E-02	3.74697E-01	7.73882E-01
21	1.66043E-01	3.12588E-01	-3.80649E-02	3.65864E-02	3.75448E-01	7.73290E-01
22	2.06141E-01	2.95025E-01	-3.58507E-02	3.65865E-02	3.76301E-01	7.72617E-01
23	2.53938E-01	2.74174E-01	-3.32407E-02	3.65869E-02	3.77313E-01	7.71820E-01
24	3.16669E-01	2.46945E-01	-2.98459E-02	3.65876E-02	3.78635E-01	7.70780E-01
25	4.70630E-01	1.80760E-01	-2.16741E-02	3.65898E-02	3.81837E-01	7.68265E-01
26	6.29025E-01	1.13596E-01	-1.35149E-02	3.65920E-02	3.85064E-01	7.65739E-01
27	6.96164E-01	8.56028E-02	-1.01303E-02	3.65929E-02	3.86412E-01	7.64687E-01
28	7.48355E-01	6.35974E-02	-7.52784E-03	3.65936E-02	3.87451E-01	7.63876E-01
29	7.92828E-01	4.50915E-02	-5.32870E-03	3.65941E-02	3.88332E-01	7.63190E-01
30	8.32382E-01	2.86901E-02	-3.38618E-03	3.65946E-02	3.89112E-01	7.62583E-01
31	8.68451E-01	1.37807E-02	-1.62481E-03	3.65950E-02	3.89820E-01	7.62031E-01
32	9.01884E-01	0.	0.	3.65954E-02	3.90475E-01	7.61522E-01

TABLE V (Cont'd)

I= 17 Q/Q-INF= 6.19865E 00

J	RHO	PSI	THETA	S	MM	M
17	8.00000E-02	3.79497E-01	-4.64135E-02	3.65880E-02	3.73397E+01	7.74909E-01
18	1.06857E-01	3.67525E-01	-4.49012E-02	3.65875E-02	3.73979E+01	7.74449E-01
19	1.35762E-01	3.54673E-01	-4.32790E-02	3.65871E-02	3.74603E+01	7.73956E-01
20	1.67265E-01	3.40704E-01	-4.15176E-02	3.65867E-02	3.75283E+01	7.73420E-01
21	2.02212E-01	3.25257E-01	-3.95722E-02	3.65866E-02	3.76035E+01	7.72827E-01
22	2.42026E-01	3.07718E-01	-3.73680E-02	3.65865E-02	3.76889E+01	7.72154E-01
23	2.89489E-01	2.86894E-01	-3.47580E-02	3.65867E-02	3.77903E+01	7.71355E-01
24	3.51786E-01	2.59697E-01	-3.13633E-02	3.65873E-02	3.79227E+01	7.70314E-01
25	5.04709E-01	1.93576E-01	-2.31914E-02	3.65894E-02	3.82435E+01	7.67797E-01
26	6.62073E-01	1.25455E-01	-1.50322E-02	3.65916E-02	3.85567E+01	7.65268E-01
27	7.28786E-01	9.82745E-02	-1.16476E-02	3.65925E-02	3.87017E+01	7.64715E-01
28	7.80649E-01	7.64762E-02	-9.04517E-03	3.65931E-02	3.88058E+01	7.63403E-01
29	8.24846E-01	5.79748E-02	-6.84601E-03	3.65937E-02	3.88940E+01	7.62716E-01
30	8.64157E-01	4.15761E-02	-4.90351E-03	3.65942E-02	3.89721E+01	7.62108E-01
31	9.00006E-01	2.66683E-02	-3.14211E-03	3.65946E-02	3.90431E+01	7.61556E-01
32	9.33237E-01	1.28884E-02	-1.51734E-03	3.65951E-02	3.91088E+01	7.61046E-01
33	9.64400E-01	0.	0.	3.65954E-02	3.91701E+01	7.60570E-01

TABLE V (Cont'd)

I= 16 P/P-INF= 6.26931E 00

J	RHO	PSI	THETA	S	MU	W
16	9.00000E-02	4.02594E-01	-4.92660E-02	3.65899E-02	3.73402E-01	7.74905E-01
17	1.15016E-01	3.91356E-01	-4.78436E-02	3.66891E-02	3.73948E-01	7.74474E-01
18	1.41688E-01	3.79402E-01	-4.63313E-02	3.66884E-02	3.74530E-01	7.74014E-01
19	1.70396E-01	3.66570E-01	-4.47091E-02	3.65878E-02	3.75155E-01	7.73521E-01
20	2.01685E-01	3.52622E-01	-4.29476E-02	3.65873E-02	3.75836E-01	7.72984E-01
21	2.36396E-01	3.37197E-01	-4.10023E-02	3.65869E-02	3.76589E-01	7.72390E-01
22	2.75944E-01	3.19681E-01	-3.87980E-02	3.65867E-02	3.77444E-01	7.71717E-01
23	3.23092E-01	2.98884E-01	-3.61880E-02	3.65867E-02	3.78460E-01	7.70917E-01
24	3.84982E-01	2.71718E-01	-3.27933E-02	3.65871E-02	3.79786E-01	7.69875E-01
25	5.36928E-01	2.05659E-01	-2.46215E-02	3.65890E-02	3.82999E-01	7.67355E-01
26	6.93322E-01	1.38583E-01	-1.64623E-02	3.65911E-02	3.86236E-01	7.64824E-01
27	7.59634E-01	1.10415E-01	-1.30776E-02	3.65920E-02	3.87588E-01	7.63769E-01
28	8.11190E-01	8.86246E-02	-1.04752E-02	3.65927E-02	3.88631E-01	7.62957E-01
29	8.55128E-01	7.01283E-02	-8.27608E-03	3.65933E-02	3.89515E-01	7.62269E-01
30	8.94210E-01	5.37329E-02	-6.33359E-03	3.65938E-02	3.90297E-01	7.61660E-01
31	9.29851E-01	3.88273E-02	-4.57220E-03	3.65943E-02	3.91008E-01	7.61108E-01
32	9.62892E-01	2.50486E-02	-2.94742E-03	3.65947E-02	3.91666E-01	7.60598E-01
33	9.93878E-01	1.21608E-02	-1.43009E-03	3.65951E-02	3.92280E-01	7.60120E-01
34	1.02319E 00	0.	0.	3.65954E-02	3.92861E-01	7.59670E-01

TABLE V (Cont'd)

I= 15 P/R-INF= 6.33700E 00

J	RHO	PSI	THETA	S	MU	H
15	1.00000E-01	4.24453E-01	-5.19709E-02	3.65924E-02	3.73407E+01	7.74901E-01
16	1.23480E-01	4.13827E-01	-5.06236E-02	3.65913E-02	3.73925E+01	7.74492E-01
17	1.48331E-01	4.02607E-01	-4.92012E-02	3.65903E-02	3.74472E+01	7.74060E-01
18	1.74828E-01	3.90672E-01	-4.76890E-02	3.65894E-02	3.75054E+01	7.73600E-01
19	2.03349E-01	3.77858E-01	-4.60667E-02	3.65887E-02	3.75681E+01	7.73106E-01
20	2.34436E-01	3.63931E-01	-4.43053E-02	3.65880E-02	3.76362E+01	7.72569E-01
21	2.68924E-01	3.48526E-01	-4.23600E-02	3.65874E-02	3.77116E+01	7.71975E-01
22	3.08220E-01	3.31034E-01	-4.01557E-02	3.65870E-02	3.77973E+01	7.71301E-01
23	3.55070E-01	3.10262E-01	-3.75457E-02	3.65868E-02	3.78990E+01	7.70501E-01
24	4.16573E-01	2.83127E-01	-3.41510E-02	3.65870E-02	3.80317E+01	7.69458E-01
25	5.67594E-01	2.17131E-01	-2.59792E-02	3.65887E-02	3.83535E+01	7.66935E-01
26	7.23069E-01	1.50099E-01	-1.78200E-02	3.65907E-02	3.86777E+01	7.64402E-01
27	7.89002E-01	1.21945E-01	-1.44354E-02	3.65916E-02	3.88131E+01	7.63346E-01
28	8.40266E-01	1.00162E-01	-1.18330E-02	3.65923E-02	3.89176E+01	7.62533E-01
29	8.83958E-01	8.16714E-02	-9.63383E-03	3.65929E-02	3.90061E+01	7.61844E-01
30	9.22824E-01	6.52799E-02	-7.69134E-03	3.65934E-02	3.90845E+01	7.61235E-01
31	9.58269E-01	5.03769E-02	-5.92995E-03	3.65939E-02	3.91557E+01	7.60682E-01
32	9.91129E-01	3.65999E-02	-4.30520E-03	3.65943E-02	3.92215E+01	7.60171E-01
33	1.02195E 00	2.37132E-02	-2.78788E-03	3.65947E-02	3.92831E+01	7.59693E-01
34	1.05110E 00	1.15528E-02	-1.35781E-03	3.65951E-02	3.93412E+01	7.59243E-01
35	1.07886E 00	0.	0.	3.65954E-02	3.93965E+01	7.58814E-01

TABLE V (Cont'd)

I= 14 P/P-INF= 6.40216E 00

J	RHO	PSI	THETA	S	MU	W
14	1.10000E-01	4.45255E-01	-5.45506E-02	3.65955E-02	3.73414E-01	7.[illegible]E-01
15	1.32172E-01	4.35151E-01	-5.32673E-02	3.65942E-02	3.73907E-01	[illegible]450[illegible]E-01
16	1.55503E-01	4.24543E-01	-5.19200E-02	3.65929E-02	3.74425E-01	7.74097E-01
17	1.80197E-01	4.13340E-01	-5.04976E-02	3.65918E-02	3.74973E-01	7.73665E-01
18	2.06526E-01	4.01422E-01	-4.89853E-02	3.65907E-02	3.75556E-01	7.73205E-01
19	2.34871E-01	3.88628E-01	-4.73831E-02	3.65897E-02	3.76183E-01	7.72710E-01
20	2.65765E-01	3.74720E-01	-4.56016E-02	3.65888E-02	3.76865E-01	7.72173E-01
21	3.00040E-01	3.59336E-01	-4.36563E-02	3.65881E-02	3.77620E-01	7.71578E-01
22	3.39096E-01	3.41867E-01	-4.14521E-02	3.65875E-02	3.78478E-01	7.70903E-01
23	3.85662E-01	3.21120E-01	-3.88420E-02	3.65871E-02	3.79496E-01	7.70103E-01
24	4.[illegible]6798E-01	2.94016E-01	-3.54473E-02	3.65870E-02	3.80826E-01	7.69059E-01
25	5.96937E-01	2.28081E-01	-2.72755E-02	3.65884E-02	3.84048E-01	7.66534E-01
26	7.51538E-01	1.61094E-01	-1.91163E-02	3.65904E-02	3.87295E-01	7.63998E-01
27	8.17109E-01	1.32953E-01	-1.57317E-02	3.65913E-02	3.88651E-01	7.62942E-01
28	8.[illegible]8096E-01	1.11179E-01	-1.31293E-02	3.65920E-02	3.89697E-01	7.62127E-01
29	9.11553E-01	9.26945E-02	-1.09301E-02	3.65926E-02	3.90583E-01	7.61438E-01
30	9.50212E-01	7.63072E-02	-8.98767E-03	3.65931E-02	3.91368E-01	7.60828E-01
31	9.85471E-01	6.14071E-02	-7.22629E-03	3.65935E-02	3.92082E-01	7.60275E-01
32	1.01816E 00	4.76323E-02	-5.60152E-03	3.65940E-02	3.92741E-01	7.597[illegible]3E-01
33	1.04881E 00	3.47470E-02	-4.08421E-03	3.65944E-02	3.93358E-01	7.592[illegible]5E-01
34	1.07782E 00	2.25875E-02	-2.65414E-03	3.65947E-02	3.93940E-01	7.58834E-01
35	1.10543E 00	1.10351E-02	-1.29634E-03	3.65951E-02	3.94494E-01	7.58406E-01
36	1.13187E 00	0.	0.	3.65954E-02	3.95023E-01	7.57996E-01

TABLE V (Cont'd)

I= 13 P/P-INF= 6.46518E 00

J	RHO	PSI	THETA	S	MU	W
13	1.20000E-01	4.65142E-01	-5.70223E-02	3.65993E-02	3.73423E+01	7.74888E-01
14	1.41043E-01	4.55490E-01	-5.57943E-02	3.65977E-02	3.73894E+01	7.74516E-01
15	1.63079E-01	4.45402E-01	-5.45111E-02	3.65962E-02	3.74387E+01	7.74127E-01
16	1.86267E-01	4.34810E-01	-5.31638E-02	3.65948E-02	3.74906E+01	7.73718E-01
17	2.10812E-01	4.23624E-01	-5.17414E-02	3.65934E-02	3.75454E+01	7.73285E-01
18	2.36983E-01	4.11725E-01	-5.02291E-02	3.65921E-02	3.76038E+01	7.72824E-
19	2.65155E-01	3.98948E-01	-4.86069E-02	3.65909E-02	3.76666E+01	7.72330E-01
20	2.95865E-01	3.85060E-01	-4.68454E-02	3.65899E-02	3.77349E+01	7.71792E-01
21	3.29937E-01	3.69697E-01	-4.49001E-02	3.65889E-02	3.78105E+01	7.71197E-01
22	3.68763E-01	3.52249E-01	-4.26958E-02	3.65881E-02	3.78963E+01	7.70522E-01
23	4.15058E-01	3.31527E-01	-4.00858E-02	3.65875E-02	3.79983E+01	7.69720E-01
24	4.75841E-01	3.04453E-01	-3.66911E-02	3.65872E-02	3.81314E+01	7.68675E-01
25	5.65137E-01	2.68580E-01	-2.85192E-02	3.65882E-02	3.84540E+01	7.66149E-01
26	7.78900E-01	1.71638E-01	-2.03601E-02	3.65901E-02	3.87792E+01	7.63610E-01
27	8.44125E-01	1.43511E-01	-1.69755E-02	3.65909E-02	3.89150E+01	7.62553E-01
28	8.94846E-01	1.21746E-01	-1.43731E-02	3.65916E-02	3.90197E+01	7.61738E-01
29	9.38080E-01	1.03267E-01	-1.21739E-02	3.65922E-02	3.91085E+01	7.61048E-01
30	9.76541E-01	8.68845E-02	-1.02314E-02	3.65927E-02	3.91871E+01	7.60438E-01
31	1.01162E 00	7.19878E-02	-8.47008E-03	3.65932E-02	3.92586E+01	7.59884E-01
32	1.04414E 00	5.82155E-02	-6.84528E-03	3.65936E-02	3.93246E+01	7.59372E-01
33	1.07465E 00	4.53319E-02	-5.32796E-03	3.65940E-02	3.93863E+01	7.58893E-01
34	1.10350E 00	3.31736E-02	-3.89791E-03	3.65944E-02	3.94447E+01	7.58442E-01
35	1.13098E 00	2.16219E-02	-2.54011E-03	3.65948E-02	3.95001E+01	7.58013E-01
36	1.15729E 00	1.05872E-02	-1.24380E-03	3.65951E-02	3.95532E+01	7.57603E-01
37	1.18258E 00	0.	0.	3.65954E-02	3.96041E+01	7.57209E-01

TABLE V (Cont'd)

I= 12 R/R-INF= 6.52634E 00

J	RHO	PSI	THETA	S	MU	W
12	1.30000E-01	4.84228E-01	-5.93997E-02	3.66038E-02	3.73433E-01	7.74880E-01
13	1.50055E-01	4.74970E-01	-5.82203E-02	3.66020E-02	3.73885E-01	7.74523E-01
14	1.70973E-01	4.65333E-01	-5.69924E-02	3.66002E-02	3.74357E-01	7.74151E-01
15	1.92878E-01	4.55261E-01	-5.57091E-02	3.65985E-02	3.74850E-01	7.73761E-01
16	2.15930E-01	4.44685E-01	-5.43618E-02	3.65968E-02	3.75369E-01	7.73352E-01
17	2.40330E-01	4.33516E-01	-5.29393E-02	3.65952E-02	3.75918E-01	7.72919E-01
18	2.66349E-01	4.21634E-01	-5.14271E-02	3.65937E-02	3.76503E-01	7.72458E-01
19	2.94357E-01	4.08875E-01	-4.98048E-02	3.65923E-02	3.77131E-01	7.71963E-01
20	3.24889E-01	3.95006E-01	-4.80434E-02	3.65910E-02	3.77815E-01	7.71425E-01
21	3.58766E-01	3.79663E-01	-4.60981E-02	3.65899E-02	3.78572E-01	7.70829E-01
22	3.97371E-01	3.62237E-01	-4.38938E-02	3.65888E-02	3.79432E-01	7.70153E-01
23	4.43405E-01	3.41540E-01	-4.12837E-02	3.65880E-02	3.80453E-01	7.69351E-01
24	5.03850E-01	3.14495E-01	-3.78890E-02	3.65874E-02	3.81785E-01	7.68306E-01
25	6.52336E-01	2.48683E-01	-2.97172E-02	3.65881E-03	3.85016E-01	7.65777E-01
26	8.05294E-01	1.81787E-01	-2.15580E-02	3.65898E-02	3.88271E-01	7.63237E-01
27	8.70186E-01	1.53674E-01	-1.81734E-02	3.65906E-02	3.89831E-01	7.62178E-01
28	9.20652E-01	1.31918E-01	-1.55710E-02	3.65913E-02	3.90680E-01	7.61363E-01
29	9.63670E-01	1.13446E-01	-1.33719E-02	3.65918E-02	3.91569E-01	7.60672E-01
30	1.00194E 00	9.70676E-02	-1.14294E-02	3.65924E-02	3.92356E-01	7.60061E-01
31	1.03685E 00	8.21746E-02	-9.66805E-03	3.65928E-02	3.93072E-01	7.59507E-01
32	1.06921E 00	6.84050E-02	-8.04327E-03	3.65933E-02	3.93733E-01	7.58995E-01
33	1.09957E 00	5.55234E-02	-6.52595E-03	3.65937E-02	3.94351E-01	7.58516E-01
34	1.12829E 00	4.33666E-02	-5.09589E-03	3.65941E-02	3.94935E-01	7.58064E-01
35	1.15563E 00	3.18159E-02	-3.73809E-03	3.65944E-02	3.95491E-01	7.57634E-01
36	1.18182E 00	2.07818E-02	-2.44176E-03	3.65948E-02	3.96022E-01	7.57224E-01
37	1.20699E 00	1.01949E-02	-1.19797E-03	3.65951E-02	3.96532E-01	7.56830E-01
38	1.23128E 00	0.	0.	3.65954E-02	3.97024E-01	7.56450E-01

TABLE V (Cont'd)

I= 11 P/P-INF= 6.58589E 00

J	RHO	PSI	THETA	S	M	W
11	1.40030E-01	5.02603E-01	-6.16941E-02	3.66090E-02	3.73445E-01	7.74871E-01
12	1.59162E-01	4.93694E-01	-6.05576E-02	3.66069E-02	3.73880E-01	7.74527E-01
13	1.79121E-01	4.84451E-01	-5.93782E-02	3.66048E-02	3.74333E-01	7.74170E-01
14	1.99918E-01	4.74829E-01	-5.81503E-02	3.66028E-02	3.74805E-01	7.73797E-01
15	2.21698E-01	4.64773E-01	-5.68670E-02	3.66009E-02	3.75299E-01	7.73407E-01
16	2.44617E-01	4.54213E-01	-5.55197E-02	3.65990E-02	3.75819E-01	7.72997E-01
17	2.68678E-01	4.43060E-01	-5.40972E-02	3.65973E-02	3.76368E-01	7.72564E-01
18	2.94750E-01	4.31195E-01	-5.25850E-02	3.65955E-02	3.76953E-01	7.72103E-01
19	3.22600E-01	4.18454E-01	-5.09627E-02	3.65939E-02	3.77582E-01	7.71608E-01
20	3.52962E-01	4.04603E-01	-4.92013E-02	3.65924E-02	3.78267E-01	7.71069E-01
21	3.86650E-01	3.89280E-01	-4.72559E-02	3.65910E-02	3.79024E-01	7.70473E-01
22	4.23042E-01	3.71876E-01	-4.50517E-02	3.65897E-02	3.79885E-01	7.69797E-01
23	4.70825E-01	3.51203E-01	-4.24416E-02	3.65886E-02	3.80907E-01	7.68995E-01
24	5.30944E-01	3.24188E-01	-3.90469E-02	3.65878E-02	3.82241E-01	7.67948E-01
25	6.73649E-01	2.58436E-01	-3.08751E-02	3.65880E-02	3.85476E-01	7.65418E-01
26	8.33831E-01	1.91585E-01	-2.27159E-02	3.65895E-02	3.88736E-01	7.62875E-01
27	8.95402E-01	1.63486E-01	-1.93313E-02	3.65903E-02	3.90097E-01	7.61816E-01
28	9.45022E-01	1.41740E-01	-1.67289E-02	3.65909E-02	3.91148E-01	7.61000E-01
29	9.88432E-01	1.23274E-01	-1.45298E-02	3.65915E-02	3.92038E-01	7.60309E-01
30	1.02652E 00	1.06901E-01	-1.25873E-02	3.65920E-02	3.92826E-01	7.59697E-01
31	1.06126E 00	9.20122E-02	-1.08259E-02	3.65925E-02	3.93542E-01	7.59142E-01
32	1.09347E 00	7.82455E-02	-9.20110E-03	3.65930E-02	3.94204E-01	7.58629E-01
33	1.12369E 00	6.53663E-02	-7.68376E-03	3.65934E-02	3.94824E-01	7.58150E-01
34	1.15227E 00	5.32112E-02	-6.25373E-03	3.65938E-02	3.95409E-01	7.57698E-01
35	1.17949E 00	4.16618E-02	-4.89595E-03	3.65941E-02	3.95965E-01	7.57268E-01
36	1.20555E 00	3.06286E-02	-3.59960E-03	3.65945E-02	3.96496E-01	7.56857E-01
37	1.23061E 00	2.00422E-02	-2.35581E-03	3.65948E-02	3.97008E-01	7.56463E-01
38	1.25479E 00	9.84751E-03	-1.15783E-03	3.65951E-02	3.97500E-01	7.56082E-01
39	1.27819E 00	0.	0.	3.65954E-02	3.97977E-01	7.55715E-01

TABLE V (Cont'd)

I= 10 P/P-INF= 6.64403E 00

J	RHO	PSI	THETA	S	MU	M
10	1.50000E-01	5.20343E-01	-6.39147E-02	3.66148E-02	3.73458E-01	7.74861E-01
11	1.68403E-01	5.11745E-01	-6.28165E-02	3.66124E-02	3.73878E-01	7.74529E-01
12	1.87477E-01	5.02851E-01	-6.16801E-02	3.66101E-02	3.74314E-01	7.74184E-01
13	2.07304E-01	4.93622E-01	-6.05007E-02	3.66079E-02	3.74768E-01	7.73827E-01
14	2.27984E-01	4.84015E-01	-5.92727E-02	3.66057E-02	3.75240E-01	7.73454E-01
15	2.49642E-01	4.73974E-01	-5.79895E-02	3.66035E-02	3.75735E-01	7.73064E-01
16	2.72434E-01	4.63430E-01	-5.66421E-02	3.66015E-02	3.76255E-01	7.72654E-01
17	2.96561E-01	4.52293E-01	-5.52197E-02	3.65995E-02	3.76805E-01	7.72220E-01
18	3.22290E-01	4.40444E-01	-5.37074E-02	3.65975E-02	3.77390E-01	7.71759E-01
19	3.49988E-01	4.27721E-01	-5.20851E-02	3.65957E-02	3.78020E-01	7.71269E-01
20	3.80184E-01	4.13888E-01	-5.03237E-02	3.65939E-02	3.78705E-01	7.70724E-01
21	4.13690E-01	3.98585E-01	-4.83784E-02	3.65923E-02	3.79464E-01	7.70128E-01
22	4.51877E-01	3.81203E-01	-4.61742E-02	3.65907E-02	3.80325E-01	7.69451E-01
23	4.97417E-01	3.60553E-01	-4.35041E-02	3.65896E-02	3.81348E-01	7.68648E-01
24	5.57221E-01	3.33567E-01	-4.01693E-02	3.65883E-02	3.82684E-01	7.67601E-01
25	7.04170E-01	2.67875E-01	-3.19975E-02	3.65881E-02	3.85922E-01	7.65069E-01
26	8.55602E-01	2.01070E-01	-2.38384E-02	3.65893E-02	3.89186E-01	7.62524E-01
27	9.19863E-01	1.72986E-01	-2.04538E-02	3.65900E-02	3.90549E-01	7.61464E-01
28	9.69845E-01	1.51249E-01	-1.78514E-02	3.65906E-02	3.91601E-01	7.60647E-01
29	1.01245E 00	1.32790E-01	-1.56522E-02	3.65912E-02	3.92493E-01	7.59956E-01
30	1.05036E 00	1.16423E-01	-1.37097E-02	3.65917E-02	3.93282E-01	7.59344E-01
31	1.08495E 00	1.01538E-01	-1.19484E-02	3.65922E-02	3.93999E-01	7.58788E-01
32	1.11701E 00	8.77742E-02	-1.03236E-02	3.65926E-02	3.94662E-01	7.58275E-01
33	1.14709E 00	7.48974E-02	-8.80624E-03	3.65930E-02	3.95282E-01	7.57796E-01
34	1.17554E 00	6.27443E-02	-7.37620E-03	3.65934E-02	3.95868E-01	7.57343E-01
35	1.20264E 00	5.11963E-02	-6.01840E-03	3.65938E-02	3.96425E-01	7.56913E-01
36	1.22858E 00	4.01642E-02	-4.72206E-03	3.65942E-02	3.96957E-01	7.56502E-01
37	1.25353E 00	2.95786E-02	-3.47830E-03	3.65945E-02	3.97469E-01	7.56107E-01
38	1.27760E 00	1.93844E-02	-2.28030E-03	3.65948E-02	3.97962E-01	7.55726E-01
39	1.30090E 00	9.53708E-03	-1.12250E-03	3.65951E-02	3.98440E-01	7.55358E-01
40	1.32350E 00	0.	0.	3.65954E-02	3.98904E-01	7.55001E-01

TABLE V (Cont'd)

I= 9 P/P-INF= 6.70092E 00

J	RHO	PSI	THETA	S	MU	M
9	1.60000E-01	5.37510E-01	-6.60692E-02	3.66214E-02	3.73472E-01	7.74849E-01
10	1.77703E-01	5.29193E-01	-6.50056E-02	3.66187E-02	3.73880E-01	7.74528E-01
11	1.96003E-01	5.20609E-01	-6.39074E-02	3.66161E-02	3.74301E-01	7.74195E-01
12	2.14973E-01	5.11728E-01	-6.27710E-02	3.66136E-02	3.74737E-01	7.73851E-01
13	2.34691E-01	5.02514E-01	-6.15916E-02	3.66111E-02	3.75191E-01	7.73493E-01
14	2.55259E-01	4.92922E-01	-6.03637E-02	3.66087E-02	3.75664E-01	7.73120E-01
15	2.76799E-01	4.82896E-01	-5.90804E-02	3.66064E-02	3.76159E-01	7.72729E-01
16	2.99467E-01	4.72367E-01	-5.77330E-02	3.66041E-02	3.76679E-01	7.72319E-01
17	3.23404E-01	4.61246E-01	-5.63105E-02	3.66018E-02	3.77230E-01	7.71886E-01
18	3.49055E-01	4.49414E-01	-5.47983E-02	3.65997E-02	3.77816E-01	7.71424E-01
19	3.76606E-01	4.36708E-01	-5.31760E-02	3.65976E-02	3.78446E-01	7.70928E-01
20	4.06642E-01	4.22893E-01	-5.14146E-02	3.65956E-02	3.79132E-01	7.70389E-01
21	4.39972E-01	4.07609E-01	-4.94692E-02	3.65937E-02	3.79891E-01	7.69792E-01
22	4.77959E-01	3.90248E-01	-4.72650E-02	3.65919E-02	3.80754E-01	7.69115E-01
23	5.23263E-01	3.69022E-01	-4.46549E-02	3.65903E-02	3.81778E-01	7.68312E-01
24	5.82762E-01	3.42065E-01	-4.12602E-02	3.65889E-02	3.83115E-01	7.67204E-01
25	7.28979E-01	2.77032E-01	-3.30883E-02	3.65882E-02	3.86357E-01	7.64730E-01
26	8.79084E-01	2.10273E-01	-2.49292E-02	3.65892E-02	3.89625E-01	7.62183E-01
27	9.43649E-01	1.82204E-01	-2.15446E-02	3.65898E-02	3.90990E-01	7.61122E-01
28	9.93395E-01	1.60476E-01	-1.89422E-02	3.65904E-02	3.92043E-01	7.60305E-01
29	1.03581E 00	1.42025E-01	-1.67430E-02	3.65909E-02	3.92935E-01	7.59613E-01
30	1.07355E 00	1.25663E-01	-1.48005E-02	3.65914E-02	3.93725E-01	7.59000E-01
31	1.10797E 00	1.10782E-01	-1.30392E-02	3.65919E-02	3.94444E-01	7.58444E-01
32	1.13990E 00	9.70217E-02	-1.14144E-02	3.65923E-02	3.95107E-01	7.57931E-01
33	1.16984E 00	8.41476E-02	-9.89710E-03	3.65927E-02	3.95728E-01	7.57451E-01
34	1.19817E 00	7.19906E-02	-8.46707E-03	3.65931E-02	3.96315E-01	7.56998E-01
35	1.22514E 00	6.04503E-02	-7.10926E-03	3.65935E-02	3.96872E-01	7.56567E-01
36	1.25098E 00	4.94195E-02	-5.81292E-03	3.65938E-02	3.97405E-01	7.56156E-01
37	1.27581E 00	3.88348E-02	-4.56915E-03	3.65942E-02	3.97918E-01	7.55761E-01
38	1.29978E 00	2.86413E-02	-3.37115E-03	3.65946E-02	3.98412E-01	7.55380E-01
39	1.32298E 00	1.87944E-02	-2.21337E-03	3.65948E-02	3.98890E-01	7.55011E-01
40	1.34548E 00	9.25749E-03	-1.09087E-03	3.65951E-02	3.99355E-01	7.54654E-01
41	1.36737E 00	0.	0.	3.65954E-02	3.99807E-01	7.54306E-01

TABLE V (Cont'd)

I= 8 P/P-INF= 6.75671E 00

J	RHO	PSI	THETA	S	MU	M
8	1.70000E-01	5.54158E-01	-6.81641E-02	3.66286E-02	3.73489E-01	7.74836E-01
9	1.87070E-01	5.46094E-01	-6.71317E-02	3.66257E-02	3.73884E-01	7.74524E-01
10	2.04677E-01	5.37790E-01	-6.60681E-02	3.66229E-02	3.74291E-01	7.74202E-01
11	2.22880E-01	5.29220E-01	-6.49700E-02	3.66201E-02	3.74713E-01	7.73870E-01
12	2.41747E-01	5.20353E-01	-6.38335E-02	3.66173E-02	3.75150E-01	7.73525E-01
13	2.61359E-01	5.11153E-01	-6.26541E-02	3.66146E-02	3.75603E-01	7.73167E-01
14	2.81817E-01	5.01575E-01	-6.14201E-02	3.66120E-02	3.76077E-01	7.72794E-01
15	3.03243E-01	4.91564E-01	-6.01428E-02	3.66094E-02	3.76572E-01	7.72403E-01
16	3.25791E-01	4.81050E-01	-5.87955E-02	3.66069E-02	3.77093E-01	7.71993E-01
17	3.49662E-01	4.69945E-01	-5.73730E-02	3.66044E-02	3.77644E-01	7.71559E-01
18	3.75119E-01	4.58129E-01	-5.58608E-02	3.66020E-02	3.78231E-01	7.71097E-01
19	4.02526E-01	4.45440E-01	-5.42385E-02	3.65997E-02	3.78862E-01	7.70601E-01
20	4.32406E-01	4.31643E-01	-5.24770E-02	3.65975E-02	3.79549E-01	7.70062E-01
21	4.65565E-01	4.16378E-01	-5.05317E-02	3.65953E-02	3.80308E-01	7.69465E-01
22	5.03358E-01	3.99038E-01	-4.83275E-02	3.65933E-02	3.81172E-01	7.68787E-01
23	5.48434E-01	3.78436E-01	-4.57174E-02	3.65913E-02	3.82197E-01	7.67983E-01
24	6.07636E-01	3.51507E-01	-4.23227E-02	3.65896E-02	3.83535E-01	7.66935E-01
25	7.53143E-01	2.85934E-01	-3.41508E-02	3.65884E-02	3.86781E-01	7.64399E-01
26	9.03142E-01	2.19220E-01	-2.59917E-02	3.65891E-02	3.90052E-01	7.61851E-01
27	9.66810E-01	1.91166E-01	-2.26071E-02	3.65896E-02	3.91419E-01	7.60789E-01
28	1.01634E 00	1.69448E-01	-2.00047E-02	3.65901E-02	3.92473E-01	7.59971E-01
29	1.05856E 00	1.51004E-01	-1.78055E-02	3.65906E-02	3.93367E-01	7.59278E-01
30	1.09613E 00	1.34647E-01	-1.58630E-02	3.65911E-02	3.94158E-01	7.58665E-01
31	1.13041E 00	1.19771E-01	-1.41017E-02	3.65916E-02	3.94877E-01	7.58109E-01
32	1.16219E 00	1.06014E-01	-1.24769E-02	3.65920E-02	3.95542E-01	7.57595E-01
33	1.19200E 00	9.31429E-02	-1.09596E-02	3.65924E-02	3.96163E-01	7.57114E-01
34	1.22021E 00	8.09942E-02	-9.52955E-03	3.65928E-02	3.96751E-01	7.56661E-01
35	1.24707E 00	6.94498E-02	-8.17178E-03	3.65932E-02	3.97309E-01	7.56230E-01
36	1.27279E 00	5.84203E-02	-6.87542E-03	3.65936E-02	3.97843E-01	7.55818E-01
37	1.29752E 00	4.78368E-02	-5.63166E-03	3.65939E-02	3.98356E-01	7.55423E-01
38	1.32139E 00	3.76441E-02	-4.43365E-03	3.65942E-02	3.98851E-01	7.55042E-01
39	1.34449E 00	2.77978E-02	-3.27586E-03	3.65945E-02	3.99329E-01	7.54673E-01
40	1.36690E 00	1.82612E-02	-2.15335E-03	3.65948E-02	3.99794E-01	7.54315E-01
41	1.38870E 00	9.00391E-03	-1.06250E-03	3.65951E-02	4.00247E-01	7.53967E-01
42	1.40994E 00	0.	0.	3.65954E-02	4.00688E-01	7.53628E-01

TABLE V (Cont'd)

I= 7 P/P-INF= 6.81152E 00

J	RHO	PSI	THETA	S	MU	M
7	1.80000E-01	5.70333E-01	-7.02052E-02	3.66366E-02	3.73507E-01	7.74822E-01
8	1.96494E-01	5.62499E-01	-6.92012E-02	3.66334E-02	3.73891E-01	7.74519E-01
9	2.13473E-01	5.54448E-01	-6.81688E-02	3.66303E-02	3.74280E-01	7.74207E-01
10	2.30987E-01	5.46157E-01	-6.71052E-02	3.66272E-02	3.74694E-01	7.73885E-01
11	2.49094E-01	5.37600E-01	-6.60071E-02	3.66242E-02	3.75115E-01	7.73552E-01
12	2.67861E-01	5.28747E-01	-6.48706E-02	3.66213E-02	3.75555E-01	7.73207E-01
13	2.87371E-01	5.19561E-01	-6.36911E-02	3.66183E-02	3.76007E-01	7.72849E-01
14	3.07722E-01	5.09997E-01	-6.24632E-02	3.66156E-02	3.76481E-01	7.72475E-01
15	3.29036E-01	5.00000E-01	-6.11799E-02	3.66127E-02	3.76977E-01	7.72085E-01
16	3.51468E-01	4.89502E-01	-5.98326E-02	3.66099E-02	3.77498E-01	7.71674E-01
17	3.75216E-01	4.78412E-01	-5.84101E-02	3.66072E-02	3.78050E-01	7.71240E-01
18	4.00542E-01	4.66612E-01	-5.68978E-02	3.66046E-02	3.78637E-01	7.70778E-01
19	4.27810E-01	4.53940E-01	-5.52755E-02	3.66020E-02	3.79268E-01	7.70282E-01
20	4.57539E-01	4.40161E-01	-5.35141E-02	3.65995E-02	3.79956E-01	7.69742E-01
21	4.90531E-01	4.24915E-01	-5.15688E-02	3.65971E-02	3.80716E-01	7.69145E-01
22	5.28136E-01	4.07595E-01	-4.93645E-02	3.65947E-02	3.81580E-01	7.68467E-01
23	5.72990E-01	3.87016E-01	-4.67544E-02	3.65926E-02	3.82607E-01	7.67662E-01
24	6.31903E-01	3.60116E-01	-4.33597E-02	3.65904E-02	3.83946E-01	7.66613E-0
25	7.76718E-01	2.94601E-01	-3.51879E-02	3.65887E-02	3.87195E-01	7.64076E-01
26	9.25030E-01	2.27933E-01	-2.70287E-02	3.65890E-02	3.90470E-01	7.61526E-01
27	9.89414E-01	1.99894E-01	-2.36441E-02	3.65895E-02	3.91838E-01	7.60463E-01
28	1.03872E 00	1.78186E-01	-2.10417E-02	3.65899E-02	3.92894E-01	7.59645E-01
29	1.08076E 00	1.59749E-01	-1.88426E-02	3.65904E-02	3.93789E-01	7.58951E-01
30	1.11817E 00	1.43396E-01	-1.69001E-02	3.65909E-02	3.94581E-01	7.58338E-01
31	1.15230E 00	1.28527E-01	-1.51387E-02	3.65913E-02	3.95301E-01	7.57781E-01
32	1.18395E 00	1.14774E-01	-1.35139E-02	3.65917E-02	3.95966E-01	7.57267E-01
33	1.21363E 00	1.01905E-01	-1.19966E-02	3.65921E-02	3.96589E-01	7.56786E-01
34	1.24172E 00	8.97591E-02	-1.05666E-02	3.65925E-02	3.97176E-01	7.56332E-01
35	1.26847E 00	7.82167E-02	-9.20881E-03	3.65929E-02	3.97735E-01	7.55901E-01
36	1.29408E 00	6.71888E-02	-7.91245E-03	3.65933E-02	3.98270E-01	7.55489E-01
37	1.31871E 00	5.66066E-02	-6.66870E-03	3.65936E-02	3.98784E-01	7.55093E-01
38	1.34248E 00	4.64148E-02	-5.47073E-03	3.65939E-02	3.99279E-01	7.54712E-01
39	1.36548E 00	3.65693E-02	-4.31293E-03	3.65942E-02	3.99759E-01	7.54343E-01
40	1.38781E 00	2.70332E-02	-3.19043E-03	3.65946E-02	4.00224E-01	7.53985E-01
41	1.40951E 00	1.77762E-02	-2.09958E-03	3.65949E-02	4.00677E-01	7.53636E-01
42	1.43066E 00	8.77248E-03	-1.03711E-03	3.65952E-02	4.01119E-01	7.53297E-01
43	1.45130E 00	0.	0.	3.65954E-02	4.01551E-01	7.52965E-01

TABLE V (Cont'd)

I= 6 P/P-INF= 6.86544E 00

J	RHO	PSI	THETA	S	MU	W
6	1.90000E-01	5.86073E-01	-7.21972E-02	3.66453E-02	3.73526E-01	7.74807E-01
7	2.05966E-01	5.78450E-01	-7.12193E-02	3.66419E-02	3.73900E-01	7.74511E-01
8	2.22374E-01	5.70629E-01	-7.02154E-02	3.66385E-02	3.74284E-01	7.74208E-01
9	2.39265E-01	5.62591E-01	-6.91829E-02	3.66352E-02	3.74680E-01	7.73896E-01
10	2.56688E-01	5.54313E-01	-6.81193E-02	3.66319E-02	3.75088E-01	7.73573E-01
11	2.74701E-01	5.45769E-01	-6.70211E-02	3.66286E-02	3.75510E-01	7.73240E-01
12	2.93372E-01	5.36929E-01	-6.58847E-02	3.66254E-02	3.75948E-01	7.72896E-01
13	3.12782E-01	5.27757E-01	-6.47052E-02	3.66223E-02	3.76402E-01	7.72537E-01
14	3.33028E-01	5.18207E-01	-6.34773E-02	3.66192E-02	3.76876E-01	7.72164E-01
15	3.54234E-01	5.08225E-01	-6.21940E-02	3.66161E-02	3.77373E-01	7.71773E-01
16	3.76553E-01	4.97741E-01	-6.08467E-02	3.66131E-02	3.77895E-01	7.71362E-01
17	4.00180E-01	4.86666E-01	-5.94242E-02	3.66102E-02	3.78447E-01	7.70928E-01
18	4.25380E-01	4.74882E-01	-5.79119E-02	3.66073E-02	3.79035E-01	7.70465E-01
19	4.52511E-01	4.62227E-01	-5.62896E-02	3.66044E-02	3.79666E-01	7.69969E-01
20	4.82093E-01	4.48465E-01	-5.45281E-02	3.66017E-02	3.80354E-01	7.69429E-01
21	5.14923E-01	4.33238E-01	-5.25828E-02	3.65990E-02	3.81115E-01	7.68831E-01
22	5.52345E-01	4.15938E-01	-5.03785E-02	3.65964E-02	3.81980E-01	7.68153E-01
23	5.96981E-01	3.95383E-01	-4.77684E-02	3.65938E-02	3.83008E-01	7.67348E-01
24	6.55613E-01	3.68510E-01	-4.43737E-02	3.65914E-02	3.84349E-01	7.66299E-01
25	7.99754E-01	3.03055E-01	-3.62018E-02	3.65890E-02	3.87601E-01	7.63760E-01
26	9.48396E-01	2.36432E-01	-2.80427E-02	3.65890E-02	3.90880E-01	7.61208E-01
27	1.01150E 00	2.08408E-01	-2.46581E-02	3.65893E-02	3.92249E-01	7.60145E-01
28	1.08060E 00	1.86710E-01	-2.20557E-02	3.65897E-02	3.93306E-01	7.59325E-01
29	1.10246E 00	1.68281E-01	-1.98506E-02	3.65902E-02	3.94202E-01	7.58632E-01
30	1.13971E 00	1.51936E-01	-1.79141E-02	3.65906E-02	3.94995E-01	7.58018E-01
31	1.17370E 00	1.37068E-01	-1.61527E-02	3.65910E-02	3.95715E-01	7.57461E-01
32	1.20521E 00	1.23319E-01	-1.45279E-02	3.65915E-02	3.96382E-01	7.56946E-01
33	1.23477E 00	1.10454E-01	-1.30106E-02	3.65919E-02	3.97005E-01	7.56465E-01
34	1.26274E 00	9.83106E-02	-1.15806E-02	3.65922E-02	3.97593E-01	7.56011E-01
35	1.28939E 00	8.67703E-02	-1.02228E-02	3.65926E-02	3.98153E-01	7.55579E-01
36	1.31489E 00	7.57441E-02	-8.92643E-03	3.65930E-02	3.98688E-01	7.55167E-01
37	1.33942E 00	6.51633E-02	-7.68267E-03	3.65933E-02	3.99202E-01	7.54771E-01
38	1.36309E 00	5.49726E-02	-6.48470E-03	3.65936E-02	3.99699E-01	7.54389E-01
39	1.38600E 00	4.51279E-02	5.32690E-03	3.65940E-02	4.00179E-01	7.54020E-01
40	1.40824E 00	3.55926E-02	-4.20438E-03	3.65943E-02	4.00645E-01	7.53661E-01
41	1.42986E 00	2.63360E-02	-3.11350E-03	3.65946E-02	4.01098E-01	7.53313E-01
42	1.45092E 00	1.73325E-02	-2.05104E-03	3.65949E-02	4.01541E-01	7.52973E-01
43	1.47148E 00	8.56021E-03	-1.01395E-03	3.65952E-02	4.01973E-01	7.52641E-01
44	1.49158E 00	0.	0.	3.65954E-02	4.02398E-01	7.52316E-01

TABLE V (Cont'd)

I= 5 P/P-INF= 6.91859E 00

J	RHO	PSI	THETA	S	MU	W
5	2.00000E-01	6.01412E-01	-7.41444E-02	3.66548E-02	3.73548E-01	7.74790E-01
6	2.13481E-01	5.93983E-01	-7.31904E-02	3.66511E-02	3.73912E-01	7.74502E-01
7	2.31365E-01	5.86373E-01	-7.22125E-02	3.66474E-02	3.74286E-01	7.74207E-01
8	2.47689E-01	5.78565E-01	-7.12085E-02	3.66438E-02	3.74671E-01	7.73903E-01
9	2.64494E-01	5.70539E-01	-7.01761E-02	3.66402E-02	3.75067E-01	7.73590E-01
10	2.81829E-01	5.62273E-01	-6.91125E-02	3.66367E-02	3.75475E-01	7.73268E-01
11	2.99750E-01	5.53743E-01	-6.80144E-02	3.66332E-02	3.75898E-01	7.72935E-01
12	3.18327E-01	5.44917E-01	-6.68779E-02	3.66298E-02	3.76335E-01	7.72590E-01
13	3.37639E-01	5.35756E-01	-6.56984E-02	3.66264E-02	3.76790E-01	7.72232E-01
14	3.57784E-01	5.26222E-01	-6.44705E-02	3.66231E-02	3.77265E-01	7.71858E-01
15	3.78884E-01	5.16253E-01	-6.31872E-02	3.66198E-02	3.77761E-01	7.71467E-01
16	4.01091E-01	5.05784E-01	-6.18398E-02	3.66165E-02	3.78284E-01	7.71056E-01
17	4.24602E-01	4.94725E-01	-6.04173E-02	3.66133E-02	3.78836E-01	7.70622E-01
18	4.49678E-01	4.82956E-01	-5.89050E-02	3.66102E-02	3.79424E-01	7.70159E-01
19	4.76676E-01	4.70317E-01	-5.72827E-02	3.66071E-02	3.80057E-01	7.69662E-01
20	5.06115E-01	4.56573E-01	-5.55213E-02	3.66041E-02	3.80745E-01	7.69122E-01
21	5.38766E-01	4.41365E-01	-5.35759E-02	3.66011E-02	3.81507E-01	7.68524E-01
22	5.75028E-01	4.24085E-01	-5.13717E-02	3.65981E-02	3.82373E-01	7.67846E-01
23	6.20453E-01	4.03552E-01	-4.87615E-02	3.65953E-02	3.83401E-01	7.67040E-01
24	6.78811E-01	3.76707E-01	-4.53668E-02	3.65924E-02	3.84743E-01	7.65990E-01
25	8.22293E-01	3.11310E-01	-3.71950E-02	3.65895E-02	3.87998E-01	7.63450E-01
26	9.70281E-01	2.44703E-01	-2.90359E-02	3.65891E-02	3.91281E-01	7.60896E-01
27	1.03312E 00	2.16724E-01	-2.56512E-02	3.65893E-02	3.92652E-01	7.59832E-01
28	1.08200E 00	1.95037E-01	-2.30488E-02	3.65896E-02	3.93710E-01	7.59012E-01
29	1.12369E 00	1.76615E-01	-2.08497E-02	3.65900E-02	3.94607E-01	7.58318E-01
30	1.16079E 00	1.60276E-01	-1.89072E-02	3.65904E-02	3.95401E-01	7.57704E-01
31	1.19463E 00	1.45413E-01	-1.71459E-02	3.65908E-02	3.96122E-01	7.57146E-01
32	1.22602E 00	1.31868E-01	-1.55211E-02	3.65912E-02	3.96789E-01	7.56631E-01
33	1.25546E 00	1.18806E-01	-1.40038E-02	3.65916E-02	3.97413E-01	7.56150E-01
34	1.28332E 00	1.06665E-01	-1.25737E-02	3.65920E-02	3.98002E-01	7.55695E-01
35	1.30985E 00	9.51270E-02	-1.12159E-02	3.65923E-02	3.98563E-01	7.55264E-01
36	1.33526E 00	8.41027E-02	-9.91960E-03	3.65927E-02	3.99098E-01	7.54851E-01
37	1.35969E 00	7.35234E-02	-8.67586E-03	3.65930E-02	3.99613E-01	7.54455E-01
38	1.38327E 00	6.33339E-02	-7.47788E-03	3.65934E-02	4.00110E-01	7.54072E-01
39	1.40609E 00	5.34902E-02	-6.32009E-03	3.65937E-02	4.00591E-01	7.53703E-01
40	1.42823E 00	4.39556E-02	-5.19758E-03	3.65940E-02	4.01057E-01	7.53344E-01
41	1.44977E 00	3.46996E-02	-4.10671E-03	3.65943E-02	4.01511E-01	7.52995E-01
42	1.47075E 00	2.56966E-02	-3.04424E-03	3.65946E-02	4.01954E-01	7.52655E-01
43	1.49123E 00	1.69245E-02	-2.00718E-03	3.65949E-02	4.02387E-01	7.52323E-01
44	1.51124E 00	8.36440E-03	-9.93212E-04	3.65952E-02	4.02811E-01	7.51998E-01
45	1.53084E 00	0.	0.	3.65954E-02	4.03226E-01	7.51680E-01

TABLE V (Cont'd)

E= 4 R/R-INF= 6.97104E 00

J	RHO	PSI	THETA	S	MU	M
4	2.10000E-01	6.16381E-01	-7.60505E-02	3.66650E-02	3.73571E-01	7.74772E-01
5	2.25034E-01	6.09131E-01	-7.51186E-02	3.66610E-02	3.73926E-01	7.74491E-01
6	2.40437E-01	6.01715E-01	-7.41647E-02	3.66571E-02	3.74291E-01	7.74203E-01
7	2.56241E-01	5.94116E-01	-7.31868E-02	3.66532E-02	3.74665E-01	7.73907E-01
8	2.72482E-01	5.86320E-01	-7.21828E-02	3.66493E-02	3.75050E-01	7.73603E-01
9	2.89203E-01	5.78307E-01	-7.11504E-02	3.66456E-02	3.75446E-01	7.73291E-01
10	3.06451E-01	5.70054E-01	-7.00868E-02	3.66418E-02	3.75855E-01	7.72969E-01
11	3.24284E-01	5.61536E-01	-6.89886E-02	3.66381E-02	3.76278E-01	7.72635E-01
12	3.42768E-01	5.52723E-01	-6.78521E-02	3.66344E-02	3.76716E-01	7.72290E-01
13	3.61984E-01	5.43577E-01	-6.66726E-02	3.66308E-02	3.77171E-01	7.71932E-01
14	3.82030E-01	5.34055E-01	-6.54447E-02	3.66272E-02	3.77646E-01	7.71558E-01
15	4.03027E-01	5.24101E-01	-6.41614E-02	3.66236E-02	3.78143E-01	7.71167E-01
16	4.25126E-01	5.13646E-01	-6.28140E-02	3.66201E-02	3.78666E-01	7.70755E-01
17	4.48522E-01	5.02602E-01	-6.13915E-02	3.66167E-02	3.79219E-01	7.70321E-01
18	4.73477E-01	4.90849E-01	-5.98792E-02	3.66133E-02	3.79807E-01	7.69858E-01
19	5.00345E-01	4.78226E-01	-5.82569E-02	3.66099E-02	3.80440E-01	7.69361E-01
20	5.29643E-01	4.64499E-01	-5.64955E-02	3.66066E-02	3.81129E-01	7.68820E-01
21	5.62159E-01	4.49309E-01	-5.45501E-02	3.66033E-02	3.81892E-01	7.68222E-01
22	5.99226E-01	4.32049E-01	-5.23458E-02	3.66001E-02	3.82758E-01	7.67544E-01
23	6.43444E-01	4.11539E-01	-4.97357E-02	3.65969E-02	3.83787E-01	7.66738E-01
24	7.01534E-01	3.84722E-01	-4.63410E-02	3.65937E-02	3.85131E-01	7.65687E-01
25	8.44373E-01	3.19383E-01	-3.81691E-02	3.65900E-02	3.88289E-01	7.63145E-01
26	9.91721E-01	2.52851E-01	-3.00100E-02	3.65892E-02	3.91675E-01	7.60590E-01
27	1.05429E 00	2.24857E-01	-2.66253E-02	3.65892E-02	3.93048E-01	7.59526E-01
28	1.10298E 00	2.03180E-01	-2.40230E-02	3.65895E-02	3.94107E-01	7.58705E-01
29	1.14449E 00	1.84766E-01	-2.18238E-02	3.65898E-02	3.95004E-01	7.58010E-01
30	1.18144E 00	1.68433E-01	-1.98813E-02	3.65902E-02	3.95799E-01	7.57396E-01
31	1.21515E 00	1.53575E-01	-1.81200E-02	3.65906E-02	3.96521E-01	7.56838E-01
32	1.24640E 00	1.39834E-01	-1.64951E-02	3.65909E-02	3.97189E-01	7.56323E-01
33	1.27573E 00	1.26975E-01	-1.49779E-02	3.65913E-02	3.97814E-01	7.55841E-01
34	1.30348E 00	1.14837E-01	-1.35478E-02	3.65917E-02	3.98404E-01	7.55386E-01
35	1.32991E 00	1.03301E-01	-1.21901E-02	3.65921E-02	3.98965E-01	7.54954E-01
36	1.35521E 00	9.22790E-02	-1.08937E-02	3.65924E-02	3.99501E-01	7.54541E-01
37	1.37955E 00	8.17013E-02	-9.64994E-03	3.65927E-02	4.00017E-01	7.54144E-01
38	1.40303E 00	7.15132E-02	-8.45197E-03	3.65931E-02	4.00514E-01	7.53762E-01
39	1.42576E 00	6.16705E-02	-7.29419E-03	3.65934E-02	4.00995E-01	7.53392E-01
40	1.44782E 00	5.21368E-02	-6.17170E-03	3.65937E-02	4.01462E-01	7.53033E-01
41	1.46927E 00	4.28815E-02	-5.08084E-03	3.65940E-02	4.01917E-01	7.52684E-01
42	1.49018E 00	3.38790E-02	-4.01836E-03	3.65943E-02	4.02360E-01	7.52344E-01
43	1.51058E 00	2.51072E-02	-2.98129E-03	3.65946E-02	4.02794E-01	7.52011E-01
44	1.53052E 00	1.65474E-02	-1.96733E-03	3.65949E-02	4.03218E-01	7.51686E-01
45	1.55003E 00	8.18310E-03	-9.74136E-04	3.65952E-02	4.03634E-01	7.51367E-01
46	1.56916E 00	0.	0.	3.65954E-02	4.04042E-01	7.51055E-01

TABLE V (Cont'd)

I= 3 P/P-INF= 7.02285E 00

J	RHO	PSI	THETA	S	MU	M
3	2.20000E-01	6.31006E-01	-7.79188E-02	3.66760E-02	3.73595E-01	7.74752E-01
4	2.34619E-01	6.23922E-01	-7.70074E-02	3.66717E-02	3.73943E-01	7.74477E-01
5	2.49578E-01	6.16684E-01	-7.60756E-02	3.66675E-02	3.74299E-01	7.74196E-01
6	2.64904E-01	6.09279E-01	-7.51217E-02	3.66633E-02	3.74664E-01	7.73908E-01
7	2.80630E-01	6.01693E-01	-7.41437E-02	3.66592E-02	3.75038E-01	7.73613E-01
8	2.96791E-01	5.93908E-01	-7.31397E-02	3.66551E-02	3.75424E-01	7.73309E-01
9	3.13429E-01	5.85907E-01	-7.21073E-02	3.66511E-02	3.75820E-01	7.72996E-01
10	3.30593E-01	5.77667E-01	-7.10436E-02	3.66471E-02	3.76229E-01	7.72674E-01
11	3.48338E-01	5.69162E-01	-6.99455E-02	3.66431E-02	3.76652E-01	7.72340E-01
12	3.66732E-01	5.60362E-01	-6.88090E-02	3.66392E-02	3.77090E-01	7.71995E-01
13	3.85855E-01	5.51229E-01	-6.76295E-02	3.66353E-02	3.77544E-01	7.71636E-01
14	4.05804E-01	5.41721E-01	-6.64016E-02	3.66315E-02	3.78021E-01	7.71262E-01
15	4.26699E-01	5.31780E-01	-6.51183E-02	3.66277E-02	3.78519E-01	7.70871E-01
16	4.48692E-01	5.21340E-01	-6.37709E-02	3.66240E-02	3.79042E-01	7.70460E-01
17	4.71977E-01	5.10310E-01	-6.23484E-02	3.66202E-02	3.79595E-01	7.70025E-01
18	4.96812E-01	4.98573E-01	-6.08361E-02	3.66166E-02	3.80184E-01	7.69562E-01
19	5.23554E-01	4.85966E-01	-5.92137E-02	3.66129E-02	3.80818E-01	7.69065E-01
20	5.52714E-01	4.72256E-01	-5.74523E-02	3.66093E-02	3.81507E-01	7.68524E-01
21	5.85079E-01	4.57084E-01	-5.55069E-02	3.66057E-02	3.82270E-01	7.67926E-01
22	6.21975E-01	4.39844E-01	-5.33026E-02	3.66022E-02	3.83137E-01	7.67247E-01
23	6.65990E-01	4.19356E-01	-5.06925E-02	3.65986E-02	3.84167E-01	7.66441E-01
24	7.23817E-01	3.92567E-01	-4.72978E-02	3.65950E-02	3.85512E-01	7.65389E-01
25	8.66026E-01	3.27285E-01	-3.91259E-02	3.65907E-02	3.88773E-01	7.62846E-01
26	1.01275E 00	2.60799E-01	-3.09668E-02	3.65894E-02	3.92063E-01	7.60289E-01
27	1.07506E 00	2.32820E-01	-2.75821E-02	3.65893E-02	3.93437E-01	7.59224E-01
28	1.12355E 00	2.11153E-01	-2.49798E-02	3.65894E-02	3.94497E-01	7.58403E-01
29	1.16489E 00	1.92747E-01	-2.27806E-02	3.65897E-02	3.95395E-01	7.57708E-01
30	1.20169E 00	1.76420E-01	-2.08381E-02	3.65900E-02	3.96191E-01	7.57093E-01
31	1.23526E 00	1.61567E-01	-1.90769E-02	3.65904E-02	3.96914E-01	7.56535E-01
32	1.26640E 00	1.47830E-01	-1.74520E-02	3.65907E-02	3.97583E-01	7.56019E-01
33	1.29561E 00	1.34975E-01	-1.59347E-02	3.65911E-02	3.98208E-01	7.55537E-01
34	1.32325E 00	1.22840E-01	-1.45047E-02	3.65914E-02	3.98799E-01	7.55082E-01
35	1.34958E 00	1.11306E-01	-1.31469E-02	3.65918E-02	3.99360E-01	7.54649E-01
36	1.37478E 00	1.00286E-01	-1.18505E-02	3.65921E-02	3.99897E-01	7.54236E-01
37	1.39903E 00	8.97099E-02	-1.06068E-02	3.65925E-02	4.00413E-01	7.53839E-01
38	1.42242E 00	7.95232E-02	-9.40883E-03	3.65928E-02	4.00911E-01	7.53457E-01
39	1.44506E 00	6.96817E-02	-8.25104E-03	3.65931E-02	4.01393E-01	7.53086E-01
40	1.46704E 00	6.01489E-02	-7.12854E-03	3.65934E-02	4.01861E-01	7.52727E-01
41	1.48841E 00	5.08944E-02	-6.03769E-03	3.65937E-02	4.02316E-01	7.52378E-01
42	1.50923E 00	4.18925E-02	-4.97520E-03	3.65940E-02	4.02760E-01	7.52038E-01
43	1.52950E 00	3.31212E-02	-3.93811E-03	3.65943E-02	4.03193E-01	7.51705E-01
44	1.54942E 00	2.45617E-02	-2.92413E-03	3.65946E-02	4.03616E-01	7.51379E-01
45	1.56886E 00	1.61976E-02	-1.93093E-03	3.65949E-02	4.04030E-01	7.51060E-01
46	1.58792E 00	8.01456E-03	-9.56808E-04	3.65952E-02	4.04444E-01	7.50747E-01
47	1.60660E 00	0.	0.	3.65954E-02	4.04846E-01	7.50440E-01

TABLE V (Cont'd)

I= 2 R/R-INF= 7.07411E 00

J	RHO	PSI	THETA	S	MU	W
2	2.30000E-01	6.45311E-01	-7.97523E-02	3.66877E-02	3.73622E-01	7.74731E-01
3	2.44234E-01	6.38380E-01	-7.88599E-02	3.66832E-02	3.73962E-01	7.74463E-01
4	2.58781E-01	6.31308E-01	-7.79486E-02	3.66787E-02	3.74310E-01	7.74188E-01
5	2.73666E-01	6.24081E-01	-7.70167E-02	3.66743E-02	3.74666E-01	7.73907E-01
6	2.88918E-01	6.16688E-01	-7.60628E-02	3.66699E-02	3.75031E-01	7.73618E-01
7	3.04567E-01	6.09113E-01	-7.50849E-02	3.66655E-02	3.75406E-01	7.73323E-01
8	3.20649E-01	6.01341E-01	-7.40809E-02	3.66612E-02	3.75791E-01	7.73019E-01
9	3.37206E-01	5.93352E-01	-7.30484E-02	3.66569E-02	3.76188E-01	7.72706E-01
10	3.54287E-01	5.85124E-01	-7.19848E-02	3.66527E-02	3.76597E-01	7.72383E-01
11	3.71947E-01	5.76631E-01	-7.08866E-02	3.66484E-02	3.77021E-01	7.72050E-01
12	3.90252E-01	5.67844E-01	-6.97501E-02	3.66443E-02	3.77459E-01	7.71705E-01
13	4.09283E-01	5.58725E-01	-6.85706E-02	3.66402E-02	3.77915E-01	7.71346E-01
14	4.29137E-01	5.49229E-01	-6.73427E-02	3.66361E-02	3.78391E-01	7.70972E-01
15	4.49933E-01	5.39303E-01	-6.60593E-02	3.66320E-02	3.78888E-01	7.70580E-01
16	4.71822E-01	5.28876E-01	-6.47120E-02	3.66280E-02	3.79412E-01	7.70169E-01
17	4.94997E-01	5.17861E-01	-6.32894E-02	3.66240E-02	3.79966E-01	7.69734E-01
18	5.19717E-01	5.06139E-01	-6.17771E-02	3.66201E-02	3.80556E-01	7.69271E-01
19	5.46334E-01	4.93549E-01	-6.01548E-02	3.66161E-02	3.81189E-01	7.68773E-01
20	5.75359E-01	4.79865E-01	-5.83034E-02	3.66122E-02	3.81879E-01	7.68232E-01
21	6.07575E-01	4.64701E-01	-5.64479E-02	3.66083E-02	3.82643E-01	7.67634E-01
22	6.44303E-01	4.47481E-01	-5.42437E-02	3.66045E-02	3.83511E-01	7.66954E-01
23	6.88120E-01	4.27015E-01	-5.16336E-02	3.66005E-02	3.84542E-01	7.66148E-01
24	7.45689E-01	4.00253E-01	-4.82388E-02	3.65965E-02	3.85887E-01	7.65096E-01
25	8.87281E-01	3.35029E-01	-4.00870E-02	3.65914E-02	3.89152E-01	7.62551E-01
26	1.03339E 00	2.68588E-01	-3.19078E-02	3.65896E-02	3.92444E-01	7.59993E-01
27	1.09545E 00	2.40624E-01	-2.85232E-02	3.65894E-02	3.93820E-01	7.58927E-01
28	1.14374E 00	2.18968E-01	-2.59208E-02	3.65894E-02	3.94881E-01	7.58106E-01
29	1.18492E 00	2.00569E-01	-2.37216E-02	3.65896E-02	3.95780E-01	7.57410E-01
30	1.22157E 00	1.84298E-01	-2.17791E-02	3.65899E-02	3.96577E-01	7.56795E-01
31	1.25502E 00	1.69401E-01	-2.00178E-02	3.65902E-02	3.97301E-01	7.56236E-01
32	1.28603E 00	1.55668E-01	-1.83930E-02	3.65905E-02	3.97970E-01	7.55720E-01
33	1.31513E 00	1.42816E-01	-1.68757E-02	3.65909E-02	3.98596E-01	7.55238E-01
34	1.34266E 00	1.30684E-01	-1.54456E-02	3.65912E-02	3.99187E-01	7.54782E-01
35	1.36889E 00	1.19153E-01	-1.40879E-02	3.65915E-02	3.99750E-01	7.54350E-01
36	1.39400E 00	1.08134E-01	-1.27915E-02	3.65919E-02	4.00287E-01	7.53936E-01
37	1.41815E 00	9.75602E-02	-1.15478E-02	3.65922E-02	4.00804E-01	7.53539E-01
38	1.44146E 00	8.73750E-02	-1.03498E-02	3.65926E-02	4.01302E-01	7.53156E-01
39	1.46401E 00	7.75348E-02	-9.19201E-03	3.65929E-02	4.01784E-01	7.52786E-01
40	1.48591E 00	6.80031E-02	-8.06950E-03	3.65932E-02	4.02253E-01	7.52426E-01
41	1.50720E 00	5.87494E-02	-6.97865E-03	3.65935E-02	4.02708E-01	7.52077E-01
42	1.52794E 00	4.97482E-02	-5.91616E-03	3.65938E-02	4.03153E-01	7.51736E-01
43	1.54819E 00	4.09774E-02	-4.87909E-03	3.65941E-02	4.03587E-01	7.51403E-01
44	1.56798E 00	3.24183E-02	-3.86510E-03	3.65944E-02	4.04012E-01	7.51078E-01
45	1.58735E 00	2.40545E-02	-2.87193E-03	3.65946E-02	4.04429E-01	7.50758E-01
46	1.60633E 00	1.58717E-02	-1.89780E-03	3.65949E-02	4.04839E-01	7.50445E-01
47	1.62495E 00	7.85722E-03	-9.41011E-04	3.65952E-02	4.05241E-01	7.50137E-01
48	1.64324E 00	0.	0.	3.65954E-02	4.05638E-01	7.49834E-01

TABLE V (Cont'd)

I= 1 P/P-INF= 7.12488E 00

J	KMO	PSI	BHETA	G	AM	M
1	2.40000E-01	6.59315E-01	-8.15536E-02	3.670038E-02	3.736508-01	7.747098-01
2	2.53874E-01	6.52528E-01	-8.06790E-02	3.668958-02	3.739838-01	7.744468-01
3	2.68039E-01	6.45609E-01	-7.97866E-02	3.669078-02	3.743248-01	7.741778-01
4	2.82516E-01	6.38548E-01	-7.88753E-02	3.668408-02	3.746728-01	7.739028-01
5	2.97329E-01	6.31332E-01	-7.79434E-02	3.668188-02	3.750288-01	7.736218-01
6	3.12507E-01	6.23951E-01	-7.69895E-02	3.667678-02	3.753948-01	7.733338-01
7	3.28080E-01	6.16388E-01	-7.60115E-02	3.667218-02	3.757698-01	7.730378-01
8	3.44086E-01	6.08627E-01	-7.50075E-02	3.666768-02	3.761548-01	7.727338-01
9	3.60564E-01	6.00650E-01	-7.39751E-02	3.666308-02	3.765518-01	7.724208-01
10	3.77563E-01	5.92439E-01	-7.29114E-02	3.665858-02	3.769618-01	7.720978-01
11	3.95138E-01	5.83955E-01	-7.18132E-02	3.665408-02	3.773848-01	7.717648-01
12	4.13357E-01	5.75180E-01	-7.06767E-02	3.664968-02	3.778238-01	7.714188-01
13	4.32299E-01	5.66073E-01	-6.94972E-02	3.664528-02	3.782798-01	7.710598-01
14	4.52059E-01	5.56591E-01	-6.82693E-02	3.664088-02	3.787568-01	7.706858-01
15	4.72758E-01	5.46678E-01	-6.69860E-02	3.663658-02	3.792598-01	7.702948-01
16	4.94545E-01	5.36266E-01	-6.56386E-02	3.663228-02	3.797778-01	7.698828-01
17	5.17613E-01	5.25265E-01	-6.42160E-02	3.662808-02	3.803318-01	7.694478-01
18	5.42218E-01	5.13559E-01	-6.27037E-02	3.662378-02	3.809218-01	7.689868-01
19	5.68713E-01	5.00984E-01	-6.10814E-02	3.661958-02	3.815568-01	7.684868-01
20	5.97600E-01	4.87307E-01	-5.93200E-02	3.661638-02	3.822468-01	7.679458-01
21	6.29077E-01	4.72171E-01	-5.73765E-02	3.661118-02	3.830108-01	7.673468-01
22	6.66240E-01	4.54970E-01	-5.51703E-02	3.660698-02	3.838798-01	7.666668-01
23	7.09862E-01	4.34526E-01	-5.25601E-02	3.660268-02	3.849118-01	7.658598-01
24	7.67179E-01	4.07791E-01	-4.91654E-02	3.659818-02	3.862588-01	7.648078-01
25	9.08165E-01	3.42624E-01	-4.09935E-02	3.659228-02	3.895268-01	7.622818-01
26	1.05367E 00	2.76228E-01	-3.28343E-02	3.658898-02	3.928218-01	7.597028-01
27	1.11548E 00	2.48280E-01	-2.94497E-02	3.658958-02	3.941978-01	7.586368-01
28	1.18358E 00	2.26634E-01	-2.68473E-02	3.658948-02	3.952608-01	7.578138-01
29	1.20460E 00	2.08243E-01	-2.46481E-02	3.658968-02	3.961608-01	7.571178-01
30	1.24111E 00	1.91928E-01	-2.27057E-02	3.658988-02	3.969578-01	7.565018-01
31	1.27443E 00	1.77085E-01	-2.09444E-02	3.659008-02	3.976828-01	7.559428-01
32	1.30532E 00	1.63357E-01	-1.93195E-02	3.659038-02	3.983528-01	7.554268-01
33	1.33431E 00	1.50509E-01	-1.78022E-02	3.659068-02	3.989708-01	7.549438-01
34	1.36174E 00	1.38379E-01	-1.63722E-02	3.659108-02	3.995718-01	7.544878-01
35	1.38788E 00	1.26851E-01	-1.50144E-02	3.659138-02	4.001338-01	7.540548-01
36	1.41288E 00	1.15835E-01	-1.37181E-02	3.659168-02	4.006728-01	7.536418-01
37	1.43694E 00	1.05262E-01	-1.24743E-02	3.659208-02	4.011898-01	7.532438-01
38	1.46016E 00	9.50788E-02	-1.12764E-02	3.659238-02	4.016888-01	7.528608-01
39	1.48264E 00	8.52400E-02	-1.01186E-02	3.659268-02	4.021718-01	7.524898-01
40	1.50445E 00	7.57094E-02	-8.99609E-03	3.659298-02	4.026398-01	7.521308-01
41	1.52566E 00	6.64566E-02	-7.90526E-03	3.659328-02	4.030968-01	7.517808-01
42	1.54633E 00	5.74581E-02	-6.84277E-03	3.659368-02	4.035408-01	7.514398-01
43	1.56650E 00	4.86860E-02	-5.80668E-03	3.659388-02	4.039758-01	7.511048-01
44	1.58622E 00	4.01274E-02	-4.79170E-03	3.659418-02	4.044018-01	7.507808-01
45	1.60552E 00	3.17639E-02	-3.79852E-03	3.659448-02	4.048188-01	7.504618-01
46	1.62443E 00	2.35814E-02	-2.82439E-03	3.659468-02	4.052288-01	7.501478-01
47	1.64299E 00	1.55671E-02	-1.86761E-03	3.659498-02	4.056318-01	7.498398-01
48	1.66120E 00	7.70992E-03	-9.26608E-04	3.659528-02	4.060288-01	7.495348-01
49	1.67910E 00	0.	0.	3.659568-02	4.064198-01	7.492348-01

3. Double Conical Shock Program Example

This program was carried out for the case where one cone is at an angle of attack for the following input data:

M_1^* = 2.03183 (M_∞ = 4.0, 15 deg. cone).

ψ_1^* = 0.165935 rad.

γ_1 = 0.38032 rad.

p_1/p_∞ = 2.4056

S_1/R = 0.067733

$M^*_{1,2}$ = 2.06346

$\psi^*_{1,2}$ = 0.12262 rad.

γ_2 = 0.342957 rad. (M_∞ = 4.0, 12.5 deg. cone).

p_2/p_∞ = 1.9441

$S_{1,2}/R$ = 0.029667

r = 2.0

q = 1.0

$\Delta\psi$ = 5.0 deg.

$\bar{\gamma}$ = 1.4

S_2/R = 0.52932

KALF = 1

α = 2.0 deg.

η/α = 0.654926

M_2^* = -0.408226

$M^*_{w,2}$ = 1.86308

ψ^*_2 =-0.505885 rad.

The program output is included in this appendix and the symbols are defined in Appendix V.3.

The intersection curve of the two conical shocks is described in terms of conical coordinates ρ and ψ, which lie on the base cone surface. The computation of this curve is terminated when the value of ψ_{max}, which represents the point where the intersection curve starts to bend back in, is reached.

The pressure, Mach number and entropy immediately behind the intersection curve in the lower and upper regions are given by Figures 49 and 50. These quantities are plotted versus the meridian angle ψ and therefore are at points along the intersection curve. As shown in the output these computations are terminated when a so-called Mach reflection is reached. This means that the normal Mach number components are too small for the necessary deflections and a cusped intersection with a normal shock region occurs. Comparison of Figures 49 and 50, shows that the pressure ratios in the lower and upper regions, at each point on the intersection curve, differ by less than 2% even though the assumption of constant shock strengths has been used instead of an iteration procedure.

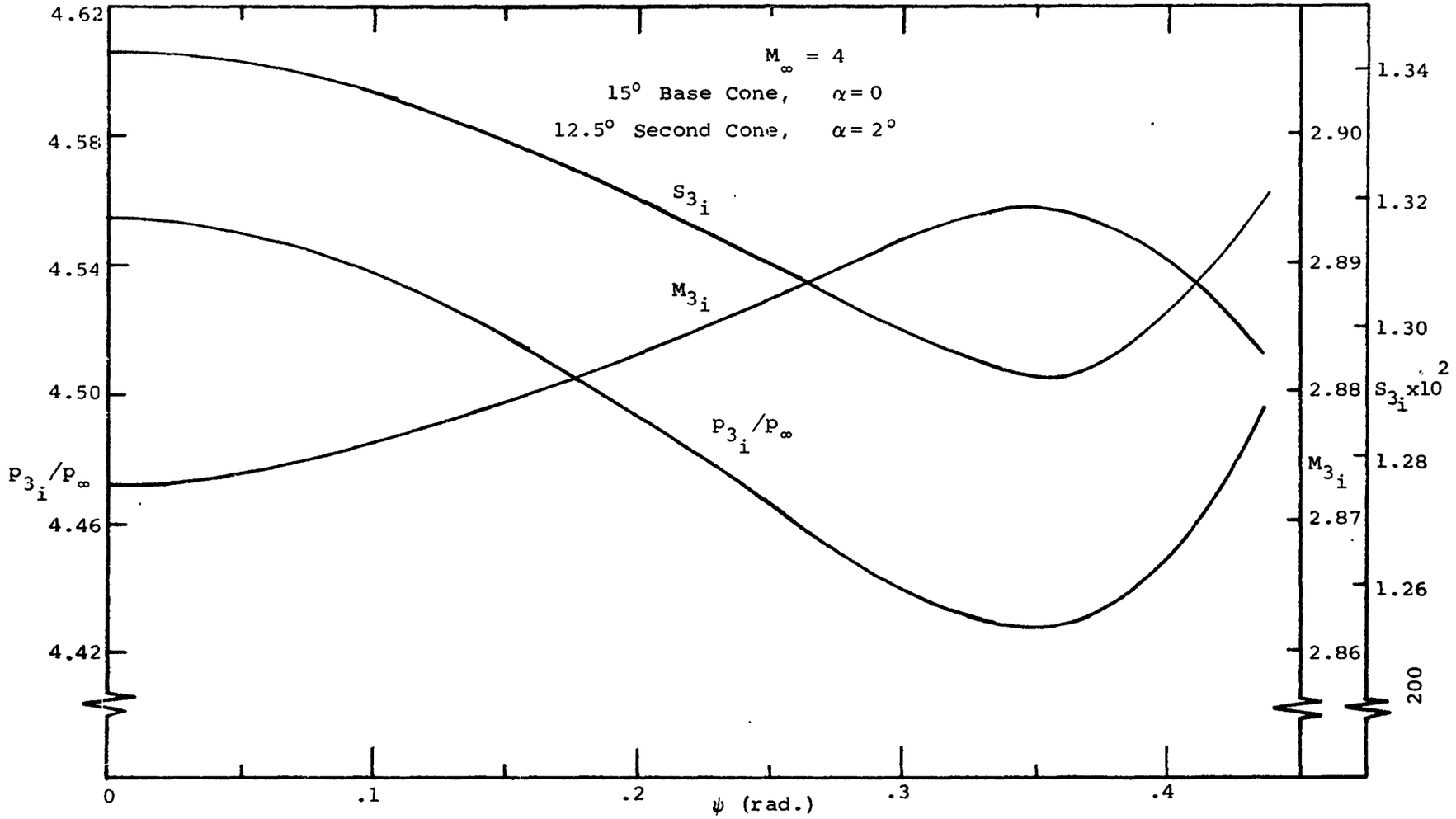

FIGURE 49 - LOWER CONICAL-CONICAL INTERSECTION REGION PROPERTIES

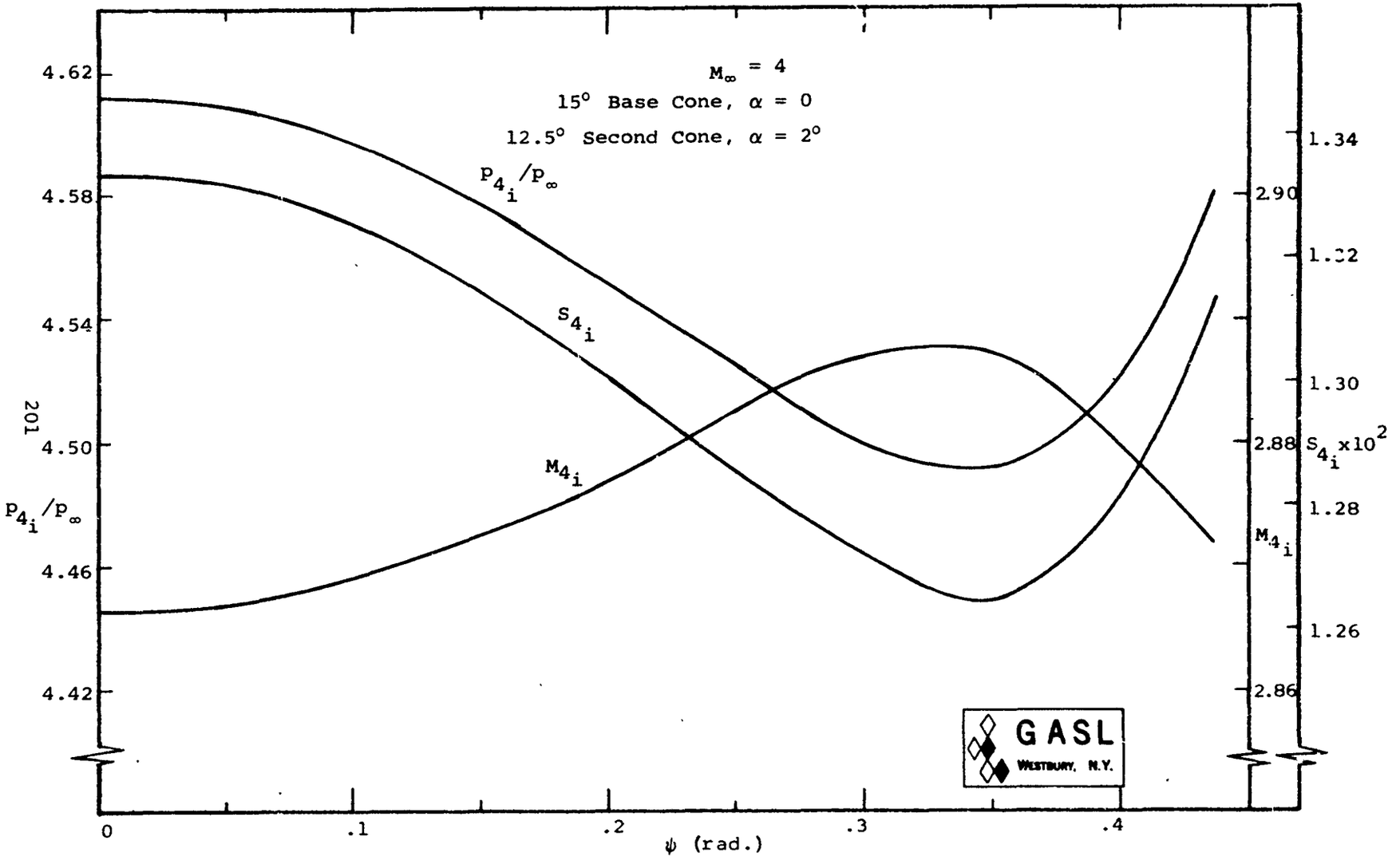

FIGURE 50 - UPPER CONICAL-CONICAL INTERSECTION REGION PROPERTIES

TABLE VI - SAMPLE OUTPUT - DOUBLE CONICAL SHOCK PROBLEM

DOUBLE CONICAL SHOCK PROGRAM

FIRST CONE

M1= 2.05183E 00 PSI1= 1.65935E-01 GAMMA1= 3.80320E-01 P1/P-INF= 2.40560E 00 S1/R= 6.77330E-02

SECOND CONE WITH NO ANGLE OF ATTACK

M12= 2.06346E 00 PSI12= 1.22620E-01 GAMMA2= 3.42957E-01 P2/P-INF= 1.94410E 00 S12/R= 2.96670E-02

DATA FOR SECOND CONE WITH ANGLE OF ATTACK

ALPHA= 2.00000E 00 ETA/ALPHA= 6.54926E-01 M2=-6.08226E-01 MN2= 1.86306E 00 PSI2=-5.05885E-01

K= 2.00000E 00 G= 1.00000E 00 DELTA PSI= 5.00000E 00 S2/R= 5.29320E-01 GAMMA-BAR= 1.40000E 00

ALPHA AND DELTA PSI ARE IN DEGREES

PSI-MAX(DEGREES)= 5.23085E 01

TERMS INDEPENDENT OF PSI(I)

THETA-1= 1.20454E-02 COS(BZ)=-3.71218E-01 RZ1= 3.27530E 00

TABLE VI (Cont'd)

PSI	COS(TX)	COS(TY)	COS(TZ)	COS(BX)	COS(BY)	COS(NX)	COS(NY)	COS(NZ)
0.	-1.0000E 00	-0.	-0.	0.	9.2855E-01	0.	-3.7122E-01	-9.2855E-01
8.7266E-02	-9.5718E-01	-3.1732E-02	-2.8774E-01	8.0928E-02	9.2501E-01	2.7795E-01	-3.7861E-01	-8.8284E-01
1.7453E-01	-8.5679E-01	-5.6978E-02	-5.1251E-01	1.5124E-01	9.1444E-01	4.8981E-01	-4.0069E-01	-7.7430E-01
2.6180E-01	-7.4500E-01	-7.4728E-02	-6.6286E-01	2.4033E-01	8.9691E-01	6.2227E-01	-4.3684E-01	-6.5024E-01
3.4907E-01	-6.4638E-01	-8.7228E-02	-7.5801E-01	3.1758E-01	8.7255E-01	6.9378E-01	-4.8068E-01	-5.3629E-01
4.3633E-01	-5.6641E-01	-9.6886E-02	-8.1841E-01	3.9242E-01	8.4155E-01	7.2469E-01	-5.3142E-01	-4.3864E-01
5.2360E-01	-5.0311E-01	-1.0550E-01	-8.5776E-01	4.6427E-01	8.0414E-01	7.2892E-01	-5.8500E-01	-3.5560E-01
6.1087E-01	-4.5282E-01	-1.1448E-01	-8.8422E-01	6.3259E-01	7.6062E-01	7.1505E-01	-6.3902E-01	-2.8345E-01
6.9813E-01	-4.1191E-01	-1.2539E-01	-9.0256E-01	5.9686E-01	7.1131E-01	6.8854E-01	-6.9161E-01	-2.1815E-01
7.8540E-01	-3.7661E-01	-1.4104E-01	-9.1557E-01	6.5658E-01	6.5658E-01	6.5350E-01	-7.4095E-01	-1.5467E-01
8.7266E-01	-3.3923E-01	-1.7104E-01	-9.2502E-01	7.1131E-01	5.9686E-01	6.1560E-01	-7.8390E-01	-8.0813E-02

PSI	RHO	GAMMA	MY1	MX1	MI-BAR 1	MN-BAR 1	MB-BAR 1	MN1
0.	3.3137E 00	3.8032E-01	5.4853E-01	0.	-0.	-3.2449E 00	-2.0651E-01	3.3209E 00
8.7266E-02	3.3311E 00	3.9804E-01	5.4644E-01	4.7808E-02	-1.0055E 00	-3.0852E 00	-2.0651E-01	3.1650E 00
1.7453E-01	3.3847E 00	4.4705E-01	5.4020E-01	9.5251E-02	-1.7910E 00	-2.7058E 00	-2.0651E-01	2.7966E 00
2.6180E-01	3.4779E 00	5.1874E-01	5.2984E-01	1.4197E-01	-2.3164E 00	-2.2323E 00	-2.0651E-01	2.3796E 00
3.4907E-01	3.6173E 00	6.0546E-01	5.1545E-01	1.8761E-01	-2.6490E 00	-1.8741E 00	-2.0651E-01	2.0029E 00
4.3633E-01	3.8138E 00	7.0233E-01	4.9714E-01	2.3182E-01	-2.8600E 00	-1.5329E 00	-2.0651E-01	1.6879E 00
5.2360E-01	4.0861E 00	8.0689E-01	4.7504E-01	2.7427E-01	-2.9975E 00	-1.2427E 00	-2.0651E-01	1.4295E 00
6.1087E-01	4.4666E 00	9.1866E-01	4.4933E-01	3.1462E-01	-3.0900E 00	-9.9055E-01	-2.0651E-01	1.2167E 00
6.9813E-01	5.0178E 00	1.0395E 00	4.2020E-01	3.5259E-01	-3.1641E 00	-7.6235E-01	-2.0651E-01	1.0394E 00
7.8540E-01	5.8857E 00	1.1760E 00	3.8787E-01	3.8787E-01	-3.1996E 00	-5.4061E-01	-2.0651E-01	8.8956E-01
8.7266E-01	7.6135E 00	1.3564E 00	3.5259E-01	4.2020E-01	-3.2328E 00	-2.8241E-01	-2.0651E-01	7.6087E-01

TABLE VI (Cont'd)

RSI	DELTA 1	X	Y	Z	PHI	U-BAR	V-BAR	W-BAR
0.	1.6594E-01	0.	1.2301E 00	3.0769E 00	0.	8.3212E-01	8.7561E-02	0.
8.7266E-02	1.7292E-01	1.0778E-01	1.2319E 00	3.0931E 00	1.5393E-01	8.3217E-01	8.7744E-02	4.0708E-03
1.7453E-01	1.9165E-01	2.1818E-01	1.2374E 00	3.1429E 00	3.0836E-01	8.3231E-01	8.8287E-02	8.0325E-03
2.6180E-01	2.1730E-01	3.3415E-01	1.2471E 00	3.2294E 00	4.6987E-01	8.3254E-01	8.9169E-02	1.1784E-02
3.4907E-01	2.4496E-01	4.5926E-01	1.2618E 00	3.3588E 00	6.1120E-01	8.3284E-01	9.0363E-02	1.5236E-02
4.3633E-01	2.7045E-01	5.9833E-01	1.2831E 00	3.5413E 00	7.6140E-01	8.3322E-01	9.1835E-02	1.8318E-02
5.2360E-01	2.8992E-01	7.5843E-01	1.3136E 00	3.7942E 00	9.1095E-01	8.3365E-01	9.3550E-02	2.0977E-02
6.1087E-01	2.9910E-01	9.5104E-01	1.3582E 00	4.1475E 00	1.0611E 00	8.3415E-01	9.5487E-02	2.3176E-02
6.9813E-01	2.9209E-01	1.1973E 00	1.4269E 00	4.6592E 00	1.2149E 00	8.3470E-01	9.7645E-02	2.4886E-02
7.8540E-01	2.5827E-01	1.5449E 00	1.5449E 00	5.4651E 00	1.3796E 00	8.3533E-01	1.0010E-01	2.6066E-02
8.7266E-01	1.6591E-01	2.1651E 00	1.8167E 00	7.0695E 00	1.5576E 00	8.3603E-01	1.0283E-01	2.6548E-02

PSI	MW	A2	MX2	MY2	MZ2
0.	2.0492 10E 00	2.4499 92E-01	0.	-4.1782105E-01	3.3818 97E 00
8.726646E-02	2.0493 79E 00	2.4495 22E-01	7.1354 57E-02	-4.1697756E-01	3.3829 47E 00
1.7453 29E-01	2.0498 78E 00	2.4481 29E-01	1.4037 97E-01	-4.1522484E-01	3.3860 60E 00
2.6179 94E-01	2.0506 91E 00	2.4458 59E-01	2.0498 06E-01	-4.1239205E-01	3.3911 28E 00
3.4906 59E-01	2.0517 90E 00	2.4427 84E-01	2.6335 73E-01	-3.1859796E-01	3.3979 90E 00
4.3633 23E-01	2.0531 45E 00	2.4389 86E-01	3.1412 46E-01	-3.1308320E-01	3.4066 57E 00
5.2359 88E-01	2.0547 25E 00	2.4345 47E-01	3.5641 67E-01	-2.0868797E-01	3.4163 40E 00
6.1086 52E-01	2.0565 08E 00	2.4295 24E-01	3.8961 73E-01	-2.0282371E-01	3.4275 10E 00
6.9813 17E-01	2.0584 95E 00	2.4239 07E-01	4.1337 21E-01	-1.0642732E-01	3.4399 81E 00
7.8539 82E-01	2.0607 53E 00	2.4177 04E-01	4.2699 38E-01	-9.1340932E-02	3.4541 75E 00
8.7266 46E-01	2.0632 72E 00	2.4110 32E-01	4.2805 02E-01	-1.1662250E-02	3.4700 46E 00

TABLE VI (Cont'd)

PSI	MT-BAR 2	MN-BAR 2	MB-BAR 2	MN2	DELTA 2
0.	-0.	-2.963654E 00	-1.697139E 00	3.412519DE 00	1.397489E-01
8.726046E-02	-1.026803E 00	-2.788899E 00	-1.684584E 00	3.258818.E 00	1.453408E-01
1.745329E-01	-1.829891E 00	-2.371838E 00	-1.647884E 00	2.888102E 00	1.401541E-01
2.617994E-01	-2.368889E 00	-1.892714E 00	-1.589801E 00	2.471805E 00	1.793911E-01
3.490659E-01	-2.712286E 00	-1.464078E 00	-1.514542E 00	2.099567E 00	2.002979E-01
4.363323E-01	-2.932875E 00	-1.085971E 00	-1.422245E 00	1.793422E 00	2.180320E-01
5.235988E-01	-3.079447E 00	-7.872122E-01	-1.333424E 00	1.548458E 00	2.306002E-01
6.108652E-01	-3.180985E 00	-5.470882E-01	-1.230447E 00	1.353904E 00	2.361569E-01
6.981317E-01	-3.254447E 00	-3.522045E-01	-1.147106E 00	1.209960E 00	2.384016E-01
7.853982E-01	-3.310185E 00	-1.860066E-01	-1.063226E 00	1.079373E 00	2.215912E-01
8.726646E-01	-3.352236E 00	-3.887907E-03	-9.935880E-01	9.935956E-01	2.104404E-01

TABLE VI (Cont'd)

MACH REFLECTION

LOOP= 7 CASE NO.= 1

PSI	M81	THETA	M3T	M3	P3/P-INF	S3
0.	2.873366E 00	4.116648E-01	-0.	2.873366E 00	4.554718E 00	1.343131E-02
8.726646E-02	2.726020E 00	4.326772E-01	-9.148747E-01	2.875444E 00	4.541939E 00	1.338228E-02
1.745329E-01	2.374730E 00	4.925270E-01	-1.631541E 00	2.881193E 00	4.506727E 00	1.324864E-02
2.617994E-01	1.969264E 00	5.860078E-01	-2.113722E 00	2.888916E 00	4.459746E 00	1.307379E-02
3.490659E-01	1.587814E 00	7.139304E-01	-2.420010E 00	2.894409E 00	4.426527E 00	1.295257E-02
4.363323E-01	1.232307E 00	8.987727E-01	-2.606381E 00	2.883020E 00	4.495577E 00	1.320679E-02

PSI	M82	THETA	M4T	M4	P4/P-INF	S4
0.	2.866119E 00	4.265092E-01	-0.	2.866119E 00	4.611187E 00	1.334597E-02
8.726646E-02	2.718533E 00	4.471016E-01	-9.146360E-01	2.868271E 00	4.598628E 00	1.327465E-02
1.745329E-01	2.366515E 00	5.084387E-01	-1.631134E 00	2.874195E 00	4.564257E 00	1.307863E-02
2.617994E-01	1.959745E 00	6.036278E-01	-2.113157E 00	2.882020E 00	4.519614E 00	1.281918E-02
3.490659E-01	1.575906E 00	7.323876E-01	-2.418992E 00	2.887040E 00	4.491620E 00	1.264519E-02
4.363323E-01	1.213386E 00	9.162864E-01	-2.603055E 00	2.871968E 00	4.581099E 00	1.312793E-02

4. Plane Shock-Conical Body Program Example

The following input data has been used as an example of the operation of this program:

$M_\infty = 4.0$

$\delta_1 = 10$ deg.

$r = 2.5$

$q = 2.0$

$\Delta z = 0.05$

$\bar{\gamma} = 1.4$

$p_c/p_\infty = 2.405$ (15 deg. cone)

$p_b/p_\infty = 2.80$

$T_c/T_\infty = 1.31$

$S_2/R = 0.067733$

$\gamma_c = 0.3803$ rad.

$M^*_{1c} = 2.03183$

$\psi_{1c} = 0.165935$ rad.

$\gamma_b = 0.261799$ (15 deg.)

$M^*_{1b} = 2.01128$

$\psi_{1b} = 0.261799$ rad.

The program output with the characteristic subroutine is included in this appendix and the symbols are defined in Appendix V-4.

The intersection curve of the plane and conical shocks in coordinates on the plane surface is given in Figure 51. As noted on the first page of the output, this computation terminates when a so-called Mach reflection is reached, which means a cusped-normal shock intersection exists in the plane normal to the intersection curve. Figure 52 shows the variation of Mach number, pressure ratio and entropy in the lower intersection region, immediately behind the intersection curve (conditions 4) versus the slope of the curve with respect to the z' axes (Ω_i).

The program next computes the intersection curve of the modified plane shock and the cone surface. To do this it is necessary to pick three points through which to construct the second order curve (Section E). The points chosen in this case are i = 1,4, and 10. This curve is terminated due to a Mach reflection. The flow properties $M_{4_{bi}}$, $p_{4_{bi}}/p_\infty$ and $S_{4_{bi}}$ immediately behind the modified plane shock near the cone surface are shown in Figure 53 and differ somewhat from those in Figure 52 since the flow upstream of the modified plane shock is conical. The flow properties immediately behind the reflected shock on the cone surface are plotted versus the slope of the reflection curve on the conical surface, β, given by

$$\beta_i = \sigma_{6_i} + \tan^{-1}\left(\frac{M_{6_{N_i}}}{M_{6_{t_i}}}\right)$$

in Figure 54. The pressure variation along the centerline on the cone surface obtained from the characteristic subroutine is given in Figure 55. The output of the characteristic subroutine is described in Appendix VI-2.

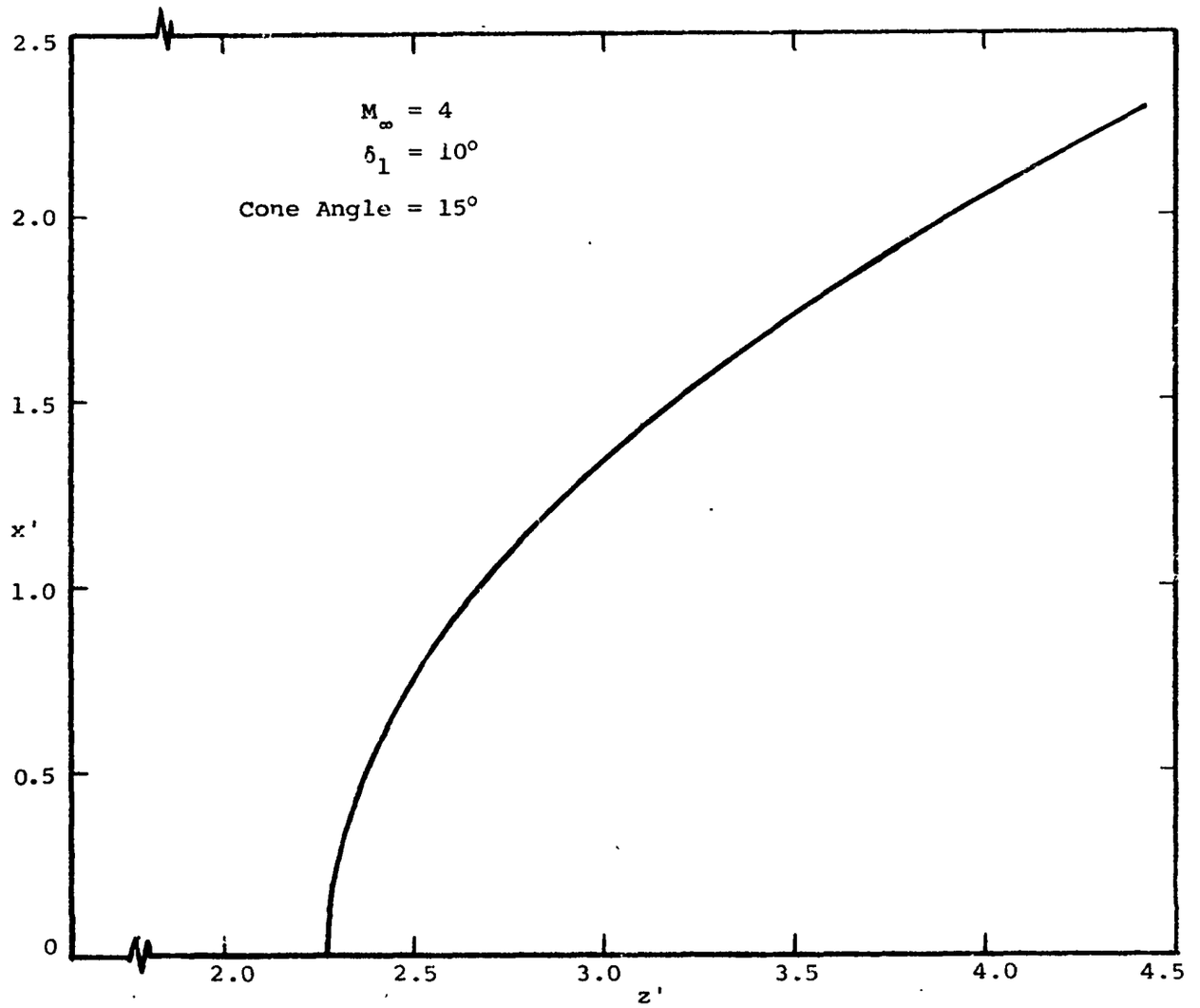

FIGURE 51 - CONICAL SHOCK-PLANE SHOCK INTERSECTION CURVE

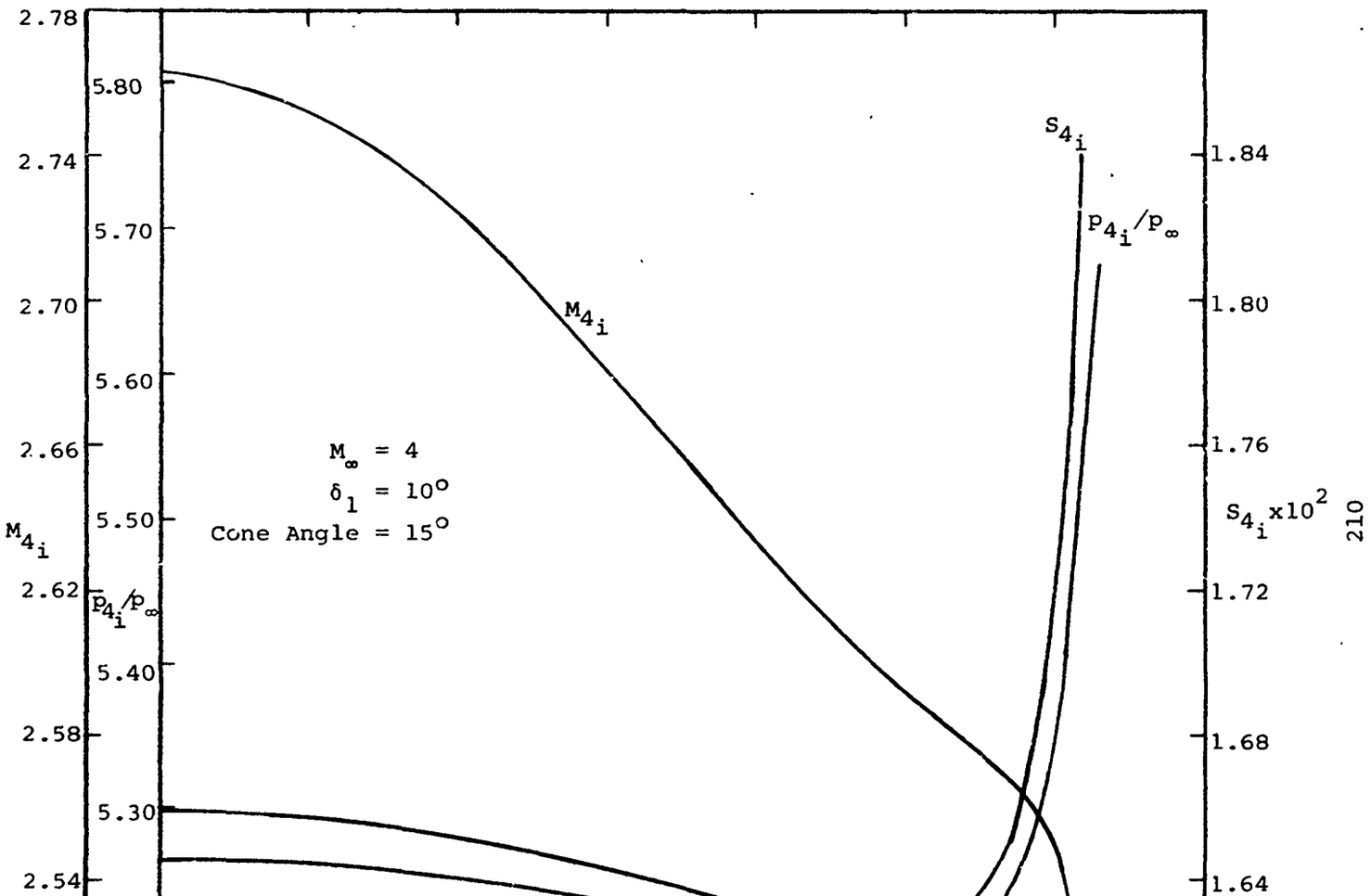

FIGURE 52 - CONDITIONS IN LOWER INTERSECTION REGION OF PLANE AND CONICAL SHOCKS

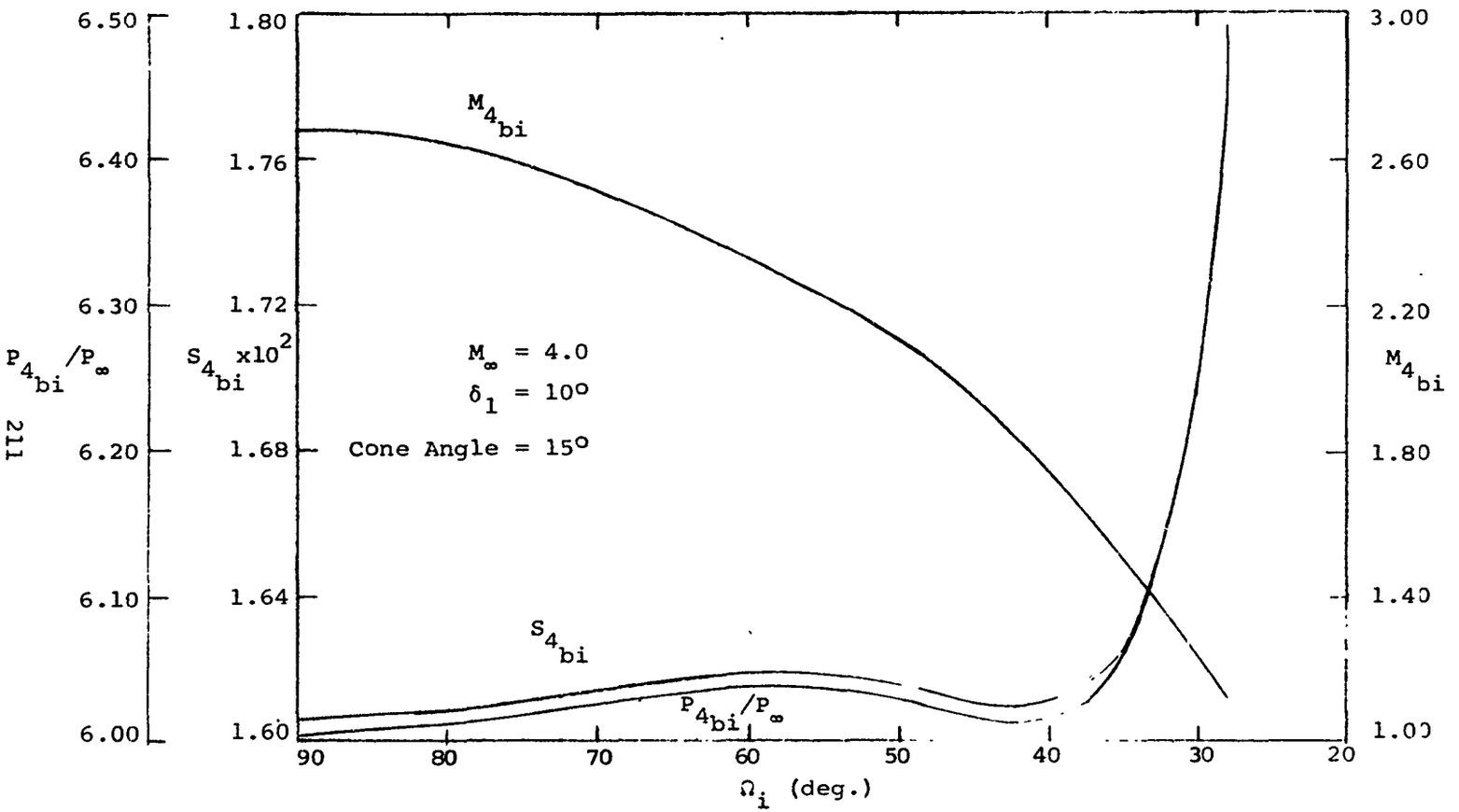

FIGURE 53. - FLOW PROPERTIES BEHIND THE MODIFIED PLANE SHOCK NEAR THE CONE SURFACE

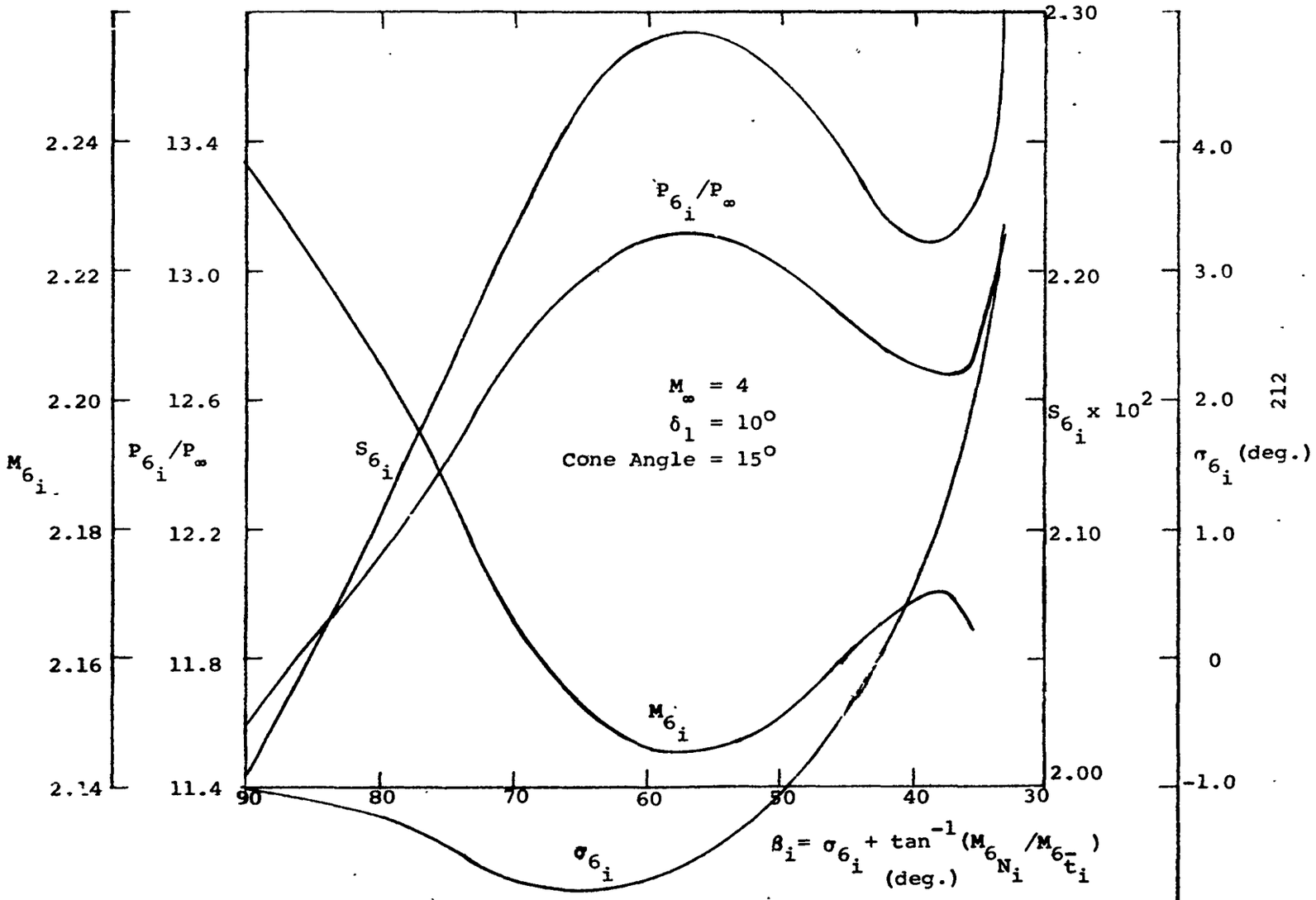

FIGURE 54 - FLOW PROPERTIES IMMEDIATELY BEHIND REFLECTION CURVE ON CONE SURFACE

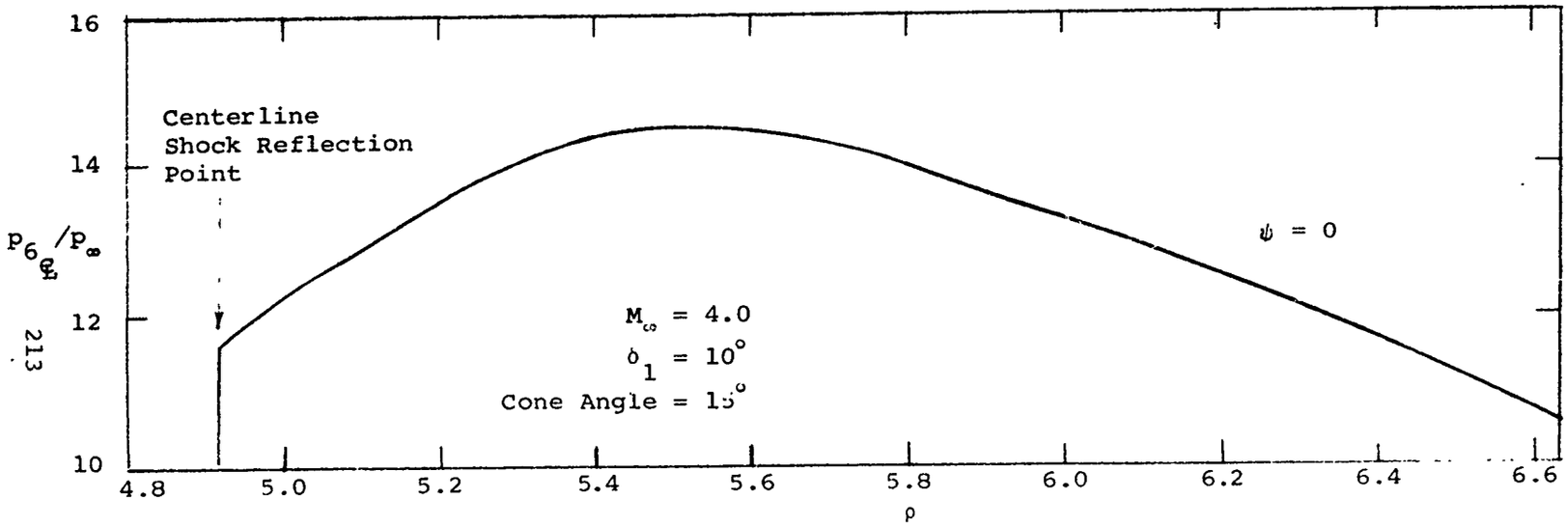

FIGURE 55 - CENTERLINE PRESSURE DISTRIBUTION ON CONE SURFACE BEHIND REFLECTED SHOCK

TABLE VII - SAMPLE OUTPUT FOR PLANE SHOCK - CONICAL BODY PROBLEM

PLANE SHOCK - CONICAL BODY WITH CHARACTERISTICS

M-INF= 4.000000E 00 [illegible]= 2.500000E 00 DELTA-1= 1.000000E 01 PC/P-INF= 2.405000E 00 DELTA Z= 5.000000E-02
GAMMA= 1.400000E 00 G= 2.000000E 00 S2/R= 6.779300E-02 PB/P-INF= 2.800000E 00 TC/T-INF= 1.310000E 00

DELTA-1 IN DEGREES

GAMMA	M1-STAR	PSI-1
3.80300E-01	2.03183E 00	1.65935E-01
2.61799E-01	2.01128E 00	2.61799E-01

GAMMA-C= 3.80300E-01 MR= 3.24491E 00 MT=-7.06449E-01

M-1= 3.28605E 00 THETA-1= 3.88059E-01 P1/P-INF= 2.50604E 00 A1/A-INF= 1.15294E 00

MACH REFLECTION

TABLE VII (Cont'd)

ZP	XP	OMEGA	M2XP	M2YP	M2ZP	M2NP	M2TP
2.27206E 00	0.	1.57080E 00	0.	1.74710E 00	2.82421E 00	2.82421E 00	0.
2.32206E 00	3.52352E-01	1.29273E 00	1.15856E-01	1.73564E 00	2.82889E 00	2.68842E 00	-7.76525E-01
2.37206E 00	4.95442E-01	1.18703E 00	1.62028E-01	1.72444E 00	2.83347E 00	2.56670E 00	-1.06089E 00
2.42206E 00	6.06751E-01	1.11146E 00	1.96265E-01	1.71348E 00	2.83795E 00	2.45677E 00	-1.25822E 00
2.47206E 00	7.01571E-01	1.05178E 00	2.24168E-01	1.70276E 00	2.84233E 00	2.35683E 00	-1.40987E 00
2.52206E 00	7.83212E-01	1.00233E 00	2.47935E-01	1.69227E 00	2.84662E 00	2.26546E 00	-1.53244E 00
2.57206E 00	8.57911E-01	9.60132E-01	2.68713E-01	1.68200E 00	2.85082E 00	2.18150E 00	-1.63469E 00
2.62206E 00	9.26591E-01	9.23382E-01	2.87190E-01	1.67194E 00	2.85493E 00	2.10401E 00	-1.72188E 00
2.67206E 00	9.91504E-01	8.90898E-01	3.03824E-01	1.66209E 00	2.85896E 00	2.03221E 00	-1.79747E 00
2.72206E 00	1.05252E 00	8.61348E-01	3.18933E-01	1.65245E 00	2.86290E 00	1.96544E 00	-1.86385E 00
2.77206E 00	1.11728E 00	8.35627E-01	3.32756E-01	1.64300E 00	2.86676E 00	1.90314E 00	-1.92277E 00
2.82206E 00	1.18125E 00	8.11776E-01	3.45474E-01	1.63374E 00	2.87055E 00	1.84485E 00	-1.97554E 00
2.87206E 00	1.21781E 00	7.89940E-01	3.57228E-01	1.62466E 00	2.87426E 00	1.79017E 00	-2.02316E 00
2.92206E 00	1.25225E 00	7.69936E-01	3.68133E-01	1.61576E 00	2.87789E 00	1.73874E 00	-2.06640E 00
2.97206E 00	1.30981E 00	7.51237E-01	3.78284E-01	1.60704E 00	2.88146E 00	1.69025E 00	-2.10590E 00
3.02206E 00	1.35570E 00	7.33957E-01	3.87759E-01	1.59848E 00	2.88496E 00	1.64446E 00	-2.14217E 00
3.07206E 00	1.41007E 00	7.17842E-01	3.96624E-01	1.59009E 00	2.88839E 00	1.60112E 00	-2.17561E 00
3.12206E 00	1.44307E 00	7.02762E-01	4.04935E-01	1.58186E 00	2.89176E 00	1.56003E 00	-2.20658E 00
3.17206E 00	1.48481E 00	6.88608E-01	4.12742E-01	1.57378E 00	2.89506E 00	1.52101E 00	-2.23537E 00
3.22206E 00	1.52540E 00	6.75286E-01	4.20086E-01	1.56585E 00	2.89830E 00	1.48390E 00	-2.26221E 00
3.27206E 00	1.56493E 00	6.62715E-01	4.27005E-01	1.55806E 00	2.90148E 00	1.44855E 00	-2.28731E 00
3.32206E 00	1.60347E 00	6.50827E-01	4.33532E-01	1.55042E 00	2.90461E 00	1.41483E 00	-2.31086E 00
3.37206E 00	1.64110E 00	6.39559E-01	4.39696E-01	1.54292E 00	2.90767E 00	1.38263E 00	-2.33300E 00
3.42206E 00	1.67789E 00	6.28858E-01	4.45523E-01	1.53555E 00	2.91069E 00	1.35183E 00	-2.35387E 00
3.47206E 00	1.71385E 00	6.18679E-01	4.51037E-01	1.52831E 00	2.91364E 00	1.32236E 00	-2.37359E 00
3.52206E 00	1.74904E 00	6.08978E-01	4.56258E-01	1.52120E 00	2.91655E 00	1.29411E 00	-2.39225E 00
3.57206E 00	1.78361E 00	5.99718E-01	4.61206E-01	1.51421E 00	2.91941E 00	1.26702E 00	-2.40995E 00
3.62206E 00	1.81747E 00	5.90868E-01	4.65898E-01	1.50735E 00	2.92221E 00	1.24100E 00	-2.42677E 00
3.67206E 00	1.85073E 00	5.82396E-01	4.70350E-01	1.50060E 00	2.92497E 00	1.21600E 00	-2.44278E 00
3.72206E 00	1.88334E 00	5.74277E-01	4.74577E-01	1.49397E 00	2.92768E 00	1.19195E 00	-2.45804E 00
3.77206E 00	1.91541E 00	5.66486E-01	4.78591E-01	1.48744E 00	2.93035E 00	1.16880E 00	-2.47261E 00
3.82206E 00	1.94695E 00	5.59001E-01	4.82406E-01	1.48103E 00	2.93297E 00	1.14649E 00	-2.48653E 00
3.87206E 00	1.97798E 00	5.51802E-01	4.86032E-01	1.47473E 00	2.93555E 00	1.12499E 00	-2.49986E 00
3.92206E 00	2.00852E 00	5.44872E-01	4.89479E-01	1.46852E 00	2.93809E 00	1.10424E 00	-2.51263E 00
3.97206E 00	2.03859E 00	5.38194E-01	4.92758E-01	1.46242E 00	2.94058E 00	1.08420E 00	-2.52489E 00
4.02206E 00	2.06822E 00	5.31753E-01	4.95877E-01	1.45642E 00	2.94303E 00	1.06484E 00	-2.53666E 00
4.07206E 00	2.09742E 00	5.25534E-01	4.98844E-01	1.45051E 00	2.94545E 00	1.04613E 00	-2.54798E 00
4.12206E 00	2.12622E 00	5.19526E-01	5.01669E-01	1.44470E 00	2.94782E 00	1.02803E 00	-2.55887E 00
4.17206E 00	2.15462E 00	5.13717E-01	5.04356E-01	1.43898E 00	2.95016E 00	1.01051E 00	-2.56937E 00
4.22206E 00	2.18265E 00	5.08095E-01	5.06914E-01	1.43335E 00	2.95246E 00	9.93536E-01	-2.57949E 00
4.27206E 00	2.21031E 00	5.02650E-01	5.09349E-01	1.42780E 00	2.95473E 00	9.77093E-01	-2.58926E 00
4.32206E 00	2.23763E 00	4.97374E-01	5.11667E-01	1.42235E 00	2.95696E 00	9.61152E-01	-2.59869E 00
4.37206E 00	2.26461E 00	4.92258E-01	5.13873E-01	1.41697E 00	2.95916E 00	9.45690E-01	-2.60781E 00
4.42206E 00	2.29126E 00	4.87294E-01	5.15972E-01	1.41168E 00	2.96132E 00	9.30685E-01	-2.61663E 00

TABLE VII (Cont'd)

ZP	M2KN	DELTA(2)	OMEGA-STAR	GAMMA	DELTA(2)STAR	DELTA(1)	DELTA(1)STAR
2.27206E 00	3.32092E 00	5.53994E-01	0.	3.88059E-01	1.65935E-01	2.13526E-01	1.74533E-01
2.32206E 00	3.23001E 00	5.73274E-01	2.78068E-01	4.01970E-01	1.71304E-01	2.21784E-01	1.80186E-01
2.37206E 00	3.09219E 00	5.91592E-01	3.83764E-01	4.15223E-01	1.76359E-01	2.29713E-01	1.85510E-01
2.42206E 00	2.99529E 00	6.09015E-01	4.59339E-01	4.27882E-01	1.81132E-01	2.37347E-01	1.90536E-01
2.47206E 00	2.90758E 00	6.25654E-01	5.19015E-01	4.40005E-01	1.85649E-01	2.44712E-01	1.95292E-01
2.52206E 00	2.82773E 00	6.41571E-01	5.68464E-01	4.51638E-01	1.89933E-01	2.51834E-01	1.99803E-01
2.57206E 00	2.75464E 00	6.56824E-01	6.10664E-01	4.62821E-01	1.94003E-01	2.58733E-01	2.04088E-01
2.62206E 00	2.68743E 00	6.71467E-01	6.47414E-01	4.73592E-01	1.97875E-01	2.65425E-01	2.08166E-01
2.67206E 00	2.62534E 00	6.85546E-01	6.79839E-01	4.83980E-01	2.01566E-01	2.71927E-01	2.12053E-01
2.72206E 00	2.56779E 00	6.99102E-01	7.08948E-01	4.94013E-01	2.05089E-01	2.78252E-01	2.15761E-01
2.77206E 00	2.51424E 00	7.12170E-01	7.35169E-01	5.03716E-01	2.08454E-01	2.84412E-01	2.19304E-01
2.82206E 00	2.46426E 00	7.24783E-01	7.59020E-01	5.13110E-01	2.11673E-01	2.90417E-01	2.22692E-01
2.87206E 00	2.41748E 00	7.36969E-01	7.80857E-01	5.22214E-01	2.14755E-01	2.96279E-01	2.25936E-01
2.92206E 00	2.37358E 00	7.48756E-01	8.00961E-01	5.31047E-01	2.17709E-01	3.02003E-01	2.29044E-01
2.97206E 00	2.33228E 00	7.60166E-01	8.19560E-01	5.39624E-01	2.20542E-01	3.07599E-01	2.32025E-01
3.02206E 00	2.29334E 00	7.71221E-01	8.36839E-01	5.47960E-01	2.23262E-01	3.13073E-01	2.34886E-01
3.07206E 00	2.25664E 00	7.81941E-01	8.52954E-01	5.56067E-01	2.25874E-01	3.18433E-01	2.37634E-01
3.12206E 00	2.22179E 00	7.92344E-01	8.68034E-01	5.63958E-01	2.28386E-01	3.23683E-01	2.40275E-01
3.17206E 00	2.18866E 00	8.02446E-01	8.82138E-01	5.71645E-01	2.30801E-01	3.28830E-01	2.42815E-01
3.22206E 00	2.15727E 00	8.12263E-01	8.95510E-01	5.79136E-01	2.33126E-01	3.33878E-01	2.45258E-01
3.27206E 00	2.12740E 00	8.21808E-01	9.08091E-01	5.86442E-01	2.35365E-01	3.38832E-01	2.47611E-01
3.32206E 00	2.09894E 00	8.31094E-01	9.19970E-01	5.93572E-01	2.37523E-01	3.43695E-01	2.49876E-01
3.37206E 00	2.07177E 00	8.40134E-01	9.31238E-01	6.00532E-01	2.39602E-01	3.48472E-01	2.52060E-01
3.42206E 00	2.04582E 00	8.48939E-01	9.41938E-01	6.07332E-01	2.41607E-01	3.53167E-01	2.54165E-01
3.47206E 00	2.02098E 00	8.57520E-01	9.52118E-01	6.13978E-01	2.43542E-01	3.57783E-01	2.56195E-01
3.52206E 00	1.99717E 00	8.65885E-01	9.61819E-01	6.20476E-01	2.45409E-01	3.62323E-01	2.58153E-01
3.57206E 00	1.97438E 00	8.74045E-01	9.71078E-01	6.26833E-01	2.47212E-01	3.66789E-01	2.60043E-01
3.62206E 00	1.95248E 00	8.82007E-01	9.79928E-01	6.33054E-01	2.48953E-01	3.71185E-01	2.61869E-01
3.67206E 00	1.93144E 00	8.89780E-01	9.88400E-01	6.39144E-01	2.50636E-01	3.75514E-01	2.63630E-01
3.72206E 00	1.91120E 00	8.97371E-01	9.96519E-01	6.45110E-01	2.52262E-01	3.79777E-01	2.65333E-01
3.77206E 00	1.89171E 00	9.04788E-01	1.00431E 00	6.50954E-01	2.53834E-01	3.83977E-01	2.66978E-01
3.82206E 00	1.87294E 00	9.12037E-01	1.01180E 00	6.56683E-01	2.55354E-01	3.88116E-01	2.68567E-01
3.87206E 00	1.85483E 00	9.19125E-01	1.01899E 00	6.62300E-01	2.56824E-01	3.92196E-01	2.70104E-01
3.92206E 00	1.83736E 00	9.26057E-01	1.02592E 00	6.67810E-01	2.58247E-01	3.96220E-01	2.71590E-01
3.97206E 00	1.82049E 00	9.32839E-01	1.03260E 00	6.73215E-01	2.59624E-01	4.00188E-01	2.73027E-01
4.02206E 00	1.80418E 00	9.39476E-01	1.03904E 00	6.78520E-01	2.60956E-01	4.04103E-01	2.74417E-01
4.07206E 00	1.78840E 00	9.45974E-01	1.04526E 00	6.83728E-01	2.62246E-01	4.07966E-01	2.75762E-01
4.12206E 00	1.77313E 00	9.52337E-01	1.05127E 00	6.88842E-01	2.63495E-01	4.11779E-01	2.77063E-01
4.17206E 00	1.75835E 00	9.58570E-01	1.05708E 00	6.93865E-01	2.64705E-01	4.15543E-01	2.78322E-01
4.22206E 00	1.74402E 00	9.64677E-01	1.06270E 00	6.98800E-01	2.65877E-01	4.19259E-01	2.79541E-01
4.27206E 00	1.73013E 00	9.70663E-01	1.06815E 00	7.03651E-01	2.67012E-01	4.22930E-01	2.80720E-01
4.32206E 00	1.71665E 00	9.76531E-01	1.07342E 00	7.08419E-01	2.68112E-01	4.26556E-01	2.81862E-01
4.37206E 00	1.70357E 00	9.82285E-01	1.07854E 00	7.13107E-01	2.69178E-01	4.30139E-01	2.82968E-01
4.42206E 00	1.69086E 00	9.87928E-01	1.08350E 00	7.17717E-01	2.70211E-01	4.33679E-01	2.84038E-01

TABLE VII (Cont'd)

TP	P4/P2	A4/A2	M4N	THETA(4)	M4T	M4	P4/P-INF
2.272066E 00	2.139746E 00	1.126246E 00	2.763446E 00	4.422266E-01	0.	2.763446E 00	5.266386E 00
2.322066E 00	2.186286E 00	1.125946E 00	2.649816E 00	4.598286E-01	-6.896696E-01	2.738096E 00	5.258016E 00
2.372066E 00	2.183026E 00	1.125656E 00	2.547976E 00	4.768136E-01	-9.424636E-01	2.716686E 00	5.250166E 00
2.422066E 00	2.179976E 00	1.125396E 00	2.455966E 00	4.932506E-01	-1.118036E 00	2.698476E 00	5.242836E 00
2.472066E 00	2.177136E 00	1.125146E 00	2.372276E 00	5.091996E-01	-1.285066E 00	2.682886E 00	5.236016E 00
2.522066E 00	2.174516E 00	1.124916E 00	2.295676E 00	5.247116E-01	-1.362286E 00	2.669446E 00	5.229706E 00
2.572066E 00	2.172106E 00	1.124706E 00	2.225176E 00	5.398306E-01	-1.453456E 00	2.657806E 00	5.223906E 00
2.622066E 00	2.169906E 00	1.124516E 00	2.159986E 00	5.545946E-01	-1.531236E 00	2.647676E 00	5.218616E 00
2.672066E 00	2.167916E 00	1.124346E 00	2.099426E 00	5.690376E-01	-1.598696E 00	2.638826E 00	5.213836E 00
2.722066E 00	2.166146E 00	1.124186E 00	2.042956E 00	5.831916E-01	-1.657966E 00	2.631066E 00	5.209576E 00
2.772066E 00	2.164596E 00	1.124056E 00	1.990106E 00	5.970316E-01	-1.710586E 00	2.624236E 00	5.205836E 00
2.822066E 00	2.163256E 00	1.123936E 00	1.940466E 00	6.107446E-01	-1.757716E 00	2.618196E 00	5.202626E 00
2.872066E 00	2.162146E 00	1.123836E 00	1.893706E 00	6.241736E-01	-1.800236E 00	2.612846E 00	5.199946E 00
2.922066E 00	2.161256E 00	1.123756E 00	1.849526E 00	6.374176E-01	-1.838846E 00	2.608076E 00	5.197806E 00
2.972066E 00	2.160536E 00	1.123706E 00	1.807576E 00	6.504886E-01	-1.874086E 00	2.603826E 00	5.196226E 00
3.022066E 00	2.160176E 00	1.123666E 00	1.767926E 00	6.634036E-01	-1.906426E 00	2.600006E 00	5.195206E 00
3.072066E 00	2.159996E 00	1.123646E 00	1.730086E 00	6.761816E-01	-1.936216E 00	2.596556E 00	5.194756E 00
3.122066E 00	2.160046E 00	1.123656E 00	1.693976E 00	6.888386E-01	-1.963766E 00	2.593436E 00	5.194916E 00
3.172066E 00	2.160336E 00	1.123686E 00	1.659446E 00	7.013916E-01	-1.989336E 00	2.590596E 00	5.195676E 00
3.222066E 00	2.160956E 00	1.123736E 00	1.626346E 00	7.138506E-01	-2.013136E 00	2.587986E 00	5.197086E 00
3.272066E 00	2.161896E 00	1.123806E 00	1.594566E 00	7.262466E-01	-2.035336E 00	2.585586E 00	5.199146E 00
3.322066E 00	2.163296E 00	1.123906E 00	1.563996E 00	7.385806E-01	-2.056106E 00	2.583336E 00	5.201896E 00
3.372066E 00	2.164896E 00	1.124036E 00	1.534516E 00	7.508736E-01	-2.075576E 00	2.581226E 00	5.205376E 00
3.422066E 00	2.166156E 00	1.124186E 00	1.506036E 00	7.631416E-01	-2.093856E 00	2.579216E 00	5.209636E 00
3.472066E 00	2.168296E 00	1.124376E 00	1.478476E 00	7.754016E-01	-2.111046E 00	2.577286E 00	5.214646E 00
3.522066E 00	2.170776E 00	1.124586E 00	1.451746E 00	7.876706E-01	-2.127246E 00	2.575406E 00	5.220536E 00
3.572066E 00	2.173526E 00	1.124836E 00	1.425776E 00	7.999686E-01	-2.142516E 00	2.573566E 00	5.227326E 00
3.622066E 00	2.176766E 00	1.125116E 00	1.400496E 00	8.123136E-01	-2.156926E 00	2.571716E 00	5.235106E 00
3.672066E 00	2.180436E 00	1.125436E 00	1.375326E 00	8.247276E-01	-2.170536E 00	2.569856E 00	5.243936E 00
3.722066E 00	2.184576E 00	1.125796E 00	1.351706E 00	8.372366E-01	-2.183396E 00	2.567946E 00	5.253406E 00
3.772066E 00	2.189246E 00	1.126206E 00	1.328066E 00	8.498646E-01	-2.195546E 00	2.565956E 00	5.265136E 00
3.822066E 00	2.194496E 00	1.126656E 00	1.304846E 00	8.626436E-01	-2.207016E 00	2.563886E 00	5.277746E 00
3.872066E 00	2.200376E 00	1.127166E 00	1.281356E 00	8.756096E-01	-2.217836E 00	2.561686E 00	5.291686E 00
3.922066E 00	2.206976E 00	1.127736E 00	1.259146E 00	8.888026E-01	-2.228036E 00	2.559316E 00	5.307766E 00
3.972066E 00	2.214396E 00	1.128386E 00	1.236916E 00	9.022726E-01	-2.237636E 00	2.556746E 00	5.325616E 00
4.022066E 00	2.222756E 00	1.129106E 00	1.214596E 00	9.160806E-01	-2.246626E 00	2.553926E 00	5.345726E 00
4.072066E 00	2.232226E 00	1.129926E 00	1.192266E 00	9.303036E-01	-2.255016E 00	2.550806E 00	5.368486E 00
4.122066E 00	2.243006E 00	1.130846E 00	1.169796E 00	9.450396E-01	-2.262806E 00	2.547296E 00	5.394406E 00
4.172066E 00	2.255376E 00	1.131916E 00	1.147046E 00	9.604206E-01	-2.269946E 00	2.543296E 00	5.424176E 00
4.222066E 00	2.269766E 00	1.133146E 00	1.123786E 00	9.766296E-01	-2.276406E 00	2.538686E 00	5.458786E 00
4.272066E 00	2.286746E 00	1.134606E 00	1.099706E 00	9.939376E-01	-2.282106E 00	2.533246E 00	5.499706E 00
4.322066E 00	2.307406E 00	1.136356E 00	1.074336E 00	1.012776E 00	-2.286876E 00	2.526656E 00	5.549316E 00
4.372066E 00	2.333436E 00	1.138566E 00	1.046826E 00	1.033916E 00	-2.290456E 00	2.518336E 00	5.611916E 00
4.422066E 00	2.368786E 00	1.141546E 00	1.015366E 00	1.058996E 00	-2.292206E 00	2.507026E 00	5.696936E 00

TABLE VII (Cont'd)

ZP	A4/A-INF	SIGMA(4)	THETAP(4)	S4
2.27206E 00	9.84001E-01	8.94070E-08	-1.11768E-01	1.65913E-02
2.32206E 00	9.8 737E-01	2.60890E 00	-1.13446E-01	1.65497E-02
2.37206E 00	9.83489E-01	2.60355E 00	-1.14769E-01	1.65108E-02
2.42206E 00	9.83257E-01	2.25506E 00	-1.15765E-01	1.64745E-02
2.47206E 00	9.83041E-01	2.13662E 00	-1.16455E-01	1.64408E-02
2.52206E 00	9.82841E-01	2.03757E 00	-1.16859E-01	1.64097E-02
2.57206E 00	9.82657E-01	1.95232E 00	-1.16994E-01	1.63813E-02
2.62206E 00	9.82489E-01	1.87750E 00	-1.16873E-01	1.63552E-02
2.67206E 00	9.82338E-01	1.81088E 00	-1.16509E-01	1.63318E-02
2.72206E 00	9.82203E-01	1.75090E 00	-1.15911E-01	1.63110E-02
2.77206E 00	9.82084E-01	1.69641E 00	-1.15088E-01	1.62927E-02
2.82206E 00	9.81982E-01	1.64655E 00	-1.14048E-01	1.62770E-02
2.87206E 00	9.81897E-01	1.60064E 00	-1.12797E-01	1.62639E-02
2.92206E 00	9.81829E-01	1.55813E 00	-1.11[illegible]E-01	1.62535E-02
2.97206E 00	9.81778E-01	1.51860E 00	-1.09[illegible]8E-01	1.62457E-02
3.02206E 00	9.81746E-01	1.48168E 00	-1.07818E-01	1.62408E-02
3.07206E 00	9.81732E-01	1.44707E 00	-1.05760E-01	1.62386E-02
3.12206E 00	9.81737E-01	1.41453E 00	-1.03506E-01	1.62394E-02
3.17206E 00	9.81761E-01	1.38384E 00	-1.01056E-01	1.62431E-02
3.22206E 00	9.81806E-01	1.35481E 00	-9.84081E-02	1.62499E-02
3.27206E 00	9.81871E-01	1.32728E 00	-9.55619E-02	1.62600E-02
3.32206E 00	9.81959E-01	1.30111E 00	-9.25143E-02	1.62734E-02
3.37206E 00	9.82069E-01	1.27619E 00	-8.92614E-02	1.62904E-02
3.42206E 00	9.82204E-01	1.25240E 00	-8.57983E-02	1.63111E-02
3.47206E 00	9.82363E-01	1.22964E 00	-8.21186E-02	1.63358E-02
3.52206E 00	9.82550E-01	1.20783E 00	-7.82147E-02	1.63647E-02
3.57206E 00	9.82766E-01	1.18689E 00	-7.40770E-02	1.63981E-02
3.62206E 00	9.83012E-01	1.16675E 00	-6.96942E-02	1.64363E-02
3.67206E 00	9.83291E-01	1.14734E 00	-6.50526E-02	1.64799E-02
3.72206E 00	9.83607E-01	1.12861E 00	-6.01358E-02	1.65293E-02
3.77206E 00	9.83962E-01	1.11049E 00	-5.49242E-02	1.65850E-02
3.82206E 00	9.84360E-01	1.09294E 00	-4.93939E-02	1.66478E-02
3.87206E 00	9.84806E-01	1.07590E 00	-4.35159E-02	1.67186E-02
3.92206E 00	9.85306E-01	1.05933E 00	-3.72548E-02	1.67983E-02
3.97206E 00	9.85868E-01	1.04317E 00	-3.05665E-02	1.68883E-02
4.02206E 00	9.86499E-01	1.02737E 00	-2.33956E-02	1.69903E-02
4.07206E 00	9.87213E-01	1.01189E 00	-1.56705E-02	1.71064E-02
4.12206E 00	9.88024E-01	9.96656E-01	-7.29784E-03	1.72394E-02
4.17206E 00	9.88953E-01	9.81608E-01	1.84986E-03	1.73933E-02
4.22206E 00	9.90031E-01	9.66660E-01	1.19515E-02	1.75737E-02
4.27206E 00	9.91301E-01	9.51699E-01	2.32739E-02	1.77890E-02
4.32206E 00	9.92835E-01	9.36557E-01	3.62430E-02	1.80530E-02
4.37206E 00	9.94763E-01	9.20950E-01	5.16216E-02	1.83905E-02
4.42206E 00	9.97367E-01	9.04281E-01	7.1058CE-02	1.88567E-02

TABLE VII (Cont'd)

K= 1 GAMMA(K)= 2.61799E-01

I	ETA	ZETA	X	Y	Z	RHO	PHI	CHECK
1	-8.44333E-02	7.52287E-01	-0.	1.27145E 00	4.76753E 00	4.93571E 00	0.	-4.47E-08
2	-8.47451E-02	7.43808E-01	1.46178E-01	1.27226E 00	4.77940E 00	4.94799E 00	1.14395E-01	-1.49E-08
3	-8.47493E-02	7.35611E-01	2.20019E-01	1.26583E 00	4.79499E 00	4.96414E 00	1.72095E-01	0.
4	-8.46335E-02	7.27984E-01	2.83995E-01	1.25824E 00	4.81395E 00	4.98376E 00	2.21988E-01	-1.49E-07
5	-8.43563E-02	7.21089E-01	3.42893E-01	1.24958E 00	4.83591E 00	5.00650E 00	2.67813E-01	-5.96E-08
6	-8.39372E-02	7.15003E-01	3.98299E-01	1.23997E 00	4.86053E 00	5.03199E 00	3.10806E-01	-1.49E-08
7	-8.34168E-02	7.09743E-01	4.50936E-01	1.22951E 00	4.88749E 00	5.05990E 00	3.51527E-01	0.
8	-8.28080E-02	7.05298E-01	5.01208E-01	1.21830E 00	4.91651E 00	5.08953E 00	3.90293E-01	-8.94E-08
9	-8.21136E-02	7.01633E-01	5.49377E-01	1.20644E 00	4.94736E 00	5.12188E 00	4.27311E-01	-5.96E-08
10	-8.13524E-02	6.98706E-01	5.95639E-01	1.19401E 00	4.97980E 00	5.15547E 00	4.62733E-01	-7.45E-08
11	-8.05110E-02	6.96447E-01	6.40147E-01	1.18108E 00	5.01365E 00	5.19052E 00	4.96683E-01	0.
12	-7.95937E-02	6.94857E-01	6.83032E-01	1.16772E 00	5.04876E 00	5.22686E 00	5.29265E-01	-1.49E-08
13	-7.85986E-02	6.93860E-01	7.24406E-01	1.15399E 00	5.08498E 00	5.26436E 00	5.60569E-01	-8.94E-08
14	-7.75225E-02	6.93398E-01	7.64370E-01	1.13994E 00	5.12219E 00	5.30288E 00	5.90678E-01	2.98E-08
15	-7.63615E-02	6.93440E-01	8.03015E-01	1.12562E 00	5.16029E 00	5.34233E 00	6.19664E-01	1.49E-08
16	-7.51111E-02	6.93947E-01	8.40422E-01	1.11106E 00	5.19919E 00	5.38260E 00	6.47592E-01	-4.47E-08
17	-7.37669E-02	6.94882E-01	8.76666E-01	1.09632E 00	5.23881E 00	5.42361E 00	6.74523E-01	-7.45E-08
18	-7.23207E-02	6.96214E-01	9.11814E-01	1.08142E 00	5.27908E 00	5.46531E 00	7.00511E-01	-2.98E-08
19	-7.07688E-02	6.97911E-01	9.45930E-01	1.06639E 00	5.31995E 00	5.50762E 00	7.25607E-01	-1.49E-07
20	-6.91038E-02	6.99948E-01	9.79069E-01	1.05126E 00	5.36136E 00	5.55049E 00	7.49856E-01	-1.19E-07
21	-6.73182E-02	7.02300E-01	1.01129E 00	1.03606E 00	5.40327E 00	5.59387E 00	7.73298E-01	-2.98E-08
22	-6.54042E-02	7.04945E-01	1.04263E 00	1.02081E 00	5.44564E 00	5.63774E 00	7.95972E-01	2.98E-08
23	-6.33531E-02	7.07862E-01	1.07314E 00	1.00553E 00	5.48843E 00	5.68204E 00	8.17912E-01	2.98E-08
24	-6.11557E-02	7.11035E-01	1.10286E 00	9.90247E-01	5.53162E 00	5.72676E 00	8.39149E-01	2.98E-08
25	-5.88015E-02	7.14446E-01	1.13183E 00	9.74981E-01	5.57519E 00	5.77186E 00	8.59711E-01	-5.96E-08
26	-5.62793E-02	7.18091E-01	1.16009E 00	9.59753E-01	5.61911E 00	5.81733E 00	8.79623E-01	-8.94E-08
27	-5.35763E-02	7.21927E-01	1.18766E 00	9.44584E-01	5.66336E 00	5.86314E 00	8.98908E-01	-2.98E-08
28	-5.06782E-02	7.25973E-01	1.21458E 00	9.29496E-01	5.70793E 00	5.90928E 00	9.17585E-01	2.98E-08
29	-4.75690E-02	7.30208E-01	1.24087E 00	9.14511E-01	5.75280E 00	5.95574E 00	9.35672E-01	5.96E-08
30	-4.42305E-02	7.34624E-01	1.26656E 00	8.99653E-01	5.79797E 00	6.00250E 00	9.53183E-01	-5.96E-08
31	-4.06915E-02	7.39212E-01	1.29167E 00	8.84946E-01	5.84343E 00	6.04956E 00	9.70128E-01	-2.98E-08
32	-3.67773E-02	7.43967E-01	1.31622E 00	8.70420E-01	5.88918E 00	6.09692E 00	9.86518E-01	-1.19E-07
33	-3.26090E-02	7.48885E-01	1.34024E 00	8.56105E-01	5.93521E 00	6.14458E 00	1.00256E 00	-8.94E-08
34	-2.81017E-02	7.53962E-01	1.36373E 00	8.42038E-01	5.98154E 00	6.19254E 00	1.01764E 00	5.96E-08
35	-2.32133E-02	7.59198E-01	1.38671E 00	8.28260E-01	6.02816E 00	6.24081E 00	1.03238E 00	0.
36	-1.78814E-02	7.64590E-01	1.40920E 00	8.14823E-01	6.07509E 00	6.28940E 00	1.04655E 00	2.98E-08
37	-1.20698E-02	7.70161E-01	1.43119E 00	8.01789E-01	6.12236E 00	6.33833E 00	1.06014E 00	-1.19E-07
38	-2.66252E-03	7.75904E-01	1.45269E 00	7.89239E-01	6.17000E 00	6.38765E 00	1.07312E 00	-2.98E-08
39	-1.44450E-03	7.80868E-01	1.47454E 00	7.74784E-01	6.21650E 00	6.43580E 00	1.08701E 00	-2.98E-08
40	-9.34428E-03	7.81960E-01	1.49947E 00	7.49798E-01	6.25674E 00	6.47746E 00	1.10712E 00	-5.96E-08
41	-1.82370E-02	7.83139E-01	1.52404E 00	7.23850E-01	6.29674E 00	6.51887E 00	1.12739E 00	-2.98E-08
42	-2.84395E-02	7.84347E-01	1.54831E 00	6.96634E-01	6.33634E 00	6.55986E 00	1.14800E 00	2.98E-08
43	-4.05340E-02	7.85484E-01	1.57238E 00	6.67605E-01	6.37525E 00	6.60015E 00	1.16928E 00	0.
44	-5.59694E-02	7.86332E-01	1.59645E 00	6.35596E-01	6.41290E 00	6.63912E 00	1.19190E 00	-1.19E-07

THREE POINT SELECTION I= 1 I= 4 I= 10

RHO-0= 4.93571E 00 RHO-1= 4.98376E 00 RHO-2= 5.15547E 00

PHI-1= 2.21988E-01 PHI-2= 4.62733E-01

TABLE VII (Cont'd)

COS(TX)	COS(TY)	COS(TZ)	COS(BX)	COS(BY)	COS(BZ)	COS(NX)	COS(NY)	COS(NZ)
1.0000E 00	0.	0.	0.	9.6593E-01	-2.5882E-01	-0.	2.5882E-01	9.6593E-01
9.8438E-01	-6.7701E-02	1.6252E-01	1.0876E-01	9.5978E-01	-2.5882E-01	-1.3846E-01	2.7245E-01	9.5216E-01
9.6465E-01	-1.0057E-01	2.4359E-01	1.6459E-01	9.5180E-01	-2.5882E-01	-2.0582E-01	2.8976E-01	9.3471E-01
9.4179E-01	-1.2707E-01	3.1127E-01	2.1267E-01	9.4222E-01	-2.5882E-01	-2.6040E-01	3.0995E-01	9.1440E-01
9.1671E-01	-1.4937E-01	3.7061E-01	2.5628E-01	9.3131E-01	-2.5882E-01	-3.0652E-01	3.3224E-01	8.9203E-01
8.9024E-01	-1.6793E-01	4.2341E-01	2.9651E-01	9.1929E-01	-2.5882E-01	-3.4577E-01	3.5595E-01	8.6818E-01
8.6302E-01	-1.8347E-01	4.7068E-01	3.3384E-01	9.0640E-01	-2.5882E-01	-3.7914E-01	3.8050E-01	8.4349E-01
8.3558E-01	-1.9621E-01	5.1314E-01	3.6860E-01	8.9283E-01	-2.5882E-01	-4.0737E-01	4.0541E-01	8.1835E-01
8.0830E-01	-2.0643E-01	5.5139E-01	4.0099E-01	8.7876E-01	-2.5882E-01	-4.3111E-01	4.3030E-01	7.9308E-01
7.8148E-01	-2.1439E-01	5.8594E-01	4.3119E-01	8.6434E-01	-2.5882E-01	-4.5097E-01	4.5491E-01	7.6791E-01
7.5530E-01	-2.2030E-01	6.1725E-01	4.5935E-01	8.4971E-01	-2.5882E-01	-4.6746E-01	4.7902E-01	7.4298E-01
7.2989E-01	-2.2436E-01	6.4569E-01	4.8563E-01	8.3497E-01	-2.5882E-01	-4.8106E-01	5.0247E-01	7.1840E-01
7.0534E-01	-2.2675E-01	6.7162E-01	5.1013E-01	8.2023E-01	-2.5882E-01	-4.9220E-01	5.2517E-01	6.9421E-01
6.8169E-01	-2.2762E-01	6.9534E-01	5.3299E-01	8.0556E-01	-2.5882E-01	-5.0123E-01	5.4704E-01	6.7045E-01
6.5892E-01	-2.2710E-01	7.1711E-01	5.5431E-01	7.9104E-01	-2.5882E-01	-5.0849E-01	5.6815E-01	6.4712E-01
6.3706E-01	-2.2531E-01	7.3715E-01	5.7419E-01	7.7673E-01	-2.5882E-01	-5.1426E-01	5.8815E-01	6.2419E-01
6.1606E-01	-2.2235E-01	7.5566E-01	5.9273E-01	7.6268E-01	-2.5882E-01	-5.1878E-01	6.0735E-01	6.0165E-01
5.9591E-01	-2.1830E-01	7.7281E-01	6.1001E-01	7.4893E-01	-2.5882E-01	-5.2228E-01	6.2565E-01	5.7946E-01
5.7656E-01	-2.1324E-01	7.8874E-01	6.2611E-01	7.3553E-01	-2.5882E-01	-5.2495E-01	6.4306E-01	5.5769E-01
5.5796E-01	-2.0724E-01	8.0358E-01	6.4111E-01	7.2249E-01	-2.5882E-01	-5.2694E-01	6.5959E-01	5.3598E-01
5.4007E-01	-2.0035E-01	8.1742E-01	6.5507E-01	7.0985E-01	-2.5882E-01	-5.2840E-01	6.7525E-01	5.1462E-01
5.2284E-01	-1.9262E-01	8.3038E-01	6.6807E-01	6.9764E-01	-2.5882E-01	-5.2945E-01	6.9007E-01	4.9344E-01
5.0623E-01	-1.8407E-01	8.4252E-01	6.8014E-01	6.8587E-01	-2.5882E-01	-5.3022E-01	7.0406E-01	4.7241E-01
4.9018E-01	-1.7476E-01	8.5392E-01	6.9136E-01	6.7456E-01	-2.5882E-01	-5.3079E-01	7.1724E-01	4.5148E-01
4.7465E-01	-1.6470E-01	8.6463E-01	7.0178E-01	6.6372E-01	-2.5882E-01	-5.3124E-01	7.2962E-01	4.3062E-01
4.5959E-01	-1.5393E-01	8.7469E-01	7.1142E-01	6.5337E-01	-2.5882E-01	-5.3166E-01	7.4123E-01	4.0978E-01
4.4493E-01	-1.4245E-01	8.8416E-01	7.2035E-01	6.4352E-01	-2.5882E-01	-5.3211E-01	7.5206E-01	3.8893E-01
4.3065E-01	-1.3028E-01	8.9307E-01	7.2859E-01	6.3417E-01	-2.5882E-01	-5.3264E-01	7.6214E-01	3.6803E-01
4.1668E-01	-1.1745E-01	9.0143E-01	7.3618E-01	6.2534E-01	-2.5882E-01	-5.3331E-01	7.7146E-01	3.4703E-01
4.0298E-01	-1.0395E-01	9.0929E-01	7.4316E-01	6.1703E-01	-2.5882E-01	-5.3416E-01	7.8004E-01	3.2590E-01
3.8950E-01	-8.9792E-02	9.1664E-01	7.4955E-01	6.0926E-01	-2.5882E-01	-5.3523E-01	7.8787E-01	3.0461E-01
3.7619E-01	-7.4986E-02	9.2350E-01	7.5538E-01	6.0201E-01	-2.5882E-01	-5.3655E-01	7.9496E-01	2.8311E-01
3.6299E-01	-5.9534E-02	9.2989E-01	7.6067E-01	5.9531E-01	-2.5882E-01	-5.3817E-01	8.0128E-01	2.6138E-01
3.4985E-01	-4.3435E-02	9.3580E-01	7.6544E-01	5.8916E-01	-2.5882E-01	-5.4009E-01	8.0685E-01	2.3937E-01
3.3672E-01	-2.6688E-02	9.4123E-01	7.6972E-01	5.8356E-01	-2.5882E-01	-5.4236E-01	8.1163E-01	2.1704E-01
3.2354E-01	-9.2902E-03	9.4617E-01	7.7352E-01	5.7852E-01	-2.5882E-01	-5.4497E-01	8.1561E-01	1.9436E-01
3.1024E-01	8.7647E-03	9.5062E-01	7.7684E-01	5.7404E-01	-2.5882E-01	-5.4797E-01	8.1878E-01	1.7128E-01
2.9676E-01	2.7487E-02	9.5456E-01	7.7971E-01	5.7014E-01	-2.5882E-01	-5.5135E-01	8.2109E-01	1.4776E-01
2.8346E-01	4.6264E-02	9.5787E-01	7.8206E-01	5.6691E-01	-2.5882E-01	-5.5500E-01	8.2248E-01	1.2452E-01
2.7181E-01	6.2894E-02	9.6029E-01	7.8374E-01	5.6459E-01	-2.5882E-01	-5.5845E-01	8.2297E-01	1.0417E-01
2.6006E-01	7.9765E-02	9.6229E-01	7.8510E-01	5.6270E-01	-2.5882E-01	-5.6212E-01	8.2280E-01	8.3713E-02
2.4823E-01	9.6791E-02	9.6385E-01	7.8614E-01	5.6125E-01	-2.5882E-01	-5.6601E-01	8.2197E-01	6.3225E-02
2.3636E-01	1.1382E-01	9.6497E-01	7.8687E-01	5.6022E-01	-2.5882E-01	-5.7006E-01	8.2048E-01	4.2851E-02
2.2464E-01	1.3057E-01	9.6565E-01	7.8730E-01	5.5961E-01	-2.5882E-01	-5.7419E-01	8.1840E-01	2.2912E-02

TABLE VII (Cont'd)

[illegible]	[illegible]	M2P	M2P	M2N	M2T	M2S
[illegible]	[illegible]	1.[illegible]E 00	2.56[illegible]E 00	2.56[illegible]E 00	1.11953E-07	3.21671E 00
1.12[illegible]E-01	[illegible]E-02	1.[illegible]E 00	2.56[illegible]E 00	2.43886E 00	-7.93693E-04	3.11725E 00
1.71[illegible]E-01	1.41[illegible]E-01	1.[illegible]E 00	2.56565E 00	2.32592E 00	-1.09216E 00	3.02562E 00
2.21991E-01	1.43[illegible]E-01	1.92743E 00	2.56878E 00	2.22124E 00	-1.30318E 00	2.94090E 00
[illegible]E-01	2.[illegible]E-01	1.91972E 00	2.57234E 00	2.12401E 00	-1.46775E 00	2.86233E 00
5.12[illegible]E-01	2.[illegible]E-01	1.[illegible]E 00	2.57625E 00	2.03350E 00	-1.60227E 00	2.78926E 00
3.52[illegible]E-01	2.47745E-01	1.89985E 00	2.58046E 00	1.94909E 00	-1.71541E 00	2.72114E 00
3.91527E-01	3.17699E-01	1.88803E 00	2.58488E 00	1.87021E 00	-1.81242E 00	2.65751E 00
4.[illegible]E-01	3.66615E-01	1.87680E 00	2.58947E 00	1.79638E 00	-1.89680E 00	2.59795E 00
4.62[illegible]E-01	3.71645E-01	1.86530E 00	2.59418E 00	1.72715E 00	-1.97100E 00	2.54212E 00
4.95598E-01	3.05922E-01	1.85362E 00	2.59895E 00	1.66213E 00	-2.03681E 00	2.48970E 00
5.29[illegible]E-01	4.18568E-01	1.84187E 00	2.60375E 00	1.60099E 00	-2.09561E 00	2.44042E 00
5.63[illegible]E-01	4.34691E-01	1.83010E 00	2.60856E 00	1.54340E 00	-2.14845E 00	2.39402E 00
5.[illegible]E-01	4.59393E-01	1.81840E 00	2.61335E 00	1.48908E 00	-2.19619E 00	2.35031E 00
6.11[illegible]E-01	4.77769E-01	1.80682E 00	2.61808E 00	1.43778E 00	-2.23951E 00	2.30907E 00
6.[illegible]E-01	4.94905E-01	1.79540E 00	2.62275E 00	1.38927E 00	-2.27896E 00	2.27014E 00
[illegible]	5.[illegible]E-01	1.78419E 00	2.62733E 00	1.34335E 00	-2.31502E 00	2.23336E 00
6.93527E-01	5.25775E-01	1.77322E 00	2.63182E 00	1.29982E 00	-2.34806E 00	2.19860E 00
7.[illegible]E-01	5.[illegible]E-01	1.76252E 00	2.63619E 00	1.25852E 00	-2.37841E 00	2.16577E 00
7.35[illegible]E-01	5.52581E-01	1.75212E 00	2.64044E 00	1.21929E 00	-2.40637E 00	2.13466E 00
7.[illegible]	5.[illegible]E-01	1.74204E 00	2.64456E 00	1.18199E 00	-2.43216E 00	2.10519E 00
7.[illegible]	5.[illegible]E-01	1.73230E 00	2.64854E 00	1.14650E 00	-2.45590E 00	2.07733E 00
7.81[illegible]E-01	5.[illegible]E-01	1.72291E 00	2.65238E 00	1.11269E 00	-2.47805E 00	2.05097E 00
7.97[illegible]E-01	5.95896E-01	1.71388E 00	2.65607E 00	1.08046E 00	-2.49848E 00	2.02603E 00
[illegible]	[illegible]E-01	1.70524E 00	2.65961E 00	1.04971E 00	-2.51744E 00	2.00243E 00
[illegible]	[illegible]E-01	1.69[illegible]E 00	2.66298E 00	1.02035E 00	-2.53503E 00	1.98011E 00
8.[illegible]E-01	6.21[illegible]E-01	1.68[illegible]E 00	2.66620E 00	9.92298E-01	-2.55136E 00	1.95902E 00
8.56[illegible]E-01	6.27479E-01	1.68166E 00	2.66924E 00	9.65478E-01	-2.56653E 00	1.93911E 00
[illegible]	[illegible]E-01	1.67462E 00	2.67212E 00	9.39820E-01	-2.58062E 00	1.92031E 00
[illegible]E-01	6.43537E-01	1.66779E 00	2.67483E 00	9.15259E-01	-2.59371E 00	1.90260E 00
8.[illegible]E-01	6.46044E-01	1.66178E 00	2.67737E 00	8.91738E-01	-2.60586E 00	1.88593E 00
8.97[illegible]E-01	6.51069E-01	1.65601E 00	2.67973E 00	8.69202E-01	-2.61712E 00	1.87026E 00
9.[illegible]E-01	6.55623E-01	1.65056E 00	2.68192E 00	8.47602E-01	-2.62757E 00	1.85556E 00
9.14[illegible]E-01	6.59749E-01	1.64575E 00	2.68392E 00	8.26892E-01	-2.63723E 00	1.84181E 00
9.[illegible]E-01	6.63432E-01	1.64128E 00	2.68575E 00	8.07033E-01	-2.64615E 00	1.82897E 00
9.29[illegible]E-01	6.66703E-01	1.63726E 00	2.68739E 00	7.87985E-01	-2.65437E 00	1.81702E 00
9.44[illegible]E-01	6.69571E-01	1.63369E 00	2.68885E 00	7.69715E-01	-2.66192E 00	1.80594E 00
9.59[illegible]E-01	6.72[illegible]E-01	1.63058E 00	2.69013E 00	7.52193E-01	-2.66883E 00	1.79571E 00
9.43556E-01	6.74069E-01	1.62800E 00	2.69118E 00	7.35429E-01	-2.67506E 00	1.78641E 00
9.46529E-01	6.75519E-01	1.62615E 00	2.69194E 00	7.19481E-01	-2.68052E 00	1.77820E 00
9.48036E-01	6.76[illegible]E-01	1.62464E 00	2.69255E 00	7.04149E-01	-2.68550E 00	1.77067E 00
9.50794E-01	6.77584E-01	1.62348E 00	2.69303E 00	6.89410E-01	-2.69002E 00	1.76380E 00
9.52088E-01	6.78213E-01	1.62266E 00	2.69336E 00	6.75242E-01	-2.69411E 00	1.75755E 00
9.52861E-01	6.77587E-01	1.62218E 00	2.69356E 00	6.61622E-01	-2.69778E 00	1.75191E 00

TABLE VII (Cont'd)

P4/P2	A4/A2	M4CN	THETA-4	S4	M4T	M4N
2.14480E 00	1.12231E 00	2.68036E 00	4.52907E-01	1.60617E-02	9.97524E-08	2.38322E 00
2.14966E 00	1.12274E 00	2.58366E 00	4.69025E-01	1.61181E-02	-7.06925E-01	2.29529E 00
2.15291E 00	1.12302E 00	2.49461E 00	4.84801E-01	1.61560E-02	-9.72515E-01	2.20963E 00
2.15491E 00	1.12320E 00	2.41225E 00	5.00271E-01	1.61792E-02	-1.16024E 00	2.12679E 00
2.15594E 00	1.12329E 00	2.33577E 00	5.15466E-01	1.61913E-02	-1.30665E 00	2.04704E 00
2.15624E 00	1.12332E 00	2.26452E 00	5.30411E-01	1.61948E-02	-1.42637E 00	1.97049E 00
2.15600E 00	1.12330E 00	2.19794E 00	5.45125E-01	1.61921E-02	-1.52712E 00	1.89717E 00
2.15539E 00	1.12324E 00	2.13555E 00	5.59628E-01	1.61849E-02	-1.61356E 00	1.82701E 00
2.15453E 00	1.12317E 00	2.07696E 00	5.73934E-01	1.61749E-02	-1.68880E 00	1.75993E 00
2.15354E 00	1.12308E 00	2.02181E 00	5.88056E-01	1.61633E-02	-1.75499E 00	1.69583E 00
2.15249E 00	1.12299E 00	1.96978E 00	6.02007E-01	1.61511E-02	-1.81374E 00	1.63457E 00
2.15148E 00	1.12290E 00	1.92061E 00	6.15795E-01	1.61393E-02	-1.86625E 00	1.57603E 00
2.15056E 00	1.12282E 00	1.87405E 00	6.29429E-01	1.61285E-02	-1.91345E 00	1.52009E 00
2.14978E 00	1.12275E 00	1.82991E 00	6.42917E-01	1.61195E-02	-1.95609E 00	1.46661E 00
2.14 9 E 00	1.12270E 00	1.78799E 00	6.56266E-01	1.61127E-02	-1.99476E 00	1.41549E 00
2.14884E 00	1.12267E 00	1.74812E 00	6.69481E-01	1.61086E-02	-2.02995E 00	1.36659E 00
2.14876E 00	1.12266E 00	1.71015E 00	6.82567E-01	1.61076E-02	-2.06208E 00	1.31991E 00
2.14897E 00	1.12268E 00	1.67395E 00	6.95527E-01	1.61101E-02	-2.09148E 00	1.27505E 00
2.14950E 00	1.12273E 00	1.63940E 00	7.08364E-01	1.61163E-02	-2.11843E 00	1.23270E 00
2.15039E 00	1.12280E 00	1.60638E 00	7.21082E-01	1.61265E-02	-2.14318E 00	1.19117E 00
2.15163E 00	1.12291E 00	1.57481E 00	7.33681E-01	1.61411E-02	-2.16594E 00	1.15188E 00
2.15327E 00	1.12306E 00	1.54459E 00	7.46162E-01	1.61601E-02	-2.18688E 00	1.11424E 00
2.15530E 00	1.12323E 00	1.51564E 00	7.58526E-01	1.61839E-02	-2.20617E 00	1.07817E 00
2.15776E 00	1.12345E 00	1.48788E 00	7.70771E-01	1.62126E-02	-2.22394E 00	1.04361E 00
2.16064E 00	1.12370E 00	1.46125E 00	7.82898E-01	1.62464E-02	-2.24031E 00	1.01049E 00
2.16397E 00	1.12399E 00	1.43569E 00	7.94913E-01	1.62854E-02	-2.25538E 00	9.78735E-01
2.16776E 00	1.12432E 00	1.41115E 00	8.06783E-01	1.63300E-02	-2.26924E 00	9.48301E-01
2.17201E 00	1.12469E 00	1.38757E 00	8.18536E-01	1.63802E-02	-2.28198E 00	9.19131E-01
2.17674E 00	1.12511E 00	1.36491E 00	8.30156E-01	1.64361E-02	-2.29367E 00	8.91176E-01
2.18194E 00	1.12556E 00	1.34313E 00	8.41638E-01	1.64980E-02	-2.30437E 00	8.64392E-01
2.18764E 00	1.12606E 00	1.32219E 00	8.52974E-01	1.65659E-02	-2.31414E 00	8.38740E-01
2.19383E 00	1.12659E 00	1.30206E 00	8.64157E-01	1.66400E-02	-2.32304E 00	8.14185E-01
2.20052E 00	1.12718E 00	1.28272E 00	8.75177E-01	1.67204E-02	-2.33111E 00	7.90696E-01
2.20770E 00	1.12780E 00	1.26414E 00	8.86023E-01	1.68071E-02	-2.33839E 00	7.68248E-01
2.21537E 00	1.12846E 00	1.24631E 00	8.96681E-01	1.69003E-02	-2.34491E 00	7.46824E-01
2.22353E 00	1.12917E 00	1.22920E 00	9.07136E-01	1.69998E-02	-2.35073E 00	7.26410E-01
2.23216E 00	1.12991E 00	1.21281E 00	9.17370E-01	1.71057E-02	-2.35586E 00	7.07005E-01
2.24125E 00	1.13069E 00	1.19714E 00	9.27359E-01	1.72178E-02	-2.36034E 00	6.88617E-01
2.25076E 00	1.13151E 00	1.18229E 00	9.37012E-01	1.73358E-02	-2.36415E 00	6.70072E-01
2.26062E 00	1.13236E 00	1.16852E 00	9.46131E-01	1.74589E-02	-2.36720E 00	6.47219E-01
2.27082E 00	1.13323E 00	1.15535E 00	9.55007E-01	1.75370E-02	-2.36977E 00	6.24638E-01
2.28132E 00	1.13413E 00	1.14276E 00	9.63622E-01	1.77197E-02	-2.37188E 00	6.02165E-01
2.29209E 00	1.13505E 00	1.13077E 00	9.71962E-01	1.78567E-02	-2.37356E 00	5.79520E-01
2.30310E 00	1.13599E 00	1.11935E 00	9.80014E-01	1.79977E-02	-2.37483E 00	5.56120E-01

TABLE VII (Cont'd)

M4B	M4TB	M4NB	M4BB	DELTA-4	M4KN
1.22[illegible]E 00	4.42776E-09	2.63964E 00	-4.65439E-01	1.74533E-01	2.68036E 00
1.18615E 00	4.72289E-01	2.58836E 00	-5.04252E-01	1.92405E-01	2.63702E 00
1.15786E 00	7.06681E-01	2.52795E 00	-5.28189E-01	2.05977E-01	2.58254E 00
1.13930E 00	9.05471E-01	2.46018E 00	-5.41069E-01	2.16484E-01	2.51897E 00
1.12492E 00	1.09370E 00	2.38692E 00	-5.45755E-01	2.24781E-01	2.44851E 00
1.11589E 00	1.23717E 00	2.30989E 00	-5.44398E-01	2.31457E-01	2.37318E 00
1.10981E 00	1.37746E 00	2.23058E 00	-5.38615E-01	2.36933E-01	2.29469E 00
1.10573E 00	1.50347E 00	2.15017E 00	-5.29627E-01	2.41510E-01	2.21444E 00
1.10291E 00	1.61678E 00	2.06957E 00	-5.18357E-01	2.45417E-01	2.13350E 00
1.10095E 00	1.71882E 00	1.98943E 00	-5.05502E-01	2.48828E-01	2.05265E 00
1.09913E 00	1.81084E 00	1.91021E 00	-4.91592E-01	2.51884E-01	1.97245E 00
1.09766E 00	1.89397E 00	1.83219E 00	-4.77029E-01	2.54706E-01	1.89327E 00
1.09660E 00	1.96924E 00	1.75554E 00	-4.62120E-01	2.57397E-01	1.81534E 00
1.09436E 00	2.03751E 00	1.68032E 00	-4.47096E-01	2.60053E-01	1.73878E 00
1.09238E 00	2.09958E 00	1.60654E 00	-4.32136E-01	2.62766E-01	1.66365E 00
1.09011E 00	2.15611E 00	1.53415E 00	-4.17371E-01	2.65625E-01	1.58991E 00
1.08752E 00	2.20769E 00	1.46307E 00	-4.02906E-01	2.68722E-01	1.51754E 00
1.08462E 00	2.25482E 00	1.39320E 00	-3.88814E-01	2.72156E-01	1.44644E 00
1.08136E 00	2.29795E 00	1.32441E 00	-3.75153E-01	2.76030E-01	1.37652E 00
1.07776E 00	2.33745E 00	1.25658E 00	-3.61966E-01	2.80464E-01	1.30767E 00
1.07387E 00	2.37356E 00	1.18958E 00	-3.49283E-01	2.85592E-01	1.23980E 00
1.06968E 00	2.40682E 00	1.12329E 00	-3.37126E-01	2.91570E-01	1.17279E 00
1.06522E 00	2.43720E 00	1.05757E 00	-3.25510E-01	2.98589E-01	1.10653E 00
1.06052E 00	2.46499E 00	9.92298E-01	-3.14447E-01	3.06877E-01	1.04093E 00
1.05554E 00	2.49035E 00	9.27356E-01	-3.03943E-01	3.16719E-01	9.75894E-01
1.05033E 00	2.51344E 00	8.62626E-01	-2.94003E-01	3.28476E-01	9.11351E-01
1.04502E 00	2.53436E 00	7.97998E-01	-2.84629E-01	3.42613E-01	8.47240E-01
1.03949E 00	2.55321E 00	7.33366E-01	-2.75825E-01	3.59742E-01	7.83521E-01
1.03382E 00	2.57006E 00	6.68628E-01	-2.67591E-01	3.80686E-01	7.20186E-01
1.02802E 00	2.58499E 00	6.03688E-01	-2.59928E-01	4.06577E-01	6.57269E-01
1.02211E 00	2.59800E 00	5.38457E-01	-2.52841E-01	4.39005E-01	5.94865E-01
1.01611E 00	2.60914E 00	4.72846E-01	-2.46333E-01	4.80274E-01	5.33163E-01
1.01004E 00	2.61843E 00	4.06772E-01	-2.40410E-01	5.33789E-01	4.72505E-01
1.00392E 00	2.62586E 00	3.40157E-01	-2.35081E-01	6.04725E-01	4.13485E-01
9.97763E-01	2.63142E 00	2.72920E-01	-2.30358E-01	7.01029E-01	3.57142E-01
9.91592E-01	2.63508E 00	2.04987E-01	-2.26258E-01	8.34683E-01	3.05307E-01
9.85418E-01	2.63681E 00	1.36277E-01	-2.22806E-01	1.02186E 00	2.61178E-01
9.79259E-01	2.63657E 00	6.67058E-02	-2.20035E-01	1.27644E 00	2.29924E-01
9.74072E-01	2.63441E 00	-1.43059E-03	-2.16545E-01	1.56419E 00	2.16549E-01
9.72910E-01	2.63106E 00	-6.01896E-02	-2.07425E-01	1.28835E 00	2.15962E-01
9.71935E-01	2.62625E 00	-1.19018E-01	-1.98231E-01	1.03008E 00	2.31216E-01
9.71240E-01	2.62002E 00	-1.77686E-01	-1.88850E-01	8.15840E-01	2.59301E-01
9.70975E-01	2.61243E 00	-2.35787E-01	-1.78963E-01	6.49240E-01	2.96012E-01
9.71428E-01	2.60366E 00	-2.92451E-01	-1.67933E-01	5.21252E-01	3.37237E-01

MACH REFLECTION

TABLE VII (Cont'd)

THETAP-6	P6/P4	A6/A4	M6N	M6T	M6	P6/P-INF	SIG4A-6	S6
3.4917E-01	1.9295E 00	1.1036E 00	2.2396E 00	4.0145E-09	2.2396E 00	1.1588E 01	0.	2.0158E-02
3.5545E-01	2.0343E 00	1.1125E 00	2.1584E 00	4.2273E-01	2.1994E 00	1.2244E 01	-2.1795E-02	2.1275E-02
3.6475E-01	2.1044E 00	1.1187E 00	2.0793E 00	6.3167E-01	2.1732E 00	1.2685E 01	-2.8174E-02	2.2080E-02
3.7680E-01	2.1673E 00	1.1225E 00	2.0009E 00	8.0663E-01	2.1574E 00	1.2956E 01	-3.0544E-02	2.2594E-02
3.9145E-01	2.1697E 00	1.1245E 00	1.9223E 00	9.6106E-01	2.1492E 00	1.3098E 01	-3.0273E-02	2.2968E-02
4.0862E-01	2.1772E 00	1.1251E 00	1.8435E 00	1.0996E 00	2.1465E 00	1.3145E 01	-2.8061E-02	2.2960E-02
4.2837E-01	2.1742E 00	1.1249E 00	1.7643E 00	1.2245E 00	2.1476E 00	1.3125E 01	-2.4350E-02	2.2922E-02
4.5081E-01	2.1644E 00	1.1240E 00	1.6848E 00	1.3376E 00	2.1512E 00	1.3063E 01	-1.9421E-02	2.2800E-02
4.7622E-01	2.1509E 00	1.1228E 00	1.6050E 00	1.4399E 00	2.1563E 00	1.2975E 01	-1.3429E-02	2.2631E-02
5.0501E-01	2.1361E 00	1.1215E 00	1.5247E 00	1.5325E 00	2.1618E 00	1.2880E 01	-6.4144E-03	2.2448E-02
5.3786E-01	2.1226E 00	1.1204E 00	1.4433E 00	1.6163E 00	2.1669E 00	1.2793E 01	1.7087E-03	2.2281E-02
5.7591E-01	2.1131E 00	1.1195E 00	1.3599E 00	1.6918E 00	2.1706E 00	1.2730E 01	1.1203E-02	2.2162E-02
6.2117E-01	2.1118E 00	1.1194E 00	1.2728E 00	1.7592E 00	2.1714E 00	1.2716E 01	2.2653E-02	2.2136E-02
6.7789E-01	2.1207E 00	1.1207E 00	1.1781E 00	1.8180E 00	2.1664E 00	1.2801E 01	3.7443E-02	2.2297E-02
7.5941E-01	2.1841E 00	1.1258E 00	1.0627E 00	1.8650E 00	2.1466E 00	1.3144E 01	6.0320E-02	2.2960E-02

TABLE VII (Cont'd)

CHARACTERISTICS PROGRAM

GAMMA= 1.400 P/P=11.588

I	J	NU	PSI	THETA	S	M	MU	M
1	1	[illegible]	5.11219E-01	6.03204E-02	2.29605E-02	2.14655E 00	4.84611E-01	6.92519E-01
[illegible]	[illegible]	[illegible]	[illegible]	3.74431E-02	2.22966E-02	2.16038E 00	4.79798E-01	6.95826E-01
[illegible]	[illegible]	[illegible]	[illegible]	2.26533E-02	2.21364E-02	2.17135E 00	4.78566E-01	6.96649E-01
4	4	[illegible]	[illegible]	1.12031E-02	2.21618E-02	2.17057E 00	4.78793E-01	6.96520E-01
5	5	[illegible]	4.95598E-01	1.70867E-03	2.22809E-02	2.16689E 00	4.79675E-01	6.95911E-01
[illegible]	[illegible]	[illegible]	[illegible]	-6.41440E-03	2.24479E-02	2.16178E 00	4.80906E-01	6.95063E-01
7	7	[illegible]	[illegible]	-1.34287E-02	2.26308E-02	2.15625E 00	4.82243E-01	6.94143E-01
[illegible]	[illegible]	[illegible]	3.91527E-01	-1.94208E-02	2.27998E-02	2.15122E 00	4.83469E-01	6.93301E-01
[illegible]	[illegible]	[illegible]	3.52901E-01	-2.43497E-02	2.29223E-02	2.14760E 00	4.84353E-01	6.92696E-01
[illegible]	1	[illegible]	[illegible]	-2.80607E-02	2.29603E-02	2.14649E 00	4.84626E-01	6.92509E-01
11	11	[illegible]	2.48541E-01	-3.02727E-02	2.28684E-02	2.14919E 00	4.83964E-01	6.92962E-01
[illegible]	[illegible]	[illegible]	2.21991E-01	-3.05443E-02	2.25937E-02	2.15737E 00	4.81972E-01	6.94329E-01
13	13	[illegible]	1.71233E-01	-2.81738E-02	2.20796E-02	2.17317E 00	4.78172E-01	6.96949E-01
14	14	[illegible]	1.13424E-01	-2.17650E-02	2.12755E-02	2.19938E 00	4.72017E-01	7.01233E-01
[illegible]	[illegible]	[illegible]	0.	0.	2.01581E-02	2.23960E 00	4.62860E-01	7.07604E-01

TABLE VII (Cont'd)

I= 14 P/P-INF= 1.31958E 01

J	RHO	PSI	THETA	S	MU	W
14	4.94799E 00	1.12836E-01	-2.17950E-02	2.12755E-02	4.72007E-01	7.01233E-01
15	5.05160E 00	5.72039E-02	-1.88131E-02	2.07406E-02	4.72981E-01	7.00553E-01
16	5.15964E 00	0.	0.	2.01581E-02	4.82170E-01	6.94193E-01

TABLE VII (Cont'd)

I= 13 P/P-INF= 1.39602E 01

J	RHO	PSI	THETA	S	MU	W
13	4.96414E 00	1.71233E-01	-2.81738E-02	2.20796E-02	4.78172E-01	6.96949E-01
14	5.01300E 00	1.44115E-01	-3.01225E-02	2.17274E-02	4.76781E-01	6.97912E-01
15	5.11461E 00	9.78293E-02	-2.71360E-02	2.11111E-02	4.77682E-01	6.97288E-01
16	5.21887E 00	3.08672E-02	-8.31418E-03	2.05020E-02	4.86976E-01	6.90903E-01
17	5.27630E 00	0.	0.	2.01581E-02	4.91079E-01	6.88114E-01

TABLE VII (Cont'd)

I= 12 P/P-INF= 1.43652E 01

J	RHO	PSI	THETA	S	MU	W
12	4.93375E 00	2.21991E-01	-3.05443E-02	2.25937E-02	4.81972E-01	6.94329E-01
13	5.02328E 00	1.99740E-01	-3.24435E-02	2.23832E-02	4.80740E-01	6.95177E-01
14	5.07196E 00	1.72299E-01	-3.43975E-02	2.20803E-02	4.79390E-01	6.96178E-01
15	5.17242E 00	1.15732E-01	-3.14083E-02	2.14573E-02	4.80299E-01	6.95487E-01
16	5.27389E 00	5.03694E-02	-1.25746E-02	2.08359E-02	4.89646E-01	6.89086E-01
17	5.33024E 00	2.86986E-02	-4.25226E-03	2.04890E-02	4.93779E-01	6.86289E-01
18	5.34295E 00	0.	0.	2.01581E-02	4.95741E-01	6.84969E-01

TABLE VII (Cont'd)

I= 11 P/P-INF= 1.45052E 01

J	RHO	PSI	THETA	S	MU	W
11	5.[illegible]	2.68541E-01	-3.02727E-02	2.28684E-02	4.83964E-01	6.92962E-01
12	5.04034E 00	2.49425E-01	-3.20057E-02	2.27633E-02	4.82930E-01	6.93671E-01
13	5.07995E 00	2.26977E-01	-3.39110E-02	2.26035E-02	4.81749E-01	6.94483E-01
14	5.12869E 00	1.99329E-01	-3.58591E-02	2.23566E-02	4.80455E-01	6.95373E-01
15	5.[illegible]	1.42765E-01	-3.28635E-02	2.17737E-02	4.81401E-01	6.94722E-01
16	5.[illegible]	8.72547E-02	-1.40346E-02	2.11640E-02	4.90803E-01	6.88301E-01
17	5.[illegible]	5.69255E-02	+5.71483E-03	2.08190E-02	4.94954E-01	6.85497E-01
18	5.43541E 00	2.83507E-02	-1.45115E-03	2.04887E-02	4.96924E-01	6.84173E-01
19	5.44752E 00	0.	0.	2.01581E-02	4.97343E-01	6.83892E-01

TABLE VII (Cont'd)

I= 10 P/P-INF= 1.44486E 01

J	RHO	PSI	THETA	S	MU	W
10	5.03199E 00	3.12005E-01	2.80607E-02	2.29603E-02	4.84626E-01	6.92509E-01
11	5.06151E 00	2.95374E-01	-2.96936E-02	2.29275E-02	4.83721E-01	6.93128E-01
12	5.09556E 00	2.76155E-01	-3.14267E-02	2.28636E-02	4.82732E-01	6.93807E-01
13	5.13540E 00	2.53632E-01	-3.33322E-02	2.27526E-02	4.81604E-01	6.94582E-01
14	5.18439E 00	2.25836E-01	-3.52806E-02	2.25635E-02	4.80374E-01	6.95429E-01
15	5.23409E 00	1.69506E-01	-3.22838E-02	2.20502E-02	4.81395E-01	6.94726E-01
16	5.39166E 00	1.15059E-01	-1.34519E-02	2.14772E-02	4.90840E-01	6.88276E-01
17	5.43608E 00	8.51736E-02	-5.13028E-03	2.11433E-02	4.95006E-01	6.85462E-01
18	5.49806E 00	5.48405E-02	-8.65683E-04	2.08181E-02	4.96982E-01	6.84134E-01
19	5.54016E 00	2.85613E-02	5.85683E-04	2.04997E-02	4.97404E-01	6.83951E-01
20	5.59285E 00	0.	0.	2.01581E-02	4.96696E-01	6.84326E-01

TABLE VII (Cont'd)

I= 9 P/P-INF= 1.42493E 01

J	RHO	PSI	THETA	S	MU	W
9	5.[illegible]E 00	3.62901E-01	-2.43497E-02	2.29223E-02	4.86353E-01	6.92696E-01
10	5.08578E 00	3.39457E-01	-2.59877E-02	2.29349E-02	4.83496E-01	6.93283E-01
11	5.11558E 00	3.21705E-01	-2.76206E-02	2.29322E-02	4.82627E-01	6.93879E-01
12	5.14394E 00	3.02544E-01	-2.93538E-02	2.29051E-02	4.81682E-01	6.94529E-01
13	5.17013E 00	2.79938E-01	-3.12595E-02	2.28393E-02	4.80606E-01	6.95269E-01
14	5.23951E 00	2.52217E-01	-3.32084E-02	2.27066E-02	4.79439E-01	6.96074E-01
15	5.33932E 00	1.96166E-01	-3.02179E-02	2.22795E-02	4.80551E-01	6.95307E-01
16	5.43541E 00	1.42907E-01	-1.13773E-02	2.17640E-02	4.90039E-01	6.88820E-01
17	5.43922E 00	1.13559E-01	-3.05427E-03	2.14517E-02	4.94220E-01	6.85992E-01
18	5.54099E 00	8.55325E-02	1.21094E-03	2.11389E-02	4.96206E-01	6.84655E-01
19	5.59314E 00	5.74137E-02	2.66207E-03	2.08174E-02	4.96635E-01	6.84367E-01
20	5.64609E 00	2.89053E-02	2.07572E-03	2.04890E-02	4.95932E-01	6.84839E-01
21	5.69975E 00	0.	0.	2.01581E-02	4.94410E-01	6.85863E-01

TABLE VII (Cont'd)

I= 8 P/P-INF= 1.39492E 01

J	<HU	PSI	THETA	S	MU	W
9	5.11260E 00	3.79357E-01	-2.11801E-02	2.28372E-02	4.82577E-01	6.93913E-01
10	5.13873E 00	3.64606E-01	-2.28180E-02	2.28700E-02	4.81747E-01	6.94484E-01
11	5.16893E 00	3.47946E-01	-2.44530E-02	2.28928E-02	4.80911E-01	6.95059E-01
12	5.21367E 00	3.28734E-01	-2.61840E-02	2.28977E-02	4.80004E-01	6.95684E-01
13	5.24429E 00	3.06162E-01	-2.80838E-02	2.28723E-02	4.78978E-01	6.96392E-01
14	5.27418E 00	2.78423E-01	-3.00391E-02	2.27920E-02	4.77873E-01	6.97156E-01
15	5.30431E 00	2.48078E-01	-2.70432E-02	2.24580E-02	4.79079E-01	6.96322E-01
16	5.33499E 00	2.17911E-01	-9.20662E-03	2.20148E-02	4.88607E-01	6.97093E-01
17	5.36242E 00	1.87237E-01	1.17329E-04	2.17335E-02	4.92805E-01	6.86945L-01
18	5.39039E 00	1.56416E-01	4.38256E-03	2.14412E-02	4.94803E-01	6.85596E-01
19	5.41639E 00	8.63162E-02	5.83347E-03	2.11332E-02	4.95251E-01	6.85297E-01
20	5.44071E 00	5.91206E-02	5.24620E-03	2.08129E-02	4.94541E-01	6.85726E-01
21	5.47538E 00	2.92492E-02	3.16917E-03	2.04859E-02	4.93050E-01	6.86781E-01
22	5.80867E 00	0.	0.	2.01581E-02	4.90952E-01	6.89200E-01

TABLE VII (Cont'd)

I= 7 P/P-INF= 1.35796E 01

J	RHO	PSI	THETA	S	MU	W
7	5.12148E 00	4.28087E-01	-1.34287E-02	2.26308E-02	4.82243E-01	6.94143E-01
8	5.11158E 00	4.17423E-01	-1.54416E-02	2.26780E-02	4.81232E-01	6.94838E-01
9	5.10457E 00	4.04951E-01	-1.72006E-02	2.27274E-02	4.80359E-01	6.95439E-01
10	5.09111E 00	3.90517E-01	-1.88392E-02	2.27760E-02	4.79551E-01	6.95996E-01
11	5.07154E 00	3.73349E-01	-2.04708E-02	2.28194E-02	4.78742E-01	6.96555E-01
12	5.05252E 00	3.54637E-01	-2.22039E-02	2.28510E-02	4.77871E-01	6.97158E-01
13	5.03794E 00	3.32195E-01	-2.41097E-02	2.28604E-02	4.76887E-01	6.97838E-01
14	5.03840E 00	3.04534E-01	-2.60591E-02	2.28269E-02	4.75839E-01	6.98565E-01
15	5.04405E 00	2.67435E-01	-2.81639E-02	2.25861E-02	4.77138E-01	6.97665E-01
16	5.05428E 00	1.98309E-01	-4.22616E-03	2.22241E-02	4.86699E-01	6.91092E-01
17	5.05354E 00	1.72477E-01	4.09842E-03	2.19798E-02	4.90917E-01	6.88224E-01
18	5.04715E 00	1.43431E-01	8.36377E-03	2.17159E-02	4.92941E-01	6.86855E-01
19	5.03971E 00	1.15795E-01	9.81338E-03	2.14284E-02	4.93406E-01	6.86541E-01
20	5.03344E 00	8.75591E-02	9.22565E-03	2.11223E-02	4.92736E-01	6.86993E-01
21	5.03827E 00	5.87591E-02	7.14715E-03	2.08041E-02	4.91243E-01	6.88003E-01
22	5.03378E 00	2.95413E-02	3.97622E-03	2.04805E-02	4.89161E-01	6.89416E-01
23	5.01372E 00	0.	0.	2.01581E-02	4.86663E-01	6.91117E-01

TABLE VII (Cont'd)

I= 6 P/P-INF= 1.31634E 01

J	RHO	PSI	THETA	S	MU	W
6	5.15547E 00	4.62734E-01	-6.41440E-03	2.24479E-02	4.80906E-01	6.95063E-01
7	5.17241E 00	4.53743E-01	-8.84235E-03	2.24942E-02	4.79680E-01	6.95908E-01
8	5.19247E 00	4.43069E-01	-1.08545E-02	2.25465E-02	4.78681E-01	6.96597E-01
9	5.21582E 00	4.30613E-01	-1.26132E-02	2.26036E-02	4.77823E-01	6.97190E-01
10	5.24275E 00	4.16216E-01	-1.42505E-02	2.26632E-02	4.77034E-01	6.97737E-01
11	5.27370E 00	3.99640E-01	-1.58828E-02	2.27220E-02	4.76247E-01	6.98282E-01
12	5.30936E 00	3.80505E-01	-1.76156E-02	2.27747E-02	4.75404E-01	6.98867E-01
13	5.35102E 00	3.58093E-01	-1.95212E-02	2.28127E-02	4.74458E-01	6.99525E-01
14	5.40212E 00	3.30545E-01	-2.14707E-02	2.28197E-02	4.73460E-01	7.00219E-01
15	5.50333E 00	2.76026E-01	-1.84820E-02	2.26669E-02	4.74842E-01	6.99258E-01
16	5.59593E 00	2.26788E-01	3.62310E-04	2.23860E-02	4.84427E-01	6.92645E-01
17	5.64844E 00	1.99314E-01	8.68729E-03	2.21851E-02	4.88665E-01	6.89753E-01
18	5.70007E 00	1.72509E-01	1.29525E-02	2.19553E-02	4.90714E-01	6.88362E-01
19	5.75293E 00	1.45173E-01	1.44020E-02	2.16949E-02	4.91207E-01	6.88027E-01
20	5.80721E 00	1.17134E-01	1.38126E-02	2.14094E-02	4.90565E-01	6.88463E-01
21	5.86268E 00	8.84639E-02	1.17325E-02	2.11057E-02	4.89098E-01	6.89458E-01
[illegible]	5.91899E 00	5.92974E-02	8.55976E-03	2.07914E-02	4.87040E-01	6.90859E-01
[illegible]	5.97581E 00	2.97699E-02	4.58150E-03	2.04734E-02	4.84563E-01	6.92552E-01
[illegible]	6.03287E 00	0.	0.	2.01581E-02	4.81789E-01	6.94456E-01

TABLE VII (Cont'd)

I= 5 P/P-INF= 1.271 E 01

J	RHO	PSI	THETA	S	MU	W
6	5.18052E 00	4.95598E-01	1.70857E-03	2.22809E-02	4.79675E-01	6.95911E-01
5	5.20484E 00	4.88154E-01	-1.35263E-03	2.23184E-02	4.78112E-01	6.96990E-01
7	5.22917E 00	4.79142E-01	-3.77985E-03	2.23639E-02	4.76895E-01	6.97833E-01
8	5.24260E 00	4.68472E-01	-5.79192E-03	2.24170E-02	4.75906E-01	6.98519E-01
9	5.26634E 00	4.56047E-01	-7.55023E-03	2.24769E-02	4.75058E-01	6.99108E-01
10	5.29369E 00	4.41703E-01	-9.18708E-03	2.25423E-02	4.74281E-01	6.99648E-01
11	5.32509E 00	4.25199E-01	-1.08190E-02	2.26108E-02	4.73511E-01	7.00184E-01
12	5.36126E 00	4.06151E-01	-1.25514E-02	2.26786E-02	4.72691E-01	7.00756E-01
13	5.40351E 00	3.83845E-01	-1.44557E-02	2.27388E-02	4.71776E-01	7.01394E-01
14	5.45529E 00	3.56441E-01	-1.64060E-02	2.27791E-02	4.70820E-01	7.02062E-01
15	5.55719E 00	3.02553E-01	-1.34178E-02	2.27054E-02	4.72274E-01	7.01047E-01
16	5.64881E 00	2.54728E-01	5.42672E-03	2.25040E-02	4.81870E-01	6.94399E-01
17	5.72109E 00	2.27931E-01	1.37519E-02	2.23466E-02	4.86174E-01	6.91484E-01
18	5.75268E 00	2.01592E-01	1.80169E-02	2.21549E-02	4.88200E-01	6.90069E-01
19	5.80589E 00	1.74583E-01	1.94657E-02	2.19270E-02	4.88727E-01	6.89711E-01
20	5.86074E 00	1.46773E-01	1.88751E-02	2.16677E-02	4.88119E-01	6.90124E-01
21	5.91694E 00	1.18257E-01	1.67935E-02	2.13843E-02	4.86686E-01	6.91101E-01
22	5.97410E 00	8.91869E-02	1.36182E-02	2.10846E-02	4.84659E-01	6.92486E-01
23	6.03187E 00	5.97087E-02	9.63856E-03	2.07759E-02	4.82210E-01	6.94166E-01
24	6.08996E 00	2.99489E-02	5.05480E-03	2.04650E-02	4.79460E-01	6.96059E-01
25	6.14813E 00	0.	0.	2.01581E-02	4.76494E-01	6.98111E-01

TABLE VII (Cont'd)

I= 4 P/P-INF= 1.22461E 01

J	RHO	PSI	THETA	S	MU	W
4	5.225836E 00	5.20786E-01	1.12031E-02	2.21618E-02	4.78793E-01	6.96520E-01
5	5.23865E 00	5.20313E-01	7.17605E-03	2.21851E-02	4.76716E-01	6.97957E-01
6	5.25340E 00	5.13322E-01	4.11511E-03	2.22160E-02	4.75161E-01	6.99036E-01
7	5.27112E 00	5.04281E-01	1.68823E-03	2.22553E-02	4.73944E-01	6.99880E-01
8	5.29196E 00	4.93627E-01	-3.23460E-04	2.23032E-02	4.72963E-01	7.00566E-01
9	5.31610E 00	4.81246E-01	-2.09136E-03	2.23600E-02	4.72119E-01	7.01155E-01
10	5.34389E 00	4.69971E-01	-3.71790E-03	2.24250E-02	4.71348E-01	7.01693E-01
11	5.37577E 00	4.50556E-01	-5.34931E-03	2.24969E-02	4.70588E-01	7.02225E-01
12	5.41247E 00	4.31615E-01	-7.08129E-03	2.25730E-02	4.69784E-01	7.02788E-01
13	5.45535E 00	4.09437E-01	-8.98619E-03	2.26484E-02	4.68892E-01	7.03413E-01
14	5.50786E 00	3.82205E-01	-1.09352E-02	2.27140E-02	4.67970E-01	7.04060E-01
15	5.61053E 00	3.28993E-01	-7.94716E-03	2.27083E-02	4.69482E-01	7.03000E-01
16	5.70123E 00	2.82597E-01	1.08972E-02	2.25798E-02	4.79075E-01	6.96325E-01
17	5.75312E 00	2.56490E-01	1.92225E-02	2.24649E-02	4.83339E-01	6.93390E-01
18	5.80491E 00	2.30637E-01	2.34872E-02	2.23127E-02	4.85442E-01	6.91950E-01
19	5.85850E 00	2.03982E-01	2.49354E-02	2.21208E-02	4.86004E-01	6.91506E-01
20	5.91396E 00	1.76430E-01	2.43437E-02	2.18927E-02	4.85437E-01	6.91954E-01
21	5.97233E 00	1.48101E-01	2.22606E-02	2.16347E-02	4.84043E-01	6.92908E-01
22	6.02900E 00	1.19159E-01	1.90842E-02	2.13547E-02	4.82054E-01	6.94273E-01
23	6.08778E 00	8.97540E-02	1.51017E-02	2.10603E-02	4.79639E-01	6.95936E-01
24	6.14694E 00	6.00432E-02	1.05157E-02	2.07586E-02	4.76921E-01	6.97815E-01
25	6.20625E 00	3.01088E-02	5.45855E-03	2.04561E-02	4.73982E-01	6.99856E-01
26	6.26557E 00	0.	0.	2.01581E-02	4.70870E-01	7.02028E-01

TABLE VII (Cont'd)

I= 3 P/P-INF= 1.17566E 01

J	RHO	PSI	THETA	S	MU	W
3	5.26434E 00	5.56396E-01	2.26533E-02	2.21364E-02	4.78606E-01	6.96649E-01
4	5.27365E 00	5.51825E-01	1.70813E-02	2.21406E-02	4.75709E-01	6.98650E-01
5	5.28592E 00	5.45749E-01	1.30534E-02	2.21497E-02	4.73637E-01	7.00097E-01
6	5.30111E 00	5.38201E-01	9.99262E-03	2.21655E-02	4.72080E-01	7.01182E-01
7	5.31925E 00	5.29153E-01	7.56600E-03	2.21899E-02	4.70863E-01	7.02032E-01
8	5.34049E 00	5.18527E-01	5.55461E-03	2.22242E-02	4.69872E-01	7.02726E-01
9	5.36557E 00	5.06205E-01	3.79702E-03	2.22694E-02	4.69024E-01	7.03320E-01
10	5.39331E 00	4.92013E-01	2.16096E-03	2.23259E-02	4.68252E-01	7.03862E-01
11	5.42569E 00	4.75704E-01	5.29875E-04	2.23931E-02	4.67494E-01	7.04395E-01
12	5.46296E 00	4.58891E-01	-1.20142E-03	2.24695E-02	4.66697E-01	7.04955E-01
13	5.50550E 00	4.34864E-01	-3.10604E-03	2.25518E-02	4.65821E-01	7.05573E-01
14	5.55979E 00	4.07832E-01	-5.05456E-03	2.26341E-02	4.64924E-01	7.06205E-01
15	5.62831E 00	3.65340E-01	-2.06659E-03	2.26832E-02	4.66477E-01	7.05110E-01
16	5.73310E 00	3.13387E-01	1.67775E-02	2.26183E-02	4.76050E-01	6.98419E-01
17	5.81479E 00	2.84994E-01	2.51026E-02	2.25429E-02	4.80318E-01	6.95468E-01
18	5.85671E 00	2.59638E-01	2.93671E-02	2.24296E-02	4.82445E-01	6.94004E-01
19	5.91774E 00	2.33363E-01	3.08146E-02	2.22753E-02	4.83043E-01	6.93593E-01
20	5.99535E 00	2.06100E-01	3.02219E-02	2.20815E-02	4.82518E-01	6.93954E-01
21	6.08465E 00	1.77990E-01	2.81375E-02	2.18533E-02	4.81170E-01	6.94881E-01
22	6.18367E 00	1.49213E-01	2.49593E-02	2.15977E-02	4.79225E-01	6.96222E-01
23	6.29359E 00	1.19937E-01	2.09748E-02	2.13223E-02	4.76850E-01	6.97864E-01
24	6.41374E 00	9.03014E-02	1.63826E-02	2.10345E-02	4.74170E-01	6.99726E-01
25	6.54430E 00	6.04076E-02	1.13270E-02	2.07409E-02	4.71264E-01	7.01752E-01
26	6.68498E 00	3.03112E-02	5.86601E-03	2.04472E-02	4.68181E-01	7.03912E-01
27	6.83557E 00	0.	0.	2.01581E-02	4.64930E-01	7.06201E-01

TABLE VII (Cont'd)

I= 2 P/P-INF= 1.12397E 01

J	RHO	PSI	THETA	S	MU	W
2	5.33294E 00	5.44514E-01	3.74481E-02	2.22966E-02	4.79798E-01	6.95826E-01
3	5.33694E 00	5.31302E-01	2.90747E-02	2.22764E-02	4.75413E-01	6.98862E-01
4	5.34452E 00	5.76553E-01	2.35011E-02	2.22528E-02	4.72513E-01	7.00849E-01
5	5.33239E 00	5.70382E-01	1.94738E-02	2.22309E-02	4.70429E-01	7.02436E-01
6	5.34211E 00	5.62797E-01	1.64129E-02	2.22147E-02	4.68954E-01	7.03443E-01
7	5.30652E 00	5.53756E-01	1.39853E-02	2.22078E-02	4.67617E-01	7.04308E-01
8	5.34818E 00	5.43174E-01	1.19749E-02	2.22129E-02	4.66604E-01	7.05029E-01
9	5.41321E 00	5.30927E-01	1.02175E-02	2.22321E-02	4.65740E-01	7.05633E-01
10	5.44194E 00	5.16438E-01	8.58177E-03	2.22667E-02	4.64953E-01	7.06145E-01
11	5.47446E 00	5.00656E-01	6.95135E-03	2.23171E-02	4.64185E-01	7.06726E-01
12	5.51276E 00	4.81995E-01	5.21999E-03	2.23827E-02	4.63386E-01	7.07292E-01
13	5.55699E 00	4.60148E-01	3.31638E-03	2.24614E-02	4.62514E-01	7.07909E-01
14	5.61111E 00	4.33352E-01	1.36818E-03	2.25499E-02	4.61633E-01	7.08534E-01
15	5.71569E 00	3.81638E-01	4.55623E-03	2.26385E-02	4.63209E-01	7.07417E-01
16	5.83467E 00	3.33152E-01	2.31998E-02	2.26259E-02	4.72741E-01	7.00721E-01
17	5.85509E 00	3.13473E-01	3.15249E-02	2.25851E-02	4.77004E-01	6.97758E-01
18	5.91819E 00	2.84661E-01	3.57890E-02	2.25085E-02	4.79149E-01	6.96274E-01
19	5.95279E 00	2.62832E-01	3.72360E-02	2.23915E-02	4.79782E-01	6.95837E-01
20	6.01953E 00	2.35867E-01	3.66424E-02	2.22337E-02	4.79361E-01	6.96169E-01
21	6.07821E 00	2.08019E-01	3.45967E-02	2.20383E-02	4.78001E-01	6.97067E-01
22	6.13826E 00	1.79451E-01	3.13758E-02	2.18112E-02	4.76105E-01	6.98381E-01
23	6.19922E 00	1.50339E-01	2.73935E-02	2.15592E-02	4.73774E-01	6.99999E-01
24	6.26072E 00	1.20929E-01	2.29030E-02	2.12898E-02	4.71141E-01	7.01838E-01
25	6.32250E 00	9.10260E-02	1.77381E-02	2.10096E-02	4.68275E-01	7.03846E-01
26	6.38441E 00	6.09868E-02	1.22745E-02	2.07246E-02	4.65229E-01	7.05990E-01
27	6.44644E 00	3.06973E-02	6.42590E-03	2.04397E-02	4.62010E-01	7.08266E-01
28	6.50885E 00	0.	0.	2.01581E-02	4.58562E-01	7.10717E-01

TABLE VII (Cont'd)

I= 1 P/P-INF= 1.06546E 01

J	RHO	PSI	THETA	S	MU	W
1	5.3[illegible]E 00	6.11219E-01	6.03204E-02	2.29605E-02	4.84611E-01	6.92519E-01
2	5.34[illegible]E 00	6.02376E-01	4.50038E-02	2.29062E-02	4.76497E-01	6.98109E-01
3	5.35[illegible]E 00	6.05978E-01	3.66364E-02	2.28172E-02	4.72081E-01	7.01181E-01
4	5.35443E 00	6.00976E-01	3.10603E-02	2.27129E-02	4.69126E-01	7.03249E-01
5	5.[illegible]E 00	5.94730E-01	2.70314E-02	2.26061E-02	4.66976E-01	7.04759E-01
6	5.[illegible]E 00	5.87129E-01	2.39694E-02	2.25063E-02	4.65333E-01	7.05917E-01
7	5.41[illegible]E 00	5.78119E-01	2.15421E-02	2.24208E-02	4.64029E-01	7.06837E-01
8	5.43505E 00	5.67607E-01	1.95303E-02	2.23550E-02	4.62958E-01	7.07594E-01
9	5.44[illegible]E 00	5.55465E-01	1.77727E-02	2.23125E-02	4.62040E-01	7.08245E-01
10	5.45[illegible]E 00	5.41512E-01	1.61399E-02	2.22953E-02	4.61210E-01	7.08833E-01
11	5.52340E 00	5.25498E-01	1.45064E-02	2.23041E-02	4.60411E-01	7.09401E-01
12	5.55198E 00	5.07035E-01	1.27756E-02	2.23384E-02	4.59588E-01	7.09986E-01
13	5.61[illegible]E 00	4.85424E-01	1.08722E-02	2.23963E-02	4.58706E-01	7.10614E-01
14	5.69211E 00	4.59929E-01	8.92475E-03	2.24756E-02	4.57826E-01	7.11242E-01
15	5.75779E 00	4.08112E-01	1.19133E-02	2.25841E-02	4.59404E-01	7.10117E-01
16	5.85623E 00	3.66173E-01	3.07555E-02	2.26101E-02	4.68864E-01	7.03432E-01
17	5.[illegible]E 00	3.42272E-01	3.99814E-02	2.25979E-02	4.73107E-01	7.00466E-01
18	5.95[illegible]E 00	3.18056E-01	4.33653E-02	2.25540E-02	4.75262E-01	6.98966E-01
19	6.01502E 00	2.92681E-01	4.47918E-02	2.24727E-02	4.75926E-01	6.98505E-01
20	6.07268E 00	2.66150E-01	4.41973E-02	2.23512E-02	4.75489E-01	6.98808E-01
21	6.13279E 00	2.39643E-01	4.21104E-02	2.21907E-02	4.74241E-01	6.99676E-01
22	6.19360E 00	2.12364E-01	3.89239E-02	2.19952E-02	4.72399E-01	7.00959E-01
23	6.25583E 00	1.81497E-01	3.49406E-02	2.17709E-02	4.70127E-01	7.02548E-01
24	6.31869E 00	1.52194E-01	3.03430E-02	2.15243E-02	4.67542E-01	7.04361E-01
25	6.38191E 00	1.22362E-01	2.52835E-02	2.12622E-02	4.64726E-01	7.06345E-01
26	6.44532E 00	9.26587E-02	1.98173E-02	2.09906E-02	4.61725E-01	7.08468E-01
27	6.50891E 00	6.24677E-02	1.39459E-02	2.07146E-02	4.58549E-01	7.10726E-01
28	6.57299E 00	3.18236E-02	7.53713E-03	2.04375E-02	4.55160E-01	7.13161E-01
29	6.63397E 00	0.	0.	2.01581E-02	4.51221E-01	7.15975E-01

REFERENCES

1. Analytical and Experimental Evaluation of the Supersonic

5.

6.

(Confidential Report).

7. Courant, R. and Friedricks, K., Supersonic Flows and Shock Waves, Interscience, John Wiley

8. Shapiro, A. H., The Dynamics and Thermodynamics of Compressible Fluid Flow, 2 Vols., The Ronal Press Co., New York (1954).

9. Von Mises, R., Mathematical Theory of Compressible Fluid Flow, Academic Press, New York (1958).

10. Powers, S. A. and O'Neill, J. B., "Determination of Hypersonic Flow Fields by the Method of Characteristics," AIAA J., 1, 7, July 1963, 1693-1694.

11. Ferri, A., "Elements of Aerodynamics of Supersonic Flows," The MacMillan Co., New York, 1949.

12. Babaev, D.A., "Numerical Solution of the Problem of Supersonic Flow Past the Lower Surface of a Delta Wing," AIAA Journal, Vol. I, No. 9 (224-231), 1963.

13. Fowell, L.R., "Exact and Approximate Solutions for the Supersonic Delta Wing," Journal of the Aeronautical Sciences, Vol. 23, No. 8, (709-770), 1956.

14. Puckett, A.E., "Supersonic Wave Drag of Thin Airfoils," Journal of the Aeronautical Sciences, Vol. 13, No. 9, (415-484), 1946.

15. Sims, J.L., "Tables for Supersonic Flow Around Right Circular Cones at Zero Angle of Attack," NASA SP-3004, 1964.

16. Sims, J.L., "Tables for Supersonic Flow Around Right Circular Cones at Small Angle of Attack," NASA SP-3007, 1964.

17. Courant, R., "Differential and Integral Calculus," Vol. II, Interscience Publishers Inc., New York, 1936. (Translated by E.J. McShane).

Unclassified

Security Classification

DOCUMENT CONTROL DATA - R & D

(Security classification of title, body of abstract and indexing annotation must be entered when the overall report is classified)

1 ORIGINATING ACTIVITY *(Corporate author)*
General Applied Science Laboratories, Inc.
A Subsidiary of The Marquardt Corporation

2a. REPORT SECURITY CLASSIFICATION
Unclassified

2b GROUP

3 REPORT TITLE
Investigation of the Low Speed Fixed Geometry Scramjet Inlet Design Practice Manual

4 DESCRIPTIVE NOTES *(Type of report and inclusive dates)*
Technical Report - September 1966 to August 1967

5 AUTHOR(S) *(First name, middle initial, last name)*
Edited by Johnson, James

6 REPORT DATE	7a. TOTAL NO OF PAGES	7b. NO OF REFS
February 1967	241	17

8a. CONTRACT OR GRANT NO	9a. ORIGINATOR'S REPORT NUMBER(S)
F-33(615)-67-C-1084	TR-667
b. PROJECT NO: 3012	
c.	9b. OTHER REPORT NO(S) *(Any other numbers that may be assigned this report)*: AFAPL-TR-68-7
d.	

10 DISTRIBUTION STATEMENT This report is subject to special export controls and each transmittal to foreign governments or foreign nationals may be made only with the prior approval of the Air Force Aero Propulsion Laboratory, Wright-Patterson AFB, Ohio 45433.

11 SUPPLEMENTARY NOTES This document may be further distributed by any holder only with specific prior approval of the Air Force Aero Propulsion Laboratory, Wright-Patterson AFB, Ohio 45433

12. SPONSORING MILITARY ACTIVITY
Air Force Aero Propulsion Laboratory, Wright-Patterson AFB, Ohio 45433

13 ABSTRACT

Computer programs have been written to aid the design and analysis of 2-D, axisymmetric, and 3-D supersonic inlets. This report presents the fundamental analytic techniques, the use and operation of the computer programs, and the application to the design of supersonic inlets. The programs are written in FORTRAN IV for use on the 7094 high speed digital computer.

The 2-D and axisymmetric programs presented herein are written for generalized inviscid supersonic internal flow problems with uniform or non-uniform inlet entry conditions for entropy, total enthalpy, pressure, Mach number and flow direction. The program capabilities include the intersections and reflections of both family waves, the formation of shocks or expansions at corners, the formation of shocks by coalescence of waves from smooth walls, and the formation of contact discontinuities.

The 3-D programs presented herein are written for the calculation of the inviscid supersonic flow fields associated with basic elements of 3-D supersonic inlets. The methods utilized exact and linearized supersonic flow theory with engineering approximations to yield solutions to the following unit problems; delta wing flow, conical shock interacting with a plane surface, plane shock interacting with a conical surface, and the interaction of two different conical flow fields.

DD FORM 1 NOV 65 1473

Unclassified

Security Classification

14. KEY WORDS	LINK A		LINK B		LINK C	
	ROLE	WT	ROLE	WT	ROLE	WT
Three-Dimensional Supersonic Flow						
Three Dimensional Computer Program						
Two-Dimensional Supersonic Flow						
Two-Dimensional Computer Program						
Supersonic Inlets						
Scramjet						